The Role of Megakaryocytes and Platelets in Infection and Immunothrombosis.

by

Galit Hocsman Frydman

B.S., Carnegie Mellon University (2007)

D.V.M., University of Florida, College of Veterinary Medicine (2013)

Submitted to the Department of Biological Engineering

in partial fulfillment of the requirements for the degree of

Doctor of Science

at the

MASSACHUSETTS INSTITUTE OF TECHNOLOGY

February 2018

Signature redacted

Author . . . . . .

Department of Biological Engineering

December 14, 2017

Signature redacted

Certified by. . . . . .

James G. Fox

Professor of Biological Engineering

Director, Division of Comparative Medicine

Thesis Supervisor

Signature redacted

Accepted by . . . . . .

Mark Bathe

Chair, Biological Engineering Graduate Committee

Preface

Chapter 1 was, in part, written in collaboration with Kelly Metcalf Pate (Johns Hopkins University, Baltimore, MD) and Allison Vitsky (Pfizer Global Research and Development, San Diego, CA), and is adapted from a chapter entitled "Platelets and Hemostasis" contained in the forthcoming third edition of *Comprehensive Toxicology* (Elsevier, Inc.). Experiments exploring the megakaryocyte as an innate immune cell, as discussed in Chapters 2 and 3, are presently being drafted as manuscripts for submission. The development of a microfluidic device for the exploration of platelet-leukocyte interactions, as described in Chapter 4, has previously been published in the *Journal of Leukocyte Biology* under the title "Technical Advance: Changes in neutrophil migration patterns upon contact with platelets in a microfluidic assay." The preliminary findings described in the Appendix regarding the changes in megakaryocyte differentiation in the presence of lipopolysaccharide will continue to be explored, with future experiments looking into related changes in resultant platelet phenotype utilizing new tools, such as those developed and described in Chapter 4.

The work presented in this thesis is the product of the author, with contributions from other laboratory members and collaborators across MIT and Harvard. I am particularly grateful to James Fox, without whose encouragement, criticism, and unwavering support this project could never have materialized. I would also like to thank Jacquin Niles, who served as my thesis committee chair and provided valuable guidance and feedback throughout this process. Other individuals from the Division of Comparative Medicine provided invaluable feedback on a variety of topics. Especially noteworthy were the contributions of Sureshkumar Muthupalani, who provided experimental guidance on experimental pathology and image analysis; Yan Feng, who aided in special staining techniques for bacterial co-localization; Ellen Buckley and Carolyn Madden, who provided bacterial cultures for experiments and clinical laboratory guidance; and Joanna Richards and Caroline Atkinson of the pathology service team, who prepared histopathology samples for analysis. Nicki Watson from the Whitehead Institute performed the immune-gold labeling and some of the electron microscopy. Two undergraduate research

students, David Olaleye and Skyler Kaufman, aided in cell toxicity assays and histopathology image analysis.

The teams at the Center for Engineering in Medicine, the BioMEMs Resource Center, and the Center for Surgery, Innovation & Bioengineering (Massachusetts General Hospital, Boston, MA), under the leadership of Daniel Irimia, Mehmet Toner, and Ronald Tompkins, were also integral to the success of this thesis. A debt of gratitude is further owed to Charles Vanderburg (Harvard NeuroDiscovery Center, Boston, MA), whose ideas and assistance proved essential to the development, maturation, and interpretation of this thesis material. Additionally, Lawrence Zuckerbeg and Martin Selig (Dept. of Pathology, Massachusetts General Hospital) aided in histopathology sample collection, analysis, and electron microscopy. Finally, a number of laboratory members and researchers were especially helpful, or co-authored one or more of the papers published during this thesis, and thus deserve special recognition. These include Felix Ellett, Shannon Tessier, Keith Wong, Caroline Jones, Anna Lee, Julianne Jorgensen, and Anika Marand. And, of course, patient sample collection would not have been possible without the assistance of the clinical diagnostic laboratory team at MGH. To all these individuals—and to others far too numerous to list here—I give my profound thanks for making this research possible.

I would like to thank and acknowledge my thesis committee for their endless support, mentorship, and guidance of this work.

This work was supported by the T32-0D019078-28 (JGF), the P30-ES002109 (JGF), the P50-GM021700 (RGT), the GM092804 and AI113937 (to D.I.), and the Harvard NeuroDiscovery Center. All microfabrication procedures were performed at the BioMEMS Resource Center (EB002503).

The Role of Megakaryocytes and Platelets in Infection and Immunothrombosis.

By

Galit Hocsman Frydman

Submitted to the Department of Biological Engineering
on December 14, 2017, in Partial Fulfillment of the
Requirements for the Degree of Doctor of Science in
Biological Engineering

Abstract

Megakaryocytes (MKs), one of the largest and rarest hematopoietic stem cells in the bone marrow, have traditionally played a primary role in hemostasis as precursors to platelets, which are importantly, one of the most abundant cell types in the peripheral circulation. While platelets are studied for their various roles in inflammation, the role of MKs within the innate immune system has not been explored. In a series of comprehensive *in vitro* experiments, we have demonstrated that both cord blood-derived MKs and MKs from a megakaryoblastic lineage have innate immune cell functions, including: phagocytosis, formation of extracellular traps, and chemotaxis towards pathogenic stimuli. MKs were also observed to directionally release platelets towards pathogenic stimuli. In addition to their primary role as immune cells, MKs were also shown to contain extranuclear histones, which the MKs release along with budding platelets into the circulation. These small packages of histones can play a major role in inflammation and immunothrombosis by promoting inflammation and coagulation. By evaluating blood and tissue samples from patients diagnosed with sepsis, we demonstrated that there is an increased MK concentration both in the peripheral circulation, as well as in the lungs and kidneys. Platelets from patients with sepsis also appeared to have a specific phenotype, including increased DNA and histone staining. MK number in the circulation and end-organs, as well as platelet histone expression appeared to be correlated with both prognosis and type of infection. This newly recognized role of MKs as functional innate immune cells may have significant implications for the role of MKs in conditions such as sepsis and, pending a more profound mechanistic understanding, may further lead to the development of novel targets for the treatment of sepsis

Thesis Supervisor: James G. Fox

Title: Professor of Biological Engineering

Table of Contents

Appendix: The Effect of Endotoxin on Megakaryocyte Differentiation

List of Figures

Appendix

List of Tables

List of Videos

Videos are in a separate electronic document

2-1 Zymosan particles co-incubated with Meg-01 cells.

2-2 Zymosan particles are internalized by Meg-01 cell.

2-3 Chemotaxis of Meg-01 cells.

2-4 Platelet-like particle budding within a well after chemotaxis

2-5 Cytoskeletal rearrangement during chemotaxis

2-6 Meg-01 cell carrying zymosan particle during chemotaxis

2-7 Meg-01 cell budding platelet-like particles in the presence of zymosan and LPS

2-8 Meg-01 cell budding platelets in the presence of SDF1α

2-9 Meg-01 cell chemotaxis negative control

4-1 Neutrophil motility in the presence of PRP

4-2 Neutrophil chemotaxis towards fMLP

List of Abbreviations

ACD	Acid citrate dextrose
ADP	Adenosine diphosphate
AKI	Acute kidney injury
APC	Antigen presenting cells
ARDS	Acute respiratory distress syndrome
Ca	Calcium
CB MKs	Cord blood-derived megakaryocytes
CBC	Complete blood cell count
CD	Cluster of Differentiation
CFU	Colony-forming unit
c-MPL	Thrompoietin receptor
COX	Cyclooxygenase
DAMPs	Danger-associated molecular patterns
DC	Dendritic cells
DIC	Disseminated intravascular coagulation
DNA	Deoxyribonucleic acid
dsDNA	Double stranded deoxyribonucleic acid
E. coli	*Escherichia coli*
EC histones	Extracellular histones
EDTA	Ethylenediaminetetraacetic acid
EET	Eosinophil extracellular trap
ET	Extracellular trap
FBS	Fetal bovine serum
fMLP	N-formylmethionine-leucyl-phenylalanine
GP	Glycoprotein
GPCR	G-protein coupled receptors
GPS	Grays Platelets Syndrome
H	Histone (ex: H2, Histone 2)

HLA	Human leukocyte antigen
HRP	Horseradish peroxidase
HSC	Hematopoietic stem cell
HT	Hepes-tyrode
IL	Interleukin
LPS	Lipopolysaccharide
Meg-01	Megakaryoblastic cell line
MET	Megakaryocyte extracellular trap
Mg	Magnesium
MHC	Major Histocompatibility Complex
MK	Megakaryocyte
MPO	Myeloperoxidase
MYH10	Non-muscle myosin IIB heavy chain
MYH9	Non-muscle myosin IIA heavy chain
NBEAL2	Neurobeachin-like protein 2
NEC	Necrotizing enterocolitis
NET	Neutrophil extracellular trap
PAR	Protease-activated receptors
PBS	Peripheral blood smear
PBS	Phosphate buffered saline
PG	Prostaglandins
PLA	Platelet-leukocyte aggregate
Plt	Platelet
PNC	Platelet-neutrophil complex
PPP	Platelet-poor plasma
PRP	Platelet-rich plasma
PTSM	Post-translational modifications
RNA	Ribonucleic acid
ROS	Reactive oxygen species
RPMI media	Roswell Park Memorial Institute media
S. aureus	*Staphylococcus aureus*

S. pyogenes	*Streptococcus pyogenes*
SDF-1α	Stromal cell-derived factor-1α
SOFA	Sequential [Sepsis-related] Organ Failure Assessment Score
TEM	Transmission electron microscopy
TF	Tissue factor
TLR	Toll-like receptor
TPO	Thrombopoietin
TX	Thromboxane
vWF	von Willebrand Factor
WBC	White blood cell
WP	Washed platelets

Chapter 1
Introduction

Adapted from:

Frydman GH, MetCalf Pate KA, Vitsky A. (2018) **Platelets and Hemostasis, In: McQueen CA, Comprehensive Toxicology, Third Edition.** Vol 12, pp. 60-113. Oxford: Elsevier Ltd.

1.1 Abstract

Platelets are circulating, anucleate cells derived from megakaryocytes. While platelets were originally thought to play a role only in primary hemostasis, these cells have recently been discovered to participate in a wide variety of pathways, including hemostasis, immunology, wound healing, and cancer biology. Dependent on their RNA and protein expression profiles, platelets may also display various phenotypes that play a part in the pathophysiology of specific diseases, such as sepsis, cancer, and autoimmune conditions. In order to understand platelets and their roles within the body, it is important to understand the origin and development of the platelet, starting from the hematopoietic stem cell. This chapter provides a bird's-eye view of the increasingly complex megakaryocyte-platelet axis and its various roles in the body.

1.2 Platelet Production

Platelets are small (1-3 μm diameter), circulating anucleate cells derived from megakaryocytes (MKs). In an adult, there are approximately 100 billion new platelets produced each day, each with a life span of 8-10 days, maintaining a platelet count of 150-400 x 10^9 platelets L^{-1}. (Kaushansky, 2005;Italiano, 2007) The production of platelets from megakaryocytes can be roughly divided into two major stages: megakaryopoiesis, the development and maturation of the

MK from the hematopoietic stem cell progenitor, and thrombopoiesis, the development and release of platelets from MKs. Each step in this complex process requires the optimal combination of physiological conditions, including many different cytokines and growth factors. Many diseases and drugs that result in changes to the peripheral platelet count and/or function may be the result of an effect on the megakaryocyte during its multiple stages of maturation and platelet production. In this section, we will review the basics of platelet production, beginning with the hematopoietic stem cell.

While platelets were originally thought to have a role only in primary hemostasis, more recently, these cells have been discovered to participate in a wide variety of pathways, including: hemostasis, immunology, wound healing, and cancer biology. Dependent on their RNA and protein expression profiles, platelets may also display various phenotypes that play a part in the pathophysiology of specific diseases, such as sepsis, cancer, and autoimmune conditions. In order to understand platelets and their roles within the body, it is important to understand the origin and development of the platelet, starting from the hematopoietic stem cell.

Platelets and their roles in pharmacology are extremely important. While platelet inhibitors have been used in a clinical setting for decades, as the understanding of the platelet grows, new pharmaceutical targets on the platelet are being elucidated and new platelet inhibitors are being developed. Because the role of the platelet is not always straight-forward, it is also becoming increasingly apparent that these platelet inhibitors may have unintended downstream effects on other functions and issues within the body, such as inflammatory pathways and cancer development. On another note, there are many pharmaceutical chemical compounds and biologics that have direct, yet unintended effects on platelets, such as antidepressants, including serotonin reuptake inhibitors (SSRIs), and non-steroidal anti-inflammatory agents (NSAIDs), including COX-1 and COX-2 inhibitors. Due to the platelets' plentiful interactions with various cell types and organ systems within the body, newer techniques are being developed to utilize the platelet as a drug delivery tool itself, including direct drug-loading and genetic manipulations of the megakaryocytes themselves to treat a number of congenital conditions involving the coagulation system.

1.2.1 Megakaryopoiesis

It has long been thought that MKs differentiate from hematopoietic stem cells (HSCs) and are the largest (50-100 μm) and rarest (0.01%) progenitor cell in the bone marrow (Nakeff and Maat, 1974). HSCs are primarily present in the bone marrow and lungs, although during early development, they are also present in the yolk sac, fetal liver, and spleen. (Long et al., 1982, Gordon et al., 1990, Ogawa, 1993, Morita et al., 2011) The HSC first becomes a common myeloid progenitor, with the MK-specific myeloid progenitor being called either MK/erythrocyte bipotent progenitor (MEP) or BFU-E/MK. After the MEP cell becomes committed to MK differentiation, it is referred to as a hematopoietic progenitor, and it loses self-renewal capabilities and pluripotency. The BFU-MK then develops, forming colonies of about 50 cells organized into sub colonies. BFU-MKs are in the G0/G1 phase of the cell cycle, and develop within 12 days in the mouse and within 21 days in the human. (Nakorn et al., 2003) The subsequent progenitor, the CFU-MK has colonies composed of 3-50 cells, are in active cell cycle, and develop within 5 days in the mouse and within 15 days in the human. (Becker RP 1976) Following the CFU-MK stage, these cells go through further maturation into fully differentiated megakaryocytes, including the megakaryoblast, promegakaryocyte, granular megakaryocyte, and the mature megakaryocyte (Figure 1-1). Recent literature suggests that megakaryocytes can arise from alternate pathways, however, including those lacking a pluripotent or bipotent development stage. (Woolthuis and Park, 2016)

Megakaryocytes differentiate from HSCs in a thrombopoietin (TPO) -dependent fashion (Kuter, 2013, Bartley et al., 1994). TPO acts on the MK c-MPL receptor, a proto-oncogene of the murine myeloproliferative leukemia virus and a member of the type 1 hematopoietic cytokine receptor family, resulting in activation of the JAK and STAT pathways, promoting the growth and maturation of the MK. (Vigon et al., 1993, Kaushansky, 2005, Kuter, 2013) The levels of circulating TPO are inversely correlated to the number of circulating platelets, as TPO is synthesized by the liver then bound and cleared by binding c-MPL on platelets in the peripheral circulation. (Kuter, 2013) Interleukin-6 (IL-6), which plays a role as an inflammatory mediator, increases TPO production both *in vivo* and *in vitro*. (Kaushansky and Hitchcock, 2013)

Although TPO has been deemed as an important factor in MK differentiation and platelet formation, c-mpl$^{-/-}$ and TPO$^{-/-}$ mice exhibit a reduction in progenitor cell numbers, a decrease in

MK ploidy, and a 90% reduction in peripheral platelet numbers, suggesting that other cytokines and growth factors are involved in the formation of approximately 10% of circulating platelets (Murone et al., 1998). Other cytokines have also been shown to promote megakaryocyte maturation and platelet formation in a dose-dependent manner. (Stahl et al., 1991, Wu et al., 2015) IL-6, for instance, works synergistically with interleukin-3 (IL-3) and stem cell factor (SCF or kit ligand or steel factor) to increase MK colony formation. (Borde and Vainchenker, 2013) Erythropoietin (Epo) is a cytokine essential for the differentiation of red blood cells, but MKs also have the Epo receptors; although the function of the Epo receptor on the MK is not well understood, if it results in MK activation, this may explain why people chronically administered Epo can exhibit a slight increase in platelet numbers (Borde and Vainchenker, 2013). Stromal cell-derived factor-1 or (SDF-1) is also a growth factor for HSCs and increases MK maturation. (Borde and Vainchenker, 2013) MKs also produce cytokines that stimulate MK colony formation, including interleukin-1β (IL-1β), IL-6, and granulocyte-macrophage colony-stimulating factor (GM-CSF), suggesting an autocrine signaling mechanism is in place in the regulation in megakaryopoiesis. (Jiang et al., 1994) Bone morphogenic protein 4 (BMP4) and its receptor expression have been shown to be induced in MKs by TPO in an autocrine loop fashion, therefore indicating that BMP4 also plays a role in megakaryopoiesis. (Borde and Vainchenker, 2013)

The molecular mechanisms regulating megakaryopoiesis are under investigation. Though delving into all of the genetic molecular mechanisms involved in megakaryopoiesis is beyond the scope of this chapter, one example of the key regulators of MK differentiation is the GATA transcription factor family and its partners. GATA-1 is present during normal erythromegakaryocytic differentiation, and MK-specific GATA-1 knockout mice present with profound macrothrombocytopenia as well as a high number of immature MKs in the bone marrow. (Borde and Vainchenker, 2013) Other transcription factors associated with GATA-1 and affecting platelet development includes: Friend of Gata-1 (FOG-1), Tal-1, and RUNX. (Borde and Vainchenker, 2013) Abnormalities in the GATA-1 and FOG-1 interaction are associated with X-linked congenital thrombocytopenias. (Borde and Vainchenker, 2013) A knockout model of FOG-1 produces a similar phenotype as the GATA-1 knockout but with an absence of MK progenitors. Knocking out TAL-1 causes a complete absence of HSCs and

subsequent embryonic lethality. Finally, abnormalities in the RUNX-1 gene have been identified in familial thrombocytopenia and acute myeloid leukemia (AML). (Borde and Vainchenker, 2013)

HSCs differentiate into pro-megakaryoblasts and then megakaryoblasts, also in a TPO-dependent manner; after which endoreplication commences. Differentiation and maturation during this time results in distinct changes in cell-surface markers, which can be used on platforms such as flow cytometry, immunohistochemistry, and immunofluorescence to identify the various cell stages. (Tomer et al., 2007) MKs first undergo a proliferative 2n stage, followed by endomitosis, accumulating DNA content ranging up to 128n in a single cell. (Zimmet and Ravid, 2000) The size and morphology of the diploid precursor resembles that of a small lymphocyte, and this stage can only be correctly identified by surface marker expression. When evaluating megakaryocytes by cytology, three maturation stages can be identified without special staining (Figure 2-1): Type I, or immature MKs, have basophilic cytoplasm with a large polyploid nucleus, cytoplasmic blebs, and a large cell volume (> 14 μm). These cells have a high nuclear to cytoplasmic (N/C) ratio and thin chromatin. Type II MKs are larger (15-40 μm), have a polylobulated nucleus, and basophilic-staining cytoplasm. The N/C ratio begins to decrease, while the amount of cytoplasm increases and becomes more azurophilic with condensed chromatin. Type III, or mature MKs, have low N/C ratio, a dark purple-staining cytoplasm and distinct nuclear lobes. (Stenberg and Levin, 1989, Borde and Vainchenker, 2013)

During maturation, MKs undergo endomitosis (DNA replication without cellular division), becoming polyploid and accumulating a large amount of mRNA, proteins, and membrane. MKs are the only cells that become polyploid during normal differentiation. As they become polyploid, the amount of cytoplasm also grows, which is thought to allow for the increased production of platelets. In mice with acute thrombocytopenia, the first change that is seen is an increase in MK ploidy, from 16N to 32N, with maximal ploidy seen at 48 hours followed by resolution at 120 hours. (Borde and Vainchenker, 2013) MK ploidy number varies based on the source of MKs, with cord blood and fetal MKs have a lower average ploidy (2-4N in culture) compared with MKs derived from adult bone marrow and peripheral blood (16-32N in culture). (van den Oudenrijn et al., 2000, Schipper et al., 2003)

Polyploidization is related to the degradation of cyclin B-dependent cell division cycle (Cdc) kinase and a defect in late cytokinesis; there is incomplete formation of the cleavage furrow, which is dependent on down-regulation of nonmuscle myosin IIB heavy chain (MYH10) in the contractile ring by runt-related transcription factor 1 (RUNX1), preventing cell separation. (Datta et al., 1996, Garcia and Cales, 1996, Zhang et al., 1996, Zhang et al., 1998, Lordier et al., 2012, Lordier et al., 2008, Geddis et al., 2007) Utilizing MK-specific double knockouts, protein-tyrosine phosphatases Src-homology-2-domain-containing protein tyrosine phosphatases 1 and 2 (Shp1 and Shp2) have been demonstrated to play an essential role in MK progression beyond the 2-4n stage. (Mazharian et al., 2013) Additionally, it has been shown that the microtubule-associated guanine nucleotide exchange factor H1 (GEF-H) 1 and epithelial cell transforming 2 (ECT2), both playing a role in RhoA localization and activation in the cleavage furrow, are down-regulated at the mRNA and protein level in the MK. (Birkenfeld et al., 2007, Melendez et al., 2011, Gao et al., 2012, Petronczki et al., 2007) While these may be essential in preventing cell division, cell-cycle regulators, such as cyclin D and E, also play an important role in the continuation of DNA replication during G1/S phase. (Zimmet et al., 1997, Muntean et al., 2007, Eliades et al., 2010) The exact mechanism and regulation of endoreplication in MKs is still under study, and it is likely that the complexity of this cell cycle phenomenon will continue to grow. Recent research in mice demonstrated a potential regulatory role for p21-activated kinase 2 (Pak2), since deletion of this gene results in increased MK ploidy, macrothrombocytopenia, increased bone marrow MK precursors, and altered MK ultrastructure. (Kosoff et al., 2015) Another gene that appears to be essential in endomitosis is Polo-like kinase 1 (Plk1); deletion of this gene results in defective polyploidization accompanied by mitotic arrest and cell death. (Trakala et al., 2015)

The purpose of MK endoreplication is also under study. A primary hypothesis behind the need for polyploidy is the increased need for mRNA and protein production for packaging into platelets, as well as an increased need for cytoplasm, lipids, and cytoskeletal components for the formation of platelets. (Zimmet and Ravid, 2000) Some studies using IL-6 and lipopolysaccharide (LPS) show a positive correlation between MK ploidy and platelet formation, and some hereditary diseases such as Fanconi anemia (FA), have been linked to a decrease in

MK ploidy as well as peripheral thrombocytopenia. (Pawlikowska et al., 2014) However, other studies utilizing both nicotimamide and cyclin D3 regulators suggest that platelet count is independent of ploidy. (Stahl et al., 1991, Wu et al., 2015) (Zimmet et al., 1997, Giammona et al., 2006, Leysi-Derilou et al., 2012, Konieczna et al., 2013)

The ultrastructure and components of the MK are quite complex and change throughout cell maturation. As with other eukaryotic cells, MKs also contain Golgi, endoplasmic reticulum, mitochondria. Megakaryocytes also contain multiple types of granules: α, dense, lysosome, and t granules; the contents and function of which will be discussed in Section 1.3.7, 'Granules'. The ER eventually gives rise to the platelet-dense tubular system, which will contain the cytochemical activity of mature platelets, including NADH-cytochrome *c* reductase, cyclooxygenase, thromboxane synthase, Ca^{2+} Mg^{2+} adenosine triphosphatase, and platelet peroxidase. (Borde and Vainchenker, 2013, Breton-Gorius and Guichard, 1972) While endoreplication is taking place, the demarcation membrane system (DMS; IMS) is developing within the cell (Figure 1-3). The DMS, a reservoir for platelet formation, is a complex of cisternae and tubules within the MK cytoplasm. (Yamada, 1957, Radley and Haller, 1982) The DMS has continuity with the plasma membrane of mature MKs, suggesting that plasma membrane invagination is involved in DMS formation. (Machlus and Italiano, 2013, Eckly et al., 2014) A study by Chen et al (2013) identified that CDC42 interacting protein 4 (CIP4), a protein that bridges the membrane and cytoskeleton and also promotes actin reorganization via its interaction with *Wiskott–Aldrich Syndrome protein (*WASP), is essential in platelet formation as both CIP4 and WASP deficiencies result in thrombocytopenia and decreased cortical actin tension. (Chen et al., 2013)

1.2.2 Thrombopoiesis

The mechanism for the development of platelets from MKs is another area under continued study and debate. Understanding the mechanism of platelet formation is important for understanding biological details, the outcome of drug effects, and for the development and optimization of *in vitro* platelet synthesis techniques. Platelet formation occurs in two basic steps: maturation, which takes about 5 days to complete, and platelet release, which occurs within hours. Platelets

survive in the bloodstream for 7-10 days in humans. (Aster, 1967, Harker and Finch, 1969, Jackson and Edwards, 1977)

Current literature is suggestive of the 'shearing hypothesis'. Once mature, MKs migrate towards the sinusoidal blood vessels and attach to the endothelium in a chemotactic and receptor-dependent manner, involving cytokines such as stromal cell-derived factor 1 (SDF-1) and its G protein-coupled chemokine receptor CXCR4 (Fusin, LESTR). (Hamada et al., 1998) (Takahashi et al., 1999, Balduini et al., 2011) They are then exposed to the shear force of the blood flowing through the blood vessels and extend long processes, called proplatelets, which undergo fission to release platelets into the bone marrow intravascular sinusoidal space. (Richardson et al., 2005, Tavassoli and Aoki, 1989, Thon and Italiano, 2012) Alternatively, spontaneous platelet formation also occurs spontaneously *in vitro* without endothelial cells, SDF-1, or shear force. (Thon and Italiano, 2012, Thon et al., 2010, Italiano et al., 1999, Patel et al., 2005a)

The MK cytoskeleton has been suggested to be one of the key components of proplatelet formation and platelet release, suggested by the marked enlargement and re-organization of the cytoplasm and DMS in the maturing MK. Actin filaments, which are linked to the plasma membrane by filamen and bound to a number of glycoproteins, are an integral cytoskeletal part of proplatelet formation and platelet release, the importance of which has been extensively demonstrated in scientific literature. Bernard-Soulier syndrome, which is characterized by macrothrombocytopenia and a decrease or absence of platelet dense granules, is associated with abnormalities in GPIba, GPIbB, and GPIX, which are also bound to filamin. (Rao et al., 2004) Defects in the filamin A (FLNA) gene and the GPIX gene have been linked to decreased platelet counts and decreased surface expression of GPIba. (Li et al., 2015, Wang et al., 2004) β1-tubulin has also been shown to play a key role in the MK cytoskeleton and the formation of platelets, as mice deficient in β1-tubulin have both fewer platelets, and platelets with structural and functional defects, and humans with an autosomal dominant β1-tubulin mutation have a macrothrombocytopenia. (Lecine et al., 2000, Patel et al., 2005b, Kunishima et al., 2009). Mutations in the *MYH9* gene, reducing non-muscle myosin heavy chain IIa activity, have been linked to May-Hegglin anomaly and macrothrombocytopenias (Italiano et al., 1999, Seri et al., 2000, Kelley et al., 2000), and utilizing mouse models of *MYH9* gene mutations, researchers

have shown that MKs produce fewer and shorter proplatelets with less branching. (Zhang et al., 2012) RUNX1 mutations have also been shown to regulate proplatelet formation via *MYL9, MYH10, and MYH9*, suggesting a potential link between humans with familial platelet disorders and acute myelogenous leukemia. (Zhang et al., 2012, Machlus and Italiano, 2013) A study by Pleines et al (2013) demonstrated the essential role of Rho GTPases RACGAP1 (Rac) and CDC42 in proplatelet formation; knockout mice had severe thrombocytopenia and decreased platelet surface receptor expression (GPIb, GPV, GPIX, GPVI and GPIIb/IIIa) with normal actin structures but severely disrupted MK tubulin organization. (Pleines et al., 2013)

The formation of MK granules is a complex process involving many components of the cytoskeletal machinery. Microtubules are involved in proplatelet elongation and transportation, as well as assembly of organelles and granules into proplatelet buds. Granule formation begins with the budding of vesicles off of the Golgi network, after which the vesicles are delivered to multivesicular bodies for protein sorting and granule formation. (Blair and Flaumenhaft, 2009, Heijnen et al., 1998, Youssefian and Cramer, 2000) These granules are then transported to the proplatelet buds via microtubules. (Richardson et al., 2005) Cytoplasmic dynein localizes along microtubules of the proplatelet and appears to directly contribute to microtubule sliding; inhibition of dynein, through disassembly of the dynactin complex, blocks proplatelet formation, demonstrating that this is a key event in proplatelet elongation. (Machlus and Italiano, 2013) The contents of the various granules and the concept of granule sorting into different platelet populations remains a controversial topic today, as some studies do show that α-granule protein composition is heterogenous during platelet activation. (Italiano et al., 2008, Kamykowski et al., 2011, Jonnalagadda et al., 2012, Peters et al., 2012, van Nispen tot Pannerden et al., 2010)

Platelet size is an important aspect of many pathologies and disease states, with an increase in platelet size and decrease in platelet count (macrothrombocytopenia) often being correlated with changes in function. Platelet size is determined by the subcellular structure and size of the DMS. In addition to some genetic abnormalities resulting in macrothrombocytopenia, autoimmune thrombocytopenia is also associated with an increase in platelet volume. Acceleration in platelet production with an associated increase in platelet volume may be a result of changes in the partition of the constriction zones within the DMS. (Borde and Vainchenker, 2013)

MKs have many different types of granules, including α, dense, lysosome, and t granules. α – Granules are present during early MK differentiation, along with the development of the DMS. Dense granules then appear at the end of MK maturation. (Borde and Vainchenker, 2013) The multivesicular body, which is present in MKs and rarely present in platelets, is a sorting compartment, representing the intermediate step between the Golgi network and α- and dense granule formation. (Borde and Vainchenker, 2013) α–Granules arise from the trans-Golgi network and acquire proteins by two mechanisms: MK biosynthesis and plasma protein endocytosis (also thought to occur in platelets).(Borde and Vainchenker, 2013)

The mechanistic study of dense vesicle trafficking and dense granule formation is being explored in the context of Hermansky-Pudlak and Chediak-Higashi syndromes, diseases in which platelets lack dense granules. Recent research has suggested that specific genes and proteins (BLOC, VPS33A, AP3, and BEACH domain-containing protein LYST) play roles in vesicle trafficking and dense granule formation. The study of α-granules is performed in the context of Quebec Platelet Disorder, Gray Platelet Syndrome (GPS) and ARC (arthrogryposis, renal dysfunction and cholestasis) syndrome. *NBEAL2* has been identified as the causative gene mutation for GPS, and a murine model of this disorder has been created. (Albers et al., 2011, Gunay-Aygun et al., 2011, Kahr et al., 2011, Deppermann et al., 2013, Kahr et al., 2013) The studies of MKs from *Nbeal2-/-* mice have resulted in controversial findings. While a study by Kahr et al (2013) displayed structural abnormalities, delayed maturation, decreased survival, decreased ploidy, and developmental defects (abnormal extracellular distribution of von Willebrand Factor), a study by Depperman et al (2013) showed normal differentiation and proplatelet formation. (Kahr et al., 2013, Deppermann et al., 2013) It is noteworthy that these two papers did use different sources for their MKs, which could explain the discrepancies between the two studies.

One longstanding hypothesis for platelet formation and release has relied upon the importance of the intrinsic apoptotic caspase cascade. (De Botton et al., 2002, Clarke et al., 2003) MKs have been documented to undergo a caspase-3 and -9 mediated apoptosis during thrombopoiesis, and activation of caspase yields functional platelets with normal lifespans. (De Botton et al., 2002, Clarke et al., 2003) Further supporting the apoptosis hypothesis, overexpression of BCL2

inhibited proplatelet formation. (De Botton et al., 2002) However, further probing into the apoptotic pathway has shown that, although caspase-mediated apoptosis does occur in the MK, this apoptosis must be restrained for platelet formation. The deletion of BCL-xL (BCL2L1, a pro-survival signal) triggers apoptosis in MKs but fails to induce thrombopoiesis (Josefsson et al., 2011). This has been corroborated with a familial thrombocytopenia linked to a mutation in cytochrome c, which enhances caspase activity. (Morison et al., 2008) A study by Iancu-Rubin C, et al., (2014) showed that MDM2 inhibition and P53 activation impairs thrombopoiesis by both promoting MK precursor apoptosis and by blocking DNA synthesis during endomitosis, impairing platelet production. (Iancu-Rubin et al., 2014) Culture of MKs with recombinant Chemokine ligand 5 (CCL5, RANTES), a cytokine stored and released by activated platelets, resulted in increased MK ploidy and proplatelet formation, a finding thought to be secondary to CCL5's interaction with the Akt pathway with subsequent suppression of apoptosis. (Machlus et al., 2016) One recent study looked at whether ER stress during MK maturation was enough to result in apoptosis-mediated thrombopoiesis; transient ER stress was identified during the maturation of MKs and the inhibition of ER stress induced apoptosis, decreased expression of MK maturation cell surface markers, and proplatelet formation. (Lopez, 2013) Recently, a study demonstrated that thrombopoiesis was unperturbed in the absence of caspase-9, providing strong evidence that the apoptotic caspase cascade is not absolutely required for platelet production. (White et al., 2012)

An alternate hypothesis of platelet formation is MK rupture, which is postulated to result in the cytoplasmic fragmentation and release of platelets. (Nishimura et al., 2015) Research has demonstrated that serum cytokines, such as interleukin-1α (IL-1α), are elevated after platelet loss or inflammation in mice, whereas TPO is not elevated. Additionally, the administration of IL-1α to mice induced MK rupture-dependent thrombopoiesis and increased platelet count. The MKs in this study showed increase caspase-3 activation, reduced plasma membrane stability, and inhibited regulation of tubulin expression and proplatelet formation, which led to MK rupture. (Nishimura et al., 2015)

Once proplatelets are formed, they are released from the MK. Multiple stages of proplatelets and platelets have been described in the peripheral circulation, suggesting that platelets may continue

their maturation while in the blood stream. (Machlus and Italiano, 2013) A pre-platelet stage has also been identified, ranging from 2-10 μm and capable of the maturing into platelets within the bloodstream. (Thon et al., 2010, Thon and Italiano, 2012) Additionally, platelets and pre-platelets have been shown to form progeny within the bloodstream, transforming from a single platelet into a barbell-shaped structured with two platelet-like structures on each end. This phenomenon has been demonstrated *in vitro* and is associated with increased protein synthesis. (Schwertz et al., 2010, Machlus and Italiano, 2013)

Platelet size (normally approximately 2 μm) is also highly regulated, being dependent on both microtubule coil diameter and tube thickness. (Thon and Italiano, 2012) Circulating pre-platelets may become trapped in small capillary beds within the lungs, spleen or bone marrow, where increased intravascular shear forces are thought to result in terminal formation of platelets of appropriate size. (Howell and Donahue, 1937) In fact, when MKs are infused into mice, they have been shown to almost exclusively localize to the lungs, releasing platelets within 2 hours. (Fuentes et al., 2010) The size of the platelet has also been correlated with platelet reactivity in different disease states, suggesting that an increase in platelet size is positively correlated with an increase in platelet aggregation, activation, and risk for cardiovascular diseases. (Bath and Butterworth, 1996, Kamath et al., 2001, Berger et al., 2010, Chu et al., 2010, Slavka et al., 2011)

1.3 Structure and content of the platelets

Platelets, although anucleate, have many functional organelles and granules. They have active metabolisms, through their glycogen granules and mitochondria, and also contain their own RNA and proteins. In fact, they contain the machinery to translate RNA into proteins for cell use and secretion, including rough and smooth endoplasmic reticulum and Golgi complexes (Figure 1-3). Platelets play various roles in the body, including promotion and inhibition of inflammation, neovascularization, wound healing, and even cancer regulation. Their complex physiology allows them to bind to other cells and substrates, subsequently signaling to them and de-

granulating, releasing specific proteins into the environment based on the stimulus received. This section will cover the basic structure of platelets and how they function.

1.3.1 Glycoproteins

Platelet glycoproteins (GPs) are located both on the cell surface and within specific platelet granules. Glycoproteins are proteins with covalently attached carbohydrate groups and are activated by the binding of specific ligands, a process that results in activation of specific pathway(s) within the platelet (Figure 1-4). Glycoproteins are also involved in inside-out signaling, where pathway activation and platelet activation is not just dependent on ligand binding, but also on internal cell signaling that induces changes in GP expression on the cell surface. Many of these GPs can be utilized as cell surface markers for the positive identification of platelets and their activation in imaging and flow cytometry (Table 1-1). In this section, we will review the main platelet GPs, including their structure, binding partners, and associated signaling pathways.

1.3.1.1 Glycoprotein Ib-IX-V

Glycoprotein complex Ib-IX-V is composed of GPIbα, GPIbβ, GPIX, and GPV. GPIbα is the ligand-binding subunit and is disulfide bonded to GPIbβ, and non-covalently associated with GPIX and GPV. (Andrews et al., 2003b, Modderman et al., 1992, Clemetson and Clemetson, 1995) GPIbα is shed from circulating platelets, with shedding and plasma concentrations increasing upon platelet activation. GPIb-IX-V plays a central role in hemostasis, with many human and animal studies demonstrating abnormalities in hemostatic function upon the absence or blocking of this complex or one of its' subunits. (Ozaki et al., 2005, Li and Emsley, 2013) Bernard Soulier Syndrome (BSS) is an inherited platelet disorder where there is a deficiency or dysfunctional GPIbα subunit; affected patients exhibit mild to severe bleeding phenotypes, along with macrothrombocytopenia. (Lopez et al., 1998) Animal models have demonstrated that vWF-GPIb axis plays an important role in the formation of blood clots, arterial thrombosis, ischemic stroke, and venous thromboembolism. (Denorme and De Meyer, 2016, Takahashi et al., 2009, Bergmeier et al., 2006, Momi et al., 2013, Berndt and Andrews, 2013) Several non-hemostatic roles of GPIb-IX-V have also been identified, including the support of cancer metastasis, positive regulation in systemic inflammation, the binding of Mac-1, playing a role in

macrophage transmigration, and interaction with bacterial components. (Suter et al., 2001, Corken et al., 2014, Jain et al., 2007, Berndt et al., 2001, Berndt and Andrews, 2013)

The primary binding ligand for GPIb-IX-V is von Willebrand Factor (vWF). Soluble vWF is always present in the plasma and is also secreted from a number of cells, including platelets and endothelial cells. (Berndt and Andrews, 2013, Clemetson and Clemetson, 1995) Recently, a mechano-sensitive mechanism by which GPIb-IX-V is activated by bound vWF was elucidated when investigators demonstrated that pulling of the vWF A1 domain that is engaged to GPIb-IX induces unfolding of an unidentified structural domain in GPIbα. (Zhang et al., 2015) Other binding ligands to GPIbα includes P-selectin (CD62P), which is expressed and shed by activated platelets and endothelial cells, and $\alpha_M\beta_2$, which is expressed on leukocytes. (Bergmeier et al., 2006) (Berndt and Andrews, 2013) GPV has also been documented to bind to collagen. (Moog et al., 2001, Berndt and Andrews, 2013) A number of coagulation factors from both the intrinsic and extrinsic pathway can bind to GPIbα, including high molecular weight kininogen, FXII, FXI, and thrombin. (Berndt and Andrews, 2013)

There are other GPs that are involved in GPIb-IX-V binding and activation. The collagen receptor, GPVI, interacts with GPIbα as an accessory protein to a noncovalent complex between GPVI and Fc receptor γ chain (FcRγ). (Jarvis et al., 2002, Nieswandt and Watson, 2003) (Berndt and Andrews, 2013) Calmodulin also binds to separate regions of the GPIb-IX-V complex and the dissociation of calmodulin from this complex regulates the ectodomain shedding of GPIbα of GPV by a disintegrin and metalloproteinase domain-containing protein 10/17 (ADAM10/17). (Gardiner et al., 2007, Mo et al., 2010, Andrews et al., 2001, Berndt and Andrews, 2013) Thrombin, ADAM10, and ADAM17 all cleave at GPV, and therefore, absence of GPV enhances platelet activation to thrombin via GPIbα. (Berndt and Andrews, 2013)

Once GPIb-IX-V is bound and activated, it results in an intracellular signaling cascade, which activates sarcome (Src) kinase, spleen tyrosine kinase (Syk), Lymphocyte cytosolic protein 2 (SLP-76), phosphoinositide 3(PI3) kinase, Bruton's tyrosine kinase (Btk), protein kinase C, and phospholipase Cγ. There is an increase in cytosolic Ca^{++}, activation of $\alpha_{IIb}\beta_3$ as well as dense and α-granule release. (Berndt and Andrews, 2013) Calmodulin-bound GPIbβ can also bind TNF

receptor-associated factor 4 (TRAF4), which enhances platelet activation via the assembly of NADPH oxidase and ROS. (Arthur et al., 2011)(Andrews et al., 2001) (Berndt and Andrews, 2013) GPIb-IX-V also interacts with actin-binding protein filamin-A, which helps regulate membrane stability under high shear conditions. (Andrews and Fox, 1992, Nakamura et al., 2006, Li and Emsley, 2013, Berndt and Andrews, 2013) Newer research suggests that the interaction between GPIbα and filamin-A is involved in force transmission, while the interaction between GPIbα and the A1 domain of vWF mediates the force transmission; this bond-transmitting force allows a strengthening of the bond and helps explain how platelets attach to sites of vascular injury via internal forces produced by cytoskeletal tension. (Feghhi et al., 2016)

1.3.1.2 Glycoprotein GPIIb-IIIa

Platelet integrin $\alpha_{IIb}\beta_3$ (GPIIb-IIIa) plays an integral role in platelet aggregation, hemostasis, and thrombosis. Two glycoproteins, GPIIb and GPIIIa, form a non-covalent heterodimer, which represents the most abundant protein on the platelet surface. (Coller and Shattil, 2008, Calvete, 1995, Jennings and Phillips, 1982, Berndt and Andrews, 2013, Kunicki et al., 1981) Integrin $\alpha_{IIb}\beta_3$ is also located in the membrane of α-granules, and can be translocated to the surface of the cell following platelet activation. $\alpha_{IIb}\beta_3$ is reported to default into a bent (closed) form, which, upon the appropriate stimulus, can open to an extended closed form and an extended open form (the active state). (Suzuki et al., 1994, Wencel-Drake et al., 1986, Berndt and Andrews, 2013) The transition from one conformation to another reveals different epitopes. The exact mechanism and utility of the different conformations of $\alpha_{IIb}\beta_3$ is still heavily researched and under debate, however, antibodies have been developed to target conformation-specific $\alpha_{IIb}\beta_3$ for flow cytometric evaluation. (Berndt and Andrews, 2013)

Integrin $\alpha_{IIb}\beta_3$ plays a critical role in hemostasis. A variety of agonists, including collagen, ADP, and thrombin, all stimulate platelets and activate signaling cascades that cause $\alpha_{IIb}\beta_3$ to open into its' activated form. When $\alpha_{IIb}\beta_3$ is in its open form, it has a very high affinity for a variety of platelet aggregation components, including fibrinogen, fibronectin, and vWF. (Reininger, 2008, Marguerie et al., 1979, Berndt and Andrews, 2013) Following agonist stimulation, there can be activation of phospholipase Cβ by Ca^{2+}, which then results in downstream activation of protein kinase C, calcium- and diacyglycerol-regulated guanine factor 1, phophoinositide 3-kinase, and

ultimately, Ras-related protein 1B (RAP1B). RAP1 binds to talin, forming a complex that targets and activates $\alpha_{IIb}\beta_3$. (Knezevic et al., 1996, Crittenden et al., 2004, Bergmeier and Stefanini, 2009, Cifuni et al., 2008)(Stefanini et al., 2009, Berndt and Andrews, 2013) *In vitro* and animal models demonstrate that absence of talin causes severe defects in platelet aggregation, as well as agonist-stimulated $\alpha_{IIb}\beta_3$ activation and frequent pathologic bleeding. However, whereas agonist stimulation of $\alpha_{IIb}\beta_3$-deficient platelets can still result in talin re-distribution, demonstrating that, although talin is imperative for platelet hemostatic function, talin it is not dependent on $\alpha_{IIb}\beta_3$. (Bertagnolli et al., 1993, Escolar et al., 1995, Petrich et al., 2007, Watanabe et al., 2008, Nieswandt et al., 2007) The kindlin family also plays a role in the activation of $\alpha_{IIb}\beta_3$, both directly and as well as indirectly, via talin. Some studies have shown that kindlins increase multivalent ligand binding via the promotion of talin-activated integrin clustering, while other show that Kindlin-3 is an essential element for integrin activation. (Ye et al., 2013, Moser et al., 2008, Shattil et al., 2010)

Once $\alpha_{IIb}\beta_3$ is ligand bound, there is further conformational change of the integrin complex and subsequent intracellular signaling is activated; at this time, granule secretion, platelet activation, platelet adhesion, platelet spreading, and clot retraction occur. The conformational change and $\alpha_{IIb}\beta_3$ clustering at this time allow transmission of signals from outside-in. One of the primary outside-in signaling cascades involves Src family kinases (SFK), where c-Src is bound to the distal β subunit. (Wu et al., 2015, Arias-Salgado et al., 2003, Senis et al., 2014, Obergfell et al., 2002) SFK phosphorylates the Tyr773 and Tyr785 residues, which protects it from cleavage by proteases, resulting in enhancement of ligand-binding events. Mice with Tyr747 and Tyr759 mutations (the equivalent to humanTyr773 and Tyr785 mutations) show increased tail bleeding times and impaired clot retraction, demonstrating the importance of these signaling cascades. (Phillips et al., 2001, Ablooglu et al., 2009, Law et al., 1999, Ye and Ginsberg, 2013) Src and Syk work together to phosphorylate and modulate p190 Rho GTPase activating protein, SLP-76, Adhesion and Degranulating Adapter Protein (ADAP), and Vav, resulting in further platelet activation and clot retraction. (Arthur et al., 2000, Ren et al., 1999, Flevaris et al., 2007, Obergfell et al., 2002, Miranti et al., 1998) More recently, Syk and Src have been identified shown to work together in the regulation of C-type lectin receptor 2 (CLEC-2)-mediated platelet adhesion to lymphatic endothelial cells. (Huveneers and Danen, 2009, Pollitt et al., 2014, Ye and

Ginsberg, 2013) Tying in talins with Src, ADAP, a hematopoietic-restricted adapter protein that promotes integrin activation, also promotes platelet activation and irreversible fibrinogen binding to platelet $\alpha_{IIb}\beta_3$ via an interaction with talin and kindlin-3. (Kasirer-Friede et al., 2014)

Due to the inside-out and outside-in signaling that plays a role in $\alpha_{IIb}\beta_3$ activity, there are multiple mutations that can result in hereditary bleeding disorders. Glanzmann thrombosthenia (GT) is a disease associated with $\alpha_{IIb}\beta_3$ deficiency or mutations, which results in bleeding disorders. (Lee et al., 1981, Nurden et al., 1987, Phillips and Agin, 1977) In some cases of GT, mutations affect the post-translational processing and transport of $\alpha_{IIb}\beta_3$, resulting in decreased surface expression or decreased binding affinity for ligands. Mutations in kindlin-3, a protein that works with talin to regulate integrin activity, can also result in bleeding disorders. (McDowall et al., 2010, Moser et al., 2008) People with leukocyte adhesion deficiency syndrome (LADIII) have kindlin-3 mutations, and subsequent defective platelet aggregation and clot retraction. (Manevich-Mendelson et al., 2009, Meller et al., 2012) (Ye and Ginsberg, 2013)

1.3.1.3 Glycoprotein GPIa/IIa

Integrins are heterodimers composed of an α and β subunit (Hynes, 2002, Barczyk et al., 2010). There are 12 known α and 8 known β subunits, allowing for 24 possible pairings. (Barczyk et al., 2010, Takada et al., 2007) Integrin $\alpha_2\beta_1$, (VLA-2; ECMR-II; GPIa/IIa) is the only known platelet integrin receptor for collagen, although it must be activated in order to reveal its high affinity binding site; for collagen, with the resting state showing shows almost no affinity for collagen. (Depraetere et al., 1997, Staatz et al., 1990, Tuckwell et al., 1995) Other integrins, such as $\alpha_5\beta_1$, $\alpha_6\beta_1$, and $\alpha_{IIb}\beta_3$ bind fibronectin, vitronectin, laminin, and/or fibrinogen. GPIa/IIa has also been found to be present on many cell types, including lymphocytes, mesenchymal cells, fibroblasts, and cancer cells. (Zwolanek et al., 2015, Pischel et al., 1988, Sottnik et al., 2013, Li et al., 2013b, Watson et al., 2013)

1.3.1.4 Glycoprotein GPVI

Platelets have two collagen receptors, $\alpha2\beta_1$ and GPVI. $\alpha2\beta_1$ has a high affinity for collagen but requires prior activation for expression, whereas GPVI has a lower binding affinity for collagen. Platelet receptor GPVI is thought to work synergistically with $\alpha2\beta_1$; with $\alpha2\beta_1$ supporting

adhesion, and GPVI supporting activation. (Nieswandt and Watson, 2003) GPVI, which is encoded in the leukocyte receptor complex on chromosome 19, is composed of an N- and C-terminal extracellular Ig domain and is a member of the immunoglobulin superfamily. (Clemetson et al., 1999, Jandrot-Perrus et al., 2000) A peptide strand links the extracellular domains and a glycosylated stem connects to a transmembrane and cytoplasmic domain that can bind calmodulin. The transmembrane domain has an arginine residue salt bridge, which supports its association with Fcrγlla. Co-expression is required for cell-surface expression of GPVI on platelets. (Moroi and Jung, 2004, Watson et al., 2013)

The platelet GPVI receptor interacts with multiple other factors, resulting in platelet activation. The Fc receptor γ-chain, for instance, is associated with GPVI and is a critical component of the collagen signaling pathway within and activation of platelets. (Berlanga et al., 2002, Watson et al., 2013) GPVI is considered to be the major signaling receptor for collagen, while the key functional motif is an immunoreceptor tyrosine-based activation motif (ITAM) on the FcγRIIa chain. (Moroi and Jung, 2004, Gibbins et al., 1997, Tsuji et al., 1997, Watson et al., 2013) GPVI forms specific structure dimerization necessary for its' binging to collagen fibrils. (Jung et al., 2009) Studies have shown that GPVI mainly binds to collagen types that can form large collagen fibrils, such as collagen type III, resulting in the formation of large platelet aggregates during flow adhesion studies. (Jung et al., 2008)

Platelets control their responsiveness via receptor shedding; primarily mediated by two metalloproteinases, ADAM10 and ADAM17 (TACE). (Andrews et al., 2007, Gardiner et al., 2007, Bender et al., 2010, Watson et al., 2013) GPVI –FcγR expression is sufficient to confer both adhesion and signal processing of collagen. GPVI-mediated collagen response is proportional to density-dependent at the receptor level, with GVI being rapidly shed from the platelet surface following activation of both receptors, GPVI and FcγRIIa. (Chen et al., 2002) Anti-GPVI antibodies can induce receptor shedding, internalization, and transient thrombocytopenia in multiple mouse models, utilizing mechanisms that are independent of ADAM10/17 but regulated by intracellular cAMP. (Boylan et al., 2008, Bender et al., 2010, Newman, 2010, Nieswandt et al., 2001, Takayama et al., 2008) One new mechanism of platelet GPVI shedding is liver-mediated, in which the inhibitory Fc receptor, FcγRIIB, on mouse liver

sinusoid endothelial cells mediate antibody-induced GPVI trapping and shedding. (Berndt and Andrews, 2016)

Other ligands that bind to GPVI include, collagen-related peptide (CRP), which is thought to stimulate tyrosine phosphorylation in platelets, similar to collagen, laminin, a basement membrane component, and snake toxins. (Newman, 2006, Polanowska-Grabowska et al., 2003, Andrews et al., 2003a, Wijeyewickrema et al., 2007, Asazuma et al., 2001, Watson et al., 2013, Inoue et al., 2006) There are many different signaling mechanisms and regulatory proteins involved with the GPVI receptors that are still being explored, including Platelet endothelial cell adhesion molecule-1 (PECAM-1), Src homology region 2 domain-containing phosphatase-1 and -2 (SHP-1 and SHP-2), and others. (Moraes et al., 2010, Cicmil et al., 2002, Pasquet et al., 2000, Mazharian et al., 2013) (Watson et al., 2013)

1.3.2 Immunomodulatory receptors and antigens

Platelets have been increasingly recognized to play an active role in the immune system. They display a number of receptors on their cell surface for various cytokines and chemokines, and they also express immunoglobulins (FcγRI, II, III; FceRI, FcaRI/CD89). Platelets also exhibit non-self-infectious detection molecules, including Toll-like receptors (TLRs). In this section, we will review some basics about these cell surface molecules and their proposed roles through the platelet. A summary of some of these proinflammatory receptors and signaling molecules associated with platelets is summarized very nicely in a paper by Garraud, *et al.* (Garraud and Cognasse, 2010)

1.3.2.1 HLA antigens

Human leukocyte antigen (HLA) encodes for the major histocompatibility complexes (MHC). HLA (Class I) antigens play a function in major histocompatibility complex (MHC) events, presenting peptides from inside of the cell. Cosgrove *et al.*, reported that several anti-HLA monoclonal antibodies, including anti-beta 2 microglobulin antibody) selectively effects platelet function and can result in both platelet aggregation and release of 14C-seratonin. (Cosgrove et al., 1988) Additionally, anti-HLA antibodies also blocked the binding of platelets agonists, including collagen, adrenalin, and ADP. A possible association between GPIIb/IIIa and HLA

Class I antigens was also postulated. More recent studies have demonstrated that platelets express T cell co-stimulatory molecules, process and present antigens (Ag) using MHC class I molecules, and directly activate naïve T cells in a platelet MHC class I-dependent manner. (Chapman et al., 2012) Chapman *et al.*, utilized a mouse model of cerebral malaria to demonstrate that platelets are capable of presenting pathogen-derived Ag to promote T cell responses and that platelets can be used in a cell-based vaccine model to induce protective immunity. (Chapman et al., 2012)

More recently, MHC class-II molecules, which allow antigen presentation to other immune cells, were identified as being expressed on human megakaryocytes. (Finkielsztein et al., 2015) Megakaryocyte progenitors, but not platelets, produced *in vitro* from mobilized peripheral blood hematopoietic stem and progenitor cells of healthy subjects were found to function as professional antigen presenting cells (APCs). (Finkielsztein et al., 2015) The presence and role of MHCs on both platelets and their progenitors is still being explored and will likely have a major impact on the understanding of the role of the platelet within the immune system.

1.3.2.2 Fc Receptors (FcγRIIa)

The Fc receptor (FcR) is a membrane receptor for immune complexes and immunoglobulin (Ig) aggregates that is expressed on many cells types, including platelets, which express IgG Fc receptors (FcγRIIa). (Rosenfeld et al., 1985, Moore and Nachman, 1981, Shido et al., 1995) FcγRIIa mediates the activation of platelets exposed to immune complexes, Ig-opsonized bacteria, or autoantibodies targeting specific platelet membrane proteins. (Lopez, 2013) The Fc receptor plays a role in platelet activation through the presence of an immunoreceptor tyrosine-based activation motif (ITAM) in its cytoplasmic domain, which phosphorylates when ligands bind to $\alpha_{IIb}\beta_3$. (Boylan et al., 2008) Zhi H, *et al.,* demonstrated that platelets from mice expressing human FcγRIIa spread better on fibrinogen, retracted clots better, formed larger thrombi, displayed increased fibrin deposition within injured vessels, and had increased Syk phosphorylation. (Zhi et al., 2013)

The Fc receptor for IgG, FcγRIIa, is expressed on both macrophages and platelets and may play an important role in immune-mediated thrombocytopenia. A study in mice has demonstrated that

the human Fc receptor FcγRIIa plays a significant role in the *in vivo* role in the immune clearance of platelets. (McKenzie et al., 1999) It has also been previously reported that circulating immune complexes (CIC) inhibit fibrinogen binding to platelet GPIIb/IIIa, and FcγRIIs were demonstrated to have a close relationship to GPIIb/IIIa, resulting in transmission of an 'outside-in' signal when bound to ligands such as fibrinogen and vWF. (Shido et al., 1995, Boylan et al., 2008) Additionally, GP Ib-IX-V has been shown to be in close physical proximity to the population of FcγRIIa that mediates platelet activation through circulating immune complexes arising from infection with two strains of viridans group streptococci. (Sullam et al., 1998, Shrimpton et al., 2002)

1.3.2.3 CD40L (CD40L/CD154)

CD40L (CD154) is a type II transmembrane protein belonging to the Tumor Necrosis Factor (TNF) superfamily and is a dominant platelet-secreted factor. (Aloui et al., 2014) It is expressed on the cell surface of a variety of cells and plays a role in both the adaptive and innate immune response. (Grewal and Flavell, 1998, Elgueta et al., 2009) In platelets, CD40L is found in the α-granules within the platelet cytoplasm. (Charafeddine et al., 2012) RNA-seq experiments have shown that CD40L mRNA is not present in platelets, suggesting that the protein is acquired only from the parent megakaryocyte. (Gnatenko et al., 2003, Rowley et al., 2011, Simon et al., 2014, Nagalla et al., 2011) Interestingly, platelets do not maintain CD40L on their surfaces for long periods of time, rather, the protein is cleaved and released in soluble form, and it may also be carried in their microparticles. (Leroyer et al., 2008)

The main receptor for CD40L is CD40, which is constitutively expressed by platelets, antigen presenting cells (APCs), neutrophils, endothelial cells, and T-cells. (Aloui et al., 2014) Platelets express CD40 on their cell surface, regardless of activation status. (Henn et al., 1998, Inwald et al., 2003) It is currently hypothesized that the soluble form acts as a competitive inhibitor for the membranous form. (Esposito et al., 2012) CD40L can also bind to GPIIb/IIIa, $\alpha_5\beta_1$ (CD49e/CD29), and Mac-1 (Complement Receptor 3, CR3, CD11b/CD18). (Aloui et al., 2014) Additionally, there may be an essential role for these integrins, as patients with Glanzmann thrombocytopenia fail to release sCD40L upon platelet activation. (Furman et al., 2004)

The CD40-40L system functions in an autocrine, paracrine, and endocrine fashion and is associated with both proinflammatory and prothrombotic effects. (Aloui et al., 2014) CD40L may be cleaved into the soluble form (sCD40L) that has cytokine-like activity, such as activating the classical and alternative NF-kB pathways. (Chen et al., 2006) Platelets are the main source for sCD40L in the circulation. (Danese et al., 2003, Viallard et al., 2002) sCD40L is a master inflammatory cytokine involved in mediating the inflammation in cardiovascular disease, such as the production of atheroma plaques, as well as adverse transfusion events, including transfusion related acute lung injury (TRALI). (Engelmann and Massberg, 2013, Aloui et al., 2014) sCD40L also induces platelet release of reactive oxygen species (ROS) and nitrogen species through activation of AKT and MAPK signaling pathways. (Chakrabarti et al., 2005, Freedman, 2008) The interaction between CD40-CD40L has also been shown to play a role in the production of auto-antibodies in a number of autoimmune diseases, including systemic lupus erythematous (SLE) and rheumatoid arthritis (RE). (Toubi and Shoenfeld, 2004, Zhang et al., 2013)

When evaluating the autocrine effects of sCD40L on platelets themselves, two receptor interactions are important to consider: CD40 and αIIbβ3. (Aloui et al., 2014) When sCD40L activates platelet via CD40, this involves a CD40-dependent TRAF2/RACi/ps8 MAPK signaling pathway that concurrently triggers the NF-kB pathway. (Hachem et al., 2012, Yacoub et al., 2010) When sCD40L binds to $\alpha_{IIb}\beta_3$, thrombus formation is enhanced via induction of platelet spreading. (Prasad 2003; Andre P 2002) It has also been identified that soluble CD14 (sCD14) from plasma contributes to lipopolysaccharide (LPS) and toll-like receptor 4 (TLR4) signaling in platelets to allow for significant release of sCD40L. (Damien et al., 2015) LPS binding protein (LBP) and CD14 are considered obligate partners for TLR4 ligation to LPS; however, platelets do not express CD14, therefore sCD14 in the plasma environment is essential. In eukaryotic cells, LPS is transferred from CD14 to a complex between TLR4 and MD2. (Damien et al., 2015)

1.3.2.5 Toll-like Receptors (TLRs)

The Pathogen Recognition Receptor (PRR), of which Toll-like receptors are a part, are involved in the innate immune system and are expressed on cell surfaces and secreted into extracellular

compartments, resulting in opsonization, blood clotting, phagocytosis, and activation of complement and proinflammatory cascades. (Garraud and Cognasse, 2010, Janeway and Medzhitov, 2002) Studies have identified that platelets express mRNA for all 10 TLR transcripts and that all transcripts are co-expressed. (Koupenova et al., 2015) Studies have also confirmed the presence of a functional TLR/MyD88 pathway in platelets, similar to that in nucleated eukaryotic cells. (Garraud and Cognasse, 2010) The TLR transduction pathway is composed of a number of receptors, including the Toll/Interleukin-1 receptor (TIR), the Myeloid differentiation factor-88 (MyD-88), amongst many others. (Garraud and Cognasse, 2010) Following ligand binding, TLRs dimerize and recruit MyD88 through their TIR domains, resulting in the expression of multiple inflammatory signals, such as NF-kB and interferon-regulatory factors (IRFs). (Garraud and Cognasse, 2010, Moynagh, 2005, Pasare and Medzhitov, 2004)(Akira and Takeda, 2004) Soluble CD14 (sCD14) in plasma is also required for optimal response to LPS stimulation via TLR4 signaling. (Damien et al., 2015) Differences in expression patterns have been noted between men and women, with women having more abundant transcripts and distinct associations with cardiovascular risk and inflammatory biomarkers. (Koupenova et al., 2015)

The role of TLRs in the platelet is still under active investigation. Typically, TLR activation in other cell types results in the release of immunomodulatory factors and the sequestration of pathogens. Zhang G, *et al.*, demonstrated that LPS simulates platelet secretion and aggregation via TLR4/MyD88 and cGMP/PKG-dependent pathways. (Zhang et al., 2009) They have also shown that the effect of LPS on platelet aggregation is abolished by anti-TLR4 blocking antibody and in MyD88-deficient mice. TLR2 has also been studied and has been documented to activate PI3K, Akt, ERK1.2, and p38, and it has also been shown to promote platelet-dependent thrombosis. (Blair and Flaumenhaft, 2009) Experiments in mice have demonstrated that platelet-derived TLR-4 is sufficient to promote microvascular thrombosis in endotoxemia. (Stark et al., 2012) A TLR4-dependent mechanism has also been reported in LPS-induced thrombocytopenia, TNF-α production, and neutrophil-dependent pulmonary sequestration in mice. (Andonegui et al., 2005, Aslam et al., 2006) Recent experiments have also demonstrated that bacteria, such as *Streptococcus (S.) pneumonia*, can activate platelets through a TLR-independent mechanism. (de Stoppelaar et al., 2016)

1.3.3 Protease-activated receptors (PARs)

Protease-activated receptors (PARs) are G protein-coupled receptors (GPCRs) that are highly expressed throughout the body, with two forms expressed on platelets: PAR1 and PAR4. It is important to note that there are a four PARs (PAR1-4), and that they are highly expressed in a number of tissues throughout the body, including immune and epithelial cells, neurons, and vascular cells. (Alexander et al., 2008, Coughlin, 2005)(Russo et al., 2009) These receptors are activated via the binding of the PAR-activation peptide (PAR-AP), collagen, and serine protease, thrombin (Factor II). Upon activation, proteolysis cleaves a part of their extracellular domain, which results in an intracellular signaling cascade. (Soh et al., 2010)

PAR receptors play a major role in thrombin signaling, with cleavage of its amino-terminal extracellular domain, exposing a new N terminus that binds intramoleculary to the body of the receptor, resulting in transmembrane signaling. (Vu et al., 1991, Rasmussen et al., 1991) While PAR1, 3 and 4 are all activated by thrombin, only PAR1 and 4 are expressed on human platelets, while only PAR 1 and 3 are expressed on murine platelets. (Coughlin, 2000) In human platelets, collagen and thrombin binding, at different sites, results in matrix metalloprotease-1 (MMP-1) activation, resulting in the cleavage and activation of PAR1. (Trivedi et al., 2009, Blackburn and Brinckerhoff, 2008) Other metalloproteases, including ADAM17, can cleave PAR1 and render the receptor unresponsive to thrombin, whereas plasmin, cleaves PAR1 and can either activate or render it unresponsive as well. (Ludeman et al., 2004, Kuliopulos et al., 1999)

PAR 1 and 4 have also been demonstrated to regulate Factor V (FV) association with the platelet surface. PAR4 stimulation was found to result in a faster and more robust thrombin generation, compared to PAR1 stimulation, which is attributed to more efficient FV release and microparticle production upon PAR4 stimulation. (Duvernay et al., 2013) A recent study by Carrim N, *et al.*, demonstrated that, when activated, GPIbα and PAR4 work together, resulting in thrombin-induced reactive oxygen species (ROS) production. (Carrim et al., 2015) PAR1 can also have an effect on sphingosine 1-phosphate (SIP) receptor and platelet-activating factor receptor (PAFR). (Soh et al., 2010) Thrombin binding and PAR4 activation has also been shown to play a role in cermide-NF-kB signaling in platelet activation. (Chen et al., 2013) PAR3 binds

to thrombin, but instead of resulting in platelet activation, localizes thrombin for the dimerization to PAR1 and subsequent PAR1 activation. (Nakanishi-Matsui et al., 2000)

While PAR4 has traditionally been thought to play a smaller role than PAR1. Racial differences in the expression and functionality of PAR4 have recently been elucidated, with healthy black people demonstrating significantly higher thrombin-induced platelet aggregation and calcium mobilization. This result has been attributed to differentially expressed RNAs, including phosphatidylcholine transfer protein (PC-TP). (Edelstein et al., 2013) Edelstein LC, *et al.*, identified that a single nucleotide polymorphism (SNP), rs773902, determines whether residue 120 in transmembrane domain 2 is an alanine (Ala) or a threonine (Thr), with the Thr120 residue being more prominent in black subjects versus white subjects, and resulting in higher PAR4-induced platelet aggregation and calcium mobilization. (Edelstein et al., 2014) Although there are very limited studies evaluating platelet and receptor function in different races and ethnicities, these studies demonstrate that it is a factor that should be taken into consideration during the development and clinical trials of new anti-platelet therapies.

1.3.4 Adrenergic receptors

Adrenergic receptors (adrenoreceptors) belong to the family of receptors coupled to GTP-binding proteins and come in two subtypes: alpha (encompassing alpha-1, A1; alpha-2, A2) and beta (encompassing beta-1, B1; beta-2, B2; beta-3, B3). The alpha-2 and beta-2 adrenergic receptors, which have been identified on platelets, are coupled to adenyl cyclase via Gi or Gs regulatory proteins. (Strosberg, 1993) Alpha-2 adrenoreceptors, which are present on platelets, mediate the effects of epinephrine and norepinephrine, and receptor agonists are commonly administered for the treatment of hypertension, pain and panic disorders, as well as other conditions. (Hein, 2001, Giovannitti et al., 2015) Catecholamine stimulation, specifically dopamine (but notably not adrenaline) stimulation, resulted in a modification of platelet behavior in a rabbit model; thrombin-induced platelet accumulation was potentiated by dopamine at low concentrations and is inhibited at high concentrations. (Emerson et al., 1999) A rabbit model of endotoxemia-associated disseminated intravascular coagulation (DIC) investigated the effects of catecholamine administration, and found that catecholamines acting on alpha-adrenoreceptors resulted in the expected effect of glomerular capillary thrombosis, while beta-adrenergic

stimulation counterbalanced the alpha-adrenergic effects that occur during endotoxemia prevented this phenomenon. (Latour and Leger-Gauthier, 1987) Beta-adrenoreceptors, on the other hand, are most commonly known for their overall regulation of cardiac function. (Wachter and Gilbert, 2012) Binding of this receptor results in intracellular signaling through cyclic adenosine monophosphate and protein kinase A. (Johnson, 2006, Kerry and Scrutton, 1983, Klysner et al., 1984, Winther et al., 1985) These receptors have also been identified and characterized as beta 2-subtype (B2) receptors on human platelets, and binding of the beta-2 adrenergic receptor is widely distributed in tissues of the respiratory tract. This receptor has long been documented to play a role in platelet aggregation, with inhibition of this aggregation occurring secondary to the addition of isoprenaline, and or other beta-agonists. (Kerry and Scrutton, 1983, Klysner et al., 1984, Winther et al., 1985, Winther and Trap-Jensen, 1988) In a rat model, catecholamines were shown to counteract a beta-adrenoreceptor-mediated platelet inhibition via the alpha 2- adrenoreceptor site. (Koutouzov et al., 1985)

Changes in alpha- and beta- adrenoreceptors on platelets during disease are currently under investigation, with several connections having been made between the levels of expressions of these receptors during common medical conditions. Patients with anorexia nervosa have been shown to express changes in adrenergic platelet receptor concentration and in [45Ca2+] uptake. (Gill et al., 1992) Adrenoreceptor-linked [45Ca2+] uptake studies in platelets from rat models suggest that diabetic conditions may be associated with an increase in alpha-adrenergic and decrease in beta-adrenergic receptors on platelets, although the influence of adrenoreceptor stimulation on platelet aggregation is not influenced by diabetes. (Gill et al., 1994, Austin et al., 1995) A systemic review and meta-analysis evaluating the effect of beta-blockers on platelet aggregation by Bonten TN, et al., (2014) concluded that beta-blockers do significantly reduce platelet aggregation and that non-selective lipophilic beta-blockers seem to have more pronounced effects. (Bonten et al., 2014) Although less commonly investigated, studies on platelet alpha 2-adrenergic receptor activity have shown them to be dynamic, and that they may then contribute to increased platelet reactivity reported in patients with stable coronary artery disease following administration of dual antiplatelet therapy, suggesting other possible therapeutic targets; this observation may provide opportunities for novel therapeutic targets. (Beres et al., 2008)

1.3.5 Prostanoids

Prostanoids, including prostaglandins (PGs) and thromboxane A_2 (TXA_2), are lipid hormones that act on GPCRs near the site of their formation. They are formed via the action of the cyclooxygenase (COX) pathways and prostanoid synthases (Figure 1-5). (Bos et al., 2004, Smyth et al., 2009) TXA_2 is synthesized and released via the COX-1 pathway in activated platelets, resulting in amplification of activity and further platelet activation and recruitment, as well as vasoconstriction, proliferation, and mitogenesis at the site of thrombus and inflammation. (Smith, 1980, Matsuoka and Narumiya, 2008, Grosser and FitzGerald, 2013) Arachidonic acid is metabolized by three groups of enzymes, with the COX enzyme being expressed on platelets and its' precursors. There are two isoforms of COX, COX-1 and COX-2, both of which both convert arachidonic acid to prostaglandin H2 (PGH_2). While COX-1 is the only isoform present in mature platelets, COX-2 is expressed in both megakaryocytes and prematurely released platelets. (Rao et al., 1985, Reiter et al., 2001, Patrignani et al., 1999, Zetterberg et al., 2003, Tanaka et al., 2004, Grosser and FitzGerald, 2013)

Platelet agonism and subsequent activation results in generation of TXA_2 by Group (G) IVA phospholipase (PL) A_2 along with a calcium signal within the platelet cytosol. (Ballou et al., 1986, Bartoli et al., 1994) This pathway can also be activated by adhesion of vWF to GPIb-V-IX on the platelets, binding of $\alpha_{IIb}\beta_3$, as well as vascular wall cells PLA_2 isoforms resulting in release of arachidonic acid for prostanoid formation. (Prevost et al., 2009, Liu et al., 2005, Grosser and FitzGerald, 2013) Prostanoids have a short half-life and are rapidly hydrolyzed to the stable, biologically inactive compound, TXB_2, in biological fluids; therefore, TXA_2 is likely not present in the circulation, but instead exerts action upon GPCRs on their target cells. (Schuette et al., 1984, Dubin et al., 1982, Grosser and FitzGerald, 2013) TXA_2-induced platelet activation is likely restricted to the site of vascular injury and platelet activation. Modulation of this signal can occur in many ways, including heterodimerization with other GPCRs, as well as with inhibitors such as PGI_2, nitric oxide, flavonoids, dietary vitamin E, and lipoproteins. (Beitz et al., 1990, Karpen et al., 1981, Fitzgerald et al., 1988, Guerrero et al., 2007, Roberts et al., 2008, Wilson et al., 2004, Grosser et al., 2006)

Patients deficient in the TXA_2 pathway, who display mild bleeding disorders, illustrate the importance of prostanoids in hemostasis. (Matijevic-Aleksic et al., 1996, Dube et al., 2001, Defreyn et al., 1981, Remuzzi et al., 1983, Grosser and FitzGerald, 2013) Additionally, a number of COX inhibitor drugs also suppress this pathway, including aspirin; some are administered to decrease platelet contribution to thrombus formation, although these medications can also lead to bleeding diatheses such as gastrointestinal and intracranial hemorrhage. (Warner et al., 2011, Schafer, 1995, Schafer, 1999, Grosser and FitzGerald, 2013) Prostacyclin (PGI_2) is the major platelet inhibitory prostanoid, which results in vasodilation and also has anti-mitogenic and anti-arthrogenic properties. PGI_2 functions as a platelet inhibitor by restraining the effect of collagen, thrombin, or TXA_2 and raising cAMP within the platelet. (Ehrman and Jaffe, 1980, Hawiger et al., 1980, Graber and Hawiger, 1982, Grosser and FitzGerald, 2013, FitzGerald et al., 2000) Non-steroidal anti-inflammatory drugs (NSAIDs) can preferentially target the COX-2 pathway. Since inhibition of the COX-2 pathway results in reduced formation of PGI_2, these compounds result in a demonstrated prothrombotic state, which may be associated with adverse events, including myocardial infarction, stroke, and venous thromboembolism. (Ungprasert et al., 2015, Howes, 2007, Alcorn and Madhok, 2015, Grosser et al., 2010)

Other types of prostanoid synthesis that the platelet is involved in are PGD_2, which is produced via platelet COX, plasma PGD synthase, and PGE_2. Increased concentration of PGE_2 in the circulation may inhibit platelet function, while lower concentrations may activate platelets. (Smith, 1981, Cooper and Ahern, 1979, Grosser and FitzGerald, 2013) Furthermore, COX-2 inhibitors, although thought to have no effect on platelet function and expression of aggregation markers, can stimulate the release of TXB_2 from activated platelets. It is thought that the combined decrease in vasodilatory PGE_2 and PGI_2 together with increased TXA_2 may contribute to COX-2 inhibitor pro-aggregation effects. (Graff et al., 2007) Finally, it has also been shown that immature, reticulated platelets have uninhibited COX-1 and -2, even in the presence of the COX-1 inhibitor aspirin, indicating aspirin resistance. (Guthikonda et al., 2007)

A close look at the prostanoid pathway within platelets also highlights an important possible role for white blood cells. Aspirin has been shown to have an inhibitory effect on the formation of platelet-neutrophil complexes (PNCs), and the formation of PNCs is an important part of platelet

activation and the immune system. (Lopez-Farre et al., 1995) With respect to PNC formation and its role in the arachidonic acid pathway, it appears as though there is platelet-mediated regulation of neutrophil function that is still under study. Platelets support the synthesis of reactive arachidonic acid metabolites, which modulate oxygen radical production in neutrophils. (Herbertsson and Bengtsson, 2001) Upon stimulation, platelet-derived arachidonate can serve as a precursor for neutrophil-derived eicosinoids (including leukotriene B4 (LTB4) and 5-Hydroxyeicosatetraenoic acid (5-HETE)), platelet-derived product 12-HETE (which can be metabolized to DHETE), and lipid mediators, including the anti-inflammatory lipoxins (LXs). (Marcus et al., 1984, Antoine et al., 1992) Recent research has shown a contradictory role for the PNC, where platelets may inhibit the neutrophil 5-lipoxygenase activities at the integrin level and may result in decreased production of LTB4 during inflammation. (Chabannes et al., 2003) This cell-cell interaction suggests an important role for the PNC in the formation of thrombi and in inflammation.

1.3.6 P2 Receptors

Prostanoids also interact with a very important class of platelet receptors: P2Y1 and P2Y12. These receptors bind to adenosine 5'-diphosphate (ADP), which is important for thrombosis and hemostasis. (Leon et al., 1996, Gachet, 2001) ADP on its own is a weak platelet agonist and induces a reversible response. However, ADP is in very high stores within platelet dense granules, and is released upon platelet activation, playing the role of a secondary agonist, amplifying platelet aggregation at the site of vascular injury. (Hechler and Gachet, 2011) The P2Y1 receptor initiates activation and aggregation via mobilization of calcium stores, and the P2Y12 receptor is coupled to adenyl cyclase inhibition for ADP response. (Gachet, 2001, Gachet et al., 1995) (Dorsam and Kunapuli, 2004, Jagroop et al., 2003) The P2Y1 receptor also plays a role in collagen-induced platelet activation and shape change in the face of absent TXA2 formation. (Leon et al., 1999, Mangin et al., 2004)

Both the P2Y1 and thromboxane-prostanoid-α (TPα) initiate platelet activation through the phospholipase C-beta (PLCβ) pathway, with TXA_2 being produced during arachidonic acid metabolism and ADP being stored in the dense granule pool. (Jin et al., 1998, Nurden et al., 2003) The P2Y1 and TPα receptors on platelets are part of the GPCR family; they are part of a

major pool associated with the membranes of α-granules and the open canalicular system. (Nurden et al., 2003) While stimulation of the P2Y1 receptor can initiate platelet aggregation, it is P2Y12 receptor stimulation that results in completion of aggregation. (Hechler et al., 2005, Soulet et al., 2005, Savi et al., 1998) P2Y12 receptors have become a common drug target for platelet inhibition, including compounds such as clopidogrel and prasugrel. (Hechler et al., 1998) Stimulation of this receptor potentiates platelet secretion, independent of TXA_2 generation and aggregate formation, and it can mediate the stabilization for the platelet aggregation induced by thrombin or TXA_2. (Cattaneo et al., 1997, Cattaneo et al., 1990, Cattaneo et al., 2000) Both receptors also indirectly play a role in CD62P exposure and platelet-leukocyte aggregate formation, as well as the exposure of phosphatidylserine (PS) on the platelet surface. (Leon et al., 2004, Leon et al., 2001, Leon et al., 2003, Storey et al., 2000)

Another set type of P2 receptors on platelets are the ATP-gated P2X Receptor Cation Channel (P2X) receptors. There are seven P2X subunit isoforms that have been identified, with each subunit having two transmembrane domains, intracellular amino and carboxy termini, and a large extracellular ligand-binding loop. (Mahaut-Smith et al., 2011) P2X receptors are ligand-gated cation channels that are activated by adenosine triphosphate (ATP). (Hechler et al., 2005) P2X1 receptor stimulation results in a significant increase in intracellular calcium, a rapid and reversible platelet shape change, activation by collagen under shear stress, and low levels of $\alpha_{IIb}\beta_3$ activation. (Hechler et al., 2005, Hechler and Gachet, 2011, Mahaut-Smith et al., 2011) Although it is thought that all platelet contain functional P2X1 receptors, research has shown that only 40% of platelets alter their shape in saline, have a large increase in intracellular calcium, and/or are activated by maximal ATP concentrations, which is all thought to be secondary to desensitization *in vitro*.(Rolf and Mahaut-Smith, 2002) In addition to ATP, P2X1 receptors have other potential (albeit less potent) agonists which are commonly found in the circulation and specifically in platelet dense granules, including: diadenosine polyphosphates and adenosine polyphophoguanosines. (Mahaut-Smith et al., 2011) In reality, most of these receptors and agonists likely work together to result in optimal platelet function; for example, there is amplification of ADP-induced P2Y1 receptor activation and platelet aggregation via the calcium influx through the P2X1 receptor.

1.3.7 Granules

Platelets play a variety of roles within the body, including hemostasis, inflammation, wound healing, atherosclerosis, and tumor angiogenesis. A key contributing factor to these activities are platelet granules, which are released upon platelet activation. Upon encountering vascular damage, or a variety of other stimuli, platelet surface receptors bind to agonists, triggering an intracellular signaling cascade and resulting in an increase in intracellular calcium and activation of several GTP-binding proteins and protein kinases. (Blockmans et al., 1995, Plow and Ginsberg, 1995) Platelet granules are then centralized by cytoskeleton rearrangement, fuse with one another, and empty into the open canalicular system, resulting in the release of their granule contents. (Blockmans et al., 1995, Geanacopoulos et al., 1993, Greenberg-Sepersky and Simons, 1985)

Platelet granules and their contents originate within the parent megakaryocyte, where they are packaged up and deployed within the resultant platelets and microparticles. When stimulated, platelets secrete contents from four granular stores: α-granules, dense granules, t-granules, and secretory lysosomes. In the section below, we will give a brief overview of the different platelet granules and their related cargo (Table 1-2).

1.3.7.1 Alpha granules

Alpha granules are the most abundant granules within the platelet with 50-80 granules per platelet, each about 200-400 nm in diameter. (Blair and Flaumenhaft, 2009) Their heterogenic content performs many roles in hemostasis, inflammation, and angiogenesis. Patient who have a genetic deficiency in alpha granules biogenesis, known as Grays Platelet syndrome (GPS), have a diverse bleeding phenotype, ranging from mild to severe (Figure 1-6). (Gunay-Aygun et al., 2010, Bottega et al., 2013, Kahr et al., 2011, Maynard et al., 2010) The internal structure of the granule contains an electron-dense nucleoid and a less-dense peripheral area that contains many factors. (Blair and Flaumenhaft, 2009, Harrison and Cramer, 1993) It is currently debated whether differential release of specific α-granule populations, or if different granule populations are simply distributed in geographically distinct regions of the organelle. (Sehgal and Storrie, 2007, Ye and Whiteheart, 2013) One recent study, utilizing microfluidic techniques,

demonstrated that the geometric orientation of the underlying matrix and platelet spreading regulates α-granule secretion. (Sakurai, 2015)

The way in which platelets acquire their α-granule content is also quite complex and is under study. Platelets have been documented to both inherit them from their parent megakaryocyte as well as through endocytosis from the plasma compartment. (Handagama, 1990)(Suehiro et al., 2005, Flaumenhaft, 2012, Italiano and Battinelli, 2009, Ye and Whiteheart, 2013) For example, factor V, vWF, fibrinogen, and vascular endothelial growth factor (VEGF), which were once thought to be solely inherited from the parent megakaryocyte, are now recognized to be acquired via endocytosis from the surrounding environment. (Suehiro et al., 2005, Salgado et al., 2001, Roussi et al., 1995, Harrison et al., 1989) In addition, the platelet concentration of α-granule Ig is dependent on the plasma pool concentration. (George et al., 1985) It is also important to note, that some of the factors that are incorporated into the megakaryocyte via endocytosis have been shown to undergo proteolysis prior to being packaged into the platelet-pool. (Ayombil et al., 2013)

The sole role of the platelet as a component of hemostasis is now being redefined, especially when the α-granule contents are taken into account. These granules have been found to promote everything from liver regeneration to nerve growth. (Chacon-Fernandez et al., 2016, Fujimura et al., 2002, Lisman and Porte, 2016, Starlinger et al., 2016) Because they also contain pro-angiogenic, proinflammatory, and anti-inflammatory components, platelets are also being recognized as potential therapeutics for wound healing, burn treatment, and bone and cartilage repair. (Sakata and Reddi, 2016, Mussano et al., 2016, Venter et al., 2016, Pallua et al., 2010, Findikcioglu et al., 2009, You et al., 2007)

1.3.7.2 Dense granules

Release of dense granule content is also important in homeostasis. Each platelet carries approximately three to eight, ~150 nm diameter, electron-dense granules. (Ye and Whiteheart, 2013) The dense granule membrane contains H^+ pumping ATPase, which maintains the granule at an acidic pH of ~ 6.1. (Ye and Whiteheart, 2013) Dense granules serve as storage for a variety of cargo, including calcium polyphosphates, sphingosine-1-phosphate, epinephrine, serotonin,

GPIb, GPIIb/IIIa, ADP and ATP (Youssefian et al., 1997, Chatterjee et al., 1990). There are platelet-based bleeding disorders that are attributed all, or in part, to deficiencies in dense granule formation. Patients with Hermansky-Pudlak syndrome (HPS) have a genetic defect in dense granule and lysosome biogenesis, and have subsequent predilection to bleeding diatheses. (Feng et al., 2002, Di Pietro and Dell'Angelica, 2005) Recent studies in mice have also shown that platelet dense granule secretion may be essential to normal lysosome and α-granule secretion. (Meng et al., 2015, Harper et al., 2015)

The roles of the dense granule cargoes are varied and their release is commonly used in the testing of platelet function and degranulation. Serotonin (5-hydroxytryptamine, 5-Ht) is released from platelets upon activation and can then bind to 5-HT_{2A} receptors on the platelet surface to promote platelet aggregation. (Siess, 1989) The importance of serotonin in platelets is demonstrated with the increased use of serotonin reuptake inhibitors (SSRIs), which many studies suggest is correlated with a decreased risk for cardiovascular disease (in contrast with other tri-cyclic antidepressants, which are correlated with an increased risk of ischemic stroke). (Schlienger and Meier, 2003, Juang et al., 2015) (Lee et al., 2013) Platelet serotonin has also been shown to promote neutrophil recruitment to sites of inflammation in mice. (Duerschmied et al., 2013) ADP and ATP are present in high concentrations, with ADP being dominant. Outside of the granules, within the cytoplasm of the platelet, ATP is dominant over ADP. Upon platelet activation, the ADP-containing dense granules move towards the open canalicular system and release their ADP, with the concentration of ADP outside of the platelet resulting in nearby platelet activation. (Fogelson and Wang, 1996, Fukami et al., 1978)

Polyphosphates (polyPs) were recently identified as components of platelet dense granules. Interestingly, inorganic polyPs are present in bacteria, fungi, algae, and protozoa, as well as eukaryotic cells. (Ruiz et al., 2004) PolyPs are present in acidocalcisomes, which contain calcium, pyrophosphates (PPi), and other ions and proton-accumulating membranes with high density on electron microscopy. (Ruiz et al., 2004) Platelet polyPs are under investigation and have been found to be localized to the dense granules. (Ruiz et al., 2004) They play many roles in both platelet activation and the coagulations cascade, activating the contact pathway of blood clotting, accelerating factor V activation, and abrogating the anticoagulant function of tissue

factor pathway inhibitor (TFPI). (Morrissey et al., 2012, Choi et al., 2011, Muller and Renne, 2011) Additionally, although outside the scope of this section, platelet polyPs have been identified to be proinflammatory, as well as prothrombotic, via the factor XII activation triggered release of bradykinin, an inflammatory mediator of the kallikrein family. (Muller et al., 2009)

1.3.7.3 Lysosomes

Primary lysosomes have been identified in both the maturing megakaryocyte and the resultant platelets. (Bentfeld-Barker and Bainton, 1982) When platelets are sufficiently activated, they undergo two waves of exocytosis; the first wave is the release of α- and dense granules and the second is the release of the lysosome contents. This process requires both ADP and the general membrane fusion protein, N-ethylmaleimide sensitive factor, which then choreographs with specific target membrane SNAL receptor (t-SNAREs) proteins to facilitate release. (Chen et al., 2000)

Lysosomes are thought to release hydrolytic enzymes that aid in thrombus remodeling. Platelet lysosomes contain a variety of acid hydrolases and glycohydrolases. (Holmsen and Weiss, 1979) Upon platelet activation, degranulation of lysosomes appears to take place at a slower rate than α- and dense granules, and requires stronger agonists. (Holmsen, 1989) Lysosome contents contribute to vascular damage, the growth inhibition of smooth muscle cells via the cleavage of heparin-like molecules by heparinases, and to the degradation of glycoproteins, glycolipids, and glycosaminoglycans by glycohydrolases. (Ciferri et al., 2000, Zhang et al., 2001, Castellot et al., 1982)

When defining a granule as a lysosome, however, one must take into account the definition of a lysosome. Lysosomes are typically characterized by an acidic interior, however mepacrine, a lysosome labeling drug, was also found to accumulate within α- and dense granules due to their acidic interiors. (Polasek, 2005) Additionally, dense granules have recently been called lysosome-related organelles, as they exhibit lysosomal membrane glycoprotein marker CD63 and LAMP2. (Polasek, 2005) Dense granules also share CD62P, GPIb, and GPIIb/IIIa with α-granules and the multivesicular bodies that give rise to α- and dense granules, are also lysosomes that contain acid hydrolases and express CD63. (Polasek, 2005) Additionally, HPS, which is

associated with decreased platelet dense granule and lysosomes, is a generalized lysosomal storage disorder involving multiple other tissue types. (Polasek, 2005) The endocytic nature of α-granules further puts them closer to the lysosomal family as well. This information provides support to the current hypothesis that all granules within the platelet are, ultimately, a type of lysosome. (Polasek, 2005)

1.3.7.4 T-granules

The t-granule was described by Thon et al. (2012) as being a unique granule compartment within the platelet for the localization and signaling of toll-like receptor 9 (TLR9). (Thon JN, 2012) The T granule is a novel electron-dense tubular system-related compartment, where TLR9 colocalizes with protein disulfide isomerase and associates with Vamp 7/8, to regulate its distribution in platelets upon activation and spreading. TLR9 is most commonly expressed within monocytes, macrophages and dendritic cells and functions as a receptor for bacterial and viral unmethylated CpG islands in DNA. (Hennessy 2010, Thon 2012) More recent studies exploring TLR9 in platelets show a possible function in oxidative stress, innate immunity, and thrombosis. (Panigrahi S, 2013) The t-granule will likely be under further study throughout the coming years.

1.4 The role of platelets in hemostasis

The function of the platelet in hemostasis is perhaps its best known and most extensively studied role. Platelets interact with the vascular wall, other platelets, soluble and membrane-bound coagulation factors, leukocytes and fibrin to build a hemostatic plug, or thrombus, that bridges a defect in the vascular wall. This thrombus acts to prevent excessive release of vascular contents into the surrounding space, thus preventing hemorrhage and ultimately death. Though many cell types and soluble factors contribute to the process, platelets are key for the initiation and maturation of such thrombi under arterial flow, essentially coordinating the ordered construction of this biological bandage. Furthermore, by gathering at the site of injury, platelets localize the thrombogenic response and coordinate the fibrinolytic process, preventing the development of pathologic thrombi.

1.4.1 An overview of hemostasis

Hemostasis is the process of stopping blood loss from a vessel with an injured wall through the construction of an insoluble thrombus to bridge the vascular defect. This process is classically described in terms of primary and secondary hemostasis, and requires flawless integration of the response of the platelet and of the coagulation cascade to tissue injury. Primary hemostasis refers to formation of the platelet plug, while secondary hemostasis refers to the deposition of the end product of the coagulation cascade, cross-linked insoluble fibrin, into and around the platelet plug to strengthen and stabilize the resultant thrombus. Rather than occurring temporally as two distinct stages of hemostasis, these happen simultaneously and are a mechanistic continuum, with platelets central to both. This process is in many ways analogous to the construction of a brick patch to bridge a hole in a wall, with platelets serving as the bricks essential for structure and fibrin as the mortar essential for strength. The process is summarized in Figure 1-7.

The process of hemostasis begins with endothelial injury, whereupon the subendothelial environment is exposed to components contained within the flowing blood. Exposed collagen from the subendothelial environment admixed with von Willebrand factor (vWF) released from the Weibel-Palade bodies of the endothelial cells interact with each other and with platelets, resulting in tethering, activation and adhesion of the platelets to the subendothelial environment. Downstream signaling from the receptors results in platelet activation, with subsequent release of factors such as adenosine diphosphate (ADP) and thromboxane A_2 (TXA_2) that cause activation of neighboring platelets in an autocrine fashion. Inside-out signaling resulting from these agonists additionally primes the platelet to bind to fibrinogen by causing the integrin $\alpha_{IIb}\beta_3$ to adopt an active confirmation.

Meanwhile, tissue factor (TF) from the subendothelial environment binds to activated Factor VII (VIIa) to initiate the extrinsic coagulation pathway. The thrombin that is generated by the activated factor Xa (Xa) formed by the extrinsic Xase of this pathway serves to activate a number of factors of the intrinsic coagulation pathway, which ultimately generates an intrinsic Xase that is 50-100 times more efficient in converting the zymogen factor X to its active form Xa, and thus more efficient in ultimately producing thrombin than its extrinsic equivalent, thereby amplifying the response. The extrinsic and intrinsic coagulation pathways converge in

the common coagulation pathway, in which the thrombin that is generated serves to catalyze the conversion of soluble fibrinogen to insoluble fibrin. Insoluble fibrin polymers bridge the gaps between platelet membranes by binding to the active conformation of integrin $\alpha_{IIb}\beta_3$ on two or more platelet surfaces, thus facilitating the process of aggregation. The end product is a mass of platelets admixed with fibrin and "innocent bystander" leukocytes and erythrocytes that bridges the defect in the endothelial monolayer of the vessel wall.

1.4.2 Platelets respond to endothelial damage by laying a foundation for a thrombus

The healthy vessel wall is composed of a confluent sheet of endothelial cells lining the inner surface of a tube composed of a basement membrane encased in additional cellular layers (the tunica media and tunica adventicia). The intact endothelium contains an ADPase (CD39) and secretes factors, such as PGI_2 and nitric oxide, that prevent the activation of platelets in the circulation. (Tateson et al., 1977, Marcus et al., 1991, de Graaf et al., 1992) Upon injury, the confluency of the endothelial monolayer is disrupted and the basement membrane exposed.

This basement membrane is an insoluble sheet of highly cross-linked glycoproteins, including multiple types of collagen. Von Willebrand factor (vWF), which is stored in Weibel-Palade bodies of endothelium and released upon activation, binds to the basement membrane matrix by binding predominantly to collagen types I, III and VI, (Pareti et al., 1987, Hoylaerts et al., 1997) and the activation step of the adhesion process results from binding of the platelet GPIb-IX-V and GPVI to vWF and collagen, respectively.

Platelet binding to vWF has been shown to be essential for the timely adhesion of platelet to a vascular defect.(Ni et al., 2000b) Once anchored to the basement membrane, the A1 domain of vWF serves as a ligand for glycoprotein (GP) Ibα (CD42) of the GPIb-IX-V receptor complex that is specific to passing platelets under shear conditions, thus facilitating the process of Tethering of the platelet to the vascular wall.(Ruggeri, 2009, Savage et al., 1996) The association of vWF with this receptor tyrosine kinase initiates outside-in signaling by activating PI-3 kinase via the Syk/Src pathway, resulting in activation of phospholipase (PLC) γ, mobilization of IP_3, and release of calcium (Ca^{+2}) from intracellular dense tubular system.(Mazzucato et al., 2002, Nesbitt et al., 2002) This initial elevation in intracellular Ca^{+2} is compounded by a second influx

from the extracellular environment.(Nesbitt et al., 2002, Mazzucato et al., 2002) Mice deficient in vWF demonstrate a delay in the initiation of thrombus formation but do eventually form stable thrombi.(Ni et al., 2000a)

Another receptor exclusive to platelets, GPVI, complexes with FcRγ dimers on the platelet's surface and occupies membrane lipid rafts that it shares with GPIb-IX-V.(Tsuji et al., 1997) The C-terminal D2 domain of GPVI binds to collagen while GPIbα binds vWF.(Horii et al., 2006, Auton et al., 2010) Signaling downstream of this receptor tyrosine kinase's immunoreceptor tyrosine-based activation motif (ITAM), FcRγ, amplifies the outside-in PLCγ signaling and further compounds the rise in intracellular Ca^{+2} levels.(Blake et al., 1994, Daniel et al., 1994)

Elevated levels of intracellular Ca^{+2} within the platelet instigate inside-out signaling to stimulate changes from an inactive to active conformation in integrin $\alpha_2\beta_1$ (GPIa-IIa, homologous to VLA2 on lymphocytes).(Margadant et al., 2011) Though activation is not a prerequisite for collagen binding by this integrin, this active integrin's α_2-subunit I domain is able to bind to collagen's GFOGER motif with increased affinity following activation.(Emsley et al., 2000, Smith et al., 2000) Collagen binding results in additional outside-in PLCγ signaling that produces peaks in Ca^{+2} levels distinct in duration and form from those produced through GPVI signaling, (Mazzucato et al., 2009) as well as providing a third point of structural integrity to the adhesion of the platelet to the defect in the vessel wall.(Sarratt et al., 2005)

The inside-out signals produced during platelet activation similarly result in a change from an inactive to active conformation to the main integrin, $\alpha_{IIb}\beta_3$, that mediates the platelet-platelet interactions necessary for stable thrombus formation and connects the actin skeleton of adjacent platelets to allow for clot retraction. $\alpha_{IIb}\beta_3$ comprises 3% of the total protein mass of the platelet and 17% of the total plasma membrane bound protein, and as such is the most prevalent integral plasma membrane protein.(Phillips et al., 1988) Platelet activation results in tethering of $\alpha_{IIb}\beta_3$ to actin filaments through interactions with cytoskeletal accessory proteins including talin, (Knezevic et al., 1996) filamin, (Pavalko et al., 1989) α-actinin, (Pavalko et al., 1991) and others.(Burridge and Fath, 1989) Platelet activation induced talin and kindlin binding of the β_3 subunit furthermore results in unclasping of the cytoplasmic tails of the α_{IIb} and β_3 subunits,

leading to a change in the spatial orientation of the extracellular domains into an active conformation recognized by the PAC-1 antibody.(Critchley and Gingras, 2008, Montanez et al., 2008, Ma et al., 2006) A groove between this active integrin's A-like domain of the β3 subunit and β-propeller of the αIIb subunit binds to the RGD peptide sequence of multivalent vWF or the KQAGDV peptide sequence at the C-terminus of divalent fibrinogen's γ chain.(Plow et al., 1985, Ruoslahti, 1996) The active conformation of this integrin is necessary for ligand binding, and ongoing platelet activation is required for the maintenance of the active conformation of this integrin.(Goto et al., 2006) Inside-out signaling from this integrin helps to maintain ongoing platelet activation through similar mechanisms to those outlined above, as does autocrine platelet-platelet signaling as outlined below. Platelet activation additionally results in alpha-granule fusion with the platelet's surface, leading to increased surface expression of $\alpha_{IIb}\beta_3$ as the subpopulation of this integrin that is resident in the alpha granule membrane is exposed.(Wencel-Drake et al., 1986) Hereditary defects in this integrin are responsible for the prolonged bleeding times observed in patients with Glanzmann's thrombasthenia.(George et al., 1990)

1.4.3 Platelets localize the coagulation cascade to the site of injury

While the platelets interact with the subendothelial environment and each other to begin to lay the structure of the thrombus, a series of enzymatic reactions simultaneously serves to produce the insoluble fibrin that will serve as a mortar to stabilize the platelet-platelet interactions. In these reactions, serine proteases (thrombin, and factors VII, IX, X, and XI) partner with membrane-bound glycoprotein cofactors (TF and factors V and VIII) to catalyze the activation of additional zymogens or cofactors. The liver is the primary producer of the coagulation factors V, VII, VIII, IX, X, XI and thrombin (factor II) in addition to fibrinogen (factor I),(Olson et al., 1966) while the subendothelial fibroblasts and pericytes produce the integral membrane protein TF (factor III, CD142).(Wilcox et al., 1989) The ultimate end product is the cleaving of soluble fibrinogen into insoluble fibrin by thrombin (factor II).

This process is traditionally described as the interplay of three coagulation pathways: the extrinsic coagulation pathway initiates the process, the intrinsic coagulation pathway amplifies the response, and the common pathway represents the convergence of the extrinsic and intrinsic pathways to form the complex of factors V and X (known as "prothrombinase") that catalyzes

the conversion of prothrombin into thrombin.(Schenone et al., 2004) Significant redundancy across these pathways allows for deficiencies in factor VIII (hemophilia A) or factor IX (hemophilia B) to be viable, though affected individuals suffer from mild to severe bleeding diatheses.(Pavlova and Oldenburg, 2013)

The subendothelium and platelet surface as an essential scaffold for facilitating and localizing the enzymatic cascade. To operate at maximum efficacy, many of these enzymatic reactions must occur either on the scaffold of the subendothelial environment (those catalyzed by VII/TF) or at the activated platelet surface (those catalyzed by IX/VIII, X/V and thrombin).(Scandura and Walsh, 1996, Baglia and Walsh, 2000) These associations are mediated by interactions of the serine protease with the negatively charged surface (tissue factor on the subendothelial space, or activated platelet phospholipid); binding to specific receptors that are expressed on activated platelets may also play a role, especially for the binding of factor Xa.(Bouchard et al., 1997) Vitamin K is required for the post-translational carboxylation of the glutamic acid residues that allows these factors (VII, IX, X, and thrombin) to bind to these surfaces.(Furie et al., 1999) This requirement for ongoing interactions with an activated platelet surface effectively localize the coagulation cascade to the core of the thrombus.

The coagulation cascade is initiated at the site of vascular injury by exposure of TF to subnanomolar levels of circulating activated factor VIIa.(Eichinger et al., 1995) Extrinsic Xase is the product of this interaction, and activates the zymogen forms of factors X or IX with a relatively low efficacy.(Lawson and Mann, 1991, Komiyama et al., 1990) The resultant enzymes Xa or IXa serve to amplify the coagulation response by associating with their respective coenzymes (Va or VIIIa) on the platelet surface scaffold and by initiating the common or intrinsic coagulation pathways, respectively, in addition to activating additional factor VII.(Rao et al., 1985, Komiyama et al., 1990) The association of Xa with platelet-bound Va to produce prothrombinase results in increased production of thrombin in the microenvironment of the activated platelets.(Nesheim et al., 1979) This thrombin initiates the intrinsic coagulation pathway, in addition to augmenting platelet activation, increasing the pool of activated factor V, and cleaving fibrinogen to fibrin, as discussed further below (4.1.4).

Thrombin initiates the intrinsic coagulation pathway by catalyzing the activation of factors XI, VIII and V.(Pieters et al., 1989, Gailani and Broze, 1991) Factor XIa then augments the production of factor IXa, which is already being produced by factor VIIa bound to TF.(Gailani et al., 2001) Factor IXa binds to the newly minted, membrane-bound cofactor VIIIa on the activated platelet surface to form intrinsic Xase. Intrinsic Xase is 50 to 100 times more efficient than extrinsic Xase (Factor VIIa/TF) (Ahmad et al., 2003), and thus further increases production of factor Xa, which binds to factor Va and to the activated platelet surface (Bouchard et al., 1997) and subsequently produces more thrombin from prothrombin.

The extrinsic and intrinsic pathways both converge in the common pathway with the formation of thrombin by prothrombinase (Xa/Va). The enzymatic activity of prothrombinase substantially differs when it is associated with an activated platelet membrane when compared with unbound forms or forms bound to synthetic vesicles. The reactions that produce thrombin by prothrombinase on an activated platelet surface proceed through an inactive intermediate, prethrombin-2, rather than the active intermediate meizothrombin.(Wood et al., 2011) Since the latter is able to competitively bind to thrombin binding sites but has markedly reduced efficacy, (Doyle and Mann, 1990) the localization of the prothrombinase complex has implications not only for the activity of the prothrombinase but also for the activity of thrombin.

Though fibrinogen, the substrate for thrombin, is synthesized by the liver, it is concentrated in the vicinity of platelets in both intracellular and membrane-associated forms.(Gokcen and Yunis, 1963) Fibrinogen that binds to inactive $\alpha_{IIb}\beta_3$ is endocytosed and stored in alpha granules to be released upon platelet activation.(Harrison et al., 1989) Fibrinogen is a linear protein composed of three chains, Aα, Bβ and γ, that exists soluble in the plasma as dimers stabilized by disulfide bonds. Thrombin hydrolyzes RG bonds at the N terminus of the Aα and Bβ chains, resulting in the production of a fibrin molecule with exposed sites in the α and β chains that allow for interaction with a site on the C terminus of the γ chain, (Scheraga, 2004) thus allowing for the formation of the fibrin polymers that serve as mortar between the platelets.

It is also important to note that other cell types have been shown to have the capacity to produce coagulation factors in vitro, (Dashty et al., 2012) and additional sources such macrophages are

important sources of coagulation factors like VII and TF in disease states such as atherosclerosis and other inflammatory states.(Wilcox et al., 2003, Lindmark et al., 2000) Furthermore, the ultimate downstream substrate for the product of these pathways, fibrinogen, is an acute phase protein with upregulated production by the liver in inflammatory states.(Mayer and Schomerus, 1975) Such increased production of these factors in the face of inflammation may contribute to the development of pathologic hypercoagulable states.

1.4.4 Platelet Activation Provides Autocrine Signaling to Localize and Amplify Response

The first layer of bricks has thus been laid through the process of adhesion of the platelets to the subendothelial environment, and the fibrin has been generated that will act as mortar to bind the platelets together. An additional consequence of the outside-in signaling that occurs is platelet activation. Activation results in platelet shape change and release of alpha and dense granule contents into the surrounding microenvironment, as well as activation of cyclooxygenase (COX)-1. As a result of these events, the local concentration of the essential components of that mortar, fibrinogen and vWF, and the surface density of their ligand, $\alpha_{IIb}\beta_3$, increases. ADP and TXA_2 are released from the platelet, and join thrombin generated by the common coagulation pathway in a series of autocrine signaling events. The sum consequence of these events is to amplify, sustain and localize the platelet activation, with the end product of a focal stable thrombus that acts as a wall to bridge the defect in the endothelium.

Activation stimulates a reorganization of the actin cytoskeleton that drives a change in shape from a resting discoid to an activated spherical platelet and subsequent development of filapods and platelet spreading. This process is initiated by intracellular calcium binding to and causing a conformational change in gelsolin, which severs actin filaments and creates new negative (-, or pointed) ends to existing actin filaments.(Fox et al., 1987) Additionally, Arp2/3 complex is upregulated in activated platelets,(Falet et al., 2002) and when bound to actin serves as a surrogate – end and nidus for the growth of the actin filament along the + end.(Machesky and Gould, 1999) β-thymosin outcompetes the – ends of actin filaments in affinity for free actin subunits in the cytoplasm, thus preventing cytoskeletal reorganization in the resting platelet.(Carlier et al., 1996) However, these new + (or barbed) ends have a greater affinity for binding free actin subunits than β-thymosin, and their exposure allows for actin assembly and

subsequent reorganization of the cytoskeleton.(Hartwig et al., 1995) Cytoskeletal reorganization brings the cytoplasmic alpha and dense granules into close proximity with the open canicular system, allowing for SNARE-mediated fusion and exocytosis of their contents which subsequently diffuse into the microenvironment surrounding the platelet.(Stenberg et al., 1984) Both alpha and dense granules are membrane bound intracellular vesicles that are trafficked into developing platelets along microtubules in the parent megakaryocyte.(Richardson et al., 2005)

α-granules outnumber dense granules tenfold, and can be more than twice the size.(Frojmovic and Milton, 1982) Alpha granules originate from the multivesicular bodies formed by fusion of outbuddings of the Golgi apparatus and endosomes in megakaryocytes.(Handagama et al., 1990) The contents of α-granules thus include proteins from the extracellular environment, such as factor Va and prothrombin, and integral membrane proteins recycled from the platelet surface, such as αIIbβ3, GPIbα-IX-V and GPVI, in addition to factors that may be synthesized by the megakaryocyte, such as fibrinogen and vWF.(McRedmond et al., 2004) α-granule fusion with the platelet membrane thus contributes to ongoing platelet activation by increasing the concentration on the platelet surface of integrins that facilitate adhesion to the subendothelium and sustain outside-in signaling (GPIbα-IX-V and GPVI), or that are essential ligands for platelet-platelet interaction ($\alpha_{IIb}\beta_3$). Alpha granule fusion also results in an increased microenvironmental concentration of the proteins necessary to bridge interactions between platelets in the core of the thrombus, whether through direct release (vWF), or release of the components necessary for synthesis of fibrin by the coagulation pathway (prothrombin, fibrinogen and factor Va).

Interestingly, these platelet-derived proteins generally have enhanced activity compared with those from other origins. For example, platelet derived vWF consists predominantly of high-molecular-weight multimers vWF with greater adhesive activity in comparison to lower molecular weight counterparts.(Gralnick et al., 1985) Additionally, platelet-derived factor Va, which exists in either membrane-bound or unbound forms and is released in a partially active form from alpha granules, demonstrates enhanced cofactor activity following activation by thrombin,(Monkovic and Tracy, 1990) and decreased susceptibility to inactivation by activated protein C (APC) compared to its plasma-derived counterpart.(Camire et al., 1995) Upon release

of α-granule contents, the concentration of factor Va in the microenvironment can exceed that of the plasma by 600 fold.(Nesheim et al., 1986)

The downstream product of the association of Va with Xa, thrombin, thus becomes concentrated within the core of the thrombus where it serves as a potent platelet activator. Thrombin is a serine protease that cleaves the N-terminal extracellular domain of protease-activated receptors (PARs), resulting in a novel N-terminus that serves as a tethered ligand for these G-protein coupled receptors;(Vu et al., 1991) peptide agonists of the PARs, such as SFLLRN as an agonist for PAR1, thus act as surrogate PAR N-termini rather than thrombin analogs.(Ramachandran and Hollenberg, 2008) Thrombin acts on PAR1 on human platelets and PAR3 in mice to initiate reversible aggregation.(Ishihara et al., 1997) Signaling through $G_{12/13}$ triggers shape change and granule release, including dense granule ADP release, through activation of Rho kinase and subsequently cofilin and myosin light chain kinase,(Klages et al., 1999) while signaling through G_q triggers the initial release of Ca^{+2} from intracellular stores.(Covic et al., 2000) Thrombin also acts on PAR4 in both species via $G_{12/13}$ and G_q signaling to result in further granule release and a sustained Ca^{+2} influx, ultimately resulting in ongoing platelet activation and irreversible aggregation.(Covic et al., 2000) The process of α-granule fusion thus serves to concentrate the components necessary for sustained platelet-platelet interactions within the stable core of the growing thrombus, where the platelets are p-selectin positive and closely packed.(Stalker et al., 2014) It is no wonder that patients with a deficiency in α-granules, known as Gray Platelet Syndrome due to the appearance of their platelets by electron microscopy, demonstrate mild to moderate bleeding diatheses.(Raccuglia, 1971)

In contrast, dense granules are similar to lysosomes as they originate in megakaryocytes from the early endosome rather than directly from the golgi.(Raposo et al., 2007) The contents of dense granules, such as ADP and serotonin, are imported through active transport by membrane pumps, including multidrug resistance protein (MRP)-4 and vesicular monoamine transporter (VMAT)-2, respectively; the concentration of dense granule contents is thought to increase as the dense granules mature.(Jedlitschky et al., 2004, Fukami et al., 1984) ADP in the dense granule releasate serves as an autocrine signal to sustain and localize platelet activation around the thrombus. ADP acts by binding $P2Y_1$ or $P2Y_{12}$ on the platelets' surface. These G-protein

coupled receptors serve to initiate and sustain adoption of the active conformation by αIIbβ3, with G_q signaling downstream of $P2Y_1$ contributing to the initiation of activation and G_i signaling downstream of $P2Y_{12}$ synergistically contributing to the maintenance of activation.(Remijn et al., 2002, Fabre et al., 1999) Such mechanisms synergize and compound the consequences of thrombin activation, and are essential to initiating and maintaining the activation in the outer shell of the thrombus, where the platelets are more likely to be p-selectin negative and loosely associated with each other through dynamic membrane tethers.(Stalker et al., 2014, Nesbitt et al., 2009, Dopheide et al., 2002) In humans with a deficiency in dense granules, such as is found in Hermansky-Pudlak syndrome, or a defect in dense granule function, such as in Chediak-Higashi syndrome, minor bleeding diatheses are observed in conjunction with myriad other symptoms.(Buchanan and Handin, 1976, White et al., 1971)

Platelet activation is additionally amplified through the action of thromboxane A_2 (TXA_2).(Brass et al., 1987) TXA_2 is synthesized by platelets following their activation. The increase in cytosolic calcium in the activated platelet results in activation of phospholipase A_2, which hydrolyzes platelet membrane phospholipids to produce arachidonic acid. Arachidonic acid is then converted to prostaglandin (PG) G_2 by cyclooxygenase-1 (COX-1), then into PGH_2 by hydroperoxidase, then into TXA_2 by the platelet-specific isomerase thromboxane synthase.(Moncada and Higgs, 1986) TXA_2 is a small molecule that freely diffuses across the platelet membrane; the effect of TXA_2 is localized as a result of the molecule's 30 second half-life. (FitzGerald, 1991) When TXA_2 binds the G-protein coupled thromboxane receptor (TP), the downstream effects that are mediated by G_q and $G_{12/13}$ signaling are analogous to that seen following stimulation by thrombin or ADP.(Knezevic et al., 1993, Offermanns et al., 1994, Djellas et al., 1999) Inhibition of these pathways, either by blocking TXA_2 synthesis by irreversibly inhibiting COX-1 with aspirin treatment, or by knocking out TP in a mouse model, results in prolonged bleeding times. However, bleeding diatheses are rarely noted secondary to defects in these pathways.(Gerstein et al., 2015, Thomas et al., 1998) This may be due to the fact that TXA_2 mediated platelet activation appears to be most essential under shear stress conditions consistent with venous rather than the high shear stress conditions associated with arterial flow.(Moake et al., 1988)

1.4.5 Cross-linked fibrin stabilizes interactions between activated platelets to form the thrombus

The monomeric fibrin generated from fibrinogen by the enzymatic activity of thrombin binds to the active conformation of integrin $\alpha_{IIb}\beta_3$ with high affinity.(Litvinov et al., 2016) Polymerization of this platelet-bound fibrin with neighboring fibrin monomers occurs through interactions of the N terminal lysine residues that are exposed following cleavage of the Aα and Bβ chains by thrombin with glutamate residues on the γ chain.(Scheraga, 2004) This bond is catalyzed by a transglutaminase, factor XIIIa, which is present in the circulation in zymogen form and activated by thrombin following binding of fibrin.(Curtis et al., 1974) Thus, the platelet bricks that were laid over the endothelial defect are stabilized by the formation of an insoluble fibrin mortar, all under the control of paracrine signaling provided by factors localized to the area by activated platelets.

It is important to note that this initial mass of platelets is heterogeneous in structure, with classically activated p-selectin + platelets embedded within this cross-linked fibrin mortar acting as the nuclear hemostatic core, and gradients of levels of activation driven by shear stress of vascular flow and localized thrombin, ADP and TXA_2 signaling radiating from that core to form a shell with a tear-drop structure.(Stalker et al., 2014) Discoid p-selectin - platelets with filamentous tethers concentrate along the lagging edge of that structure, and primarily depend upon shear stress rather than paracrine signaling for their activation.(Nesbitt et al., 2009) Growth of the thrombus beyond these confines is inhibited by prostacyclin (PGI2), endothelial-ADPase (CD39), and nitric oxide from the surrounding intact endothelium.(Tateson et al., 1977, Marcus et al., 1991, de Graaf et al., 1992)

1.5 Platelets in inflammation

Platelets play key roles in hemostasis and immunity. Despite the seeming disparity between these two systems, there is considerable redundancy in the roles that platelets play and the mechanisms through which they fulfill their function. In both hemostasis and immunity, platelets promptly react to stimuli through post-translational mechanisms, and directly interact with endothelium,

leukocytes and other platelets to modulate their behavior and release factors from their α- and dense granules to locally amplify a response. Though the initiating stimuli substantially differ, the downstream mechanisms echo each other and overlap, and as a result, pathologic thrombi are not uncommon as a sequela to the immune response to pathogens. This section will concentrate on the mechanisms that underlie what we currently understand about the platelet's role in inflammation.

1.5.1 Direct functions

1.5.1.1 Sequestration and thrombus formation

It is not surprising that platelets likely have direct interactions with pathogens, as they are one of the most numerous blood cell type in the peripheral circulation. Upon contact with pathogens, such as bacteria, platelet can bind these invaders via many different mechanisms, dependent on the type of pathogen (bacteria, virus, etc.). They are capable of directly binding to pathogens and also indirectly binding them through bridging molecules. (Fitzgerald JR, 2006) As discussed in Section 1.3.2, 'Immunomodulatory receptors and antigens', platelets have many immune receptors, which, when bound, subsequently activate the platelets. This activation leads to a signaling cascade, which results in the activation of other nearby platelets and the activation of the coagulation system. This enables the platelets to sequester the pathogens, usually bacteria, within a cross-linked fibrin clot which subsequently holds the pathogen 'hostage' until the nearby leukocytes come and finish the job. The platelets themselves also contain a number of antimicrobial peptides within their granules, such as their lysosomes, and when sufficiently activated, the platelet can degranulate and release these toxins onto the bacteria, resulting in bacterial killing.(Yeaman MR) In some cases, platelets can be activated by bacterial toxins without direct interaction with bacteria; this can result in peripheral thrombocytopenia and/or sterile thrombus formation within the body, such as in the case with *Helicobacter pylori* (*H. pylori*) and haemolytic uremic syndrome (HUS) caused by *Escherichia coli* (*E. coli*). (Hambleton J, 2002; Proulx F, 2001)

Platelets have multiple bacterial-response mechanisms, including responding to antigen-antibody complexes, antigens alone, and complement. (Humphrey JH, 1955; Hawiger J, 1972; Weksler BB, 1971) One of the most studied platelet-bacterial interactions is with *Staphylococcus aureus* (*S. aureus*), which triggers platelet activation via secreted α-toxin, protein A, IgG, and the

FcγRIIa platelet receptor. (Fitzgerald JR, 2006) *S. aureus* even has its' own surface receptors that can directly bind to platelets and fibrinogen, such as clumping factor A (ClfA) and fibronectin-binding proteins (FnBPA and FnBPB), propagating aggregation and thrombus formation. (Schwarz-Linek U, 2003; Massey RC, 2001). *Streptococcus sanguis* (*S. sanguis*) and *Streptococcus pyogenes* (*S. pyogenes*) also activate platelets in a complement- and antibody-dependent fashion. *S. sanguis* expresses platelet-aggregation-associated protein (PAAP), which results in rapid platelet activation and aggregation. Another example includes *Porphyromonas gingivalis* (*P. gingivalis*), which can both accelerate the generation of atherosclerosis as well as directly secrete platelet-activating proteases. (Fitzgerald JR 2006) Some bacteria can bind to platelet surface receptors, such as in the case of *Borrelia burgdorferi* (*B. burgdorferi*) binding to $\alpha_{IIb}\beta_3$, either directly or through plasma protein linkers. *Escherichia coli* (*E. coli*) results in platelet activation via both FcγRIIa and $\alpha_{IIb}\beta_3$, although bacterial killing was dependent on IgG opsonization. (Watson CN 2016; Riaz AH 2012) There are even differences in bacterial-platelet interactions dependent on the specific strain of bacteria. (Fitzgerald JR, 2006) *E. coli* O111 has been shown to activate platelets in a TLR4-dependent manner, resulting in an increase in tissue factor expression and faster thrombin generation, as well as an increase in platelet adhesion to endothelial cells. (Matus V 2017; Matus V 2014) Studies of platelet interactions with a wide range of bacteria, including various different strains, has been explored, although is beyond the scope of this chapter.

1.5.1.2 Antimicrobial peptides

Platelets harbor a wide variety of antimicrobial peptides within their granule stores, which they can release upon appropriate stimulation; in fact, platelets are considered granulocytes, similar to neutrophils, eosinophils, and basophils. (Yeaman ME 2014) When platelets detect and bind to bacteria or bacterial pathogens they release a multitude of factors, including: ADP and ATP, which further stimulate platelet activation, and platelet microbicidal proteins (PMPs) and kinocidids, which both activate neighboring leukocytes and kill the inciting pathogen. (Yeaman 2014; Hamzeh-cognasse H 2015) The microbicidal proteins that platelets have been shown to contain include, kinocidins (CXCL4, CXCL7, and CCL5), defensins (BD2), and thymosin β4. (Yeaman 2014) Kinocidins are capable of acting as both chemokines and antimicrobials. (Yeaman 2014; Yeaman 2007; Yount NY 2004) Platelets are also capable of generating and releasing reactive

oxygen species (ROS), such as hydrogen peroxide. (Dorit M, 2009) These factors can have potent effects on a variety of pathogens, including bacteria, viruses, fungi, and protozoans. (Yeaman 2014)

1.5.1.3 Pathogen internalization

The ability of platelets to internalize pathogens has been widely debated and is partially dependent on the type of pathogen. Thrombocytes, the nucleated, primitive relative of the platelet, which are present in non-mammalian vertebrates, have been shown to phagytose bacteria; suggesting that this may be a conserved function. (Negasawa T 2014) While various studies on the ability of mammalian platelets to phagocytize bacteria have shown internalization, one study by *White JG* (2000) concluded that platelets are, in fact, not phagocytes but are covercytes; bacteria appear to passively enter the platelet through the open canalicular system but are not actively phagocytosed. (White JG, 2000 and 2004; Absolom DR 1982; Youssefian T 2002) This topic is still currently under debate.

A separate mechanism by which pathogens can be found in platelets is as a sequela to the infection of their 'parent' MK cell. Viruses and viral genetic material, as one example, are frequently found in circulating platelets, but the entry of these pathogens into the platelet is via another mechanism: internalization by the 'parent' MK and subsequent development and release of 'daughter' platelets with viral particles or RNA/DNA. (Lee TH 1998; Kopko PM 2001; Youssefian T 2002; Sakaguchi M 1991) Dengue virus has been found to infect megakaryocytes and be found in circulating platelets. (Noisakran S 2012; Hsu AY 2015; Clark KB, 2012) *Anaplasma phygocytophilium* (*E. phagocytophilium*), an obligate intracellular bacterium, has been shown to infect megakaryoblasts (Meg-01 cells) and is somewhat dependent on the presence of sialylated ligands and PSGL-1 (CD162); although this infection results in a peripheral thrombocytopenia, it appears to be antigen-dependent as this bacterium is not located within the platelet itself. (Granick JL 2008) *Anaplasma platys* (*A. platys;* formerly *Ehrlichia platys*), on the other hand, is known to result in both megakaryocyte infections within the bone marrow and platelet intracellular inclusion bodies in the peripheral blood. (Inokuma H 2002; Loeffelholz MJ 2014) Although the 'infected' platelets are not always infectious, they can still be bound by anti-virus IgG and be subsequently targeted by leukocytes, resulting in a peripheral thrombocytopenia. (Assinger A 2014)

1.5.2 Indirect functions

1.5.2.1 Platelet-leukocyte aggregates

Activated platelets have a powerful tool belt of cytokines and chemokines which, upon appropriate stimulation, they release into the surrounding blood and tissue for the subsequent recruitment and activation of nearby leukocytes. While platelets themselves are able to detect all four structural classes of cytokines (C, CC, CXC, and CX_3C) and potentially undergo chemotaxis towards these signals towards sites of infection and injury, one primary way for platelets to migrate into these stimulated location is by hitching a ride on a nearby leukocyte. (36-38 of and Yeaman 2014) This interaction is primarily mediated by the CD62P-CD162 interaction. (Frydman GH 2017) Platelets can release microbicidal chemokines (aka kinocidins), such as CXC chemokine ligand 4 (CXCL4; PF-4) and CCL5 (RANTES), attracting neighboring granulocytes. (Yeaman 2014)

When platelets bind to leukocytes it is called a platelet-leukocyte aggregate; these are reported to be increased in the peripheral circulation in a number of inflammatory conditions and infections. (Michelson AD 2007; Semple JW 2011) These aggregates can have multiple functions within the body, ranging from serving as a nidus for thrombus formation to serving as a vehicle for platelet and leukocyte diapedesis and extravasation into peripheral organs and sites of infection and injury. (Semple JW 2011; Mueller WA 2013; Zuchtriegel G 2016) Depending on the type of stimulation and the specific white blood cell type, platelets can stimulate antigen presentation by antigen presenting cells, stimulate degranulation, and even stimulate extracellular trap formation. (Semple JW 2011; Morrell CN 2014) Extracellular traps are discussed further in the section 1.6, 'Extracellular traps and histones'.

1.5.2.2 Antigen presentation

Both the platelet and the megakaryocyte have important roles in antigen presentation (AP); while platelets are known to activate dendritic cells (DCs), promoting their maturation and pathogen presentation to B and T cells, megakaryocytes have been shown to act as antigen presenting cells (APCs) themselves. (Yeaman MR 2014; Kang HK 2012) Platelets are able to propagate AP in dendritic cells by attracting cells to the antigen and also binding to the pathogen, even clustering

the pathogen, in order to increase the accumulation of the pathogen in the vicinity of the APC cells. (Yeaman MR 2014) This clustering and sequestration of the bacteria by platelet binding can enhance their processing and AP to T cells. Binding to *Listeria monocytegenes (L. monocytogenes)* was also shown to expand $CD8^+$ cytotoxic T cell expansion. (Verschoor A, 2011) In the case of MKs, bipotent megakaryocyte/erythroid progenitors (MM cells) in the bone marrow and those derived from peripheral blood mononuclear cells, were demonstrated to be MHC Class II-presenting cells and have the capability of inducing Th17 in response to lupus autoantigens and foreign antigens, including *Candida albicans*. (Kang HK 2012; Finkelstein A 2015)

1.6 Extracellular traps and histones

1.6.1 Extracellular traps

Extracellular traps (ETs) are entangled net-like structures, derived from leukocytes and composed of DNA, histones, and other intracellular contents, such as cell-specific granule contents and mitochondria. ETs were originally discovered to be a controlled form of cell death performed by neutrophils (neutrophil extracellular trap; NET) in response to pathogenic stimuli. The formation of NETs is distinct from both apoptosis and necrosis, and is a reactive oxygen species (ROS) - dependent cell death. (Fuchs TA 2007) Upon sufficient stimulation, neutrophils undergo a shape change and homogenization of their eu- and heterochromatin, followed by nuclear envelope and granule membrane disintegration which allows for mixing of cytoplasmic and nuclear cell components; these mixtures are then released into the extracellular space through a break in the cell membrane. (Fuchs TA 2007)

One of the earliest and most essential steps of ET formation is the re-organization of nuclear contents by the manipulation of histone post-translational modifications (PTSMs). Histones (His; H) are highly positive proteins that are in the form of octamers (H2A, H2B, H3 and H4) and linkers (H1 and H5) that attach to and condense DNA within the nucleus. On a more molecular level, peptidylgarginine deiminase 4 (PAD4) is an essential component of successful NET formation, playing a role in histone hypercitrullination and leading to chromatin decondensation during early NET formation. (Li P 2010; Rohrbach AS 2012) NETosis can be triggered by direct stimulation

of TLRs, Fc receptors, complement receptors, and other pathogenic stimulus such as bacteria. Once sufficiently activated, an intracellular calcium flux activates NADPH oxidase, resulting in the formation of ROS. (Yang H 2016) Upon bacterial stimulation, NET formation appears to be dependent on the lipoxygenase pathway. (Clark SR 2011)

The effects of ETs within the body appear to be both beneficial and dangerous. While they appear to perform an integral function in the defense against pathogens, by entrapping them and killing them, they are considered very 'sticky' and 'irritating', both instigating and perpetuating thrombosis and inflammation. (Kaplan MJ 2012) The presence of ETs has been detected in a number of acute and chronic inflammatory conditions and are thought to serve as a nidus for intravascular clot formation as well as a source of danger-associated molecular patterns (DAMPs), such as extracellular histones, which is discussed in Section 1.6.2, 'Extracellular histones'. (Lee KH 2017; Wright TK 2016; Jorch SK 2017) The contents of the released cytokines and chemokines is directly related to the cell of origin, where NETs release myeloperoxidase (MPO) and neutrophil elastase (NE) and EETs release eosinophil granule contents. (Ueki S 2013)

1.6.2 Extracellular histones

Histones are the proteins that hold together DNA in the form of nucleosomes. There are 6 types of histones (H1, H2A, H2B, H3, H4, and H5) which all work together to form an octamer and linkers tightly condensing DNA into chromatin. In addition to their role as DNA 'glue', they also function as guides for DNA expression based on their own post-translational modifications (PTSMs), either activating or silencing transcription. Although histones are traditionally located within the nucleus of the cell, they have recently been found to be in other cellular compartments, such as in the cytoplasm and cell membrane during cellular apoptosis, or possible even attached to mitochondria as functional proteins. (Zanin MK, 2010; Choi YS, 2011) With the discovery of ET formation, extracellular histones have been more recently explored for their role in the immune and coagulation system. (Chen R 2014)

Histones, once outside the protective shell of the cell membrane, can act as DAMPs and be highly prothrombotic and proinflammatory. Histones can be present within the circulation attached to extracellular traps, attached to DNA in the form of nucleosomes, or be completely free. Histones

have been shown to interact with TLRs, activating platelets and leukocytes, complement, activating the coagulation system, and even the phospholipids of endothelial and epithelial cells, resulting in cytotoxicity. (Silk E 2017) It is postulated that extracellular histones are part of the pathophysiological mechanism of intravascular coagulation and end organ injury, not only being prothrombotic, but also being anti-fibrinolytic. (Silk E 2017; Varju I 2015; Allam R 2014) Interestingly, recent research has been elaborating on the differences between free dsNDA, free histones, and bound histones and DNA in the form of nucleosomes. (Marcsman G 2016) Currently, neutrophil DNA and histones are both pro-coagulant, but the pro-coagulant properties of neutrophil extracellular traps is being debated. (Noubouossie DF 2017)

1.7 Sepsis

Sepsis was first described by the Greeks in 700 BCE, recognizing a cause of death as 'rotting' blood, and terming the condition 'sepsis', the Greek work for decomposition or rot. (Abraham E 2016) Sepsis is the result of the body's response to an infection. It is not uncommon for this inflammatory response to become out of control and result in life-threatening complications, including shock, disseminated intravascular coagulation (DIC) and end organ dysfunction, which can include multiple organ dysfunction syndrome (MODS), acute respiratory distress syndrome (ARDS), and acute kidney injury (AKI). Although originally, the pathophysiology of sepsis was thought to be a result of a hyper-inflammatory response to a pathogenic stimulus, currently, there appears to be a shift in this paradigm, where the heterogeneity of patient's immune systems and the dynamic phases of sepsis challenge this paradigm; while some patients are immuno-stimulated, others present as immuno-suppressed. (Remick DG 2007) Changes involved in sepsis range from cellular to metabolic derangements, leading to cellular apoptosis, necrosis, and stimulation of the immune, complement, and coagulation system. (Remick DG 2007) Currently, the definition of sepsis is overly-broad and fluid, with treatment recommendations are symptomatic and supportive at best.

1.7.1 Clinical diagnosis and treatment

When diagnosing a patient with sepsis, it is important to keep in mind that the term 'sepsis' describes a syndrome and not a specific condition. What this means, is that an individual will

typically display a combination of individual symptoms that are suggestive of a serious, systemic reaction to a confirmed or suspected infection. In addition to diagnosing a patient with sepsis, there are multiple levels of sepsis, with septic shock being a more critical level, indicating active or impending hypoperfusion and end organ damage. (Howell MD, 2017) The current clinical definition of sepsis, as determined by the American Medical Association in 2016, is: evidence of infection plus life-threatening organ dysfunction, clinically characterized by an acute change of 2 points or greater in the Sequential [Sepsis-related] Organ Failure Assessment Score (SOFA). Septic shock is defined as sepsis with circulatory and cellular/metabolic abnormalities profound enough to increase mortality, characterized by the need for vasopressor therapy and elevated blood lactate after adequate fluid resuscitation. (Abraham E, 2016; Singer M 2016; Shankar-Hari M, 2016)

Once a patient is diagnosed with sepsis, the earlier treatment is started the lower the chance of long-lasting morbidity and mortality. Currently, sepsis is a leading cause of morbidity, mortality, and expense in hospitals, and can be accountable for up to half of the deaths of hospitalized patients. (Howell MD 2017) Most recently, a meta-analysis of sepsis clinical studies demonstrated a mortality rate between 38.5-51.7%. (Shankar-Hari M, 2016) The major recommendations include: infection management with broad-spectrum intravenous antimicrobials within 1 hour after sepsis recognition, infection source control, fluid resuscitation with a target mean arterial pressure (MAP) of 65 mm Hg, with vasopressors administered as needed, and mechanical ventilation in patients with sepsis-related ARDS. (Howell MD 2017) Despite the vast improvements in science and medicine, the complex pathophysiology and heterogeneity of sepsis has doctors and scientists continuing to struggle in the identification and understanding of the mechanisms underlying this deadly syndrome. Uncovering the cellular and molecular mechanisms underlying sepsis and its' acute and chronic complications are imperative in the development of new and better therapeutic tools moving forward.

1.7.2 Platelets in sepsis

Platelets have long been identified as a key player in the pathophysiology and diagnosis of sepsis. Changes in platelet indices have not only been associated with sepsis, but also correlated with prognosis. Thrombocytopenia (decreased platelet count), macrothrombocytopenia (giant platelets

in conjunction with a decreased platelet count), and reticulated platelets (platelets that stain RNA-positive with thiazole orange stain) have all been identified as negative prognostic indicators. (Gao Y, 2014) There are many hypotheses for the mechanism of these platelet changes, including decreased platelet production, secondary to decreases in mature megakaryocytes, and sequestration, from platelets forming platelet-leukocyte aggregates (PLAs) or from disseminated intravascular coagulation. (Semple JW, 2011) Platelet activation and function has also been superficially evaluated in patients with sepsis, demonstrating increased spontaneous activation concurrent with a decrease in platelet aggregation in response to various agonists. (Hurley SM 2016; Yaguchi A, 2004) Additionally, similar to other cell types, platelet have been shown to display mitochondrial dysfunction during sepsis, which coincides with general platelets hypo-responsiveness to agonists. (Protti A 2015)

Due to the heterogeneity of human patients with sepsis, various animal models are used in research, with the role of platelets during various stages and complications of sepsis being multifaceted in a number of studies. A recent mouse model of *S. pyogenes* sepsis demonstrated the dynamics of platelet activation during sepsis, with CD62P and integrin expression not increasing during bacterial dissemination, but platelet-neutrophil complexes (PNCs) increasing during early sepsis and decreasing to significantly lower levels during late sepsis. Additionally, the removal of these PNC complexes coincided with a significant increase in organ damage and the accumulation of platelets in the liver sinusoids. (Hurley SM, 2016) Another *S. pyogenes* study demonstrated that platelets may actually promote bacterial dissemination, with thrombocytopenia also coinciding with platelet activation, PNC formation, and neutrophil activation. (Kahn F 2013) A model of pneumonia-derived sepsis, utilizing *Klebsiella pneumonia*, showed that platelets are essential in the survival of gram negative sepsis, with severe thrombocytopenia resulting in infection-site hemorrhage, enhanced coagulation and endothelial cell activation, and increased proinflammatory cytokine levels. (de Stoppelaar SF 2015) While severe thrombocytopenia may promote activation of coagulation, platelets themselves play an essential role in coagulation, with platelets even working with neutrophil extracellular traps in the promotion of intravascular coagulation. (McDonald B 2017) Platelets have also been shown to be protective from septic shock, through mechanisms such as the inhibition of macrophage-dependent inflammation and activation through the COX1 signaling pathway. (Xiang B, 2013) Together, these results demonstrate that the role of

the platelet is complex and dynamic during sepsis, and may be dependent on both the type of infection and the model species.

While changes in platelet count and function appears to be a consistent factor in the diagnosis and pathology of sepsis, interestingly, the administration of platelet inhibitors also appears to have a protective effect, reducing mortality in both animal models and human patients. (Akinosoglou K 2014; Toner P 2015) Studies of sepsis have demonstrated that platelets can rapidly accumulate in the lungs and liver, resulting in life-threatening complications. (Zhao L 2002; Yadav H 2015) In light of these studies, it is not surprising that there is complimentary data to suggest that the reduction of platelet activation can be protective. For example, a mouse model of lipopolysaccharide (LPS) –induced sepsis has elucidated that inhibition of the GPIb-IX receptor complex results in decreased thrombosis in the renal glomeruli. (Yin H 2013) Clopidogrel, a P2Y12 inhibitor, was also shown to be protective in mouse models of polymicrobial sepsis. (Siedel M 2009) Many human studies also demonstrate the benefit of anti-platelet therapy on patients with sepsis, with some reports even demonstrating high-on-treatment platelet reactivity (HPR); although, the mechanism of protective effects is currently under debate. (Valerio-Rojas JC 2013; Akinosoglou K 2017; Storey RF 2014; Kiers HD 2016)

1.7.3 Megakaryocytes in sepsis

The role of megakaryocytes in sepsis is a bit more nebulous than the role of platelets. Traditionally, the only role of the MK has been the production of platelets, primarily within the bone marrow niche, as well as in the lung and other sites of extramedullary hematopoiesis (liver, spleen, and lymph nodes). MKs have been shown to potentially have other roles, such as emperipolesis (the presence of an intact cell within the cytoplasm of another cell), which has been described in conditions such as hematolymphoid disorders, including myeloproliferative and myelodysplastic disorders, and non-hematological malignancies, including multiple myeloma and neuroblastoma (Rastogi V 2014; Cashell AW, 1992). MKs may also play a more significant role in the immune system; they have recently been demonstrated to serve as a primary antigen presenting cell (APC) stimulating the Th17 response in Lupus. (Kang HK, 2012). While there are many animal models of infection that have demonstrated MK infection with viruses, such as HIV and Dengue virus, their interaction with bacteria and fungus is less

explored (Sato T 2000; Noisakran S 2012). There are rare clinical case reports that describe the presence of pathogens such as Histoplasma and Cryptococcus within MKs in the bone marrow (Ferry JA 1991). Whether this is a rare occurrence or whether it is just not investigated more frequently is not known at this time.

In the context of sepsis, there is a dearth of research into the megakaryocyte. In neonatal sepsis and necrotizing enterocolitis (NEC), thrombopoietin (TPO), the growth factor that stimulates differentiation and maturation of hematopoietic stem cells (HSCs) into MKs, has been reported to be elevated; this was more common in gram negative sepsis. This elevation in TPO was correlated with an increase in circulating MK progenitor concentrations and reticulated platelets. (Brown RE 2008) It is important to note, that there are differences in cord blood-derived MKs and adult peripheral blood derived MKs, therefore studies in the neonate may not be completely translatable to adults. (Mattia G 2002) Circulating MK fragments have been reported in adult patients with sepsis as well; the presence of these MK fragments were also demonstrated to be misidentified by the automated hematology analyzer. (Sanford D 2013) MKs are known to be increased within the lungs in the case of ARDS and their numbers have also been shown to be significantly increased within the renal glomeruli of patients with sepsis. (Broghamer WL Jr, 1981; Mandal RV 2007) Taken together, these findings suggest that changes in megakaryopoiesis and thrombopoiesis may be a factor in sepsis and that abnormal circulating MK progenitors and fragments are likely missed with automated analyzers.

Up until now, very limited controlled studies have been performed to explore the potential effect of sepsis on megakaryocyte development and maturation. There have recently been a few studies looking at the effect of lipopolysaccharide (LPS) on megakaryocyte and platelet biology. While typically, MKs bud off platelets through a controlled apoptosis mechanism, when exposed to inflammatory cytokine IL-1α they have been shown to undergo a new 'rupture' mechanism of platelet development. (Nishimura S 2015) A mouse model of sepsis also showed a molecular change within MKs during sepsis, displaying altered mRNA profiles with changes in platelet phenotype, allowing them to mediate lymphocyte toxicity through a granzyme B mechanism. (Freishtat RJ 2009). Further supporting this concept of sepsis-induced changes in the MK with subsequent platelet phenotype change is a study evaluating both the interaction of platelets with

pathogens and platelets directly from human patients with sepsis, which revealed that *Tissue factor* mRNA is spliced and results in a pro-coagulant platelet phenotype. (Rondina MT 2011) Based on the dynamic role of platelets in sepsis, as discussed in the section 1.7.3, 'Platelets in sepsis', the role of the MK both inside and outside the bone marrow niche and deviations in megakaryo- and thrombopoiesis in the context of sepsis warrant further study.

1.7.4 Extracellular traps and histones in sepsis

Recently, the formation of extracellular traps (ETs) has been discovered. Extracellular traps are extracellular 'webs' of DNA, histones, and other cellular contents that form in response to a number of stimuli, ranging from pathogenic stimulus to contact with hydrophobic surfaces. (Sperling C 2016; Delgado-Rizo V 2017) The role of extracellular traps ranges from protective, allowing for the entrapment of pathogens such as bacteria, to pathologic, stimulating and propagating intravascular thrombosis. (Sorensen OE 2016) ETs were originally described as a phenomenon performed by neutrophils (NETs); although more recently, this behavior has been demonstrated in other cell types, such as eosinophils (EETs). (Ueki S 2013) These ETs are currently under investigation and have been correlated to a number of conditions, including sepsis, autoimmune disease, and chronic inflammatory diseases.

Current research suggests that NETs are of great importance in the pathogenesis of sepsis, with NETs being significantly increased in both the peripheral circulation and end organs. (Camicia G 2014; Yang S 2017) These NETs are thought to result in further stimulation of inflammation and coagulation, potentially leading to further cell death and intravascular thrombosis, which can lead to end organ dysfunction and, ultimately death. (Sorenson OE 2016) In specific, platelets have been shown to interact with and stimulate NET formation in the context of sepsis. (Carestia A 2016; McDonald B 2017) The detection and quantification of ETs is somewhat difficult, with DNA and histones usually being rapidly degraded in the plasma and the histopathologic evaluation of NETs in tissue is rudimentary at best. (Ekaney ML 2014) Additionally, the identification of the cellular origin of free DNA and histones is not possible, as all mammalian cells are composed of the same DNA and histones; at this point in time, it is an assumption that the majority of extracellular DNA and histones during sepsis originate from neutrophils.

Extracellular (EC) histones play a large role in the pro-coagulant and proinflammatory phenotype of many conditions, and they are an essential part of ETs. (Chen R 2014) In addition to direct stimulation of white blood cells and activation of the coagulation system, EC histones are able to stimulate the complement system and can even result in direct cytotoxicity of endothelial and epithelial cells. (Chen R 2014; Silk E 2017) In autoimmune conditions, such as lupus, auto-histone antibodies have also been detected as part of the pathophysiology of the disease. (Liu CL 2012) EC histones, including H3 and H4, have been shown to be significantly increased during sepsis. (Kawasagi K 2015; Ekaney ML 2014) In specific, citrullinated histone 3 (citH3) has been shown to be necessary for NET formation and increased in the blood of septic patients. (Pan B, 2017; Li Y 2011) Studies inhibiting citH3 have even been shown to be protective and improve survival in mouse models of sepsis. (Li Y 2014) One caveat to the study of EC histones in both the research and the clinical setting is the lack of consistent and accurate histones detection assays available; specifically, one study shows that quantification of citH3 using various commercially-available and laboratory-made assays result in very different concentration measurements. (Neeli L 2016) More reliable assays have been developed, such as MALDI-TOF and other mass spectrometry methods, but are cost and training restrictive. (Garcia-Gimenez JL 2017) Additionally, there appears to be a difference in the effect of histones and DNA that is dependent on whether they are truly free or bound to each other, such as in the form of a nucleosome. (Marsman G 2016) At this time, there are no reliable methods to differentiate between free and DNA-bound EC histones. As more tools are developed for the evaluation of EC histones, in addition to quantitation, post-translational modifications (PTSMs) should also be explored in the context of sepsis.

1.8 Approach and aims of this thesis

The cumulative work described in this thesis was intended to explore the potential role of the megakaryocyte as an innate immune cell, investigate how it can transfer immune cell function to its' platelet progeny, and explore how these novel findings may play a role in the pathophysiology of end organ function in the context of sepsis. Platelets have been demonstrated to play an integral role in the pathophysiology of sepsis, in both human and animal models, while the potential role of the megakaryocyte as an immune cell has been largely ignored. (Semple JW 2011) Although

megakaryocyte and platelet number have been shown to be prognostic indicators in sepsis, the associated change in phenotype is just starting to be explored. (Rondina MT 2012) Combining the common knowledge that platelets have innate immune cell functions and that they derive their cellular contents and functions from their 'parent' megakaryocytes, our primary goal with this work was to demonstrate that the megakaryocyte must therefore also have innate immune cell functions.

The second chapter in this thesis describes the testing of megakaryocyte immune cell function. In order to test whether MKs have innate immune cell functions, we utilized a combination of *in vitro* methods, using both cord blood-derived megakaryocytes (CB MKs) and cells from a megakaryoblastic lineage (Meg-01). Experiments included a combination of approaches to determine whether MKs were capable of phagocytosis, chemotaxis, and MK extracellular trap (MET) formation to a variety of pathogenic stimulus. Although MKs were demonstrated to have many immune cell functions, the physiological relevance of these findings were somewhat questionable if the MKs are primarily constrained to the bone marrow stroma. Therefore, we utilized a combination of imaging flow cytometry on whole blood and immunohistochemistry on histopathology samples from patients with sepsis to explore whether MKs were present in the peripheral circulation and end organs during sepsis. Through retrospective evaluation of the patient medical records, we were also able to explore whether the circulating MKs had any relationship with end organ damage and prognosis, as well as with the type of infection present. Putting these results together, we then developed a hypothesis towards the mechanisms of megakaryocyte immune cell function and their role in the pathophysiology of sepsis-related complications such as end organ damage.

In chapter three, we continue with exploring the observation that CB MKs and Meg-01 cells frequently have extranuclear histones. Taking into account that platelets are pre-packaged buds of the MK cell membrane and cytoplasm, we then explored whether platelets contained histones, and whether these histones could be derived directly from their 'parent' MK cell. Using a combination of immunofluorescence, flow cytometry, and transmission electron microscopy with immuno-gold labeling, we were able to investigate whether MKs do indeed have extranuclear histones and whether their progeny platelets have histones as a result. Additionally, we used imaging flow

cytometry to evaluate the platelet phenotype of patients with sepsis, testing for the presence of histones, DNA, and platelet activation. By retrospectively reviewing patient medical records, we were then able to correlate the platelet phenotype with both, patient prognosis and the type of infection present. With this information, we were able to add on to the role of the megakaryocyte and platelets in the pathophysiology of sepsis and end organ damage.

In chapters four and appendix chapter one, we developed a new tool for the evaluation of platelet phenotypes and performed preliminary experiments on the effect of endotoxin on megakaryocyte phenotype. In order to further the exploration of megakaryocyte and platelet phenotypes in inflammation and sepsis, we had to develop a novel approach for the evaluation of platelet-leukocyte interactions. In order to do this, we utilized a microfluidic approach, where the platelet-neutrophil interaction could be analyzed *in vitro* on a single-cell level. Combining this technique with fluorescent imaging and cell-tracking software, we characterized the neutrophil chemotaxis phenotype when alone, when in the presence of platelets, and when attached and carrying a platelet. In appendix chapter one, we then cultured and differentiated megakaryocytes in the presence of *Escherichia coli* (*E. coli*) endotoxin and evaluated whether this pathogenic stimulation resulted in an altered megakaryocyte phenotype. Using both imaging and flow cytometry, we were able to morphologically characterize cell changes. These preliminary experiments and results demonstrate that phenotype changes in megakaryocytes most likely occur during systemic infections and further warrant exploration of resultant platelet phenotypes.

Overall, our results indicate that the megakaryocyte does have an active role in the innate immune system and that properties of the megakaryocyte are passed on to its' progeny platelets. Taken together, the *in vitro* and *ex vivo* experimental results suggest that both MKs and platelets likely play an important role in sepsis and end organ damage.

1.9 Acknowledgements

We would like to acknowledge both Dr. Kelly A Metcalf Pate and Dr. Allison Vitsky, who co-authored part of this introduction. Martin Selig for the transmission electron microscopy images of megakaryocytes and platelets. J. Woodland Pomeroy for his aid in generating original figures

for this work. Nathan M. Pate for his aid in referencing this work. Alyssa Pappa for her assistance in bibliography management.

1.10 References

1. Kaushansky K. The molecular mechanisms that control thrombopoiesis. The Journal of clinical investigation 2005;115:3339-47.
2. Italiano JE, Jr., Patel-Hett S, Hartwig JH. Mechanics of proplatelet elaboration. Journal of thrombosis and haemostasis : JTH 2007;5 Suppl 1:18-23.
3. Nakeff A, Maat B. Separation of megakaryocytes from mouse bone marrow by velocity sedimentation. Blood 1974;43:591-5.
4. Long MW, Williams N, Ebbe S. Immature megakaryocytes in the mouse: physical characteristics, cell cycle status, and in vitro responsiveness to thrombopoietic stimulatory factor. Blood 1982;59:569-75.
5. Gordon MY, Bearpark AD, Clarke D, et al. Haemopoietic stem cell subpopulations in mouse and man: discrimination by differential adherence and marrow repopulating ability. Bone marrow transplantation 1990;5 Suppl 1:6-8.
6. Ogawa M. Differentiation and proliferation of hematopoietic stem cells. Blood 1993;81:2844-53.
7. Morita Y, Iseki A, Okamura S, et al. Functional characterization of hematopoietic stem cells in the spleen. Experimental hematology 2011;39:351-9 e3.
8. Nakorn TN, Miyamoto T, Weissman IL. Characterization of mouse clonogenic megakaryocyte progenitors. Proceedings of the National Academy of Sciences of the United States of America 2003;100:205-10.
9. Woolthuis CM, Park CY. Hematopoietic stem/progenitor cell commitment to the megakaryocyte lineage. Blood 2016;127:1242-8.
10. Kuter DJ. The biology of thrombopoietin and thrombopoietin receptor agonists. International journal of hematology 2013;98:10-23.
11. Bartley TD, Bogenberger J, Hunt P, et al. Identification and cloning of a megakaryocyte growth and development factor that is a ligand for the cytokine receptor Mpl. Cell 1994;77:1117-24.
12. Vigon I, Florindo C, Fichelson S, et al. Characterization of the murine Mpl proto-oncogene, a member of the hematopoietic cytokine receptor family: molecular cloning, chromosomal location and evidence for a function in cell growth. Oncogene 1993;8:2607-15.
13. Kaushansky K, Hitchcock I. Chapter 25: Thrombopoietin. In: Marder VJ, Aird WC, Bennett JS, Schulman S, White GC, eds. Hemostasis and thrombosis : basic principles and clinical practice. 6th ed. Philadelphia: Wolters Kluwer/Lippincott Williams & Wilkins Health; 2013:373-81.
14. Murone M, Carpenter DA, de Sauvage FJ. Hematopoietic deficiencies in c-mpl and TPO knockout mice. Stem cells 1998;16:1-6.
15. Stahl CP, Zucker-Franklin D, Evatt BL, et al. Effects of human interleukin-6 on megakaryocyte development and thrombocytopoiesis in primates. Blood 1991;78:1467-75.
16. Wu D, Xie J, Wang X, et al. Micro-concentration Lipopolysaccharide as a Novel Stimulator of Megakaryocytopoiesis that Synergizes with IL-6 for Platelet Production. Scientific reports 2015;5:13748.
17. Borde EC, Vainchenker W. Chapter 23: Platelet Production: Cellular and Modular Regulation. In: Marder VJ, Aird WC, Bennett JS, Schulman S, White GC, eds. Hemostasis and thrombosis : basic principles and clinical practice. 6th ed. Philadelphia: Wolters Kluwer/Lippincott Williams & Wilkins Health; 2013:349-64.

18. Jiang S, Levine JD, Fu Y, et al. Cytokine production by primary bone marrow megakaryocytes. Blood 1994;84:4151-6.
19. Tomer A, Bar-Lev S, Fleisher S, et al. Antiphospholipid antibody syndrome: the flow cytometric annexin A5 competition assay as a diagnostic tool. British journal of haematology 2007;139:113-20.
20. Zimmet J, Ravid K. Polyploidy: occurrence in nature, mechanisms, and significance for the megakaryocyte-platelet system. Experimental hematology 2000;28:3-16.
21. Stenberg PE, Levin J. Mechanisms of platelet production. Blood cells 1989;15:23-47.
22. van den Oudenrijn S, von dem Borne AE, de Haas M. Differences in megakaryocyte expansion potential between CD34(+) stem cells derived from cord blood, peripheral blood, and bone marrow from adults and children. Experimental hematology 2000;28:1054-61.
23. Schipper LF, Brand A, Reniers N, et al. Differential maturation of megakaryocyte progenitor cells from cord blood and mobilized peripheral blood. Experimental hematology 2003;31:324-30.
24. Datta NS, Williams JL, Caldwell J, et al. Novel alterations in CDK1/cyclin B1 kinase complex formation occur during the acquisition of a polyploid DNA content. Molecular biology of the cell 1996;7:209-23.
25. Garcia P, Cales C. Endoreplication in megakaryoblastic cell lines is accompanied by sustained expression of G1/S cyclins and downregulation of cdc25C. Oncogene 1996;13:695-703.
26. Zhang Y, Wang Z, Ravid K. The cell cycle in polyploid megakaryocytes is associated with reduced activity of cyclin B1-dependent cdc2 kinase. The Journal of biological chemistry 1996;271:4266-72.
27. Zhang Y, Wang Z, Liu DX, et al. Ubiquitin-dependent degradation of cyclin B is accelerated in polyploid megakaryocytes. The Journal of biological chemistry 1998;273:1387-92.
28. Lordier L, Bluteau D, Jalil A, et al. RUNX1-induced silencing of non-muscle myosin heavy chain IIB contributes to megakaryocyte polyploidization. Nature communications 2012;3:717.
29. Lordier L, Jalil A, Aurade F, et al. Megakaryocyte endomitosis is a failure of late cytokinesis related to defects in the contractile ring and Rho/Rock signaling. Blood 2008;112:3164-74.
30. Geddis AE, Fox NE, Tkachenko E, et al. Endomitotic megakaryocytes that form a bipolar spindle exhibit cleavage furrow ingression followed by furrow regression. Cell cycle (Georgetown, Tex) 2007;6:455-60.
31. Mazharian A, Mori J, Wang YJ, et al. Megakaryocyte-specific deletion of the protein-tyrosine phosphatases Shp1 and Shp2 causes abnormal megakaryocyte development, platelet production, and function. Blood 2013;121:4205-20.
32. Birkenfeld J, Nalbant P, Bohl BP, et al. GEF-H1 modulates localized RhoA activation during cytokinesis under the control of mitotic kinases. Developmental cell 2007;12:699-712.
33. Melendez J, Stengel K, Zhou X, et al. RhoA GTPase is dispensable for actomyosin regulation but is essential for mitosis in primary mouse embryonic fibroblasts. The Journal of biological chemistry 2011;286:15132-7.
34. Gao Y, Smith E, Ker E, et al. Role of RhoA-specific guanine exchange factors in regulation of endomitosis in megakaryocytes. Developmental cell 2012;22:573-84.
35. Petronczki M, Glotzer M, Kraut N, et al. Polo-like kinase 1 triggers the initiation of cytokinesis in human cells by promoting recruitment of the RhoGEF Ect2 to the central spindle. Developmental cell 2007;12:713-25.
36. Zimmet JM, Ladd D, Jackson CW, et al. A role for cyclin D3 in the endomitotic cell cycle. Molecular and cellular biology 1997;17:7248-59.

37. Muntean AG, Pang L, Poncz M, et al. Cyclin D-Cdk4 is regulated by GATA-1 and required for megakaryocyte growth and polyploidization. Blood 2007;109:5199-207.
38. Eliades A, Papadantonakis N, Ravid K. New roles for cyclin E in megakaryocytic polyploidization. The Journal of biological chemistry 2010;285:18909-17.
39. Kosoff RE, Aslan JE, Kostyak JC, et al. Pak2 restrains endomitosis during megakaryopoiesis and alters cytoskeleton organization. Blood 2015;125:2995-3005.
40. Trakala M, Partida D, Salazar-Roa M, et al. Activation of the endomitotic spindle assembly checkpoint and thrombocytopenia in Plk1-deficient mice. Blood 2015;126:1707-14.
41. Pawlikowska P, Fouchet P, Vainchenker W, et al. Defective endomitosis during megakaryopoiesis leads to thrombocytopenia in Fanca-/- mice. Blood 2014;124:3613-23.
42. Giammona LM, Fuhrken PG, Papoutsakis ET, et al. Nicotinamide (vitamin B3) increases the polyploidisation and proplatelet formation of cultured primary human megakaryocytes. British journal of haematology 2006;135:554-66.
43. Leysi-Derilou Y, Duchesne C, Garnier A, et al. Single-cell level analysis of megakaryocyte growth and development. Differentiation; research in biological diversity 2012;83:200-9.
44. Konieczna IM, Panuganti S, DeLuca TA, et al. Administration of nicotinamide does not increase platelet levels in mice. Blood cells, molecules & diseases 2013;50:171-6.
45. Breton-Gorius J, Guichard J. Ultrastructural localization of peroxidase activity in human platelets and megakaryocytes. The American journal of pathology 1972;66:277-93.
46. Yamada E. The fine structure of the megakaryocyte in the mouse spleen. Acta anatomica 1957;29:267-90.
47. Radley JM, Haller CJ. The demarcation membrane system of the megakaryocyte: a misnomer? Blood 1982;60:213-9.
48. Machlus KR, Italiano JE, Jr. The incredible journey: From megakaryocyte development to platelet formation. The Journal of cell biology 2013;201:785-96.
49. Eckly A, Heijnen H, Pertuy F, et al. Biogenesis of the demarcation membrane system (DMS) in megakaryocytes. Blood 2014;123:921-30.
50. Chen WF, Lee JJ, Chang CC, et al. Platelet protease-activated receptor (PAR)4, but not PAR1, associated with neutral sphingomyelinase responsible for thrombin-stimulated ceramide-NF-kappaB signaling in human platelets. Haematologica 2013;98:793-801.
51. Aster RH. Studies of the mechanism of "hypersplenic" thrombocytopenia in rats. The Journal of laboratory and clinical medicine 1967;70:736-51.
52. Harker LA, Finch CA. Thrombokinetics in man. The Journal of clinical investigation 1969;48:963-74.
53. Jackson CW, Edwards CC. Biphasic thrombopoietic response to severe hypobaric hypoxia. British journal of haematology 1977;35:233-44.
54. Hamada T, Mohle R, Hesselgesser J, et al. Transendothelial migration of megakaryocytes in response to stromal cell-derived factor 1 (SDF-1) enhances platelet formation. The Journal of experimental medicine 1998;188:539-48.
55. Takahashi R, Sekine N, Nakatake T. Influence of monoclonal antiplatelet glycoprotein antibodies on in vitro human megakaryocyte colony formation and proplatelet formation. Blood 1999;93:1951-8.
56. Balduini A, Malara A, Balduini CL, et al. Megakaryocytes derived from patients with the classical form of Bernard-Soulier syndrome show no ability to extend proplatelets in vitro. Platelets 2011;22:308-11.

57. Richardson JL, Shivdasani RA, Boers C, et al. Mechanisms of organelle transport and capture along proplatelets during platelet production. Blood 2005;106:4066-75.
58. Tavassoli M, Aoki M. Localization of megakaryocytes in the bone marrow. Blood cells 1989;15:3-14.
59. Thon JN, Italiano JE. Platelets: production, morphology and ultrastructure. Handb Exp Pharmacol 2012:3-22.
60. Thon JN, Montalvo A, Patel-Hett S, et al. Cytoskeletal mechanics of proplatelet maturation and platelet release. The Journal of cell biology 2010;191:861-74.
61. Italiano JE, Jr., Lecine P, Shivdasani RA, et al. Blood platelets are assembled principally at the ends of proplatelet processes produced by differentiated megakaryocytes. The Journal of cell biology 1999;147:1299-312.
62. Patel SR, Hartwig JH, Italiano JE, Jr. The biogenesis of platelets from megakaryocyte proplatelets. The Journal of clinical investigation 2005;115:3348-54.
63. Rao AK, Jalagadugula G, Sun L. Inherited defects in platelet signaling mechanisms. Seminars in thrombosis and hemostasis 2004;30:525-35.
64. Li J, Dai K, Wang Z, et al. Platelet functional alterations in a Bernard-Soulier syndrome patient with filamin A mutation. Journal of hematology & oncology 2015;8:79.
65. Wang Z, Zhao X, Duan W, et al. A novel mutation in the transmembrane region of glycoprotein IX associated with Bernard-Soulier syndrome. Thrombosis and haemostasis 2004;92:606-13.
66. Lecine P, Italiano JE, Jr., Kim SW, et al. Hematopoietic-specific beta 1 tubulin participates in a pathway of platelet biogenesis dependent on the transcription factor NF-E2. Blood 2000;96:1366-73.
67. Patel SR, Richardson JL, Schulze H, et al. Differential roles of microtubule assembly and sliding in proplatelet formation by megakaryocytes. Blood 2005;106:4076-85.
68. Kunishima S, Kobayashi R, Itoh TJ, et al. Mutation of the beta1-tubulin gene associated with congenital macrothrombocytopenia affecting microtubule assembly. Blood 2009;113:458-61.
69. Seri M, Cusano R, Gangarossa S, et al. Mutations in MYH9 result in the May-Hegglin anomaly, and Fechtner and Sebastian syndromes. The May-Heggllin/Fechtner Syndrome Consortium. Nature genetics 2000;26:103-5.
70. Kelley MJ, Jawien W, Ortel TL, et al. Mutation of MYH9, encoding non-muscle myosin heavy chain A, in May-Hegglin anomaly. Nature genetics 2000;26:106-8.
71. Zhang Y, Conti MA, Malide D, et al. Mouse models of MYH9-related disease: mutations in nonmuscle myosin II-A. Blood 2012;119:238-50.
72. Pleines I, Dutting S, Cherpokova D, et al. Defective tubulin organization and proplatelet formation in murine megakaryocytes lacking Rac1 and Cdc42. Blood 2013;122:3178-87.
73. Blair P, Flaumenhaft R. Platelet alpha-granules: basic biology and clinical correlates. Blood reviews 2009;23:177-89.
74. Heijnen HF, Debili N, Vainchencker W, et al. Multivesicular bodies are an intermediate stage in the formation of platelet alpha-granules. Blood 1998;91:2313-25.
75. Youssefian T, Cramer EM. Megakaryocyte dense granule components are sorted in multivesicular bodies. Blood 2000;95:4004-7.
76. Italiano JE, Jr., Richardson JL, Patel-Hett S, et al. Angiogenesis is regulated by a novel mechanism: pro- and antiangiogenic proteins are organized into separate platelet alpha granules and differentially released. Blood 2008;111:1227-33.

77. Kamykowski J, Carlton P, Sehgal S, et al. Quantitative immunofluorescence mapping reveals little functional coclustering of proteins within platelet alpha-granules. Blood 2011;118:1370-3.
78. Jonnalagadda D, Izu LT, Whiteheart SW. Platelet secretion is kinetically heterogeneous in an agonist-responsive manner. Blood 2012;120:5209-16.
79. Peters CG, Michelson AD, Flaumenhaft R. Granule exocytosis is required for platelet spreading: differential sorting of alpha-granules expressing VAMP-7. Blood 2012;120:199-206.
80. van Nispen tot Pannerden H, de Haas F, Geerts W, et al. The platelet interior revisited: electron tomography reveals tubular alpha-granule subtypes. Blood 2010;116:1147-56.
81. Albers CA, Cvejic A, Favier R, et al. Exome sequencing identifies NBEAL2 as the causative gene for gray platelet syndrome. Nature genetics 2011;43:735-7.
82. Gunay-Aygun M, Falik-Zaccai TC, Vilboux T, et al. NBEAL2 is mutated in gray platelet syndrome and is required for biogenesis of platelet alpha-granules. Nature genetics 2011;43:732-4.
83. Kahr WH, Hinckley J, Li L, et al. Mutations in NBEAL2, encoding a BEACH protein, cause gray platelet syndrome. Nature genetics 2011;43:738-40.
84. Deppermann C, Cherpokova D, Nurden P, et al. Gray platelet syndrome and defective thrombo-inflammation in Nbeal2-deficient mice. The Journal of clinical investigation 2013.
85. Kahr WH, Lo RW, Li L, et al. Abnormal megakaryocyte development and platelet function in Nbeal2(-/-) mice. Blood 2013;122:3349-58.
86. De Botton S, Sabri S, Daugas E, et al. Platelet formation is the consequence of caspase activation within megakaryocytes. Blood 2002;100:1310-7.
87. Clarke MC, Savill J, Jones DB, et al. Compartmentalized megakaryocyte death generates functional platelets committed to caspase-independent death. The Journal of cell biology 2003;160:577-87.
88. Josefsson EC, James C, Henley KJ, et al. Megakaryocytes possess a functional intrinsic apoptosis pathway that must be restrained to survive and produce platelets. The Journal of experimental medicine 2011;208:2017-31.
89. Morison IM, Cramer Borde EM, Cheesman EJ, et al. A mutation of human cytochrome c enhances the intrinsic apoptotic pathway but causes only thrombocytopenia. Nature genetics 2008;40:387-9.
90. Iancu-Rubin C, Mosoyan G, Glenn K, et al. Activation of p53 by the MDM2 inhibitor RG7112 impairs thrombopoiesis. Experimental hematology 2014;42:137-45 e5.
91. Machlus KR, Johnson KE, Kulenthirarajan R, et al. CCL5 derived from platelets increases megakaryocyte proplatelet formation. Blood 2016;127:921-6.
92. Lopez JA. The platelet Fc receptor: a new role for an old actor. Blood 2013;121:1674-5.
93. White MJ, Schoenwaelder SM, Josefsson EC, et al. Caspase-9 mediates the apoptotic death of megakaryocytes and platelets, but is dispensable for their generation and function. Blood 2012;119:4283-90.
94. Nishimura S, Nagasaki M, Kunishima S, et al. IL-1alpha induces thrombopoiesis through megakaryocyte rupture in response to acute platelet needs. The Journal of cell biology 2015;209:453-66.
95. Schwertz H, Koster S, Kahr WH, et al. Anucleate platelets generate progeny. Blood 2010;115:3801-9.

96. Howell WH, Donahue DD. THE PRODUCTION OF BLOOD PLATELETS IN THE LUNGS. The Journal of experimental medicine 1937;65:177-203.
97. Fuentes R, Wang Y, Hirsch J, et al. Infusion of mature megakaryocytes into mice yields functional platelets. The Journal of clinical investigation 2010;120:3917-22.
98. Bath PM, Butterworth RJ. Platelet size: measurement, physiology and vascular disease. Blood coagulation & fibrinolysis : an international journal in haemostasis and thrombosis 1996;7:157-61.
99. Kamath S, Blann AD, Lip GY. Platelet activation: assessment and quantification. European heart journal 2001;22:1561-71.
100. Berger JS, Eraso LH, Xie D, et al. Mean platelet volume and prevalence of peripheral artery disease, the National Health and Nutrition Examination Survey, 1999-2004. Atherosclerosis 2010;213:586-91.
101. Chu SG, Becker RC, Berger PB, et al. Mean platelet volume as a predictor of cardiovascular risk: a systematic review and meta-analysis. Journal of thrombosis and haemostasis : JTH 2010;8:148-56.
102. Slavka G, Perkmann T, Haslacher H, et al. Mean platelet volume may represent a predictive parameter for overall vascular mortality and ischemic heart disease. Arteriosclerosis, thrombosis, and vascular biology 2011;31:1215-8.
103. Andrews RK, Gardiner EE, Shen Y, et al. Glycoprotein Ib-IX-V. The international journal of biochemistry & cell biology 2003;35:1170-4.
104. Modderman PW, Admiraal LG, Sonnenberg A, et al. Glycoproteins V and Ib-IX form a noncovalent complex in the platelet membrane. The Journal of biological chemistry 1992;267:364-9.
105. Clemetson KJ, Clemetson JM. Platelet GPIb-V-IX complex. Structure, function, physiology, and pathology. Seminars in thrombosis and hemostasis 1995;21:130-6.
106. Ozaki Y, Asazuma N, Suzuki-Inoue K, et al. Platelet GPIb-IX-V-dependent signaling. Journal of thrombosis and haemostasis : JTH 2005;3:1745-51.
107. Li R, Emsley J. The organizing principle of the platelet glycoprotein Ib-IX-V complex. Journal of thrombosis and haemostasis : JTH 2013;11:605-14.
108. Lopez JA, Andrews RK, Afshar-Kharghan V, et al. Bernard-Soulier syndrome. Blood 1998;91:4397-418.
109. Denorme F, De Meyer SF. The VWF-GPIb axis in ischaemic stroke: lessons from animal models. Thrombosis and haemostasis 2016;116:597-604.
110. Takahashi M, Yamashita A, Moriguchi-Goto S, et al. Critical role of von Willebrand factor and platelet interaction in venous thromboembolism. Histology and histopathology 2009;24:1391-8.
111. Bergmeier W, Piffath CL, Goerge T, et al. The role of platelet adhesion receptor GPIbalpha far exceeds that of its main ligand, von Willebrand factor, in arterial thrombosis. Proceedings of the National Academy of Sciences of the United States of America 2006;103:16900-5.
112. Momi S, Tantucci M, Van Roy M, et al. Reperfusion of cerebral artery thrombosis by the GPIb-VWF blockade with the Nanobody ALX-0081 reduces brain infarct size in guinea pigs. Blood 2013;121:5088-97.
113. Berndt MC, Andrews RK. Chapter 26a: Major Platelet Glycoproteins: Platelet Glycoprotein Ib-IX-V. In: Marder VJ, Aird WC, Bennett JS, Schulman S, White GC, eds. Hemostasis and thrombosis : basic principles and clinical practice. 6th ed. Philadelphia: Wolters Kluwer/Lippincott Williams & Wilkins Health; 2013:382-5

114. Suter CM, Hogg PJ, Price JT, et al. Identification and characterisation of a platelet GPIb/V/IX-like complex on human breast cancers: implications for the metastatic process. Japanese journal of cancer research : Gann 2001;92:1082-92.
115. Corken A, Russell S, Dent J, et al. Platelet glycoprotein Ib-IX as a regulator of systemic inflammation. Arteriosclerosis, thrombosis, and vascular biology 2014;34:996-1001.
116. Jain S, Zuka M, Liu J, et al. Platelet glycoprotein Ib alpha supports experimental lung metastasis. Proceedings of the National Academy of Sciences of the United States of America 2007;104:9024-8.
117. Berndt MC, Shen Y, Dopheide SM, et al. The vascular biology of the glycoprotein Ib-IX-V complex. Thrombosis and haemostasis 2001;86:178-88.
118. Zhang W, Deng W, Zhou L, et al. Identification of a juxtamembrane mechanosensitive domain in the platelet mechanosensor glycoprotein Ib-IX complex. Blood 2015;125:562-9.
119. Moog S, Mangin P, Lenain N, et al. Platelet glycoprotein V binds to collagen and participates in platelet adhesion and aggregation. Blood 2001;98:1038-46.
120. Jarvis GE, Atkinson BT, Snell DC, et al. Distinct roles of GPVI and integrin alpha(2)beta(1) in platelet shape change and aggregation induced by different collagens. Brit J Pharmacol 2002;137:107-17.
121. Nieswandt B, Watson SP. Platelet-collagen interaction: is GPVI the central receptor? Blood 2003;102:449-61.
122. Gardiner EE, Karunakaran D, Shen Y, et al. Controlled shedding of platelet glycoprotein (GP)VI and GPIb-IX-V by ADAM family metalloproteinases. Journal of thrombosis and haemostasis : JTH 2007;5:1530-7.
123. Mo X, Nguyen NX, Mu FT, et al. Transmembrane and trans-subunit regulation of ectodomain shedding of platelet glycoprotein Ibalpha. The Journal of biological chemistry 2010;285:32096-104.
124. Andrews RK, Munday AD, Mitchell CA, et al. Interaction of calmodulin with the cytoplasmic domain of the platelet membrane glycoprotein Ib-IX-V complex. Blood 2001;98:681-7.
125. Arthur JF, Shen Y, Gardiner EE, et al. TNF receptor-associated factor 4 (TRAF4) is a novel binding partner of glycoprotein Ib and glycoprotein VI in human platelets. Journal of thrombosis and haemostasis : JTH 2011;9:163-72.
126. Andrews RK, Fox JE. Identification of a region in the cytoplasmic domain of the platelet membrane glycoprotein Ib-IX complex that binds to purified actin-binding protein. The Journal of biological chemistry 1992;267:18605-11.
127. Nakamura F, Pudas R, Heikkinen O, et al. The structure of the GPIb-filamin A complex. Blood 2006;107:1925-32.
128. Feghhi S, Munday AD, Tooley WW, et al. Glycoprotein Ib-IX-V Complex Transmits Cytoskeletal Forces That Enhance Platelet Adhesion. Biophysical journal 2016;111:601-8.
129. Coller BS, Shattil SJ. The GPIIb/IIIa (integrin alphaIIbbeta3) odyssey: a technology-driven saga of a receptor with twists, turns, and even a bend. Blood 2008;112:3011-25.
130. Calvete JJ. On the structure and function of platelet integrin alpha IIb beta 3, the fibrinogen receptor. Proceedings of the Society for Experimental Biology and Medicine Society for Experimental Biology and Medicine (New York, NY) 1995;208:346-60.

131. Jennings LK, Phillips DR. Purification of glycoproteins IIb and III from human platelet plasma membranes and characterization of a calcium-dependent glycoprotein IIb-III complex. The Journal of biological chemistry 1982;257:10458-66.
132. Kunicki TJ, Pidard D, Rosa JP, et al. The formation of Ca++-dependent complexes of platelet membrane glycoproteins IIb and IIIa in solution as determined by crossed immunoelectrophoresis. Blood 1981;58:268-78.
133. Suzuki H, Kaneko T, Sakamoto T, et al. Redistribution of alpha-granule membrane glycoprotein IIb/IIIa (integrin alpha IIb beta 3) to the surface membrane of human platelets during the release reaction. Journal of electron microscopy 1994;43:282-9.
134. Wencel-Drake JD, Plow EF, Kunicki TJ, et al. Localization of internal pools of membrane glycoproteins involved in platelet adhesive responses. The American journal of pathology 1986;124:324-34.
135. Reininger AJ. Function of von Willebrand factor in haemostasis and thrombosis. Haemophilia : the official journal of the World Federation of Hemophilia 2008;14 Suppl 5:11-26.
136. Marguerie GA, Plow EF, Edgington TS. Human platelets possess an inducible and saturable receptor specific for fibrinogen. The Journal of biological chemistry 1979;254:5357-63.
137. Knezevic I, Leisner TM, Lam SC. Direct binding of the platelet integrin alphaIIbbeta3 (GPIIb-IIIa) to talin. Evidence that interaction is mediated through the cytoplasmic domains of both alphaIIb and beta3. The Journal of biological chemistry 1996;271:16416-21.
138. Crittenden JR, Bergmeier W, Zhang Y, et al. CalDAG-GEFI integrates signaling for platelet aggregation and thrombus formation. Nature medicine 2004;10:982-6.
139. Bergmeier W, Stefanini L. Novel molecules in calcium signaling in platelets. Journal of thrombosis and haemostasis : JTH 2009;7 Suppl 1:187-90.
140. Cifuni SM, Wagner DD, Bergmeier W. CalDAG-GEFI and protein kinase C represent alternative pathways leading to activation of integrin alphaIIbbeta3 in platelets. Blood 2008;112:1696-703.
141. Stefanini L, Roden RC, Bergmeier W. CalDAG-GEFI is at the nexus of calcium-dependent platelet activation. Blood 2009;114:2506-14.
142. Bertagnolli ME, Locke SJ, Hensler ME, et al. Talin distribution and phosphorylation in thrombin-activated platelets. Journal of cell science 1993;106 (Pt 4):1189-99.
143. Escolar G, Diaz-Ricart M, White JG. Talin does not associate exclusively with alpha 2b beta 3 integrin in activated human platelets. The Journal of laboratory and clinical medicine 1995;125:597-607.
144. Petrich BG, Marchese P, Ruggeri ZM, et al. Talin is required for integrin-mediated platelet function in hemostasis and thrombosis. The Journal of experimental medicine 2007;204:3103-11.
145. Watanabe N, Bodin L, Pandey M, et al. Mechanisms and consequences of agonist-induced talin recruitment to platelet integrin alphaIIbbeta3. The Journal of cell biology 2008;181:1211-22.
146. Nieswandt B, Moser M, Pleines I, et al. Loss of talin1 in platelets abrogates integrin activation, platelet aggregation, and thrombus formation in vitro and in vivo. The Journal of experimental medicine 2007;204:3113-8.
147. Ye F, Petrich BG, Anekal P, et al. The mechanism of kindlin-mediated activation of integrin alphaIIbbeta3. Current biology : CB 2013;23:2288-95.

148. Moser M, Nieswandt B, Ussar S, et al. Kindlin-3 is essential for integrin activation and platelet aggregation. Nature medicine 2008;14:325-30.
149. Shattil SJ, Kim C, Ginsberg MH. The final steps of integrin activation: the end game. Nature reviews Molecular cell biology 2010;11:288-300.
150. Arias-Salgado EG, Lizano S, Sarkar S, et al. Src kinase activation by direct interaction with the integrin beta cytoplasmic domain. Proceedings of the National Academy of Sciences of the United States of America 2003;100:13298-302.
151. Senis YA, Mazharian A, Mori J. Src family kinases: at the forefront of platelet activation. Blood 2014;124:2013-24.
152. Obergfell A, Eto K, Mocsai A, et al. Coordinate interactions of Csk, Src, and Syk kinases with [alpha]IIb[beta]3 initiate integrin signaling to the cytoskeleton. The Journal of cell biology 2002;157:265-75.
153. Phillips DR, Prasad KS, Manganello J, et al. Integrin tyrosine phosphorylation in platelet signaling. Current opinion in cell biology 2001;13:546-54.
154. Ablooglu AJ, Kang J, Petrich BG, et al. Antithrombotic effects of targeting alphaIIbbeta3 signaling in platelets. Blood 2009;113:3585-92.
155. Law DA, DeGuzman FR, Heiser P, et al. Integrin cytoplasmic tyrosine motif is required for outside-in alphaIIbbeta3 signalling and platelet function. Nature 1999;401:808-11.
156. Ye F, Ginsberg MH. Chapter 26b: Major Platelet Glycoproteins: Integrin αIIbβ3 (GPIIb-IIIa). In: Marder VJ, Aird WC, Bennett JS, Schulman S, White GC, eds. Hemostasis and thrombosis : basic principles and clinical practice. 6th ed. Philadelphia: Wolters Kluwer/Lippincott Williams & Wilkins Health; 2013:386-92

157. Arthur WT, Petch LA, Burridge K. Integrin engagement suppresses RhoA activity via a c-Src-dependent mechanism. Current biology : CB 2000;10:719-22.
158. Ren XD, Kiosses WB, Schwartz MA. Regulation of the small GTP-binding protein Rho by cell adhesion and the cytoskeleton. The EMBO journal 1999;18:578-85.
159. Flevaris P, Stojanovic A, Gong H, et al. A molecular switch that controls cell spreading and retraction. The Journal of cell biology 2007;179:553-65.
160. Miranti CK, Leng L, Maschberger P, et al. Identification of a novel integrin signaling pathway involving the kinase Syk and the guanine nucleotide exchange factor Vav1. Current biology : CB 1998;8:1289-99.
161. Huveneers S, Danen EH. Adhesion signaling - crosstalk between integrins, Src and Rho. Journal of cell science 2009;122:1059-69.
162. Pollitt AY, Poulter NS, Gitz E, et al. Syk and Src family kinases regulate C-type lectin receptor 2 (CLEC-2)-mediated clustering of podoplanin and platelet adhesion to lymphatic endothelial cells. The Journal of biological chemistry 2014;289:35695-710.
163. Kasirer-Friede A, Kang J, Kahner B, et al. ADAP interactions with talin and kindlin promote platelet integrin alphaIIbbeta3 activation and stable fibrinogen binding. Blood 2014;123:3156-65.
164. Lee H, Nurden AT, Thomaidis A, et al. Relationship between fibrinogen binding and the platelet glycoprotein deficiencies in Glanzmann's thrombasthenia type I and type II. British journal of haematology 1981;48:47-57.
165. Nurden AT, Rosa JP, Fournier D, et al. A variant of Glanzmann's thrombasthenia with abnormal glycoprotein IIb-IIIa complexes in the platelet membrane. The Journal of clinical investigation 1987;79:962-9.

166. Phillips DR, Agin PP. Platelet membrane defects in Glanzmann's thrombasthenia. Evidence for decreased amounts of two major glycoproteins. The Journal of clinical investigation 1977;60:535-45.
167. McDowall A, Svensson L, Stanley P, et al. Two mutations in the KINDLIN3 gene of a new leukocyte adhesion deficiency III patient reveal distinct effects on leukocyte function in vitro. Blood 2010;115:4834-42.
168. Manevich-Mendelson E, Feigelson SW, Pasvolsky R, et al. Loss of Kindlin-3 in LAD-III eliminates LFA-1 but not VLA-4 adhesiveness developed under shear flow conditions. Blood 2009;114:2344-53.
169. Meller J, Malinin NL, Panigrahi S, et al. Novel aspects of Kindlin-3 function in humans based on a new case of leukocyte adhesion deficiency III. Journal of thrombosis and haemostasis : JTH 2012;10:1397-408.
170. Hynes RO. Integrins: bidirectional, allosteric signaling machines. Cell 2002;110:673-87.
171. Barczyk M, Carracedo S, Gullberg D. Integrins. Cell and tissue research 2010;339:269-80.
172. Takada Y, Ye X, Simon S. The integrins. Genome biology 2007;8:215.
173. Depraetere H, Wille C, Gansemans Y, et al. The integrin alpha 2 beta 1 (GPIa/IIa)-I-domain inhibits platelet-collagen interaction. Thrombosis and haemostasis 1997;77:981-5.
174. Staatz WD, Walsh JJ, Pexton T, et al. The alpha 2 beta 1 integrin cell surface collagen receptor binds to the alpha 1 (I)-CB3 peptide of collagen. The Journal of biological chemistry 1990;265:4778-81.
175. Tuckwell D, Calderwood DA, Green LJ, et al. Integrin alpha 2 I-domain is a binding site for collagens. Journal of cell science 1995;108 (Pt 4):1629-37.
176. Zwolanek D, Flicker M, Kirstatter E, et al. beta1 Integrins Mediate Attachment of Mesenchymal Stem Cells to Cartilage Lesions. BioResearch open access 2015;4:39-53.
177. Pischel KD, Bluestein HG, Woods VL, Jr. Platelet glycoproteins Ia, Ic, and IIa are physicochemically indistinguishable from the very late activation antigens adhesion-related proteins of lymphocytes and other cell types. The Journal of clinical investigation 1988;81:505-13.
178. Sottnik JL, Daignault-Newton S, Zhang X, et al. Integrin alpha2beta 1 (alpha2beta1) promotes prostate cancer skeletal metastasis. Clinical & experimental metastasis 2013;30:569-78.
179. Li X, Ishihara S, Yasuda M, et al. Lung cancer cells that survive ionizing radiation show increased integrin alpha2beta1- and EGFR-dependent invasiveness. PloS one 2013;8:e70905.
180. Watson SP, Farndale RW, Moroi M, et al. Chapter 30: Platelet Collagen Receptors. In: Marder VJ, Aird WC, Bennett JS, Schulman S, White GC, eds. Hemostasis and thrombosis : basic principles and clinical practice. 6th ed. Philadelphia: Wolters Kluwer/Lippincott Williams & Wilkins Health; 2013:420-30

181. Clemetson JM, Polgar J, Magnenat E, et al. The platelet collagen receptor glycoprotein VI is a member of the immunoglobulin superfamily closely related to FcalphaR and the natural killer receptors. The Journal of biological chemistry 1999;274:29019-24.
182. Jandrot-Perrus M, Busfield S, Lagrue AH, et al. Cloning, characterization, and functional studies of human and mouse glycoprotein VI: a platelet-specific collagen receptor from the immunoglobulin superfamily. Blood 2000;96:1798-807.
183. Moroi M, Jung SM. Platelet glycoprotein VI: its structure and function. Thrombosis research 2004;114:221-33.

184. Berlanga O, Tulasne D, Bori T, et al. The Fc receptor gamma-chain is necessary and sufficient to initiate signalling through glycoprotein VI in transfected cells by the snake C-type lectin, convulxin. European journal of biochemistry 2002;269:2951-60.
185. Gibbins JM, Okuma M, Farndale R, et al. Glycoprotein VI is the collagen receptor in platelets which underlies tyrosine phosphorylation of the Fc receptor gamma-chain. FEBS letters 1997;413:255-9.
186. Tsuji M, Ezumi Y, Arai M, et al. A novel association of Fc receptor gamma-chain with glycoprotein VI and their co-expression as a collagen receptor in human platelets. The Journal of biological chemistry 1997;272:23528-31.
187. Jung SM, Tsuji K, Moroi M. Glycoprotein (GP) VI dimer as a major collagen-binding site of native platelets: direct evidence obtained with dimeric GPVI-specific Fabs. Journal of thrombosis and haemostasis : JTH 2009;7:1347-55.
188. Jung SM, Takemura Y, Imamura Y, et al. Collagen-type specificity of glycoprotein VI as a determinant of platelet adhesion. Platelets 2008;19:32-42.
189. Andrews RK, Karunakaran D, Gardiner EE, et al. Platelet receptor proteolysis: a mechanism for downregulating platelet reactivity. Arteriosclerosis, thrombosis, and vascular biology 2007;27:1511-20.
190. Bender M, Hofmann S, Stegner D, et al. Differentially regulated GPVI ectodomain shedding by multiple platelet-expressed proteinases. Blood 2010;116:3347-55.
191. Chen H, Locke D, Liu Y, et al. The platelet receptor GPVI mediates both adhesion and signaling responses to collagen in a receptor density-dependent fashion. The Journal of biological chemistry 2002;277:3011-9.
192. Boylan B, Gao C, Rathore V, et al. Identification of FcgammaRIIa as the ITAM-bearing receptor mediating alphaIIbbeta3 outside-in integrin signaling in human platelets. Blood 2008;112:2780-6.
193. Newman PJ. GPVI and the not so eager cleaver. Blood 2010;116:3124-6.
194. Nieswandt B, Schulte V, Bergmeier W, et al. Long-term antithrombotic protection by in vivo depletion of platelet glycoprotein VI in mice. The Journal of experimental medicine 2001;193:459-69.
195. Takayama H, Hosaka Y, Nakayama K, et al. A novel antiplatelet antibody therapy that induces cAMP-dependent endocytosis of the GPVI/Fc receptor gamma-chain complex. The Journal of clinical investigation 2008;118:1785-95.
196. Berndt MC, Andrews RK. Liver-mediated shedding of platelet GPVI. Blood 2016;128:751-2.
197. Newman PJ. New role for the GPVI/FcR chain complex Blood 2006;107:1248-9.
198. Polanowska-Grabowska R, Gibbins JM, Gear AR. Platelet adhesion to collagen and collagen-related peptide under flow: roles of the [alpha]2[beta]1 integrin, GPVI, and Src tyrosine kinases. Arteriosclerosis, thrombosis, and vascular biology 2003;23:1934-40.
199. Andrews RK, Gardiner EE, Shen Y, et al. Structure-activity relationships of snake toxins targeting platelet receptors, glycoprotein Ib-IX-V and glycoprotein VI. Current medicinal chemistry Cardiovascular and hematological agents 2003;1:143-9.
200. Wijeyewickrema LC, Gardiner EE, Moroi M, et al. Snake venom metalloproteinases, crotarhagin and alborhagin, induce ectodomain shedding of the platelet collagen receptor, glycoprotein VI. Thrombosis and haemostasis 2007;98:1285-90.
201. Asazuma N, Marshall SJ, Berlanga O, et al. The snake venom toxin alboaggregin-A activates glycoprotein VI. Blood 2001;97:3989-91.

202. Inoue O, Suzuki-Inoue K, McCarty OJ, et al. Laminin stimulates spreading of platelets through integrin alpha6beta1-dependent activation of GPVI. Blood 2006;107:1405-12.
203. Moraes LA, Barrett NE, Jones CI, et al. Platelet endothelial cell adhesion molecule-1 regulates collagen-stimulated platelet function by modulating the association of phosphatidylinositol 3-kinase with Grb-2-associated binding protein-1 and linker for activation of T cells. Journal of thrombosis and haemostasis : JTH 2010;8:2530-41.
204. Cicmil M, Thomas JM, Leduc M, et al. Platelet endothelial cell adhesion molecule-1 signaling inhibits the activation of human platelets. Blood 2002;99:137-44.
205. Pasquet JM, Quek L, Pasquet S, et al. Evidence of a role for SHP-1 in platelet activation by the collagen receptor glycoprotein VI. The Journal of biological chemistry 2000;275:28526-31.
206. Garraud O, Cognasse F. Platelet Toll-like receptor expression: the link between "danger" ligands and inflammation. Inflammation & allergy drug targets 2010;9:322-33.
207. Cosgrove LJ, Vaughan HA, Tjandra JJ, et al. HLA (class I) antigens on platelets are involved in platelet function. Immunology and cell biology 1988;66 (Pt 1):69-77.
208. Chapman LM, Aggrey AA, Field DJ, et al. Platelets present antigen in the context of MHC class I. J Immunol 2012;189:916-23.
209. Finkielsztein A, Schlinker AC, Zhang L, et al. Human megakaryocyte progenitors derived from hematopoietic stem cells of normal individuals are MHC class II-expressing professional APC that enhance Th17 and Th1/Th17 responses. Immunology letters 2015;163:84-95.
210. Rosenfeld SI, Looney RJ, Leddy JP, et al. Human platelet Fc receptor for immunoglobulin G. Identification as a 40,000-molecular-weight membrane protein shared by monocytes. The Journal of clinical investigation 1985;76:2317-22.
211. Moore A, Nachman RL. Platelet Fc receptor. Increased expression in myeloproliferative disease. The Journal of clinical investigation 1981;67:1064-71.
212. Shido K, Ahmad G, Hsu L, et al. Characterization of human platelet IgG Fc receptor associated with membrane glycoprotein. Journal of clinical & laboratory immunology 1995;46:1-11.
213. Zhi H, Rauova L, Hayes V, et al. Cooperative integrin/ITAM signaling in platelets enhances thrombus formation in vitro and in vivo. Blood 2013;121:1858-67.
214. McKenzie SE, Taylor SM, Malladi P, et al. The role of the human Fc receptor Fc gamma RIIA in the immune clearance of platelets: a transgenic mouse model. J Immunol 1999;162:4311-8.
215. Sullam PM, Hyun WC, Szollosi J, et al. Physical proximity and functional interplay of the glycoprotein Ib-IX-V complex and the Fc receptor FcgammaRIIA on the platelet plasma membrane. The Journal of biological chemistry 1998;273:5331-6.
216. Shrimpton CN, Borthakur G, Larrucea S, et al. Localization of the adhesion receptor glycoprotein Ib-IX-V complex to lipid rafts is required for platelet adhesion and activation. The Journal of experimental medicine 2002;196:1057-66.
217. Aloui C, Prigent A, Sut C, et al. The signaling role of CD40 ligand in platelet biology and in platelet component transfusion. International journal of molecular sciences 2014;15:22342-64.
218. Grewal IS, Flavell RA. CD40 and CD154 in cell-mediated immunity. Annual review of immunology 1998;16:111-35.
219. Elgueta R, Benson MJ, de Vries VC, et al. Molecular mechanism and function of CD40/CD40L engagement in the immune system. Immunological reviews 2009;229:152-72.

220. Charafeddine AH, Kim EJ, Maynard DM, et al. Platelet-derived CD154: ultrastructural localization and clinical correlation in organ transplantation. American journal of transplantation : official journal of the American Society of Transplantation and the American Society of Transplant Surgeons 2012;12:3143-51.
221. Gnatenko DV, Dunn JJ, McCorkle SR, et al. Transcript profiling of human platelets using microarray and serial analysis of gene expression. Blood 2003;101:2285-93.
222. Rowley JW, Oler AJ, Tolley ND, et al. Genome-wide RNA-seq analysis of human and mouse platelet transcriptomes. Blood 2011;118:e101-11.
223. Simon LM, Edelstein LC, Nagalla S, et al. Human platelet microRNA-mRNA networks associated with age and gender revealed by integrated plateletomics. Blood 2014;123:e37-45.
224. Nagalla S, Shaw C, Kong X, et al. Platelet microRNA-mRNA coexpression profiles correlate with platelet reactivity. Blood 2011;117:5189-97.
225. Leroyer AS, Rautou PE, Silvestre JS, et al. CD40 ligand+ microparticles from human atherosclerotic plaques stimulate endothelial proliferation and angiogenesis a potential mechanism for intraplaque neovascularization. Journal of the American College of Cardiology 2008;52:1302-11.
226. Henn V, Slupsky JR, Grafe M, et al. CD40 ligand on activated platelets triggers an inflammatory reaction of endothelial cells. Nature 1998;391:591-4.
227. Inwald DP, McDowall A, Peters MJ, et al. CD40 is constitutively expressed on platelets and provides a novel mechanism for platelet activation. Circulation research 2003;92:1041-8.
228. Esposito P, Rampino T, Dal Canton A. Soluble CD40 as a modulator of CD40 pathway. Immunology letters 2012;147:85-6.
229. Furman MI, Krueger LA, Linden MD, et al. Release of soluble CD40L from platelets is regulated by glycoprotein IIb/IIIa and actin polymerization. Journal of the American College of Cardiology 2004;43:2319-25.
230. Chen Y, Chen J, Xiong Y, et al. Internalization of CD40 regulates its signal transduction in vascular endothelial cells. Biochemical and biophysical research communications 2006;345:106-17.
231. Danese S, Katz JA, Saibeni S, et al. Activated platelets are the source of elevated levels of soluble CD40 ligand in the circulation of inflammatory bowel disease patients. Gut 2003;52:1435-41.
232. Viallard JF, Solanilla A, Gauthier B, et al. Increased soluble and platelet-associated CD40 ligand in essential thrombocythemia and reactive thrombocytosis. Blood 2002;99:2612-4.
233. Engelmann B, Massberg S. Thrombosis as an intravascular effector of innate immunity. Nature reviews Immunology 2013;13:34-45.
234. Chakrabarti S, Varghese S, Vitseva O, et al. CD40 ligand influences platelet release of reactive oxygen intermediates. Arteriosclerosis, thrombosis, and vascular biology 2005;25:2428-34.
235. Freedman JE. Oxidative stress and platelets. Arteriosclerosis, thrombosis, and vascular biology 2008;28:s11-6.
236. Toubi E, Shoenfeld Y. The role of CD40-CD154 interactions in autoimmunity and the benefit of disrupting this pathway. Autoimmunity 2004;37:457-64.
237. Zhang B, Wu T, Chen M, et al. The CD40/CD40L system: a new therapeutic target for disease. Immunology letters 2013;153:58-61.
238. Hachem A, Yacoub D, Zaid Y, et al. Involvement of nuclear factor kappaB in platelet CD40 signaling. Biochemical and biophysical research communications 2012;425:58-63.

239. Yacoub D, Hachem A, Theoret JF, et al. Enhanced levels of soluble CD40 ligand exacerbate platelet aggregation and thrombus formation through a CD40-dependent tumor necrosis factor receptor-associated factor-2/Rac1/p38 mitogen-activated protein kinase signaling pathway. Arteriosclerosis, thrombosis, and vascular biology 2010;30:2424-33.
240. Damien P, Cognasse F, Eyraud MA, et al. LPS stimulation of purified human platelets is partly dependent on plasma soluble CD14 to secrete their main secreted product, soluble-CD40-Ligand. BMC immunology 2015;16:3.
241. Janeway CA, Jr., Medzhitov R. Innate immune recognition. Annual review of immunology 2002;20:197-216.
242. Koupenova M, Mick E, Mikhalev E, et al. Sex differences in platelet toll-like receptors and their association with cardiovascular risk factors. Arteriosclerosis, thrombosis, and vascular biology 2015;35:1030-7.
243. Moynagh PN. TLR signalling and activation of IRFs: revisiting old friends from the NF-kappaB pathway. Trends in immunology 2005;26:469-76.
244. Pasare C, Medzhitov R. Toll-like receptors and acquired immunity. Seminars in immunology 2004;16:23-6.
245. Akira S, Takeda K. Toll-like receptor signalling. Nature reviews Immunology 2004;4:499-511.
246. Shiraki R, Inoue N, Kawasaki S, et al. Expression of Toll-like receptors on human platelets. Thrombosis research 2004;113:379-85.
247. Zhang G, Han J, Welch EJ, et al. Lipopolysaccharide stimulates platelet secretion and potentiates platelet aggregation via TLR4/MyD88 and the cGMP-dependent protein kinase pathway. J Immunol 2009;182:7997-8004.
248. Stark RJ, Aghakasiri N, Rumbaut RE. Platelet-derived Toll-like receptor 4 (Tlr-4) is sufficient to promote microvascular thrombosis in endotoxemia. PloS one 2012;7:e41254.
249. Andonegui G, Kerfoot SM, McNagny K, et al. Platelets express functional Toll-like receptor-4. Blood 2005;106:2417-23.
250. Aslam R, Speck ER, Kim M, et al. Platelet Toll-like receptor expression modulates lipopolysaccharide-induced thrombocytopenia and tumor necrosis factor-alpha production in vivo. Blood 2006;107:637-41.
251. de Stoppelaar SF, Claushuis TA, Schaap MC, et al. Toll-Like Receptor Signalling Is Not Involved in Platelet Response to Streptococcus pneumoniae In Vitro or In Vivo. PloS one 2016;11:e0156977.
252. Alexander SP, Mathie A, Peters JA. Guide to Receptors and Channels (GRAC), 3rd edition. Brit J Pharmacol 2008;153 Suppl 2:S1-209.
253. Coughlin SR. Protease-activated receptors in hemostasis, thrombosis and vascular biology. Journal of thrombosis and haemostasis : JTH 2005;3:1800-14.
254. Russo A, Soh UJ, Trejo J. Proteases display biased agonism at protease-activated receptors: location matters! Molecular interventions 2009;9:87-96.
255. Soh UJ, Dores MR, Chen B, et al. Signal transduction by protease-activated receptors. Brit J Pharmacol 2010;160:191-203.
256. Vu TK, Hung DT, Wheaton VI, et al. Molecular cloning of a functional thrombin receptor reveals a novel proteolytic mechanism of receptor activation. Cell 1991;64:1057-68.
257. Rasmussen UB, Vouret-Craviari V, Jallat S, et al. cDNA cloning and expression of a hamster alpha-thrombin receptor coupled to Ca2+ mobilization. FEBS letters 1991;288:123-8.

258. Coughlin SR. Thrombin signalling and protease-activated receptors. Nature 2000;407:258-64.
259. Trivedi V, Boire A, Tchernychev B, et al. Platelet matrix metalloprotease-1 mediates thrombogenesis by activating PAR1 at a cryptic ligand site. Cell 2009;137:332-43.
260. Blackburn JS, Brinckerhoff CE. Matrix metalloproteinase-1 and thrombin differentially activate gene expression in endothelial cells via PAR-1 and promote angiogenesis. The American journal of pathology 2008;173:1736-46.
261. Ludeman MJ, Zheng YW, Ishii K, et al. Regulated shedding of PAR1 N-terminal exodomain from endothelial cells. The Journal of biological chemistry 2004;279:18592-9.
262. Kuliopulos A, Covic L, Seeley SK, et al. Plasmin desensitization of the PAR1 thrombin receptor: kinetics, sites of truncation, and implications for thrombolytic therapy. Biochemistry 1999;38:4572-85.
263. Duvernay M, Young S, Gailani D, et al. Protease-activated receptor (PAR) 1 and PAR4 differentially regulate factor V expression from human platelets. Molecular pharmacology 2013;83:781-92.
264. Carrim N, Arthur JF, Hamilton JR, et al. Thrombin-induced reactive oxygen species generation in platelets: A novel role for protease-activated receptor 4 and GPIbalpha. Redox biology 2015;6:640-7.
265. Nakanishi-Matsui M, Zheng YW, Sulciner DJ, et al. PAR3 is a cofactor for PAR4 activation by thrombin. Nature 2000;404:609-13.
266. Edelstein LC, Simon LM, Montoya RT, et al. Racial differences in human platelet PAR4 reactivity reflect expression of PCTP and miR-376c. Nature medicine 2013;19:1609-16.
267. Edelstein LC, Simon LM, Lindsay CR, et al. Common variants in the human platelet PAR4 thrombin receptor alter platelet function and differ by race. Blood 2014;124:3450-8.
268. Strosberg AD. Structure, function, and regulation of adrenergic receptors. Protein science : a publication of the Protein Society 1993;2:1198-209.
269. Hein L. [The alpha 2-adrenergic receptors: molecular structure and in vivo function]. Zeitschrift fur Kardiologie 2001;90:607-12.
270. Giovannitti JA, Jr., Thoms SM, Crawford JJ. Alpha-2 adrenergic receptor agonists: a review of current clinical applications. Anesthesia progress 2015;62:31-9.
271. Emerson M, Paul W, Page CP. Regulation of platelet function by catecholamines in the cerebral vasculature of the rabbit. Brit J Pharmacol 1999;127:1652-6.
272. Latour JG, Leger-Gauthier C. Vasoactive agents and production of thrombosis during intravascular coagulation. 3. Comparative effects of catecholamines. The American journal of pathology 1987;126:569-80.
273. Wachter SB, Gilbert EM. Beta-adrenergic receptors, from their discovery and characterization through their manipulation to beneficial clinical application. Cardiology 2012;122:104-12.
274. Johnson M. Molecular mechanisms of beta(2)-adrenergic receptor function, response, and regulation. The Journal of allergy and clinical immunology 2006;117:18-24; quiz 5.
275. Kerry R, Scrutton MC. Platelet beta-adrenoceptors. Brit J Pharmacol 1983;79:681-91.
276. Klysner R, Andersen PH, Geisler A, et al. Characterization of the beta-adrenergic receptor on the human platelet: a beta 2-subtype. Acta pharmacologica et toxicologica 1984;54:265-9.
277. Winther K, Klysner R, Geisler A, et al. Characterization of human platelet beta-adrenoceptors. Thrombosis research 1985;40:757-67.

278. Winther K, Trap-Jensen J. Effects of three beta-blockers with different pharmacodynamic properties on platelet aggregation and platelet and plasma cyclic AMP. European journal of clinical pharmacology 1988;35:17-20.
279. Koutouzov S, Cothenet-Vernoux L, Dausse JP, et al. Influence of adrenoceptors on thrombin-induced phosphoinositide metabolism in rat platelets. Biochemical and biophysical research communications 1985;132:1051-8.
280. Gill J, DeSouza V, Wakeling A, et al. Differential changes in alpha- and beta-adrenoceptor linked [45Ca2+] uptake in platelets from patients with anorexia nervosa. The Journal of clinical endocrinology and metabolism 1992;74:441-6.
281. Gill J, Thompson CS, Jeremy JY, et al. Adrenoceptor-linked [45Ca2+] uptake in platelets from diabetic rats: a model for human platelets. Laboratory animals 1994;28:143-7.
282. Austin CE, Otter DJ, Chess-Williams R. Influence of adrenoceptor stimulation on aggregation of platelets from diabetic and control rats. Journal of autonomic pharmacology 1995;15:169-76.
283. Bonten TN, Plaizier CE, Snoep JJ, et al. Effect of beta-blockers on platelet aggregation: a systematic review and meta-analysis. British journal of clinical pharmacology 2014;78:940-9.
284. Beres BJ, Toth-Zsamboki E, Vargova K, et al. Analysis of platelet alpha2-adrenergic receptor activity in stable coronary artery disease patients on dual antiplatelet therapy. Thrombosis and haemostasis 2008;100:829-38.
285. Bos CL, Richel DJ, Ritsema T, et al. Prostanoids and prostanoid receptors in signal transduction. The international journal of biochemistry & cell biology 2004;36:1187-205.
286. Smyth EM, Grosser T, Wang M, et al. Prostanoids in health and disease. Journal of lipid research 2009;50 Suppl:S423-8.
287. Smith JB. The prostanoids in hemostasis and thrombosis: a review. The American journal of pathology 1980;99:743-804.
288. Matsuoka T, Narumiya S. The roles of prostanoids in inflammation, allergy, and immunity. Inflammation and Regeneration 2008;28:423-33.
289. Grosser T, FitzGerald GA. Chapter 34: Platelet Prostanoid Metabolism. In: Marder VJ, Aird WC, Bennett JS, Schulman S, White GC, eds. Hemostasis and thrombosis : basic principles and clinical practice. 6th ed. Philadelphia: Wolters Kluwer/Lippincott Williams & Wilkins Health; 2013:462-7

290. Rao LV, Bajaj SP, Rapaport SI. Activation of human factor VII during clotting in vitro. Blood 1985;65:218-26.
291. Reiter R, Resch U, Sinzinger H. Do human platelets express COX-2? Prostaglandins, leukotrienes, and essential fatty acids 2001;64:299-305.
292. Patrignani P, Sciulli MG, Manarini S, et al. COX-2 is not involved in thromboxane biosynthesis by activated human platelets. Journal of physiology and pharmacology : an official journal of the Polish Physiological Society 1999;50:661-7.
293. Zetterberg E, Lundberg LG, Palmblad J. Expression of cox-2, tie-2 and glycodelin by megakaryocytes in patients with chronic myeloid leukaemia and polycythaemia vera. British journal of haematology 2003;121:497-9.
294. Tanaka N, Sato T, Fujita H, et al. Constitutive expression and involvement of cyclooxygenase-2 in human megakaryocytopoiesis. Arteriosclerosis, thrombosis, and vascular biology 2004;24:607-12.

295. Ballou LR, DeWitt LM, Cheung WY. Substrate-specific forms of human platelet phospholipase A2. The Journal of biological chemistry 1986;261:3107-11.
296. Bartoli F, Lin HK, Ghomashchi F, et al. Tight binding inhibitors of 85-kDa phospholipase A2 but not 14-kDa phospholipase A2 inhibit release of free arachidonate in thrombin-stimulated human platelets. The Journal of biological chemistry 1994;269:15625-30.
297. Prevost N, Mitsios JV, Kato H, et al. Group IVA cytosolic phospholipase A2 (cPLA2alpha) and integrin alphaIIbbeta3 reinforce each other's functions during alphaIIbbeta3 signaling in platelets. Blood 2009;113:447-57.
298. Liu J, Pestina TI, Berndt MC, et al. Botrocetin/VWF-induced signaling through GPIb-IX-V produces TxA2 in an alphaIIbbeta3- and aggregation-independent manner. Blood 2005;106:2750-6.
299. Schuette AH, Huttemeier PC, Hill RD, et al. Regional blood flow and pulmonary thromboxane release after sublethal endotoxin infusion in sheep. Surgery 1984;95:444-53.
300. Dubin NH, Blake DA, Egner PG, et al. Effect of platelet-generated thromboxane on contractions of the pregnant rat uterus. Biology of reproduction 1982;26:289-95.
301. Beitz A, Nikitina NA, Giessler C, et al. Modulation of TXA2 generation of platelets by human lipoproteins. Prostaglandins, leukotrienes, and essential fatty acids 1990;40:57-61.
302. Karpen CW, Merola AJ, Trewyn RW, et al. Modulation of Platelet thromboxane A2 and arterial prostacyclin by dietary vitamin E. Prostaglandins 1981;22:651-61.
303. Fitzgerald DJ, Fragetta J, FitzGerald GA. Prostaglandin endoperoxides modulate the response to thromboxane synthase inhibition during coronary thrombosis. The Journal of clinical investigation 1988;82:1708-13.
304. Guerrero JA, Navarro-Nunez L, Lozano ML, et al. Flavonoids inhibit the platelet TxA(2) signalling pathway and antagonize TxA(2) receptors (TP) in platelets and smooth muscle cells. British journal of clinical pharmacology 2007;64:133-44.
305. Roberts W, Riba R, Homer-Vanniasinkam S, et al. Nitric oxide specifically inhibits integrin-mediated platelet adhesion and spreading on collagen. Journal of thrombosis and haemostasis : JTH 2008;6:2175-85.
306. Wilson SJ, Roche AM, Kostetskaia E, et al. Dimerization of the human receptors for prostacyclin and thromboxane facilitates thromboxane receptor-mediated cAMP generation. The Journal of biological chemistry 2004;279:53036-47.
307. Grosser T, Fries S, FitzGerald GA. Biological basis for the cardiovascular consequences of COX-2 inhibition: therapeutic challenges and opportunities. The Journal of clinical investigation 2006;116:4-15.
308. Matijevic-Aleksic N, McPhedran P, Wu KK. Bleeding disorder due to platelet prostaglandin H synthase-1 (PGHS-1) deficiency. British journal of haematology 1996;92:212-7.
309. Dube JN, Drouin J, Aminian M, et al. Characterization of a partial prostaglandin endoperoxide H synthase-1 deficiency in a patient with a bleeding disorder. British journal of haematology 2001;113:878-85.
310. Defreyn G, Machin SJ, Carreras LO, et al. Familial bleeding tendency with partial platelet thromboxane synthetase deficiency: reorientation of cyclic endoperoxide metabolism. British journal of haematology 1981;49:29-41.
311. Remuzzi G, Benigni A, Dodesini P, et al. Reduced platelet thromboxane formation in uremia. Evidence for a functional cyclooxygenase defect. The Journal of clinical investigation 1983;71:762-8.

312. Warner TD, Nylander S, Whatling C. Anti-platelet therapy: cyclo-oxygenase inhibition and the use of aspirin with particular regard to dual anti-platelet therapy. British journal of clinical pharmacology 2011;72:619-33.
313. Schafer AI. Effects of nonsteroidal antiinflammatory drugs on platelet function and systemic hemostasis. Journal of clinical pharmacology 1995;35:209-19.
314. Schafer AI. Effects of nonsteroidal anti-inflammatory therapy on platelets. The American journal of medicine 1999;106:25S-36S.
315. Ehrman ML, Jaffe EA. Prostacyclin (PGI2) inhibits the development in human platelets of ADP and arachidonic acid-induced shape change and procoagulant activity. Prostaglandins 1980;20:1103-16.
316. Hawiger J, Parkinson S, Timmons S. Prostacyclin inhibits mobilisation of fibrinogen-binding sites on human ADP- and thrombin-treated platelets. Nature 1980;283:195-7.
317. Graber SE, Hawiger J. Evidence that changes in platelet cyclic AMP levels regulate the fibrinogen receptor on human platelets. The Journal of biological chemistry 1982;257:14606-9.
318. FitzGerald GA, Austin S, Egan K, et al. Cyclo-oxygenase products and atherothrombosis. Annals of medicine 2000;32 Suppl 1:21-6.
319. Ungprasert P, Srivali N, Wijarnpreecha K, et al. Non-steroidal anti-inflammatory drugs and risk of venous thromboembolism: a systematic review and meta-analysis. Rheumatology (Oxford, England) 2015;54:736-42.
320. Howes LG. Selective COX-2 inhibitors, NSAIDs and cardiovascular events - is celecoxib the safest choice? Therapeutics and clinical risk management 2007;3:831-45.
321. Alcorn N, Madhok R. Non-steroidal anti-inflammatory drugs and venous thromboembolism. Rheumatology (Oxford, England) 2015;54:570-1.
322. Grosser T, Yu Y, Fitzgerald GA. Emotion recollected in tranquility: lessons learned from the COX-2 saga. Annual review of medicine 2010;61:17-33.
323. Smith JB. Prostaglandins and platelet aggregation. Acta medica Scandinavica Supplementum 1981;651:91-9.
324. Cooper B, Ahern D. Characterization of the platelet prostaglandin D2 receptor. Loss of prostaglandin D2 receptors in platelets of patients with myeloproliferative disorders. The Journal of clinical investigation 1979;64:586-90.
325. Graff J, Skarke C, Klinkhardt U, et al. Effects of selective COX-2 inhibition on prostanoids and platelet physiology in young healthy volunteers. Journal of thrombosis and haemostasis : JTH 2007;5:2376-85.
326. Guthikonda S, Lev EI, Patel R, et al. Reticulated platelets and uninhibited COX-1 and COX-2 decrease the antiplatelet effects of aspirin. Journal of thrombosis and haemostasis : JTH 2007;5:490-6.
327. Lopez-Farre A, Caramelo C, Esteban A, et al. Effects of aspirin on platelet-neutrophil interactions. Role of nitric oxide and endothelin-1. Circulation 1995;91:2080-8.
328. Herbertsson H, Bengtsson T. Role of platelets and the arachidonic acid pathway in the regulation of neutrophil oxidase activity. Scandinavian journal of clinical and laboratory investigation 2001;61:641-9.
329. Marcus AJ, Broekman MJ, Safier LB, et al. Production of arachidonic acid lipoxygenase products during platelet-neutrophil interactions. Clinical physiology and biochemistry 1984;2:78-83.

330. Antoine C, Murphy RC, Henson PM, et al. Time-dependent utilization of platelet arachidonic acid by the neutrophil in formation of 5-lipoxygenase products in platelet-neutrophil co-incubations. Biochimica et biophysica acta 1992;1128:139-46.
331. Chabannes B, Moliere P, Merhi-Soussi F, et al. Platelets may inhibit leucotriene biosynthesis by human neutrophils at the integrin level. British journal of haematology 2003;121:341-8.
332. Leon C, Vial C, Cazenave JP, et al. Cloning and sequencing of a human cDNA encoding endothelial P2Y1 purinoceptor. Gene 1996;171:295-7.
333. Gachet C. ADP receptors of platelets and their inhibition. Thrombosis and haemostasis 2001;86:222-32.
334. Hechler B, Gachet C. P2 receptors and platelet function. Purinergic signalling 2011;7:293-303.
335. Gachet C, Cattaneo M, Ohlmann P, et al. Purinoceptors on blood platelets: further pharmacological and clinical evidence to suggest the presence of two ADP receptors. British journal of haematology 1995;91:434-44.
336. Dorsam RT, Kunapuli SP. Central role of the P2Y12 receptor in platelet activation. The Journal of clinical investigation 2004;113:340-5.
337. Jagroop IA, Burnstock G, Mikhailidis DP. Both the ADP receptors P2Y1 and P2Y12, play a role in controlling shape change in human platelets. Platelets 2003;14:15-20.
338. Leon C, Hechler B, Freund M, et al. Defective platelet aggregation and increased resistance to thrombosis in purinergic P2Y(1) receptor-null mice. The Journal of clinical investigation 1999;104:1731-7.
339. Mangin P, Ohlmann P, Eckly A, et al. The P2Y1 receptor plays an essential role in the platelet shape change induced by collagen when TxA2 formation is prevented. Journal of thrombosis and haemostasis : JTH 2004;2:969-77.
340. Jin J, Daniel JL, Kunapuli SP. Molecular basis for ADP-induced platelet activation. II. The P2Y1 receptor mediates ADP-induced intracellular calcium mobilization and shape change in platelets. The Journal of biological chemistry 1998;273:2030-4.
341. Nurden P, Poujol C, Winckler J, et al. Immunolocalization of P2Y1 and TPalpha receptors in platelets showed a major pool associated with the membranes of alpha -granules and the open canalicular system. Blood 2003;101:1400-8.
342. Hechler B, Cattaneo M, Gachet C. The P2 receptors in platelet function. Seminars in thrombosis and hemostasis 2005;31:150-61.
343. Soulet C, Hechler B, Gratacap MP, et al. A differential role of the platelet ADP receptors P2Y1 and P2Y12 in Rac activation. Journal of thrombosis and haemostasis : JTH 2005;3:2296-306.
344. Savi P, Beauverger P, Labouret C, et al. Role of P2Y1 purinoceptor in ADP-induced platelet activation. FEBS letters 1998;422:291-5.
345. Hechler B, Eckly A, Ohlmann P, et al. The P2Y1 receptor, necessary but not sufficient to support full ADP-induced platelet aggregation, is not the target of the drug clopidogrel. British journal of haematology 1998;103:858-66.
346. Cattaneo M, Lombardi R, Zighetti ML, et al. Deficiency of (33P)2MeS-ADP binding sites on platelets with secretion defect, normal granule stores and normal thromboxane A2 production. Evidence that ADP potentiates platelet secretion independently of the formation of large platelet aggregates and thromboxane A2 production. Thrombosis and haemostasis 1997;77:986-90.

347. Cattaneo M, Canciani MT, Lecchi A, et al. Released adenosine diphosphate stabilizes thrombin-induced human platelet aggregates. Blood 1990;75:1081-6.
348. Cattaneo M, Lecchi A, Lombardi R, et al. Platelets from a patient heterozygous for the defect of P2CYC receptors for ADP have a secretion defect despite normal thromboxane A2 production and normal granule stores: further evidence that some cases of platelet 'primary secretion defect' are heterozygous for a defect of P2CYC receptors. Arteriosclerosis, thrombosis, and vascular biology 2000;20:E101-6.
349. Leon C, Alex M, Klocke A, et al. Platelet ADP receptors contribute to the initiation of intravascular coagulation. Blood 2004;103:594-600.
350. Leon C, Freund M, Ravanat C, et al. Key role of the P2Y(1) receptor in tissue factor-induced thrombin-dependent acute thromboembolism: studies in P2Y(1)-knockout mice and mice treated with a P2Y(1) antagonist. Circulation 2001;103:718-23.
351. Leon C, Ravanat C, Freund M, et al. Differential involvement of the P2Y1 and P2Y12 receptors in platelet procoagulant activity. Arteriosclerosis, thrombosis, and vascular biology 2003;23:1941-7.
352. Storey RF, Sanderson HM, White AE, et al. The central role of the P(2T) receptor in amplification of human platelet activation, aggregation, secretion and procoagulant activity. British journal of haematology 2000;110:925-34.
353. Mahaut-Smith MP, Jones S, Evans RJ. The P2X1 receptor and platelet function. Purinergic signalling 2011;7:341-56.
354. Rolf MG, Mahaut-Smith MP. Effects of enhanced P2X1 receptor Ca2+ influx on functional responses in human platelets. Thrombosis and haemostasis 2002;88:495-502.
355. Jones S, Evans RJ, Mahaut-Smith MP. Ca2+ influx through P2X1 receptors amplifies P2Y1 receptor-evoked Ca2+ signaling and ADP-evoked platelet aggregation. Molecular pharmacology 2014;86:243-51.
356. Blockmans D, Deckmyn H, Vermylen J. Platelet activation. Blood reviews 1995;9:143-56.
357. Plow EF, Ginsberg MH. Hematology: Basic Principles and Practice, 2nd ed. New York, NY: Churchill Livingson; 1995.
358. Geanacopoulos M, Turner J, Bowling KE, et al. The role of protein kinase C in the initial events of platelet activation by thrombin assessed with a selective inhibitor. Thrombosis research 1993;69:113-24.
359. Greenberg-Sepersky SM, Simons ER. Release of a fluorescent probe as an indicator of lysosomal granule secretion by thrombin-stimulated human platelets. Analytical biochemistry 1985;147:57-62.
360. Gunay-Aygun M, Zivony-Elboum Y, Gumruk F, et al. Gray platelet syndrome: natural history of a large patient cohort and locus assignment to chromosome 3p. Blood 2010;116:4990-5001.
361. Bottega R, Pecci A, De Candia E, et al. Correlation between platelet phenotype and NBEAL2 genotype in patients with congenital thrombocytopenia and alpha-granule deficiency. Haematologica 2013;98:868-74.
362. Maynard DM, Heijnen HF, Gahl WA, et al. The alpha-granule proteome: novel proteins in normal and ghost granules in gray platelet syndrome. Journal of thrombosis and haemostasis : JTH 2010;8:1786-96.
363. Harrison P, Cramer EM. Platelet alpha-granules. Blood reviews 1993;7:52-62.

364. Sehgal S, Storrie B. Evidence that differential packaging of the major platelet granule proteins von Willebrand factor and fibrinogen can support their differential release. Journal of thrombosis and haemostasis : JTH 2007;5:2009-16.
365. Ye S, Whiteheart SW. Chapter 32: Molecular Basis for Platelet Secretion. In: Marder VJ, Aird WC, Bennett JS, Schulman S, White GC, eds. Hemostasis and thrombosis : basic principles and clinical practice. 6th ed. Philadelphia: Wolters Kluwer/Lippincott Williams & Wilkins Health; 2013:441-8

366. Suehiro Y, Veljkovic DK, Fuller N, et al. Endocytosis and storage of plasma factor V by human megakaryocytes. Thrombosis and haemostasis 2005;94:585-92.
367. Flaumenhaft R. Monitoring granule traffic in megakaryocytes. Blood 2012;120:3869-70.
368. Italiano JE, Jr., Battinelli EM. Selective sorting of alpha-granule proteins. Journal of thrombosis and haemostasis : JTH 2009;7 Suppl 1:173-6.
369. Salgado R, Benoy I, Bogers J, et al. Platelets and vascular endothelial growth factor (VEGF): a morphological and functional study. Angiogenesis 2001;4:37-43.
370. Roussi J, Drouet L, Sigman J, et al. Absence of incorporation of plasma von Willebrand factor into porcine platelet alpha-granules. British journal of haematology 1995;90:661-8.
371. Harrison P, Wilbourn B, Debili N, et al. Uptake of plasma fibrinogen into the alpha granules of human megakaryocytes and platelets. The Journal of clinical investigation 1989;84:1320-4.
372. George JN, Saucerman S, Levine SP, et al. Immunoglobulin G is a platelet alpha granule-secreted protein. The Journal of clinical investigation 1985;76:2020-5.
373. Ayombil F, Abdalla S, Tracy PB, et al. Proteolysis of plasma-derived factor V following its endocytosis by megakaryocytes forms the platelet-derived factor V/Va pool. Journal of thrombosis and haemostasis : JTH 2013;11:1532-9.
374. Andia I, Maffulli N. Platelet-rich plasma for managing pain and inflammation in osteoarthritis. Nature reviews Rheumatology 2013;9:721-30.
375. Chacon-Fernandez P, Sauberli K, Colzani M, et al. Brain-derived Neurotrophic Factor in Megakaryocytes. The Journal of biological chemistry 2016;291:9872-81.
376. Fujimura H, Altar CA, Chen R, et al. Brain-derived neurotrophic factor is stored in human platelets and released by agonist stimulation. Thrombosis and haemostasis 2002;87:728-34.
377. Lisman T, Porte RJ. Mechanisms of platelet-mediated liver regeneration. Blood 2016;128:625-9.
378. Starlinger P, Haegele S, Offensperger F, et al. The profile of platelet alpha-granule released molecules affects postoperative liver regeneration. Hepatology (Baltimore, Md) 2016;63:1675-88.
379. Sakata R, Reddi AH. Platelet-Rich Plasma Modulates Actions on Articular Cartilage Lubrication and Regeneration. Tissue engineering Part B, Reviews 2016;22:408-19.
380. Mussano F, Genova T, Munaron L, et al. Cytokine, chemokine, and growth factor profile of platelet-rich plasma. Platelets 2016;27:467-71.
381. Venter NG, Marques RG, Santos JS, et al. Use of platelet-rich plasma in deep second- and third-degree burns. Burns : journal of the International Society for Burn Injuries 2016;42:807-14.
382. Pallua N, Wolter T, Markowicz M. Platelet-rich plasma in burns. Burns : journal of the International Society for Burn Injuries 2010;36:4-8.

383. Findikcioglu K, Findikcioglu F, Yavuzer R, et al. Effect of platelet-rich plasma and fibrin glue on healing of critical-size calvarial bone defects. The Journal of craniofacial surgery 2009;20:34-40.
384. You TM, Choi BH, Zhu SJ, et al. Platelet-enriched fibrin glue and platelet-rich plasma in the repair of bone defects adjacent to titanium dental implants. The International journal of oral & maxillofacial implants 2007;22:417-22.
385. Youssefian T, Masse JM, Rendu F, et al. Platelet and megakaryocyte dense granules contain glycoproteins Ib and IIb-IIIa. Blood 1997;89:4047-57.
386. Chatterjee D, Anderson GM, Chakraborty M, et al. Human platelet dense granules: improved isolation and preliminary characterization of [3H]-serotonin uptake and tetrabenazine-displaceable [3H]-ketanserin binding. Life sciences 1990;46:1755-64.
387. Feng L, Novak EK, Hartnell LM, et al. The Hermansky-Pudlak syndrome 1 (HPS1) and HPS2 genes independently contribute to the production and function of platelet dense granules, melanosomes, and lysosomes. Blood 2002;99:1651-8.
388. Di Pietro SM, Dell'Angelica EC. The cell biology of Hermansky-Pudlak syndrome: recent advances. Traffic (Copenhagen, Denmark) 2005;6:525-33.
389. Meng R, Wu J, Harper DC, et al. Defective release of alpha granule and lysosome contents from platelets in mouse Hermansky-Pudlak syndrome models. Blood 2015;125:1623-32.
390. Harper MT, van den Bosch MT, Hers I, et al. Platelet dense granule secretion defects may obscure alpha-granule secretion mechanisms: evidence from Munc13-4-deficient platelets. Blood 2015;125:3034-6.
391. Siess W. Molecular mechanisms of platelet activation. Physiological reviews 1989;69:58-178.
392. Schlienger RG, Meier CR. Effect of selective serotonin reuptake inhibitors on platelet activation: can they prevent acute myocardial infarction? American journal of cardiovascular drugs : drugs, devices, and other interventions 2003;3:149-62.
393. Juang HT, Chen PC, Chien KL. Using antidepressants and the risk of stroke recurrence: report from a national representative cohort study. BMC neurology 2015;15:86.
394. Lee YC, Lin CH, Lin MS, et al. Effects of selective serotonin reuptake inhibitors versus tricyclic antidepressants on cerebrovascular events: a nationwide population-based cohort study. Journal of clinical psychopharmacology 2013;33:782-9.
395. Duerschmied D, Suidan GL, Demers M, et al. Platelet serotonin promotes the recruitment of neutrophils to sites of acute inflammation in mice. Blood 2013;121:1008-15.
396. Fogelson AL, Wang NT. Platelet dense-granule centralization and the persistence of ADP secretion. The American journal of physiology 1996;270:H1131-40.
397. Fukami MH, Bauer JS, Stewart GJ, et al. An improved method for the isolation of dense storage granules from human platelets. The Journal of cell biology 1978;77:389-99.
398. Ruiz FA, Lea CR, Oldfield E, et al. Human platelet dense granules contain polyphosphate and are similar to acidocalcisomes of bacteria and unicellular eukaryotes. The Journal of biological chemistry 2004;279:44250-7.
399. Morrissey JH, Choi SH, Smith SA. Polyphosphate: an ancient molecule that links platelets, coagulation, and inflammation. Blood 2012;119:5972-9.
400. Choi SH, Smith SA, Morrissey JH. Polyphosphate is a cofactor for the activation of factor XI by thrombin. Blood 2011;118:6963-70.
401. Muller F, Renne T. Platelet polyphosphates: the nexus of primary and secondary hemostasis. Scandinavian journal of clinical and laboratory investigation 2011;71:82-6.

402. Muller F, Mutch NJ, Schenk WA, et al. Platelet polyphosphates are proinflammatory and procoagulant mediators in vivo. Cell 2009;139:1143-56.
403. Bentfeld-Barker ME, Bainton DF. Identification of primary lysosomes in human megakaryocytes and platelets. Blood 1982;59:472-81.
404. Chen D, Lemons PP, Schraw T, et al. Molecular mechanisms of platelet exocytosis: role of SNAP-23 and syntaxin 2 and 4 in lysosome release. Blood 2000;96:1782-8.
405. Holmsen H, Weiss HJ. Secretable storage pools in platelets. Annual review of medicine 1979;30:119-34.
406. Holmsen H. Physiological functions of platelets. Annals of medicine 1989;21:23-30.
407. Ciferri S, Emiliani C, Guglielmini G, et al. Platelets release their lysosomal content in vivo in humans upon activation. Thrombosis and haemostasis 2000;83:157-64.
408. Zhang ZG, Zhang L, Tsang W, et al. Dynamic platelet accumulation at the site of the occluded middle cerebral artery and in downstream microvessels is associated with loss of microvascular integrity after embolic middle cerebral artery occlusion. Brain research 2001;912:181-94.
409. Castellot JJ, Jr., Favreau LV, Karnovsky MJ, et al. Inhibition of vascular smooth muscle cell growth by endothelial cell-derived heparin. Possible role of a platelet endoglycosidase. The Journal of biological chemistry 1982;257:11256-60.
410. Polasek J. Platelet secretory granules or secretory lysosomes? Platelets 2005;16:500-1.
411. Thon JN, Peters CG, Mechlus KR, et al. T granules in human platelets function in TLR9 organization and signaline. J Cell Biol, 2012; 198(4): 561-74.
412. Hennessy EJ, Parker AE, O;Neill LA. Targeting Toll-like receptors: emerging therapeutics? Nat Rev Drug Discov, 2010; doi:10.1038/nrd3203
413. Panigrahi S, Ma Y, Hong L, et al. Engagement of platelet toll-like receptor 9 by novel endogenous ligands promotes platelet hyperreactivity and thrombosis. Circ Res, 2013; 112(1): 103-12.
414. Tateson JE, Moncada S, Vane JR. Effects of prostacyclin (PGX) on cyclic AMP concentrations in human platelets. Prostaglandins 1977;13:389-97.
415. Marcus AJ, Safier LB, Hajjar KA, et al. Inhibition of platelet function by an aspirin-insensitive endothelial cell ADPase. Thromboregulation by endothelial cells. The Journal of clinical investigation 1991;88:1690-6.
416. de Graaf JC, Banga JD, Moncada S, et al. Nitric oxide functions as an inhibitor of platelet adhesion under flow conditions. Circulation 1992;85:2284-90.
417. Fitzgerald JR, Foster TJ, Cox D. The interaction of bacterial pathogens with platelets. Nature Reviews, 2006.
418. Hambleton J, Leung LL, Levi M. Coagulation: consultative hemostasis. Hematology, 2002;335-352.
419. Proulx F, Seidman EG, Karpman D. Pathogenesis of Shiga toxin-associated hemolytic uremic syndrome. Pediatr Res, 2001;50:163-171.
420. Humphrey JH, Jacues R. The release of histamine and 5-hydroxytryptamine (serotonin) from platelets by antigen-antibody reactions (in vitro). J Physiol, 1955;128:9.
421. Hawiger J, Marney SR Jr, Colley DG, et al. Complement-dependent platelet injury by staphylococcal protein A. J Exp Med, 1972;136:68-80.
422. Weksler BB, Nachman R. Rabbit platelet bacterial protein. J Exp Med, 1971;134:1114-1130.

423. Schwarz-Linek U, et al. Pathogenic bacteria attach to human fibronectin through a tandem B-zipper. Nature, 2003;423:177-181.
424. Massey RC, et al. Fibronectin-binding protein A of Staphylococcus aureus has multiple, substituting, binding regions that mediate adherence to fibronectin and invasion of endothelial cells. Cell Microbiol, 2001;3:839-851.
425. Watson CN, Kerrigan SW, Cox D, et al. Human platelet activation by Escherichia coli: roles for FcyRIIA and integrin aIIbB3. Platelets, 2016;27(6):535-540.
426. Riaz AH, Tasma BE, Woodman ME, et al. Human platelets efficiently kill IgG-opsonized E. coli. FEMS Immunol Med Microbiol, 2012; 65(1):78-83.
427. Matus V, Valenzuela JG, Hidalgo P, et al. Human platelet interaction with E. coli O111 promotes tissue-factor-dependent procoagulant activity, involving Toll like receptor 4. PLoS One, 2017;doi.
428. Matus V, Valenzuela JG, Saez CG, et al. Interaction of human platelets with enterohemorrhagic E. coli O111, induces an increase in the provoagulant activity, thrombin generation and adhersion to endothelial cells. Blood, 2014;124:4989.
429. White JG. Platelets are covercytes, not phagocytes: uptake of bacteria involves channels of the open canalicular system. Platelets, 2005;16(2):121-31.
430. Absolom DR, Francis DW, Zingg W, et al. Phagocytosis of bacteria by platelets: surface thermodynamics. J of Colloidal and Interface Science, 1982;85(1):168-177.
431. White JG. Platelets are covercytes, not phagocytes. Blood, 2004:104;3533.
432. Youssefian T, Drouin A, Masse JM, et al. Host defense role of platelets: engulfment of HIV and staphylococcus aureus occurs in a specific subcellular compartment and is enhanced by platelet activation. Blood, 2002; 99(11): 4021-4029.
433. Nagasawa T, Nakayasu C, Rieger AM, et al. Phagocytosis by thrombocytes is a conserved innate immune mechanism in lower vertebrates. Front Immunol, 2014;5:445.
434. Assinger A. Platelets and infection – an emerging role of platelets in viral infection. Front Immunol, 2014;5:649.
435. Lee TH, Stromberg RR, Heitman JW, et al. Distribution of HIV type 1 (HIV-1) in blood components: detection and significance of high levels of HIV-1 associated with platelets. Trasnfusion, 1998;38(6):580-588.
436. Kopko PM, Fernando LP, Bonney EN, et al. HIV transmissions from a window-period platelet donation. Am J Clin Pathol, 2001;116(4):562-566.
437. Sakaguchi M, Sato T, Groopman JE. Human immunodeficiency virus infection of megakaryocytic cells. Blood, 1991;77(3):481-485.
438. Noisakran S, Onlamoon N, Hsiao HM, et al. Infection of bone marrow cells by dengue virus in vivo. Exp Hematol, 2012;40(3):250-259.
439. Hsu AY, Wu SR, Tsai JJ. Infectious dengue vesicles derived from CD61+ cells in acute patient plasma exhibited a diaphanous appearance. Sci Rep, 2015;11(5):17990.
440. Clark KB, Moisekran S, Onlamoon N, et al. Multiploid CD61+ cells are the pre-dominant cell lineage infected during acute dengue virus infection in bone marrow. PLoS One, 2012;7(12):e52902.
441. Granick JL, Reneer DV, Carlyon JA, et al. Anaplasma phagocytophilium infects cells of the megakaryocytic lineage through sialylated ligands but fails to alter platelet production. J Med Microbiol, 2008;57(Pt4):416-423.
442. Inokuma H, Fujii K, Matsumoto K, et al. Demonstration of anaplasma (ehrlichia) platys inclusions in peripheral blood platelets in dogs in Japan. Vet parasitol, 2002;110(1-2):145-152.

443. Loeffelholz MJ. Anaplasma platys in bone marrow megakaryocytes of young dogs. J Clin Microbiol, 2014; 52(6):2231-2234.
444. Yeaman MR. Platelets: at the nexus of antimicrobial defence. Nature Reviews, 2014;12:426.
445. Yeaman MR, Yount NY, Waring AJ, et al. Modular determinants of antimicrobial activity in platelet factor-4 family kinocidins. Biochim Biophys Acta, 2007; 1768(3):609-619.
446. Hamzeh-Cognasse H, Damien P, Chabert A, et al. Platelets and infections – complex interactions with bacteria. Front Immunol, 2015;doi.
447. Dorit M, Zander W, Kilinger MHF. The blood platelets contribution to innate host defense-what they have learned from their big brothers. Biotechnol J, 2009;4:914-926.
448. Verschoor A, et al. A platelet-mediated system for shuttling blood-borne bacteria to CD8a+ dendritic cells depends on glycoprotein GPIb and complement C3. Nature Immunol, 2011;12:1194-1201.
449. Yount NY, Grank KD, Xiong YQ, et al. Platelet microbicidal protein 1: structural themes of a multifunctional antimicrobial peptide. Antimicrob Agent Chemother, 2004;48(11):4395-4404.
450. Kang HK, Chiang MY, Ecklund D, et al. Megakaryocyte progenitors are the main antigen presenting cells inducing Th17 response to lupus autoantigens and foreign antigens. J Immunol, 2012;188(12):5970-5980.
451. Finklestein A, Schlinker AC, Zhang L. Human megakaryocytes progenitors derived from hematopoietic stem cells of normal individuals are MHC class II-expressing professional APC that enhance Th17 and Th1/Th17 responses. Immunol Lett, 2015;163(1):84-95.
452. Michelson AD, Newburger PE. Platelets and leukocytes: aggregate knowledge. Blood, 2007;110:794-795.
453. Mueller WA. Getting leukocytes to the site of inflammation. Vet Pathol, 2013;50(1):7-22.
454. Zuchtriegel G, Uhl B, Puhr-Westerheide D, et al. Platelets guide leukocytes to their sites of extravasation. PLoS Biology, 2016;doi.
455. Morrell CN, Aggrey AA, Chapman LM, et al. Emerging roles for platelets as immune and inflammatory cells. Blood, 2014;123:2759-2767.
456. Fuchs TA, Abed U, Goosmann C, et al. Novel cell death leads to neutrophil extracellular traps. J Cell Biol, 2007;176(2):231-241.
457. Li P, Li M, Lindberg MR, et al. PAD4 is essential for antibacterial innate immunity mediated by neutrophil extracellular traps. JEM, 2010;207(9):1853.
458. Rohrbach AS, Slade DJ, Thompson PR, Mowen KA. Activation of PAD4 in NET formation. Front Immunol, 2012;3:360.
459. Yang H, Biermann MH, Brauner JM, et al. New insights into neutrophil extracellular traps: mechanisms of formation and role in inflammation. Front Immun, 2016.
460. Clark SR, Guy CJ, Scurr MJ, et al. Esterified eicosanoids are acutely generated by 5-lipoxygenase in primary neutrophils and in human and murine infection. Blood, 2011;117(6):2033-2043.
461. Kaplan MJ, Radic M. Neutrophil extracellular traps: double-edged swords of innate immunity. J Immunol, 2012;189(6):2689-2695.
462. Lee KH, Kronbichler A, Park DD, et al. Neutrophil extracellular traps (NETs) in autoimmune diseases: A comprehensive review. Autoimmune Rev, 2017;16(11):1160-1173.
463. Wright TK, Gibson PG, Simpson JL, et al. Neutrophil extracellular traps are associated with inflammation in chronic airway disease. Respirology, 2016;21(3):467-475.

464. Jorch SK, Kubes P. An emerging role for neutrophil extracellular traps in noninfectious disease. Nature Medicine, 2017;23:279-287.
465. Ueki S, Melo RCN, Ghiran I, et al. Eosinophil extracellular DNA trap cell death mediates lytic release of free secretion-competent eosinophil granules in humans. Blood, 2013;121:2074-2083.
466. Zanin MK, Donohue JM, Everitt BA. Evidence that core histone H3 is targeted to the mitochondria in Brassica oleracea. Cell Biol Int, 2010;34(10):997-1003.
467. Choi YS, Hoon J, Min HK. Shot-gun proteomic analysis of mitochondrial D-loop DNA binding proteins: identification of mitochondrial histones. Mol Biosyst, 2011;7(5):1523-1536.
468. Chen R, Kang R, Tang D. Release and activity of histones in disease. Cell Death and Disease, 2014;5:e1370.
469. Silk E, Zhao Y, Weng H, et al. The role of extracellular histones in organ injury. Cell Death and Disease, 2017;8(5):e28012.
470. Kim JE, Lee N, Gu J, et al. Circulating levels of DNA-histone complex and ds DNA are independent prognostic factors of disseminated intravascular coagulation. Thromb Res, 2015;135(6):1064-1069.
471. Varju I, Longstaff C, Szabo L, et al. DNA, histones and neutrophil extracellular traps exert anti-fibrinolytic effects in a plasma environment. Thromb Haemost, 2015;113(6):1289-1298.
472. Noubouossie DF, Whelihan MF, Yu YB, et al. In vitro activation of coagulation by human neutrophil DNA and histone proteins but not neutrophil extracellular traps. Blood, 2017;129(8):1021-1029.
473. Marsman G, Zeerleder S, Luken BM. Extracellular histones, cell-free DNA, or nucleosomes: differences in immunostimulation. Cell Death Dis, 2016;7(12):e2518.
474. Allam R, Kumar SV, Darisipudi MN, et al. Extracellular histones in tissue injury and inflammation. J mol Med (Berl), 2014;92(5):465-472.
475. Remick DG. Pathophysiology of sepsis. Am J Pathol, 2007;170(5):1435-1444.
476. Howell MD, Davis AM. Management of sepsis and septic shock. JAMA, 2017;847-848.
477. Abraham E. New definitions for sepsis and septic shock: continuing evolution but with much still to be done. JAMA, 2016;315(8):757-759.
478. Singer M, Deutschman CS, Seymour CW, et al. The third international consensus definitions for sepsis and septic shock (Sepsis-3). JAMA, 2016;315(8):801-808.
479. Shankar-Hari M, Phillips GS, Levy ML, et al. Developing a new definition and assessing new clinical criteria for septic shock: for the third international consensus definitions for sepsis and septic shock (sepsis-3). JAMA, 2016;315(8):775-787.
480. Hurley SM, Lutay N, Holmqvist B, et al. The dynamics of platelet activation during the progression of Streptococcal sepsis. PLoS One, 2016;11(9): e0163531.
481. De Stoppelaar SF, van 't Veer C, Claushuis TAM, et al. Thrombocytopenia impairs host defense in gram-negative pneumonia-derived sepsis in mice. Blood, 2015;124(25):3781-3790.
482. Xiang B, Zhang G, Guo L, et al. Platelets protect from septic shock by inhibiting macrophage-dependent inflammation via the cyclooxygenase 1 signalling pathway. Nat Commun, 2013;4:2657.
483. McDonald B, Davis RP, Kim SJ, et al. Platelets and neutrophil extracellular traps collaborate to promote intravascular coagulation during sepsis in mice. Blood, 2017;129(10):1357-1367.

484. Yin H, Stojanovic-Terp A, Xu W, et al. Role of platelet glycoprotein Ib-IX and effects of its inhibition in endotoxemia-induced thrombosis, thrombocytopenia, and mortality. Arterioscler Thromb Vasc Biol, 2013;33(11):2529-2537.
485. Zhao L, Ohtaki Y, Yamaguchi K, et al. LPS-induced platelet response and rapid shock in mice: contribution of O-antigen region of LPS and involvement of the lectin pathway of the complement system. Blood, 2002;100(9):3233-3239.
486. Yadav H, Kor D. Platelets in the pathogenesis of acute respiratory distress syndrome. Am J Physiol Lung Cell Mol Physiol, 2015;309(9):L915-923.
487. Akinosoglou K, Alexopoulos D. Use of antiplatelet agents in sepsis: a glimpse into the future. Thromb Res, 2014;133(2):131-138.
488. Kahn F, Hurley S, Shannon O. Platelet promote bacterial dissemination in a mouse model of streptococcal sepsis. Microbes and Infection, 2013;15(10-11):669-676.
489. Gao Y, Yu X, Guo S, et al. The impact of various platelet indices as prognostic markers of septic shock. PLoS One, 2014;9(8):e103761.
490. Hurley SM, Lutay N, Holmqvist B, et al. The dynamics of platelet activation during the progression of Streptococcal sepsis. PLoS One, 2016;11(9):e0163531.
491. Yaguchi A, Lobo FL, Vincent JL, et al. Platelet function in sepsis. J Thromb Haemost, 2004;2(12):2096-2102.
492. Protti A, Fortunato F, Artoni A, et al. Platelet mitochondrial dysfunction in critically ill patients: comparison between sepsis and cardiogenic shock. Critical Care, 2015;19:39.
493. Toner P, McAuley DF, Shyamsundar M. Aspirin as a potential treatment in sepsis or acute respiratory distress syndrome. Crit Care, 2015;19:374.
494. Seidel M, Winning J, Claus RA, et al. Beneficial effect of clopidogrel in a mouse model of polymicrobial sepsis. Thromb Haemost, 2009;7:1030-1032.
495. Akinosoglou K, Perperis A, Theodoraki S, et al. Sepsis favors high-on-clopidogrel platelet reactivity. Platelets, 2017;21:1-3.
496. Kiers HD, Kox M, van der Heijden WA, et al. Aspirin may improve outcome in sepsis by augmentation of the inflammatory response. Intensive Care Medicine, 2016;42(6):1096-1096.
497. Valerio-Rojas JC, Jaffer IJ, Kor DJ, et al. Outcomes of severe sepsis and septic shock on chronic antiplatelet treatment: A historical cohort study. Crit Care Res Pract, 2013;2013:782573.
498. Storey RF, James SK, Siegbahn A, et al. Lower mortality following pulmonary adverse events and sepsis with ticagrelor compared to clopidogrel in the PLATO study. Platelets, 2014;25(7):517-525.
499. Varun R, Sharma R, Misra SR, et al. Emperipolesis – A review. J Clin DIagn Res, 2014;8(12):ZM01-ZM02.
500. Cashell AW, Buss DH. The frequency and significance of megakaryocytic emperipolesis in myeloproliferative and reactive states. Ann Hematol, 1992;64(6):273-276.
501. Kang HK, Chiang MY, Ecklund D, et al. Megakaryocyte progenitors are the main APCs inducing Th17 response to lupus autoantigens and foreign antigens. J Immunol, 2012;188(12):5970-5980.
502. Sato T, Sekine H, Kakuda H, et al. HIV infection of megakaryocytic cell lines. Leuk Lymphoma, 2000;36(3-4):397-404.
503. Noisakran S, Onlamoon N, Hsiao HM, et al. Infection of bone marrow cells by dengue virus in vivo. Exp Hemaol, 2012;40(3):250-259.

504. Ferry JA, Pettit CK, Rosenberg AE, et al. Fungi in megakaryocytes. An unusual manifestation of fungal infection in bone marrow. Am J Clin Pathol, 1991;96(5):577-581.
505. Brown RE, Rimsza LM, Pastos K, et al. Effects of sepsis on neonatal thrombopoiesis. Pediatr Res, 2008;64(4):399-404.
506. Mattia G, Vulcano F, Milazzo L, et al. Different ploidy levels of megakaryocytes generated from peripheral or cord blood CD34+ cells are correlated with different levels of platelet release. Blood, 2002;99:888-897.
507. Broghamer WL Jr, Weakley-Jones B. Megakaryocytes in renal glomeruli. Am J Clin Pathol, 1981;76(2):178-82.
508. Mandal RV, Mark EJ, Kradin RL. Megakaryocytes and platelet homeostasis in diffuse alveolar damage. Exp Mol Pathol, 2007;83(3):327-331.
509. Nishimura S, Nagasaki M, Kunishima S, et al. IL-1α induces thrombopoiesis through megakaryocyte rupture in response to acute platelet needs. J Cell Biol, 2015;209(3):453-466.
510. Freishtat RJ, Natale J, Benton AS, et al. Sepsis alters the megakaryocyte-platelet transcriptional axis resulting in granzyme B-mediated lymphotoxicity. Am J Respir Crit Care Med, 2009;179(6):467-473.
511. Rondina MT, Schwertz H, Harris ES, et al. The septic milieu triggers expression of spliced tissue factor mRNA in human platelets. J Thromb Haemost, 2011;9(4):748-758.
512. Sperling X, Fischer M, Maitz MF, et al. Biomaterial induced NET formation on hydrophobic surfaces supports blood coagulation. Frontiers Bioeng Biotechnol Conference Abstract:10th world biomaterials congress.
513. Degaldo-Rizo V, Matrinez-Guzman MA, Iniguez-Gutierrez L, et al. Neutrophil extracellular traps and its implications in inflammation: An overview. Front Immunol, 2017; https://doi.org/10.3389/fimmu.2017.00081
514. Sorensen OE, Borregaard N. Neutrophil extracellular traps – the dark side of neutrophils. J Clin Invest, 2016;126(5):1612-1620.
515. Ueki S, Melo RCN, Ghiran I, et al. Eosinophil extracellular DNA trap cell death mediates lytic release of free secretion-competent eosinophil granules in humans. Blood, 2013;121(11):2074-2083.
516. Camicia G, Pozner R, Larranaga G. Neutrophil extracellular traps in sepsis. Shock, 2014;42(4):286-294.
517. Yang S, Qi H, Kan K, et al. Neutrophil extracellular traps promote hypercoagulability in patients with sepsis. Shock, 2017;47(2):132-139.
518. Carestia A, Kauffman T, Schattner M. Platelets: new bricks in the building block of neutrophil extracellular traps. Front Immunol, 2016;7:271.
519. McDonald B, Davis RP, Kim SJ, et al. Platelets and neutrophil extracellular traps collaborate to promote intravascular coagulation during sepsis in mice. Blood, 2017;129(10):1357-1367.
520. Ekaney ML, Otto GP, Sossdorf M, et al. Impact of plasma histones in human sepsis and their contribution to cellular injury and inflammation. Crit Care, 2014;18(5):543.
521. Chen R, Kang H, Fan XG, et al. Release and activity of histone in diseases. Cell Death and Disease, 2014;5:e1370.
522. Silk E, Zhao H, Weng H, et ak. The role of extracellular histone in organ injury. Cell Death and Disease, 2017;8(5):e2812.

523. Liu CL, Tangsombatvisit S, Rosenberg JM, et al. Specific post-translational modifications of neutrophil extracellular traps as immunogens and potential targets of lupus autoantibodies. Arthritis Res Ther, 2012;14(1):R25.
524. Kawasugi K, Yamamoto T, Shirafuji N, et al. Increase levels of histone in human plasma in septic patients with DIC. Blood, 2015;126:1104.
525. Ekaney ML, Otto GP, Sossdorf M, et al. İmpact of plasma histones in human sepsis and their contribution to cellular injury and inflammation. Crit Care, 2014;18(5):543.
526. Li Y, Liu B, Fukudome EY, et al. Identification of citrullinated histone H3 as a potential serum protein biomarker in a lethal model of lipopolysaccharide-induced schock. Surgery, 2011;150(3):442-451.
527. Pan B, Alam HB, Chong W, et al. CitH3: a reliable blood biomarker for diagnosis and treatment of endotoxic shock. Sci Rep, 2017;7(1):8972.
528. Li Y, Liu Z, Zhao T, et al. Citrullinated histone H3: a novel target for the treatment of sepsis. Surgery, 2014;156(2):229-234.
529. Neeli L, Radic M. Current challenges and limitation in antibody-based detection of citrullinated histones. Front Immunol, 2016;7:528.
530. Garcia-Gimenez JL, Roma-Mateo C, Carbonell N, et al. A new mass spectrometry-based method for the quantification of histones in plasma from septic shock patients. Sci Reports, 2017; doi:10.1038/s41598-017-10830-z.
531. Marsman G, Zeerleder S, Luken BM, et al. Extracellular histones, cell-free DNA, or nucleosomes: differences in immunostimulation. Cell Death Dis, 2016;7(12):e2518.
532. Semple JW, Italiano JE, Freedman J. Platelets and the immune continuum. Nature Reviews Immunol, 2011;11:264-274.

Figures:

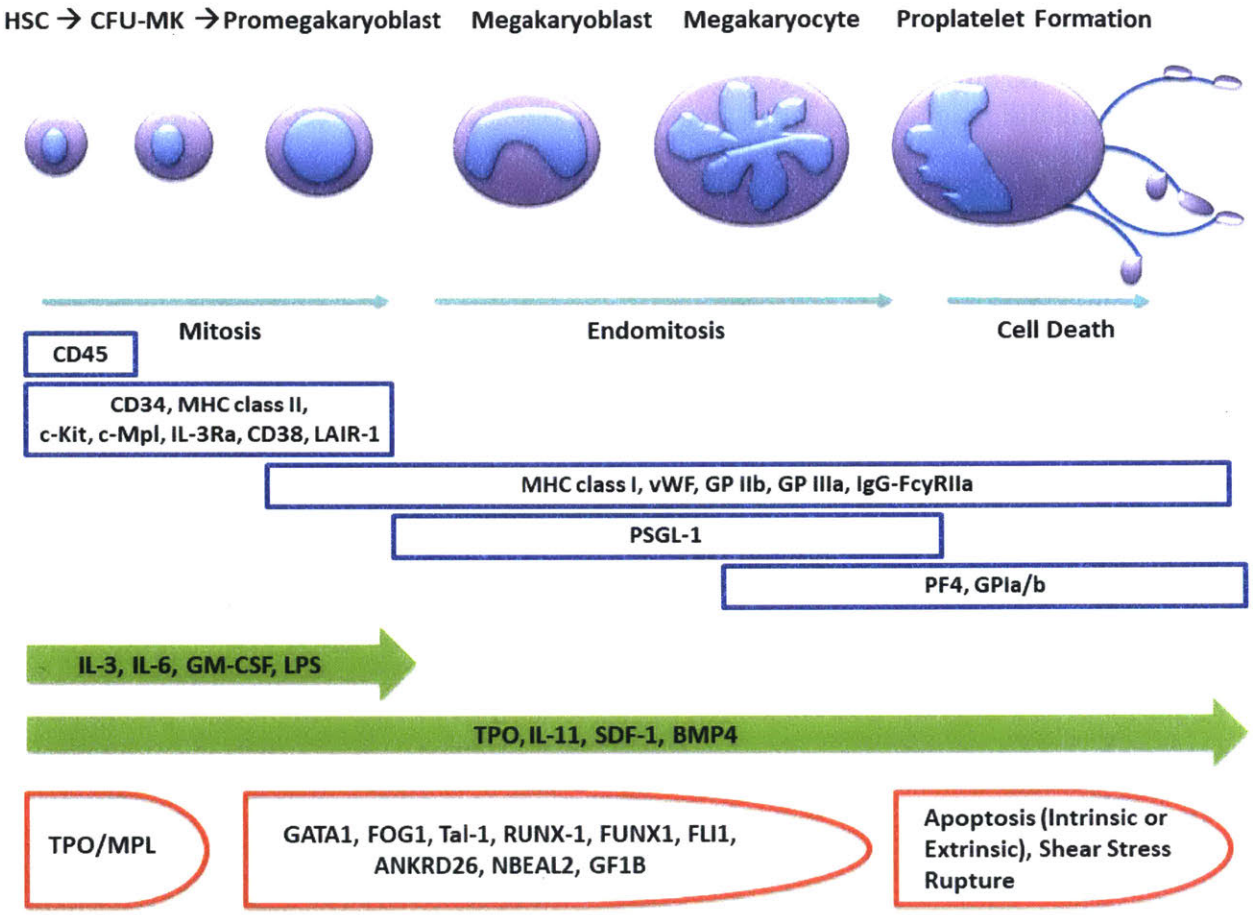

Figure 1-1: Megakaryocyte maturation and signaling.

This figure describes the maturation of the megakaryocyte originating from the hematopoietic stem cell to the proplatelet-forming mature megakaryocyte. The aqua arrows label the stage of nuclear development and cell cycle. The blue boxes include some of the markers expressed on the cell surface at various time points. The large green arrows include various stimulants to both cell proliferation and megakaryocyte commitment and maturation. The red bullets at the bottom are examples of some important pathways involved in megakaryocyte development. The listed signals, factors, and pathways in this figure are not all-inclusive and only include a few select important pathways.

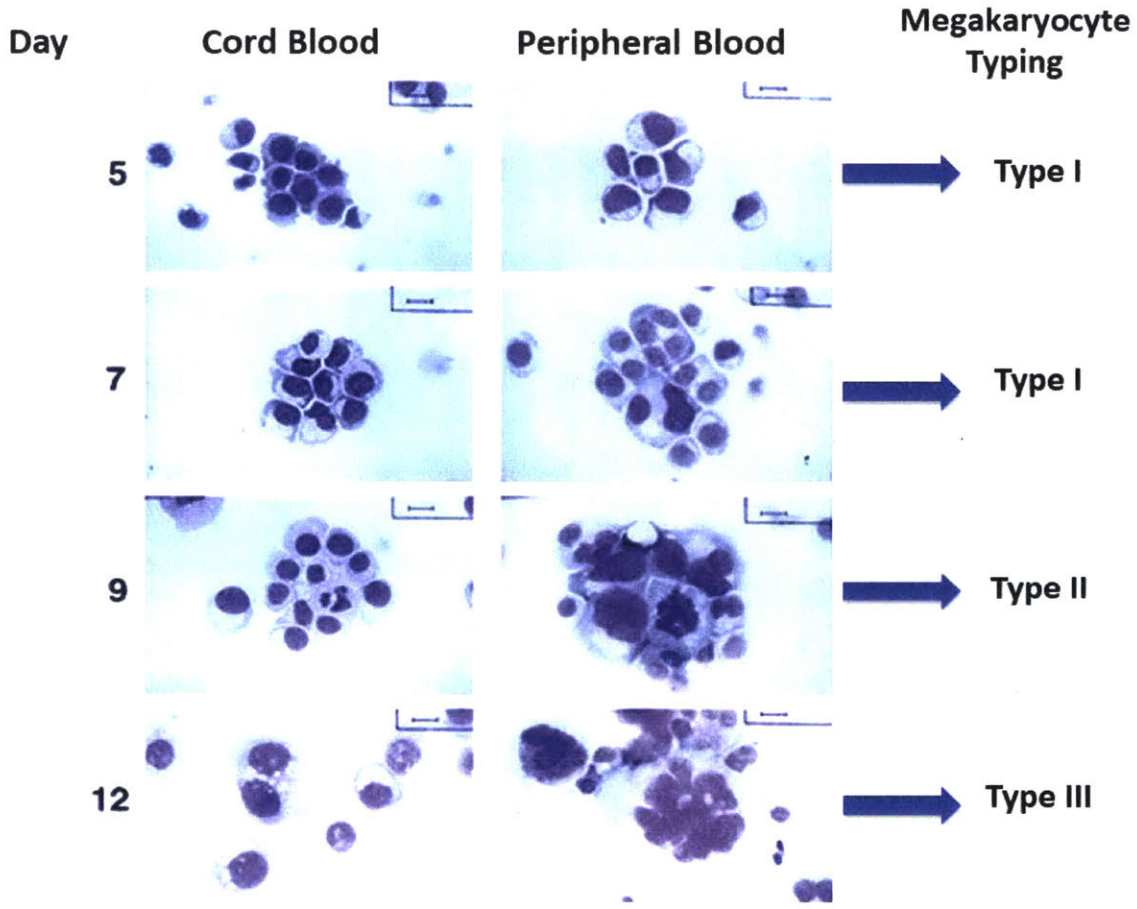

Figure 1-2: Megakaryocyte maturation.

This figure shows cytology pictures of maturing megakaryocytes from two different sources: cord blood (CB) and peripheral blood (PB). The cord blood-derived megakaryocytes are smaller and have a lower nuclear ploidy than the peripheral blood-derived cells. On the right side of the figure, the megakaryocyte type is labeled: Type I have basophilic cytoplasms with a large nuclear to cytoplasmic ratio (N:C); Type II are larger, a smaller N:C, and more azurophilic; Type III have a low N:C and distinct nuclear lobes. These maturation differences are easier to distinguish with the PB-derived cells, as the CB-derived cells maintaining a small size and somewhat resemble activated lymphocytes. Adapted from: Mattia G, Vulcano F, Milazzo L, et al. Different ploidy levels of megakaryocytes generated from peripheral or cord blood $CD34^+$ cells are correlated with different levels of platelet release. Blood, 2002;99:888-897.

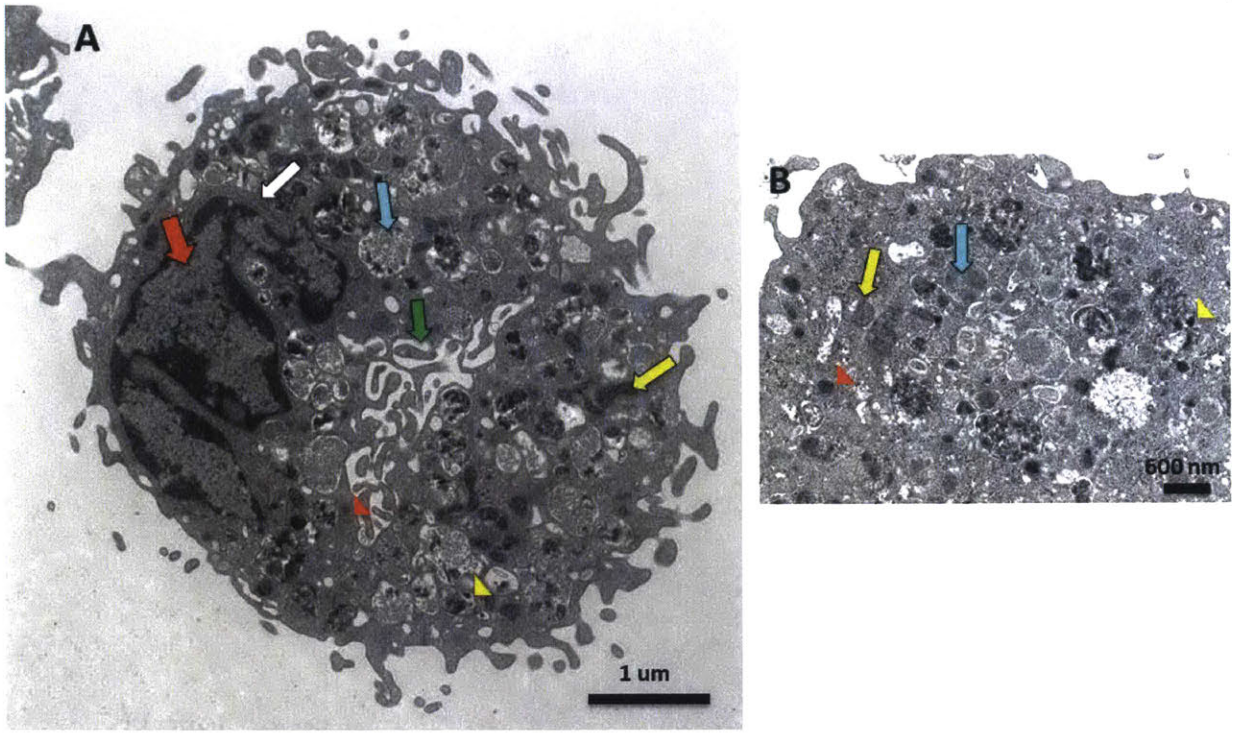

Figure 1-3: Megakaryocyte EM

Electron microscopy image of a cord blood-derived megakaryocyte with components labeled: nucleus, red arrow; multivesicular body, blue arrow; demarcation membrane system (DMS), green arrow; mitochondria, yellow arrow; rough endoplasmic reticulum (RER), white arrow; alpha granule, red arrow head; dense granule, yellow arrow head.

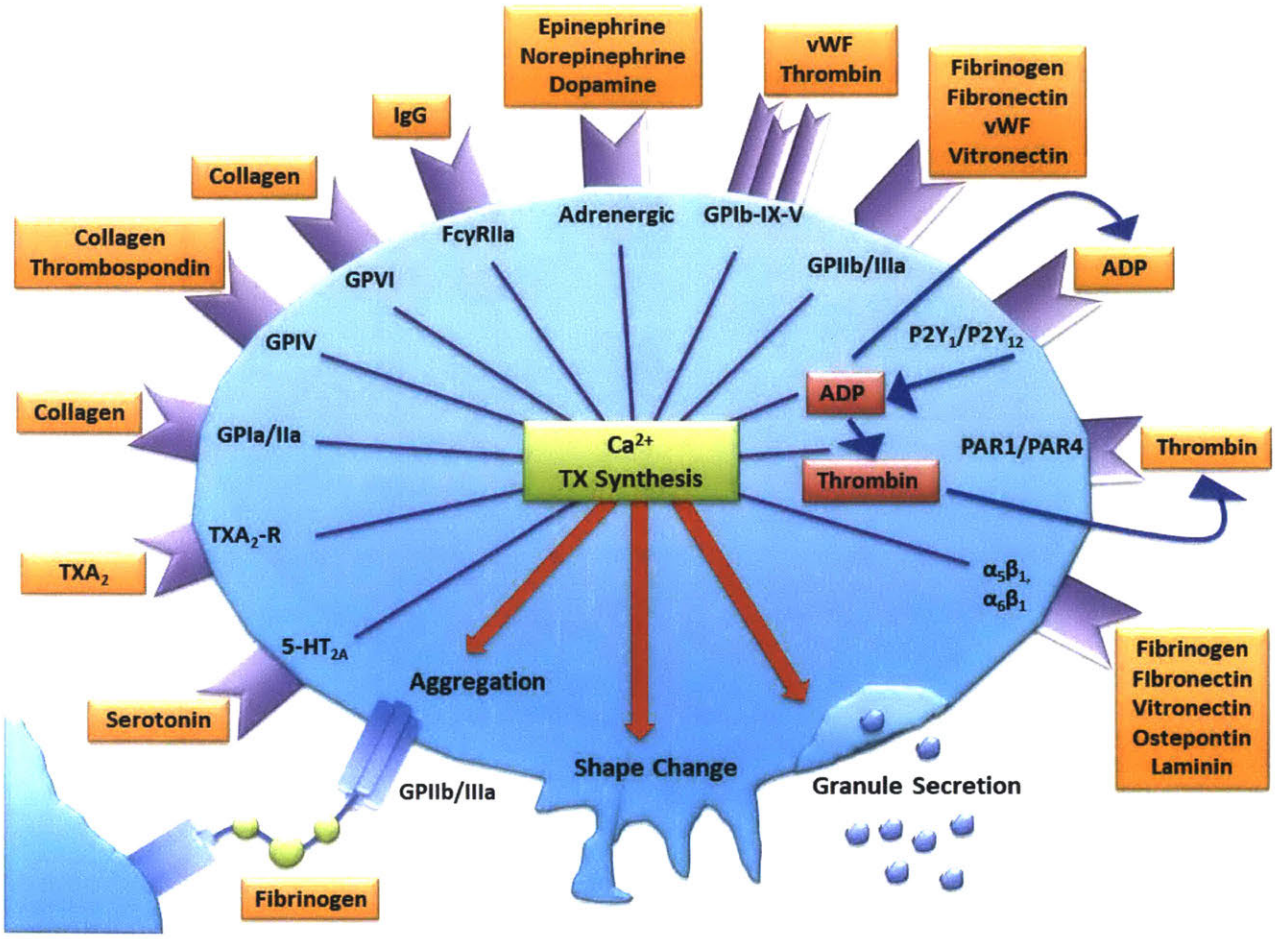

Figure 1-4: Platelet receptors and activation.

In this figure, a platelet is depicted with multiple surface receptors (purple) and some of their primary agonists (orange). The $P2Y_1/P2Y_{12}$ and PAR1/PAR4 receptors are shown to play a part in intracellular signaling (inside-out). Activation of the platelet via many of these receptors results in an increase in intracellular calcium and also TXA_2 synthesis, in a receptor-dependent fashion. Based on which agonist is bound to which receptor and the amount of stimulus, the platelet may then continue on to a reversible shape change or to an irreversible granule secretion and platelet aggregation, via the cross-linking of fibrinogen with glycoprotein receptor GPIIb/IIIa. This figure does not include all pathways, including many of the immuno-modulatory receptors.

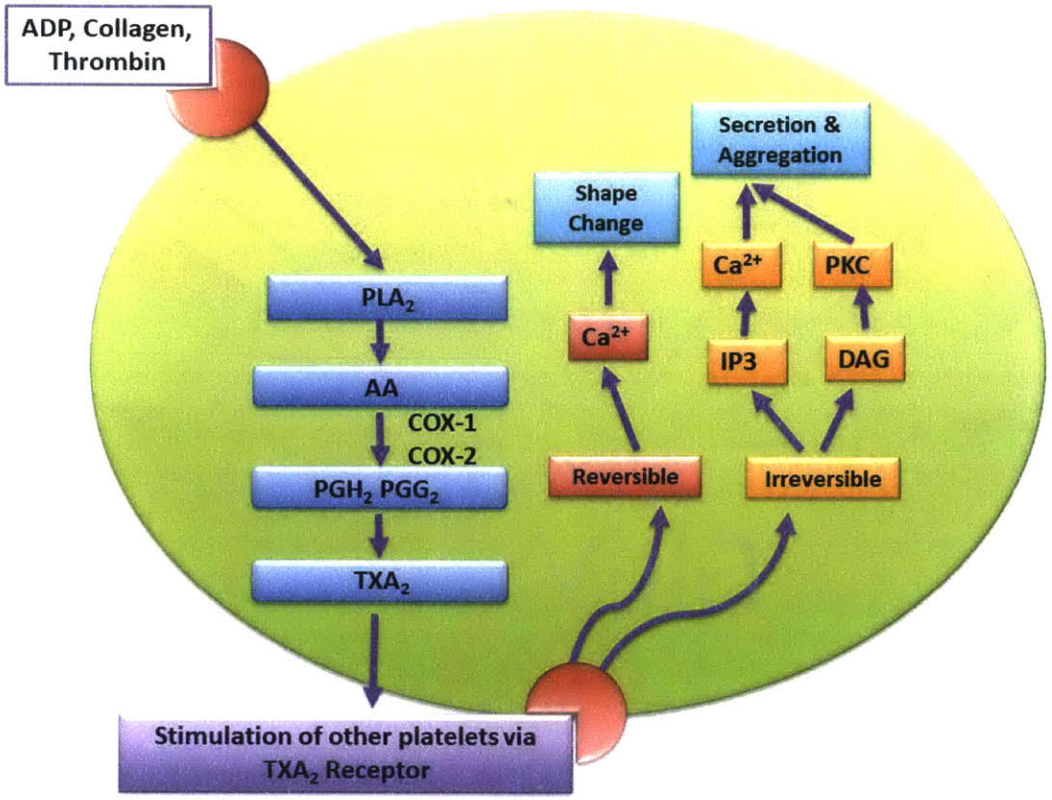

Figure 1-5: Prostanoids and the COX Pathway in Platelets

On the left of the diagram, the synthesis of thromboxane A_2 (TXA_2) is shown. Upon platelet stimulation and subsequent phospholipase A_2 (PLA_2) activation, TXA_2 is synthesized. PLA_2 cleaves membrane phosphoglycerides to release arachidonate acid (AA), which is converted by COX enzymes (primarily COX-1) to endoperoxides prostaglandin H_2 (PGH_2) and prostaglandin G_2 (PGG_2). TXA_2 is then synthesized via the conversion of these endoperoxidases by TXA_2 synthase. TXA_2 then passively diffuses across the platelet membrane, where it may interact with other cell types and activate surrounding platelets. The right side of the diagram depicts the direct interaction between TXA_2 and the platelet. A proposed model of the binding sites identified by GR32191 in human platelets and their effector systems is shown here, where reversible, high affinity binding event, results in an increase in intracellular calcium and shape change, whereas an irreversible, low affinity binding event results in platelet granule secretion and aggregation. DAG: diacylglycerol; PKC: protein kinase C; IP3: inositol triphosphate; TXA_2: thromboxane A_2; phospholipase A_2: PLA_2: prostaglandin H_2: PGH_2; prostaglandin G_2: PGG_2. Adapted from: Platelets in thrombotic and non-thrombotic disorders. Edited by: Paolo Gisele et al. 2002 Cambridge University Press.

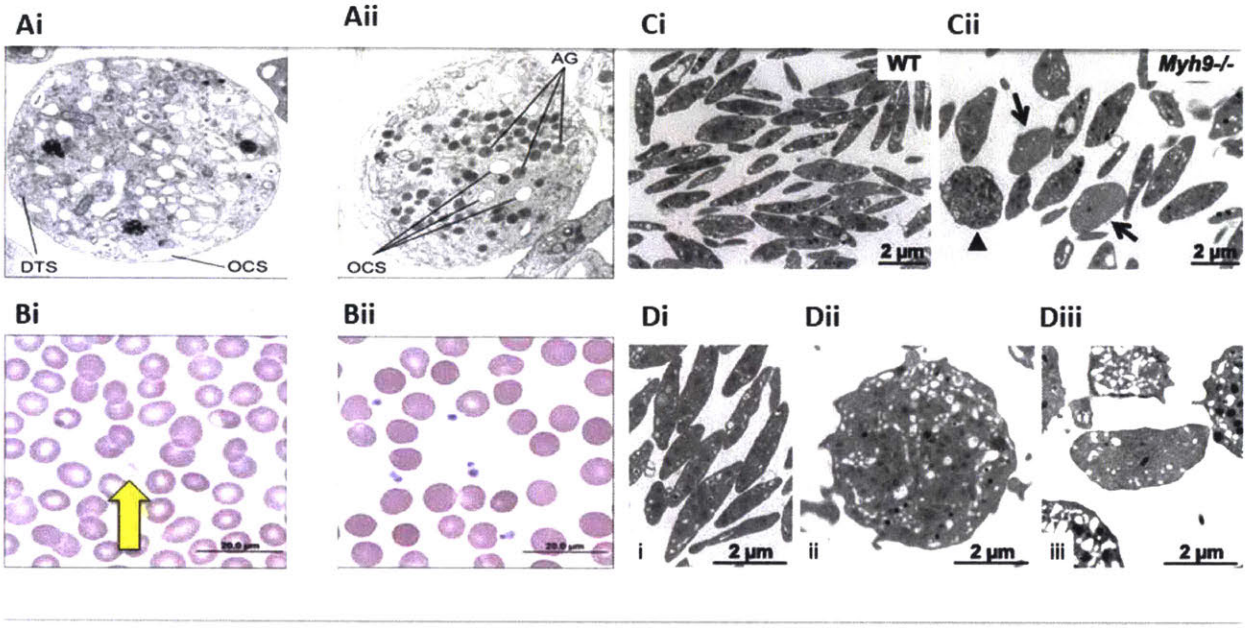

Figure 1-6: Platelets from humans and animal models with GPS and MYH9 disorders.
(Ai) EM of thin sections of a platelet from a patient showing absence of α-granules and abundant channels of the open canalicular system (labeled as OCS) in comparison with EM of a control platelet (Aii) showing normal alpha granules (labeled as AG). DTS: Dense tubule system. (Bi) Light microscopy of the peripheral smear of a GPS patient showing a large pale gray platelet (yellow arrow) without the cytoplasmic color of α-granules, in comparison with a normal smear (Bii). (Ci) Wide-field electron micrographs of mouse platelets showing the heterogeneous content of *Myh9*$^{-/-}$ platelets (right) as compared with WT cells (left) (Cii). Arrows point to low-content platelets and the arrowhead to a high-content platelet. Ultrastructure of human platelets from a control individual (Di) as compared with a MYH9-RD patient (Dii-iii). GPS images adapted from: Gunay-Aygun M, Zivony-Elboum Y, Gumruk F, et al. Gray platelet syndrome: natural history of a large patient cohort and locus assignment to chromosome 3p. Blood, 2010;116:4990-5001. *MYH9*$^{-/-}$ images adapted from: Pertuy F, Eckly A, Weber J, et al. Myosin IIA is critical for organelle distribution and F-actin organization in megakaryocytes and platelets. Blood, 2014;123:1261-1269.

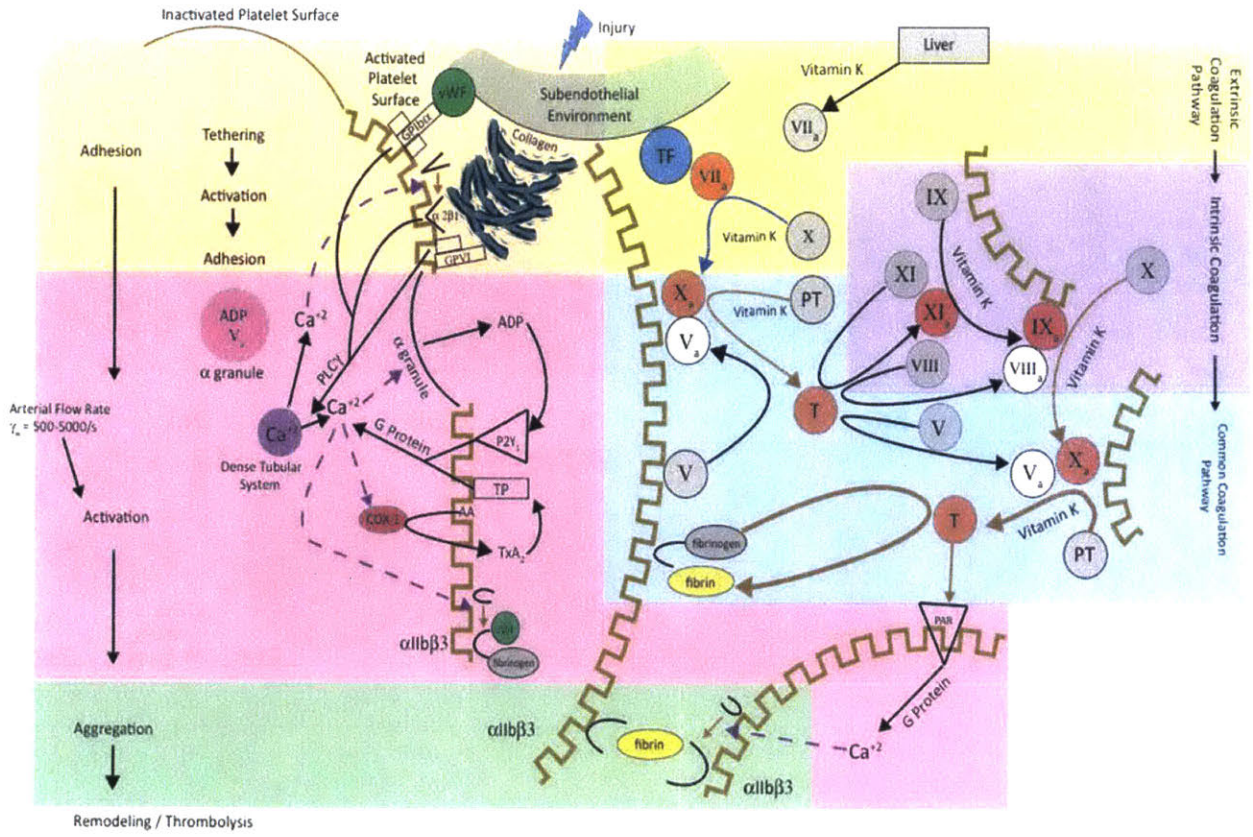

Figure 1-7: Mechanisms underlying normal hemostasis.

The intersection between primary platelet plug formation, platelet activation and the coagulation cascade is illustrated. The processes of platelet adhesion, activation and aggregation are highlighted in different color boxes, as are the extrinsic, intrinsic and common coagulation pathways. The brown lines represent the platelet surface, with the palisading lines representing the activated platelet surface. Brown arrows indicate processes that rely on the platelet surface to occur at maximum efficacy; blue arrows indicate processes that require the subendothelial environment; purple arrows indicate processes that are calcium dependent; processes that are vitamin K dependent are noted. Gray circles represent hepatic derived factors; white circles activated coenzymes; red circles activated enzymes.

Tables:

Table 1-1: Platelet Cell Surface Markers

Marker	Target	Significance
CD41	GPIIb/IIIa	Surface marker
CD42a	GPIX	Surface marker
CD42b	GPIb	Surface marker
CD61	GPIIIa	Surface marker; Vitronectin receptor
PAC-1	GPIIb/IIIa	Activation marker; against fibrinogen binding site exposed by conformational change in GPIIb/IIIa
CD62P	P-selectin	Activation marker; component of α-granule membrane, mediates adhesion to neutrophil and monocytes
CD31	PECAM	Activation marker
CD63		Activation marker; protein in dense granule and lysosomal membrane
Mepacrine	quinacrine	Activation marker; taken up by platelet dense granules and emits a green fluorescence (FL1) – washing step is required
Anexin V binding	Phosphateidylserine	Activation marker; Calcium-dependent phospholipid protein, allows the detection of PS exposure on cell surface (fluorescent conjugated annexin V)
HLA-ABC	MHC Class I	Surface marker; antigen presentation
HLA-DR	MHC Class II	Surface marker (early differentiation); antigen presentation
CD34	CD34	Hematopoietic stem cell marker
CD32a	FcγRIIa	IgG Receptor
CD123	IL3Ra	IL-3 Receptor
PF4	Platelet Factor 4	alpha granule content
CD162	PSGL-1; P-selectin glycoprotein ligand-1; SELPG	Cell adhesion molecule; binds to P- and L-selectin
vWF	Von Willebrand Factor	alpha granule content
Platelet-leukocyte complexes	Any platelet/leukocyte marker, example: CD45/CD42b positive events	Platelet and leukocyte activation; activated platelets adhere to isolated fractions of monocytes and neutrophils, mediated primarily through CD62P

Table 1-2: Platelet granule contents.

α-granules		dense-granules		lysosomes	
Membrane	Matrix	Membrane	Matrix	Membrane	Matrix
GTP binding proteins: rab4, GMP33, Rap1[b]	Proteoglycans: betaTG, PF4, serglycin, HRGP	GTP binding protein: Ral1	Adenine nucleotides: ATP, ADP	LIMP1/CD63[a]	Cathepsin D, E
GPIIbIIIa[a, b]	Adhesive: fibronectin, vitronectin, vWF, thrombospondin	Glycoproteins: GPIb[a,b], IIbIIIa[a,b]	Serotonin (5-HT)	LAMP1, LAMP2	Carboxypeptidases(A,B)
GPIb-IX[b]	Haemostasis: fibrinogen, FV/VIII/XI/XIII, kininogen, protein S, plasminogen	Granulpphysin (LIMP1/CD63)[c]	Calcium, magnesium		Prolinecarboxypeptidase
GPIV (CD63)[b]	Cellular mitogens: PDGF, TGFbeta, ECGF, EGF, VEGF/VPF, IGF, ILbeta	LAMP 2[c]	Pyrophosphate		Collagenase
P24 (CD9)[b]	Protease inhibitors: a2-macroglobulin, a2-antitrypsin, PDCI, a2-antiplasmin, PAI1, TFPI, PN-2/APP, C1 inhibitor	Src[b]	Guanine nucleotides: GTP, GDP		Acid phosphatase
P-selectin (CD62P)[a, b]	Immunoglobulins: IgG, IgA, IgM	P-selectin (CD62P)[a,b]	Histamine		Arylsulfatase
PECAM (CD31)[b]	Albumin				Heparinase
GLUT-3	GPI1/multimerin				Glycohydrolases
Vitronectin receptor	Binds vitronectin: can alter binding to fibrinogen, decrease agg, bind to endothelium				
Osteonectin	Binds thrombosponding: adhesive platelet glycoprotein				

Table modified from Chart 7.1-7.3 in: Platelets in thrombotic and non-thrombotic disorders. Edited by: Paolo Gisele et al. 2002 Cambridge University Press.

Chapter 2

Megakaryocytes as Functional Innate Immune Cells

2.1 Abstract

Megakaryocytes (MKs) are precursors to platelets, the second largest cell population in blood. While platelets are under investigation for their role in inflammation, the role of MKs within the innate immune system has not yet been explored. We have performed a set of comprehensive *in vitro* experiments demonstrating that both cord blood-derived MKs and MKs from a megakaryoblastic lineage (Meg-01 cells) have innate immune cell functions. MKs can phagocytose bacteria, form extracellular traps, and chemotaxis towards pathogenic stimuli. Evaluation of samples from patients with sepsis revealed increased numbers of $CD61^+$ cells in the kidneys and lungs, and an increased number of $CD41^+CD61^+$ cells in the peripheral blood. Overall, our study suggests that MK cells participate in the immune responses during severe inflammation and infection.

2.2 Introduction

Megakaryocytes (MKs), the largest and rarest cell in the bone marrow, are commonly recognized as key participants in the hemostasis processes through the production of platelets. (Kaushansky K, 2005; Machlus KR, 2013) In addition to their presence in the bone marrow, MKs are frequently located in the lungs, lymph nodes, spleen, and liver during times of increased extra medullary hematopoiesis. (Alamo IG, 2017; Lefrancais E, 2017; Yacoub A, 2013; Yassin MA, 2016; Hill AD, 2000) Notably, MKs have also been reported to be significantly increased in the lungs during severe pulmonary inflammation, such as in acute respiratory distress syndrome (ARDS), where they are believed to promote inflammation via the release of platelets. (Weyrich As, 2013; Mandal RV, 2007; Yadav H, 2015) The current paradigm by which MKs are increased in the lungs during ARDS revolves around passive escape from the bone marrow, secondary to vasodilation and increased vascular permeability, where they enter the arterial circulation and,

due to their large size, become trapped within the microcirculatory bed of the alveoli. (Lefrancais E, 2017; Sharma GK, 1986; Kaufman RM, 1965)

An alternate or complimentary paradigm, where MKs have immune functions, is suggested by several observations; however, this has not been tested systematically. At various points of maturations, MKs have been shown to express both major histocompatibility complex (MHC) class I and II molecules, and a variety of toll-like receptors (TLRs) on their cell surface. (Finkelstein A, 2015; Undi RB, 2016; D'Atri LP, 2015; Beaulieu LM, 2010; Shiraki R, 2004; Beulieu LM, 2011) MKs, just as platelets, are considered granulocytes and contain various granule types, including lysosomes, which are typically present in most mammalian cells and participate in the endocytosis and degradation of pathogens by innate immune cells (Bentfeld-Barker ME, 1982). Recent studies have elucidated the role of the MK as a primary antigen-presenting-cell (APCs) in stimulating the Th-17 response in Lupus. (Finkelstein A, 2015; Kang HP, 2012) Thrombocytes, the amphibian equivalent of the mammalian MK and plt, have been demonstrated to actively phagocytose pathogens, both *in vitro* and *in vivo*; although, there is still debate as to whether mammalian platelets are phagocytes or covercytes. (White JG, 2005; Lewis JC 1976; Absolom DR, 1982) In mammals, MKs have been documented to internalize various viruses, including dengue virus and HIV, and there are two case reports demonstrating internalization of fungal organisms. (Zucker-Franklin 1989; Ferry JA, 1991; Clark KB, 2016; Clark KB, 2012) These reports provide support for the participation of MKs in the immune response against infection.

Here, we explore the ability of human MKs to phagocytize pathogens, form extracellular traps, and undergo chemotaxis towards pathogenic stimuli. Moreover, we find that during sepsis $CD61^{+}CD41^{+}$ cells are increased in the peripheral circulation and $CD61^{+}$ cells are increased in the peripheral organs. The number of these cells appears to correlate with the type of infection and prognosis, being elevated during acute kidney injury (AKI) and ARDS, as well as in disseminated intravascular coagulation (DIC).

2.3 Materials and Methods

2.3.1 Cell culture

Cord blood $CD34^+$ hematopoietic stem cells and Meg-01 cells were cultured and differentiated into megakaryocytes (CB MKs). Cord blood $CD34^+$ hematopoietic stem cells were purchased and cultured in StemSpanII media with the megakaryocyte supplemental cytokines, according to the culture and differentiation protocols from Stemcell Technologies (Stemcell Technologies Inc. Cambridge, MA). A megakaryoblastic cell line (Meg-01) was purchased and cultured in RPMI with 10% FBS, according to the standard cultures protocols from ATCC (American Type Culture Collection, Manassas, VA).

2.3.2 Flow cytometry

Flow cytometry was performed in order to verify appropriate cellular differentiation and for the evaluation of cell surface markers. Briefly, cells were stained with antibodies at a concentration of 1:200 for 15 minutes, with the exception of CD41, which was at a concentration of 1:100. Cells were then stained with Draq5 (Thermo Fisher Scientific, Waltham, MA) at a concentration of 1:10000 for 5 minutes. Antibodies included: anti-human CD41, HLA-ABC (MHC class I), HLA-DR (MHC class II), CD162 (p-glycoprotein-1; SELPG), CD61 (GPIIIa), CD41 (GPIIb), CD34 (Biolegend, San Diego, Ca), CD66b, and CD62P (P-selectin) (BD Biosciences, San Jose, CA). Data was obtained through the Amnis ImageStreamX Mark II imaging flow cytometer and INSPIRE Software (EMD Millipore, Billerica, MA). The accompanying IDEAS Software was used to perform data analysis. Data is reported as the percent of the total cell population that stained positive for the specific marker.

2.3.3 Bacterial preparation

Bacteria, including *Escherichia coli (E. coli), Staphylococcus aureus (S. aureus), and Streptococcus pyogenes (S. pyogenes)*, were conjugated to pHrodo for phagocytosis experiments. Bacteria was provided by the Division of Comparative Medicine at the Massachusetts Institute of Technology (Cambridge, MA). For the killed-bacteria experiments, organisms were heat killed at 75°C for 25 minutes. Bacteria were then conjugated to pHrodo succinimidyl ester dye (Thermo Fisher Scientific) according to the manufacturer's protocols. Briefly, bacteria were pelleted from

cultures by centrifugations at 5100 rpm for 10 minutes. Pellets were resuspended in PBS (pH 9.0) at a concentration of $1x10^8$ per mL. 200 µL of this suspension was then added to 5 µL of 10 mg/mL pHrodo succinimidyl ester dye and mixed thoroughly by pipetting. Bacteria were then stained for 30 mins in the dark with gentle shaking. Following staining, 1 mL of PBS (pH 8.0) was added to the solution, and bacteria were pelleted at 13,400 rpm for 3 minutes in a benchtop centrifuge. The supernatant was removed and the pellet thoroughly resuspended in Tris Buffer (pH 8.5). The bacteria were then pelleted at 13,400 rpm for 3 mins in a benchtop centrifuge, the supernatant was removed, and the bacteria were resuspended in 1 mL of PBS (pH 7.4), and stored at 4°C in the dark.

2.3.4 Immunofluorescent imaging

MKs were co-incubated with either the pHrodo-conjugated bacteria, Zymosan A *S. cerevisiae* BioParticles (ThermoFisher Scientific), or various concentrations of *E. coli* lipopolysaccharide (O111:B4; Sigma Aldrich, St Louis, MO) for 60 minutes at 37°C on poly-lysine coated slides (Sigma Aldrich, St Louis, MO, USA). The slides were then rinsed gently three times with PBS and the adhered cells were subsequently stained for live imaging or fixed and then stained. For evaluation of live cells, cells were stained with Hoechst (Thermo Fisher Scientific) at a concentration of 1:2000 for 5 minutes. For the calcein green-stained cells, cells were also stained with calcein (Thermo Fisher Scientific) at 1:1000 for 5 minutes. For extracellular trap evaluation, cells were also stained with SYTOX orange (Thermo Fisher Scientific) at 1:50 for 5 minutes. For histone staining of extracellular traps, cells co-incubated with *E. coli* LPS for 60 minutes at 37°C. They were then fixed with 4% paraformaldehyde (Santa Cruz Biotechnology, Dallas, TX, USA) for 30 minutes and then concentrated onto a poly-lysine coated slide using the Cytospin 4 cytocentrifuge (Thermo Fisher Scientific), for 5 minutes at 1250 rpm, rinsed once with di-water and stored at -80°C until staining and evaluation. For staining, the slides were thawed at room temperature and blocked with 5% donkey serum (Jackson Immunoresearch) for 2 hours. The slides were rinsed three times with PBS and then treated with the following primary antibodies for three hours: mouse anti-human neutrophil elastase (NE; ELA2) antibody (950334, Novus Biologicals, Littleton, CO, USA) at 1:300, rat anti-Histone H3 (phospho S28) antibody (HTA28, Abcam, Cambridge, MA, USA) at 1:500, and rabbit anti-human myeloperoxidase (A039829-2, Dako, USA) at 1:300. The slides were then rinsed three times with PBS and incubated with

secondary antibodies, including donkey anti-rabbit 488, donkey anti-rat 647, and donkey anti-mouse 568 (Life Technologies) at 1:500 for 30 minutes. Slides were then rinsed three times with PBS and then covered with Vectashield antifade mounting medium with DAPI (Vector Labs, Burlingame, Ca, USA). The cells were then images with one of two fluorescent microscopes: Life Technologies EVOS FL (Thermo Fisher Scientific) or Nikon Eclipse 90i microscope (Nikon Instruments Inc., Melville, NY). Composites and videos were made and images were analyzed using either Fiji or GIMP software. (Schindelin J, 2012)

2.3.5 Extracellular trap induction

Meg-01 cells underwent various treatments to induce extracellular trap formation. Meg-01 cells were co-incubated with various pathogenic stimuli, including *E. coli* LPS and live pHrodo conjugated *E. coli*, for 30-60 minutes at 37°c on a polylysine-coated slide. The poly-lysine slide was outlined with a hydrophobic pen prior to the experiment to set a boundary for the liquid. The slide was then rinsed three times in PBS. The slides were stained with 1:1000 Hoechst and 1:500 SYTOX orange and cover slipped. For the GFP-H2B experiments, Meg-01 cells were transfected with CellLight Histone 2B-GFP (Bacmam 2.0, ThermoFisher Scientific) for 48-72 hours and then labeled with MitoSox Red mitochondrial superoxide indicator (ThermoFisher Scientific) and Hoechst. Unstained slides were stored and evaluated with immunofluorescence techniques, as described above. The cells were imaged using one of two fluorescent microscopes: Life Technologies EVOS FL (Thermo Fisher Scientific) or Nikon Eclipse 90i microscope (Nikon Instruments Inc., Melville, NY).

2.3.6 Free double stranded DNA (dsDNA) quantification

Meg-01 cells were co-incubated with various concentrations of *E. coli* LPS (20 pg/mL to 2 ug/mL) for 30 minutes at 37°C. The cells were then pelleted down at 1900 g for 10 minutes and the supernatant was immediately stored at -80°c. The experiment was performed in biological triplicates (cells from 3 different culture flasks) and in technical triplicates, on two different days. Double stranded DNA (dsDNA) was quantified using the Quant-iT™ PicoGreen™ dsDNA Assay Kit (Thermo Fisher Scientific) following the recommended protocol. Briefly, the supernatant samples were thawed and 50 uL was placed in a 96-well plate, followed by 50 uL of the aqueous working solution. A standard curve using the provided DNA standard was created

for a reference. The plate was incubated at room temperature for 5 minutes and then read at standard fluorescein wavelengths (excitation ~480 nm, emission ~520 nm) on a SpectraMax Gemini XS plate reader (Molecular Devices, Sunnyvale, CA, USA). The mean fluorescent intensities (MFIs) were then converted to free dsDNA concentration according to the standard curve.

2.3.7 Transmission Electron microscopy

Meg-01 cells were co-incubated with live bacteria for 1 hour at 37°C. The cells were then pelleted down at 1900 g for 10 minutes. Immediately after removal of the culture medium, KII fixative (2.5% glutaraldehyde, 2.0% paraformaldehyde, 0.025 % Calcium Chloride in a 0.1M Sodium Cacodylate buffer, pH 7.4) was added to the cell/bacteria pellet, mixed, and allowed to fix for 20 minutes. A rubber tipped cell scraper was then used to gently remove the fixed monolayer from the plastic substrate. The samples were centrifuged, the fixative removed, replaced with buffer, and stored at 4°C until further processing. To make a cell block, the material was centrifuged again and resuspended in warm 2% agar in a warm water bath to keep the agar fluid. The material was then centrifuged again and the agar allowed to gel in an ice water bath. The tissue containing tip of the centrifuge tube was cut off resulting in an agar block with the material embedded within it. This agar block was then processed routinely for electron microscopy in a Leica Lynx™ automatic tissue processor. Subsequent processing was done using a Lieca Lynx™ automatic tissue processor. Briefly, they were post-fixed in osmium tetroxide, stained En Bloc with uranyl acetate, dehydrated in graded ethanol solutions, infiltrated with propylene oxide/Epon mixtures, embedded in pure Epon, and polymerized overnight at 60°C. One micron sections were cut, stained with toluidine blue, and examined by light microscopy. Representative areas were chosen for electron microscopic study and the Epon blocks were trimmed accordingly. Thin sections were cut with an LKB 8801 ultramicrotome and diamond knife, stained with lead citrate, and examined in a FEI Morgagni transmission electron microscope. Images were captured with an AMT (Advanced Microscopy Techniques) 2K digital camera.

2.3.8 Transwell chemotaxis

Meg-01 cells were used for chemotaxis experiments in both transwell plates and in a custom-made microfluidic device (described in the following section). SDF1α was used as a positive control, cell culture media was the negative control, and experimental condition consisted of various concentrations of *E. coli* LPS and zymosan particles. Growth factor reduced (GFR) matrigel coated transwell inserts with 8 um pores (Biocoat Matrigel Invasion Chambers, Corning, New Jersey, USA) were thawed for 30 minutes at 37°c. 1 million Meg-01 cells were loaded in a total volume of 200uL of RPMI with 10% FBS in the top chamber, while the bottom chamber was loaded with 600 uL of various conditions, including: RPMI with 10% FBS (negative control), 200 ng/mL SDF1α (CXCL12, Peprotech, New Jersey, USA) (positive control), 220 pg/mL and 2.2 ng/mL *E. coli* LPS, Zymosan particles alone, and zymosan particles with 220 ng/mL *E. coli* LPS or with 200 ng/mL SDF1α. The wells were incubated for 24 hrs. at 37°C. The cells in that migrated through the transwell insert into the bottom chamber were counted using Cellometer Vision automated cell counter (Niexcelom, Bioscience LLC., Lawrence, MA, USA).

2.3.9 Microfluidic device fabrication

The microfluidic devices were manufactured using standard microfabrication techniques. Briefly, a two-layer photoresist design (SU8, Microchem, Newton, MA), with a first and second layer that were 3 and 50 μm thick, were patterned on one silicon wafer via sequential photolithography masks and processing cycles according to the manufacturer's protocols. The resulting patterned wafer was then used as a mold to produce PDMS (Polymidemethylsiloxane, Fished Scientific, Fair Lawn, NJ) devices, which were subsequently irreversibly bonded to glass slides (1x3 inches, Fisher). The microfluidic device was designed to allow the formation of a chemical gradient in two steps, as previously described (Caroline JN, 2014). First: an array of circular wells (50 μm diameter, 50 μm height), connected to a side channel (10 μm width, 5 μm height) by orthogonal side-combs (5 μm width, 5 μm height), were primed. During the second step, the central channel was extensively washed with cell culture media (RPMI + 10% FBS). The diffusion of the chemoattractant from the circular wells, serving as sources, to the central channel, serving as sink, produced the guiding gradient for the cells in the central channels.

2.3.10 Microfluidic chemotaxis

The cellular nucleic acid was stained with Hoechst at 1:2000 (Thermo Fisher Scientific Inc, Grand Island, NY). The microfluidic chip was placed under vacuum for 10 minutes. The media and conditions were loaded into each microfluidic device. Various concentrations of *E. coli* LPS were co-incubated with Meg-01 cells in order to determine the optimal concentration at which immediate cell death was not instigated. The conditions included the following: RPMI with 10% FBS (negative control), 200 ng/mL SDF1α (CXCL12, Peprotech, New Jersey, USA) (positive control), 22 pg/mL, 220 pg/mL and 2.2 ng/mL *E. coli* LPS, zymosan particles, zymosan particles (1 million/mL) with 220 ng/mL *E. coli* LPS and zymosan particles (1 million/mL) with 200 ng/mL SDF1α. 200 uL RPMI +10% FBS was used to wash the main channel. Cells were then loaded into the main channel at 30 million/mL. The chip was imaged for 18 hrs. every 10 minutes using time-lapse imaging on a fully automated Nikon TiE microscope with the biochamber at 37°C and 80% humidity, and in the presence of 5% carbon dioxide gas. Images were acquired automatically from distinct locations on each microfluidic device, with each image including a minimum of 3 circular wells. A minimum of 18 wells per condition were analyzed. ImageJ manual tracking software (NIH) was used for the analysis of MK and platelet migration and behavior. The videos were tracked for cells migrating into the (1) comb – attempts, (2) channel, and (3) well – through. The platelets in the well were counted at the final frame to determine platelet budding into the well.

2.3.11 Megakaryocyte quantification in patient blood samples

Venous blood from patient diagnosed with sepsis was collected and evaluated for circulating megakaryocytes (IRB protocol numbers, MGH No: 2014P002087; MIT No:150100681R001). A patient was categorized as sepsis when one of the diagnoses for the patient was 'sepsis' and when there was a confirmed infection. Twenty-one samples were evaluated with 13 sepsis samples (age 34-75 yrs., 4 females, 9 males) and 5 control samples (age 25-50 yrs., 3 females, 1 male) (Table 2-1). Three of the sepsis samples (1 female and 2 males) had follow-up blood evaluation 3 days later. Cell surface markers were selected to determine cell type by differential marker expression. CD162 was utilized in order to break up any platelet-leukocyte aggregates prior to analyzing the samples. (Frydman GH, 2017) White blood cell concentration was used as an internal control for the quantification method and whole blood spiked with MKs were used to

validate surface marker identification of MKs in samples (Figure 1-1). Sample preparation and staining methods are described in the Supplemental Methods section.

Cell surface markers were selected to determine cell type by differential marker expression: CD41 (glycoprotein IIb; GPIIb) and CD61 (glycoprotein IIIb; GPIIIb) are found on the cell surface of platelets and megakaryocytes, where they form a GPIIb/IIIa complex and find to fibrinogen and von Willebrand Factor (vWF) during platelet activation. CD45 (protein tyrosine phosphatase, receptor type, C; PTPRC; leukocyte common antigen; LCA) and CD162 (P-selectin glycoprotein ligand-1; PSGL1; SELPLG) are both present on leukocytes where CD45 hi and lo populations can be used to identify both neutrophils and lymphocytes. Draq5 is a nuclear marker that was used to differentiate between $CD41^{+}CD61^{+}$ anuclear platelets and nucleated megakaryocytes.

First, white blood cells were identified and quantified and were then compared to the total white blood cell count in the complete blood cell count (CBC) that was performed on the same blood sample at the Massachusetts General Hospital clinical pathology lab as part of the patient's routine diagnostics in order to verify our concentration calculation methods (Figure 1-1 A-C). Once white blood cell count was verified, cellular events staining positive for megakaryocyte markers were then collected and quantified. The concentrations of MKs and leukocytes in the patient samples were then back-calculated, taking into account the total volume of sample analyzed and the initial 1:200 dilution of the blood.

In order to quantify circulating megakaryocytes in peripheral venous samples, blood collected in EDTA vacutainer tubes was diluted 1:200 in calcium-free hepes-tyrode buffer (Boston Scientific, Boston, MA, USA) with 20% volume of acid citrate dextrose (ACD, Boston Scientific). The diluted blood was then stained with CD41 PacBlue, CD61 FITC, CD45 CY5/594, and CD162 PE at 1:100-1:200 for 20 minute, and 1:1000 Draq5 for 5 minutes. The samples were then run using the Amnis flow cytometer and the data was analyzed with IDEAS software. Megakaryocytes were defined as $CD41^{+}CD61^{+}Draq5^{+}$ cells. Leukocytes were defined as $CD162^{+}CD45^{+}Draq5^{+}$ cells. The concentrations of MKs and leukocytes in the patient samples

were then back-calculated, taking into account the total volume of sample analyzed by Amnis and the initial 1:200 dilution of the blood.

As a control, venous blood collected in EDTA was spiked with various concentrations of Meg-01 cells and cord-blood derived megakaryocytes (day 14 of differentiation) in order to verify the accuracy of megakaryocyte detection in whole blood patient samples. Pure megakaryocytes and the spiked whole blood samples were analyzed with flow cytometry, as described above and also run on the automated CBC analyzer in order to determine whether an automated analyzer detects megakaryocytes and how it categorizes them. Pure MKs were counted manually with a hemacytometer to compare with the automated analyzer (Figure 1-1 D-E).

2.3.12 Histopathology

Histopathology samples from patients that underwent autopsies were retrospectively collected and evaluated. All samples and patient information were collected and handled according to MGH and Massachusetts Institute of Technology (Cambridge, MA, USA) IRB protocol (MGH No: 2014P002087; MIT No:150100681R001). A patient was categorized as sepsis when the cause of death was determined to be sepsis by the official pathology report. Control patients were defined as having primary cardiac disease as the cause of death. Fifteen samples were evaluated with 9 sepsis samples (age 60-90 yrs., 2 females, 3 males) and 5 control samples (age 68-87 yrs., 7 females, 2 males) (Table 2-3). Paraffin embedded tissue samples, including kidney, and the right middle lung lobe were sectioned and stained with either Haematoxylin & Eosin (H&E), gram stain, or with HRP-labeled CD61 antibodies by the Division of Comparative Medicine (MIT, Cambridge, MA, USA) and the Massachusetts General Hospital (Boston, MA, USA), respectively. The percent of CD61 staining per renal glomerulus was quantified using Fiji software. Twenty renal glomeruli were evaluated for each patient. For evaluation of the lungs, the number of MKs were counted in ten 40x magnification views of the right middle lung lobe for each patient.

2.3.13 Statistical Analysis

Statistics were performed using both Microsoft Excel and GraphPad Prism Software (GraphPad Software, Inc.). Either one-way ANOVA or student t-tests were performed to compare between conditions. A p-value of <0.05 was considered significant.

2.4 Results

2.4.1 Megakaryocyte are capable of phagocytosis

CB MKs and Meg-01 cells are able to phagocytize multiple types of pathogens (Figure 2-2). Cells were co-incubated with either *E. coli, S. aureus, S. pyogenes*, or zymosan particles and subsequently imaged. Light microscopy showed bacteria very closely associated to the cell wall, while electron microscopy imaging showed bacterial association with both MK and platelets, as well as internalization of pathogens (Figure 2-2 A-B and Videos 2-1 and 2-2). Electron micrograph images of a contaminated CB MK culture at day 14 of differentiation uncovered a large cell with multiple bacteria of unknown origin within a large vacuole inside of the MKs (Figure 2-2 B). We confirmed internalization of *E. coli, S. aureus,* and *S. pyogenes* bacteria by CB MKs and Meg-01 cells using pHrodo as a marker for pathogen acidification and association with a phagosome or lysosome. depicted by the fluorescent orange-red bacteria within the cells (Figure 2-2 C). CB MKs were then incubated with bacteria during different stages of differentiation (day 0-14). Flow cytometry of these cells was performed during these various stages of differentiation in order to profile their surface-marker expression and confirm appropriate megakaryocyte maturation (Figure 2-3). CB MKs were observed to be capable of phagocytosis starting at day 3 of differentiation (Figure 2-4). Interestingly, the CB MKs appear to start expression of p-selectin glycoprotein ligand 1 (CD162) and MHC Class II (HLADR) on day 3 as well (Figure 2-3).

2.4.2 Megakaryocytes undergo chemotaxis towards pathogenic stimuli

Meg-01 cells are able to undergo chemotaxis towards LPS and zymosan particles, both in a microfluidic assay as well as in a traditional transwell format (Figure 2-5). In the transwell experiments, chemotaxis to SDF1α, as positive control, was between 13.7-20.4 %, consistent

with the previous literature. (Hamada T, 1998) Chemotaxis was pronounced towards LPS concentrations of 220 pg/mL and 2.2 ng/mL (4.1-8.5 % and 16.0-21.0 %, respectively), as well as zymosan particles (7.6-21.8%). When LPS or SDF1α was combined with zymosan particles, the amount of chemotaxis was increased (7.1-33.7%). The trends in Meg-01 chemotaxis towards the various stimuli were consistent between the traditional transwell assay and the new microfluidic assay (Figure 2-5 E-F). The cell migration within the microfluidic device was separated into 3 groups: the cells that entered the circular cell, the cells that remained in the side channels, and the cells with projections inside the side channels (Figure 2-5 B-C and Figure 2-6). Cells (some up to 75 μm in diameter) were observed actively migrating through 5 μm channels, displacing both their nuclei and organelles as they crawled through the narrow tunnels (Video 2-3 through 5), sometimes taking zymosan particles with them (Video 2-6). A fraction of cells did not fully go through the channel, but were observed to extend proplatelets and release platelets into the side channels with the chemoattractant; indicating a possible directed release of platelets towards the stimulus (Figure 2-5 D and Video 2-7). This phenomenon of platelet-budding could not be quantified, as the visualization of platelets within the device was not consistently possible in the same plane of focus of the cells in the videos. Another unique observation included cells migrating into the side channels and then budding platelets, essentially obstructing the side channel and preventing other cells from migrating (Video 2-8). The microfluidic assay allowed for visualization of cells extending pseudopods and proplatelets as well as re-arrangement of cellular components, which would be much more difficult with the transwell assay.

2.4.3 Megakaryocytes form extracellular traps in response to pathogenic stimuli

Megakaryocytes form extracellular traps (METs) in response to both LPS and live bacteria (Figure 2-7). When Meg-01 cells were co-incubated with live bacteria, the cell morphology changed significantly and resulted in what appeared to be extracellular traps associated with bacteria (Figure 2-7 A). In order to explore whether MKs were able to form extracellular traps to various pathogenic stimuli, *in vitro* experiments were performed using multiple techniques. Meg-01 cells were co-incubated with various concentrations of *E. coli* LPS and METs were quantified by quantifying extracellular DNA in the supernatant (Figure 2-7 B). Immunofluorescent imaging of CB MKs co-incubated with live pHrodo conjugated *E. coli* demonstrated a unique, jelly-fish-like live formation of METs, which we believe is the beginning phase of MET formation (Figure

2-7 C). The positive Hoechst staining indicates that, although a MET is being formed, the cell still has a viable nucleus; this is consistent with a recent paper which discovered that NET formation is not always a terminal event. (Yipp BG, 2017) In order to differentiate between MET formation and proplatelet budding, calcein stain was used to demonstrate the lack of cell membrane around the extracellular DNA, as compared to platelet budding, where the platelet buds stained positive for calcein and negative for DNA (Figure 2-7 D). Some extracellular traps were visualized in the negative controls, usually around or on the hydrophobic pen marking.; this may be due to the contact with the hydrophobic barrier on the slide. (Sperling C, 2017) MET formation was subjectively less in with the cells co-incubated with the killed bacteria as compared to the live bacteria, which may be due to the lack of bacterial toxins, motility, or receptor-specific interactions. METs were also evaluated with immunofluorescent imaging to confirm the presence of histones and myeloperoxidase along with the extracellular DNA (Figure 2-8). Electron micrograph imaging of Meg-01 cells co-incubated with live bacteria confirmed the formation of extracellular traps with bacteria entangled within the extracellular DNA and various organelles, which included extracellular mitochondria, granules, and nucleosomes (Figure 2-7 E-F). Other cell morphology changes included swollen nuclei, breakdown of the nuclear membrane, condensed chromatin, and re-localization of the cytoplasmic organelles and mitochondria. (Pilsczek FH, 2010; Ueki S, 2013) Meg-01 cells expressing GFP-H2B were imaged forming METs; which confirmed the perinuclear rearrangement of organelles (notably, mitochondria) during MET formation (Figure 2-7 G-H).

2.4.4 Identification of circulating megakaryocytes using automated analyzers

Control samples were first analyzed to validate identification and quantification methods for MKs in the peripheral circulation (Figure 2-1). Pure CB MKs were positively identified by the automated CBC analyzer and, interestingly, were categorized as an unknown type of white blood cells (WBCs) with an error notification. When spiked whole blood samples were analyzed, the automated analyzer identified a corresponding increase in the WBC and, more specifically, the neutrophil count, and did not display an error message (Figure 2-1 D). Meg-01 cells were unable to be counted or analyzed accurately by the automated analyzer, both as a pure population and as spiked whole blood. We suspect that this may be due to the differences in morphology between

these two populations; while CB MKs are 10-30 μm and resemble small, granular lymphocytes on light microscopy, Meg-01 cells range from 15-75 μm and are often found in large clusters.

2.4.5 $CD61^+CD41^+Draq5^+$ cells are increased in the peripheral circulation of patients with sepsis

Patient samples were then analyzed using imaging flow cytometry (Figure 2-9 A). Circulating MKs were defined as $CD61^+CD41^+Draq5^+$ cells. These cells were about 10 μm in size and ranged from having one large nucleus to having paler DNA staining, which could represent apoptotic cells. Interestingly, whereas both Meg-01 cells and CB MKs are usually $CD162^+$, the circulating $CD61^+CD41^+Draq5^+$ cells identified in the patient samples were $CD162^-$, which may indicate that adult megakaryocytes are different in phenotype than neonatal megakaryocytes, which are $CD162^+$ (Figure 2-3). The number of $CD61^+CD41^+Draq5^+$ cells were identified to be significantly higher in peripheral circulation in patients with sepsis as compared to controls ($p = 0.05$; 9565 ± 1675 vs 3502 ± 741, respectively) (Figure 2-9 Bi). Surprisingly, the number of MKs were also significantly increased in patients with 'complicated' versus 'uncomplicated' sepsis ($p = 0.01$; 11077 ± 6256 MK/mL vs 3587 ± 1219 MK/mL, respectively), as defined by the development of acute kidney injury (AKI) or acute respiratory distress syndrome (ARDS) based on medical records (Figure 2-9 Bii). When further subdividing the sepsis patient population into the source of the infection, gram negative bacterial infections had significantly higher MKs than the gram positive or mixed infections (15070 ± 5158 MK/mL, 5140 ± 2082 MK/mL, 10146 ± 7675 MK/mL, respectively) (Figure 2-9 Biii). We analyzed data of three patients at 2 time-points and observed a decrease in circulating MKs in the patient that was recovered and discharged from the hospital as compared to the two patients that remained in the hospital for multiple weeks and developed AKI (Figure 2-9 Biv). Platelet count did not significantly differ in sepsis versus control patients ($p = 0.98$; 251.1 ± 207.6 plt x 10^6/mL and 253.6 ± 34.5 plt x 10^6/mL, respectively), whereas there was a significant difference between sepsis and control patients with reference to total white blood cell counts ($p = 0.015$; 14.7 ± 9.6 WBC x 10^6/mL and 5.2 ± 1.1 WBC x 10^6/mL, respectively). There was no correlation between circulating MKs and platelet or white blood cell count (Figure 2-10). Although the sample size is quite small and no definitive conclusions can be drawn from these observation, it does suggest circulating MKs should be further explored in the context of sepsis-related complications.

2.4.6 $CD61^+$ cells are increased in the lungs and overall $CD61^+$ staining is increased in the glomeruli of patients with sepsis

$CD61^+$ cells were increased in the peripheral organs of patients with sepsis. There was a significantly increased number of large $CD61^+$ cells (MKs) in the alveoli of septic patients as compared to controls per 40x field of view (FOV) ($p = 0.013$: 0.4 ± 0.1 MK/FOV vs 1.5 ± 0.2 MK/FOV, respectively) (Figure 2-11 A-B). As seen in the H&E images, as compared to the companion CD61 IHC image, while MKs could generally be identified on H&E by their large, darkly-stained nucleus, this was not always the case and demonstrates the utility of utilizing IHC for accurate cell-type assessment (Figure 2-11 A). There was one 'control' patient that was removed from pulmonary MK analysis because, although the cause of death was cardiac failure, a patchy bronchopneumonia was diagnosed at autopsy; this patient also had an increased number of MKs in the lungs (5.4 ± 3.5 MK/FOV), suggesting that MKs may be increased within the pulmonary parenchyma during localized as well as systemic infections. One patient that died from sepsis complicated by DIC was noted to have severe pulmonary inflammation and hemorrhage, as well as a micro-abscess, as defined by an increased number of neutrophils and macrophages, in the lung pathology section (Figure 2-12). Gram staining and CD61 IHC was positive for intracellular gram positive cocci, along with multiple large, homogeneously stained, $CD61^+$ cells concentrated in the center of the abscess. This may indicate that these MKs actively migrated out of the intravascular space and into the center of the abscess in response to inflammatory signals or response to the bacteria.

Renal glomeruli from septic patients also had a significantly increased amount of CD61+ positive staining than the controls ($p = 0.018$; $0.16 \pm 0.08\%$ CD61/Glomerulus vs $1.07 \pm 0.23\%$ CD61/Glomerulus, respectively) (Figure 2-11 C-D). As seen from the paired H&E and CD61 IHC glomeruli images, it was not possible to differentiate with any certainty whether large CD61+ areas had associated MKs or whether they were platelet-rich fibrin thrombi (Figure 2-11 C). One patient, which had substantial microvascular thrombosis within the kidney and was diagnosed with disseminated intravascular coagulation (DIC), had significantly elevated CD61 staining (2.29 ± 3.0 % CD61/Glomerulus), consistent with the presence of platelet-rich micro thrombi within the glomerular capillaries (Figure 2-11 D).

2.5 Discussion

Megakaryocytes (MKs) have long been thought to have one primary role - the production of platelets (plts). (Machlus KR, 2013) Plts are small, circulating anucleate cells which have been reported to be one of the 'first responders' to pathogens and inflammatory insults, resulting in the recruitment and subsequent activation of white blood cells and even directly trapping pathogens themselves. (Semple JW, 2011; Morrell CN, 2014; de Stoppelaar SF, 2014) Because plts derive their cellular components and functionality from their parent MK cell, it is logical to deduce that the MK cell also harnesses immune cell capabilities. In this study, we explore the role of the MK as an innate immune cell, and we demonstrate its ability to perform immune cell functions, including: phagocytosis, chemotaxis, and extracellular trap formation. We then explore its potential role in the peripheral circulation and end-organs of adult patients with sepsis. To our knowledge, this is the first study exploring the dynamic role of the megakaryocyte as an innate immune cell.

Two essential roles of innate immune cells include their ability to sense and chemotax towards a pathogen and to interact and phagocytose the pathogen. Megakaryocytes have been documented to internalize a number of pathogens, both *in vitro* and *in vivo*, including dengue virus, human immunodeficiency virus, and aspergillus. (Zucker-Franklin S, 1989; Ferry JA, 1991; Clark KB, 2016; Clark KB, 2012) In this study, we utilize both electron microscopy and pHrodo conjugated bacteria to demonstrate that, not only do MKs internalize bacteria, but they also localize the bacteria to lysosomal-type granules, which is indicative of an active killing process. (Prosser A, 2013; Naqvi AR, 2015) Additionally, cord blood-derived hematopoietic stem cells (HSCs) were observed to have phagocytic capabilities starting at day 3 of megakaryocyte differentiation; this is consistent with previous literature which demonstrates that primitive HSCs are quiescent, and as they differentiate into monocytes they develop progressive phagocytic capabilities (starting at day 3). (Kolb-Maurer A, 2002) Chemotactic ability was also explored in MKs. In this study, we demonstrated that Meg-01 cells undergo active chemotaxis towards pathogenic stimuli. MKs are able to migrate through a ≤ 6 μm channels/pores, which is within the range of a small capillary vessel or intercellular pore, indicating that these cells may not merely get 'trapped' in microcirculatory beds, but may be able to move through them and even potentially diapedese

into surrounding tissues. (Alamo IG, 2017; Zuchtriegel G, 2016; Haemerle M, 2016; Lisman T, 2010; Singer G, 2006; Croner RS, 2006) Additionally, the budding of platelets into the channels, acting as a sort of 'loaded gun', as well as the obstruction of the channels by the cells and platelets may indicate a mechanism for the formation of microthombi within small capillary vessels and potentially provide another mechanism for platelet extravasation. (Yadav H, 2015; de Stoppelaar SF, 2014; Stokes KY, 2012; Wells S, 1984; Aabo K, 1978; Fuchs TA, 2007)

MKs were also demonstrated to be able to form megakaryocyte extracellular traps (METs). Extracellular trap (ET) formation, or ETosis, is a type of cell death which has been demonstrated in a number of immune cells, including: neutrophils (NETs) and eosinophils (EETs). (Ueki S, 2013; Fuchs TA, 2007) NETs are thought to be an essential part of the immune and coagulation system, both entrapping pathogens and signaling to nearby inflammatory cells and the coagulation system that there is an intruder in the system, while EETs have recently been shown to play an important role in the lungs in chronic obstructive pulmonary disease (COPD) and allergic airway conditions. (Dworksi R, 2011; Dworski R, 2011; Echevarria LU, 2017) Extracellular DNA and histones are considered danger-associated molecular patterns (DAMPs) in the peripheral circulation have been associated with sepsis as well as a number of autoimmune diseases, while increased extracellular DNA and histones has been associated with both ARDS and acute kidney injury (AKI). (Narasaraju T, 2011; Lv X, 2017; Xu Z, 2015; Jansen MPB, 2017; Xu J, 2009) We have also demonstrated that extracellular mitochondria, which are proinflammatory and released from platelets during activation, are also released during MET formation, providing another DAMP. (Maeda A, 2014; Boudreau LH, 2014) Up until now, it has been postulated that most extracellular DNA and histones originate from neutrophils or eosinophils. Our results suggest that one potential source of these DAMPs may be MKs; such as during ARDs, when there are increased numbers of MKs within the pulmonary parenchyma. (Wells S, 1984; Sulkowski S, 1999; Kadas L, 1981)

In this study, we were also able to show that MKs are increased in both the peripheral circulation and in peripheral organs during sepsis. It was necessary in this study to utilize special staining in order to positively identify and quantify MKs within the body and automated hematology analyzers were unable to positively identify the presence of these abnormal cells. (Sanford D,

2013; Erber WN, 1987) These findings are consistent with previous studies, showing that there are increased MK precursors in the peripheral circulation of neonates with sepsis, in the renal glomeruli of adults with sepsis, and in the lungs of patients with sepsis and ARDS. (Brown RE, 2008; Broghamer WL, 1981) Our results demonstrate that the average circulating MK was between 10-15 μm in diameter with a scant cytoplasm, indicating that either small MKs (micromegakaryocytes) are being prematurely released into the circulation from locations of hematopoiesis due to the sepsis syndrome (increased vascular permeability and vasodilation), or that these cells have shed their cytoplasm in the lung space and have subsequently entered the circulation as naked nuclei. (Scheinin TM, 1963; Pederson NT, 1978) Additionally, it was noted that treatment with anti-CD162 antibodies was necessary for the detection of circulating large $CD61^{+}CD41^{+}Draq5^{+}$ cells; based on previous work, we hypothesize that the possible cause for this is that these cells are more likely to be in the circulation in the form of 'clusters' with other peripheral blood cell types, such as neutrophils. (Frydman GH, 2017; Wang X, 2014; Asaduzzaman M, 2009)

In conclusion, we have shown that that MKs have innate immune cell capabilities, including phagocytosis, chemotaxis, and extracellular trap formation. We have also shown that MKs have an increased presence in the peripheral circulation, lungs, and kidneys in adult patients with sepsis, which show evidence of being correlated with both, prognosis and type of infection. These findings suggest that there may be a link between the presence of MKs and the pathogenesis of sepsis and its' related complications. The implications of having an increased MK presence in the body is now more complex, as they are now no longer merely sources of platelets, but may also serve as an innate immune cell and contribute to the proinflammatory state present in sepsis.

2.6 Acknowledgements

The authors would like to thank Carolyn Madden at the Division of Comparative Medicine (MIT) for her isolation and preparation of the bacterial cultures used in this paper. Dr. Felix Ellet and Julianne Jorgensen helped with the microfluidic design and experiments. Dr. Shannon Tessier helped with the flow cytometry of the patient samples. Dr. Keith Wong provided guidance in the immunofluorescent extracellular trap staining. Martin Selig performed the

electron microscopy and Dr. Lawrence Zukerberg provided the histopathology samples. David Olaleye performed the image analysis on the kidney pathology samples. This work was supported by the T32-0D019078-28 (JGF), the P30-ES002109 (JGF), the P50-GM021700 (RGT), the GM092804 and AI113937 (to D.I.), and the Harvard NeuroDiscovery Center. All microfabrication procedures were performed at the BioMEMS Resource Center (EB002503).

2.7 References

1. Kaushansky K. The molecular mechanisms that control thrombopoiesis. J Clin Invest. 2005;115(12):3339–3347.
2. Machlus KR, Italiano JE. The incredible journey: From megakaryocyte development to platelet formation. J Cell Biol. 2013;201(6):785-796.
3. Alamo IG, Kannan KB, Loftus TJ, et al. Severe trauma and chronic stress activates extramedullary erythropoiesis. J Trauma Acute Care Surg. 2017;83(1):144-150.
4. Lefrancais E, Ortiz-Munoz G, Caudrillier E, et al. The lung is a site of platelet biogenesis and a reservoir for haematopoietic progenitors. Nature, 2017;544(7648):105-109.
5. Yacoub A, Brockman A. Extramedullary hematopoiesis and splenic vein thrombosis, a unique presentation of pre-clinical essential thrombocythemia. Blood, 2013; 122:5257.
6. Yassin MA, Nashwan A, Mohamed S. Extramedullary hematopoiesis in patient with primary myelofibrosis rare and serious complications. Blood, 2016;128:5490.
7. Hill AD, Swanson PE. Myocardial extramedullary hematopoiesis: A clinicopathologic study. Mod Pathol, 2000;13(7):779-787.
8. Weyrich AS, Zimmerman GA. Platelets in lung biology. Annu. Rev. Physiol., 2013;75:569-591.
9. Mandal RV, Mark EJ, Kradin RL. Megakaryocytes and platelet homeostasis in diffuse alveolar damage. Exp Mol Pathol., 2007;83(3):327-31.
10. Yadav H, Kor DJ. Platelets in the pathogenesis of acute respiratory distress syndrome. Am J Physiol Lung Cell Mol Physiol., 2015;309(9):L915-L923.
11. Sharma GK, Tablot IC. Pulmonary megakaryocytes: "missing link" between cardiovascular and respiratory disease? J Clin Pathol, 1986;39(9):969-976.
12. Kaufman RM, Airo R, Pollack S, et al. Origin of pulmonary megakaryocytes. Blood, 1965;25(5):767-775.
13. Finkielsztein A, Schlinker AC, Zhang L, et al. Human megakaryocyte progenitors derived from hematopoietic stem cells of normal individuals are MHC class II-expressing professional APC that enhance Th17 and Th1/Th17 responses. Immunol Lett., 2015;163(1):84-95.
14. Undi RB, Sarvothaman S, Narasaiah K, et al. Toll-like receptor 2 signalling: Significance in megakaryocyte development through wnt signaling cross-talk and cytokine induction. Cytokine, 2016;83:245-249.
15. D'Atri LP, Etulain J, Rivadeneyra L, et al. Expression and functionality of toll-like receptor 3 in megakaryocytic lineage. J Thromb Haemost., 2015;13(5):839-850.
16. Beaulieu LM, Freedman JE. The role of inflammation in regulating platelet production and function: Toll-like receptors in platelets and megakaryocytes. Thromb Res., 2010:125(3):205-209.
17. Shiraki R, Inoue N, Kawasaki S, et al. Expression of Toll-like receptors on human platelets. Thromb Res., 2004;113(6):379-85.
18. Beulieu LM, Lin E, Morin KM, et al. Regulatory effects of TLR2 on megakaryocytic cell function. Blood, 2011;117(22):5963-5974.
19. Bentfeld-Barker ME, Bainton DF. Identification of primary lysosomes in human megakaryocytes and platelets. Blood, 1982;59(3):472-81.
20. Kang HP, Chiang MY, Ecklund D, et al. Megakaryocyte progenitors are the main antigen presenting cells inducing Th17 response to lupus autoantigens and foreign antigens. J

Immunol., 2012;188(12):5970-5980.
21. Nagasawa T, Nakayasu C, Rieger AM, et al. Phagocytosis by thrombocytes is a conserved innate immune mechanism in lower vertebrates. Front Immunol., 2014;5:445.
22. White JG. Platelet are covercytes, not phagocytes: uptake of bacteria involves channels of the open canalicular system. Platelets, 2005;16(2):121-31.
23. Lewis JC, Maldonado JE, Mann KG. Phagocytosis in human platelets: localization of acid phosphatase-positive phagosomes following latex uptake. Blood, 1976;47(5):833-840.
24. Absolom DR, Francis DW, Zingg W, et al. Phagocytosis of bacteria by platelets: surface thermodynamics. J of Colloidal and Interface Science, 1982;85(1):168-177.
25. Zucker-Franklin S, Cao Y. Megakaryocytes of human immunodeficiency virus-infected individuals express viral RNA. Proc. Natl. Acad. Sci. USA, 1989;86:5595-5599.
26. Ferry JA, Petit CK, Rosenberg AE, et al. Fungi in megakaryocytes: an unusual manifestation of fungal infection in bone marrow. Am J Clin Pathol, 1991;96(5):577-81.
27. Clark KB, Hsiao HM, Bassit L, et al. Characterization of dengue virus 2 growth in megakaryocyte-erythrocyte progenitor cells. Virology, 2016;493:162-172.
28. Clark KB, Noisakran S, Onlamoon N, et al. Multiploid CD61+ cells are the pre-dominant cell lineage infected during acute dengue virus infection in bone marrow. PLOS one, 2012.
29. Schindelin, J, Arganda-Carreras I, Frise E, et al. Fiji: an open-source platform for biological-image analysis, Nature methods, 2012;9(7):676-682.
30. Frydman GH, Le A, Ellett F, et al. Technical advance: changes in neutrophil migration patterns upon contact with platelets in a microfluidic assay. J Leukoc Biol., 2017;101(3):797-806.
31. Hamada T, Mohle R, Hesselgesser J, et al. Transendothelial migration of megakaryocytes in response to stromal cell-derived factor 1 (SDF-1) enhances platelet formation. J Exp Med, 1998;188(3):539-548.
32. Yipp BG, Kubes P. NETosis: how vital is it? Blood, 2013;122(16):2784-2794.
33. Sperling C, Fischer M, Maitz MF, et al. Neutrophil extracellular trap formation upon exposure of hydrophobic materials to human whole blood causes thrombogenic reactions. Biomater Sci., 2017;5:1998-2008.
34. Pilsczek FH, Salina D, Poon KKH, et al. A novel mechanism of rapid nuclear neutrophil extracellular trap formation in response to Staphylococcus aureus. J Immunol, 2010;185(12):7413-7425.
35. Ueki S, Melo RCN, Ghiran I, et al. Eosinophil extracellular DNA trap cell death mediates lytic release of free secretion-competent eosinophil granules in humans. Blood, 2013;121:2074-2083.
36. Semple JW, Italiano JE, Freedman J. Platelet and the immune continuum. Nature Reviews Immunol., 2011;11:264-274.
37. Morrell CN, Aggrey AA, Chapman LM, et al. Emerging roles for platelets as immune and inflammatory cells. Blood, 2014;123:2759-2767.
38. de Stoppelaar SF, van 't Veer C, van der Poll T. The role of platelets in sepsis. Thromb Haemost., 2014;112(4):666-777.
39. Prosser A, Hibbert J, Strunk T, et al. Phagocytosis of neonatal pathogens by peripheral blood neutrophils and monocytes from newborn preterm and term infants. Pediatric Research, 2013;74:503-510.
40. Naqvi AR, Fordham JB, Nares S. miR-24, miR-30b, and miR-142-3p regulate phagocytosis in myeloid inflammatory cells. J Immunol., 2015;194(4);1916-1927.

41. Kolb-Maurer A, Wilhelm M, Weissinger F, et al. Interaction of human hematopoietic stem cells with bacterial pathogens. Blood, 2002;100(10):3703-3709.
42. Zuchtriegel G, Uhl B, Puhr-Westerheide D, et al. Platelets guide leukocytes to their sites of extravasation. PLOS Biol., 2016.
43. Haemmerle M, Bottsford-Miller J, Pradeep S, et al. FAK regulates platelet extravasation and tumor growth after antiangiogenic therapy withdrawal. J Clin Invest., 2016;126(5):1885-1896.
44. Lisman T, Porte RJ. The role of platelets in liver inflammation and regeneration. Semin Thromb Hemost., 2010;36(2):170-174.
45. Singer G, Urakami H, Specian RD, et al. Platelet recruitment in the murine hepatic microvasculature during experimental sepsis: role of neutrophils. Microcirculation, 2006;13(2):89-97.
46. Croner RS, Hoerer E, Kulu Y, et al. Hepatic platelet and leukocyte adherence during endotoxemia. Crit Care, 2006;10(1):R15.
47. Stokes KY, Granger DN. Platelets: a critical link between inflammation and microvascular dysfunction. J Physiol, 2012;590(pt 5):1023-1034.
48. Wells S, Sissons M, Hasleton PS. Quantitation of pulmonary megakaryocytes and fibrin thrombi in patients dying from burns. Histopathology, 1984;8(3):517-527.
49. Aabo K, Hansen KB. Megakaryocyte in pulmonary blood vessels: Incidence at autopsy, clinicopathological relations especially to disseminated intravascular coagulation. Acta Pathologica, Microbiologica et Immunologica Scandinavica, 1978;1(6):285-291.
50. Fuchs TA, Abed U, Goosman C, et al. Novel cell death program leads to neutrophil extracellular traps. JCB, 2007;176(2):231-241.
51. Papayannopoulos V. Neutrophil extracellular traps in immunity and disease. Nature Reviews Immunology, 2017; doi.10.1038/nri.2017.105.
52. Echevarria LU, Leimgruber C, Gonzalez JG, et al. Evidence of eosinophil extracellular trap cell death in COPD: does it represent the trigger that switches on the disease? Int J Chron Obstruct Pulmon Dis, 2017;12:885-896.
53. Dworksi R, Simon HU, Hoskins A, et al. Eosinophil and neutrophil extracellular DNA traps in human allergic asthmatic airways. J Allergy Clin Immunol, 2011;127(5):1260-1266.
54. Narasaraju T, Yang E, Samy RP, et al. Excessive neutrophils and neutrophil extracellular traps contribute to acute lung injury of influenza pneumonitis. AJP, 2011;179(1):199-210.
55. L X, Wen T, Song J, et al. Extracellular histones are clinically relevant mediators in the pathogenesis of acute respiratory distress syndrome. Respir Res, 2017;18:165.
56. Xu Z, Huang Y, Mao P, et al. Sepsis and ARDS: the dark side of histones. Mediators Inflamm, 2015;2015:205054.
57. Jansen MPB, Emal D, Teske GJD, et al. Release of extracellular DNA influences renal ischemia reperfusion injury by platelet activation and formation of neutrophil extracellular traps. Kidney Int, 2017;91(2):352-364.
58. Xu J, Zhang X, Pelayo R, et al. Extracellular histones are major mediators of death in sepsis. Nat Med., 2009;15(11):1318-1321.
59. Maeda A, Fadeel B. Mitochondria released by cells undergoing TNF-α-induced necroptosis act as danger signals. Cell Death and Disease, 2014;5:e1312.
60. Boudreau LH, Duchez AC, Cloutier N, et al. Platelets release mitochondria serving as substrate for bactericidal group IIA-secreted phospholipase A_2 to promote inflammation. Blood, 2014;124:2173-2183.

61. Sulkowski S, Terlikowski S, Sulkowski M. Occlusion of pulmonary vessels by megakaryocytes after treatment with tumour necrosis factor-alpha (TNF-α). J Comp Pathol., 1999;120(3):235-245.
62. Kadas L, Szell K. The role of megakaryocytes and tissue mast cells in the respiratory distress syndrome of adults. Acta Morphol Acad Sci Hung, 1981;29(4):395-404.
63. Sanford D, Hsia C. Value of the peripheral blood film: megakaryocytic fragments misidentified by automated counter. Blood, 2013; 122:4163.
64. Erber WN, Jacobs A, Oscier DG, et al. Circulating micromegakaryocytes in myelodysplasia. J Clin Pathol, 1987;40:1349-1352.
65. Brown RE, Rimsza LM, Pastos K, et al. Effects of sepsis on neonatal thrombopoiesis. Pediatric Research, 2008;64(4):399-404.
66. Broghamer WL Jr, Weakley-Jones B. Megakaryocytes in renal glomeruli. AJCP, 1981;76(2):178-182.
67. Scheinin TM, Koivuniemi AP. Megakaryocytes in the pulmonary circulation. Blood, 1963;22(1):82-87.
68. Pederson NT. Occurrence of megakaryocytes in various vessels and their retention in the pulmonary capillaries in man. Scand J Haematol., 1978;21(5):369-375.
69. Wang X, Qin E, Sun B. New strategy for sepsis: targeting a key role of the platelet-neutrophil interaction. Burns Trauma, 2014;2(3):114-120.
70. Asaduzzaman M, Rahman M, Jeppsson B, et al. P-selectin glycoprotein-ligand-1 regulates pulmonary recruitment of neutrophils in a platelet-independent manner in abdominal sepsis. Br J Pharmacol., 2009;156(2):307-315.

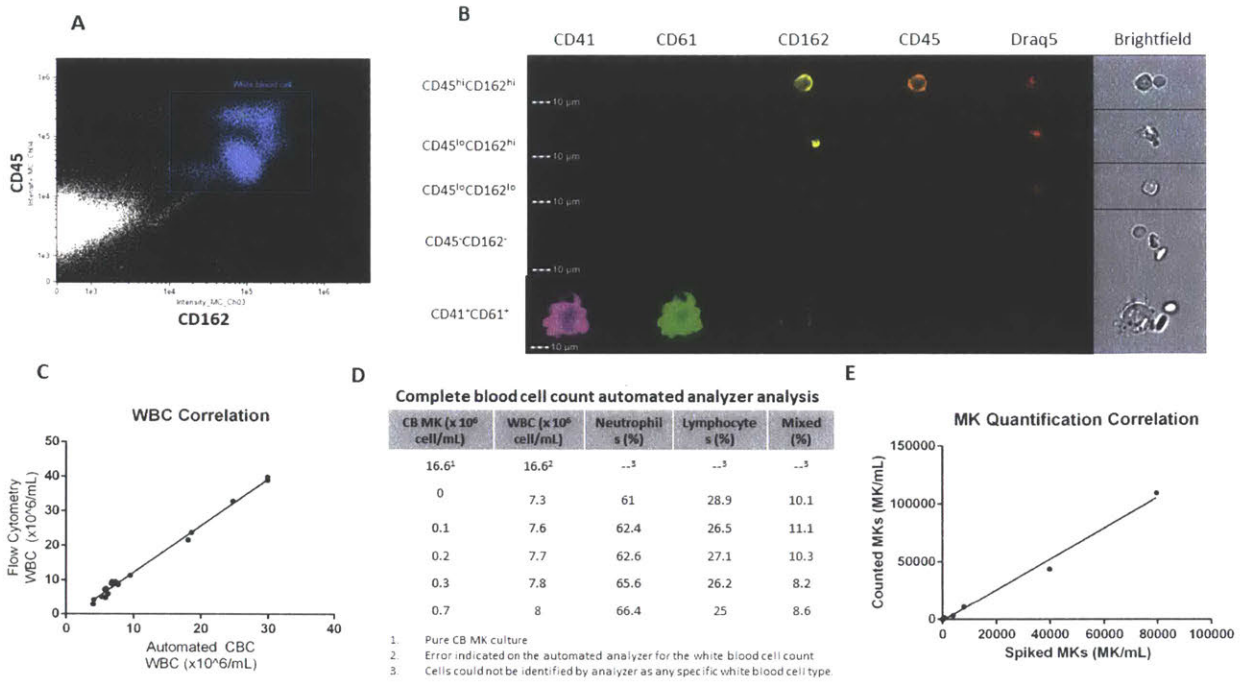

Figure 2-1: Quantification of MKs in peripheral blood using flow cytometry.

The positive identification and quantification of MKs in whole blood samples was evaluated. (A & B) A flow cytometry protocol was optimized for the accurate quantification of the total white blood cell population in whole blood. White blood cells were identified by being double positive for CD162 and CD45. Both CD45 and CD162 hi and lo populations were present, representing different types of white blood cells. The cells that were double negative for CD45 and CD162 were either platelets or red blood cells, and the large cells that were positive for CD41 and CD61 were Meg-01 cells, as shown in panel B. Cells that were negative for all markers are erythrocytes. (C) The total white blood cells per mL calculated by flow cytometry were then compared to the automated CBC WBC count and showed a strong correlation with an r of 0.998, confirming this as an accurate method of cell quantification based on cell surface markers. (D & E) Meg-01 cells were spiked into whole blood and quantified using the flow cytometry protocol. The MK manual count spiked correlated well with the flow cytometry quantified MK count with an r value of 0.980.

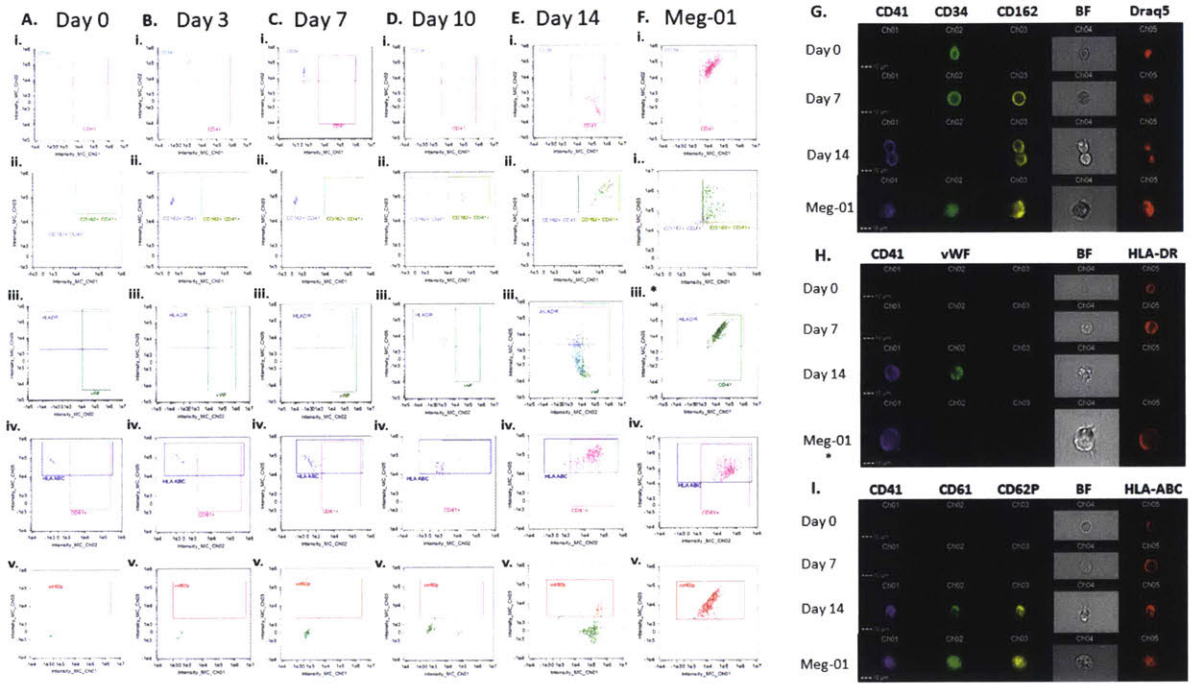

Figure 2-2: Flow cytometry analysis of cell phenotype

Imaging flow cytometry was used to characterize cord blood (CB)-derived MKs and Meg-01 cells by various cell surface markers, including: CD41 (i-ii), CD34 (i), CD162 (ii), HLA-DR (iii), vWF (iii). HLA-ABC (iv), CD61 (iv), and CD62P (v). Scatter plots of CB MKs at days 0, 3, 7, 10, and 14 of differentiation are shown in panel A-E and scatter plots of Meg-01 cells are shown in panel F. Images of representative cells for various days of differentiation are shown in panel G-I. *vWF was not evaluated in Meg-01 cells, therefore the scatter plot is of CD41 vs HLA-DR (E-iv).

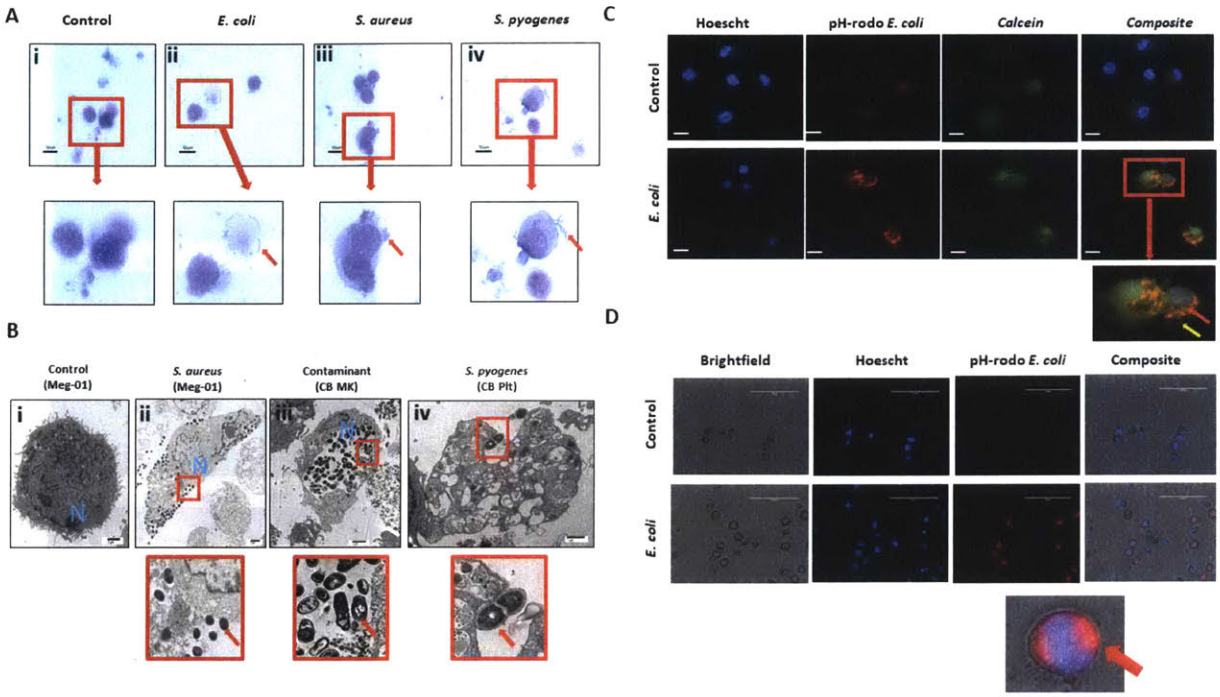

Figure 2-3: Megakaryocytes are capable of phagocytosis of pathogens.

Megakaryocytes were tested for their ability to phagocytose a number of pathogens. (A) Meg-01 cells were co-incubated with various bacteria. Light microscopy with diff-quick staining shows that bacteria appear to be associated with the cytoplasm and cell membrane of the cells. (B) Transmission electron microscopy of both Meg-01 and CB MKs exhibiting bacterial association with the cell membrane as well as internalization into vacuoles within the cytoplasm. Panel i is a control Meg-01 cell, while panel ii is a Meg-01 cell that was co-incubated with live *S. aureus.* Panel ii shows a CB MK with multiple bacteria within a large cytoplasmic vacuole from a contaminated cell culture. Panel iii is from a CB MK culture co-incubated with live *S. pyogenes* showing association of the bacteria with a platelet cell membrane. (C) CB MKs were co-incubated with live pHrodo-conjugated bacteria. This is a representative image of a control cell along with a cell co-incubated with *E. coli*. (D) Meg-01 cells were co-incubated with pHrodo-conjugated live *E. coli* and then imaged. Bacteria, red arrow; pseudopods, yellow arrow.

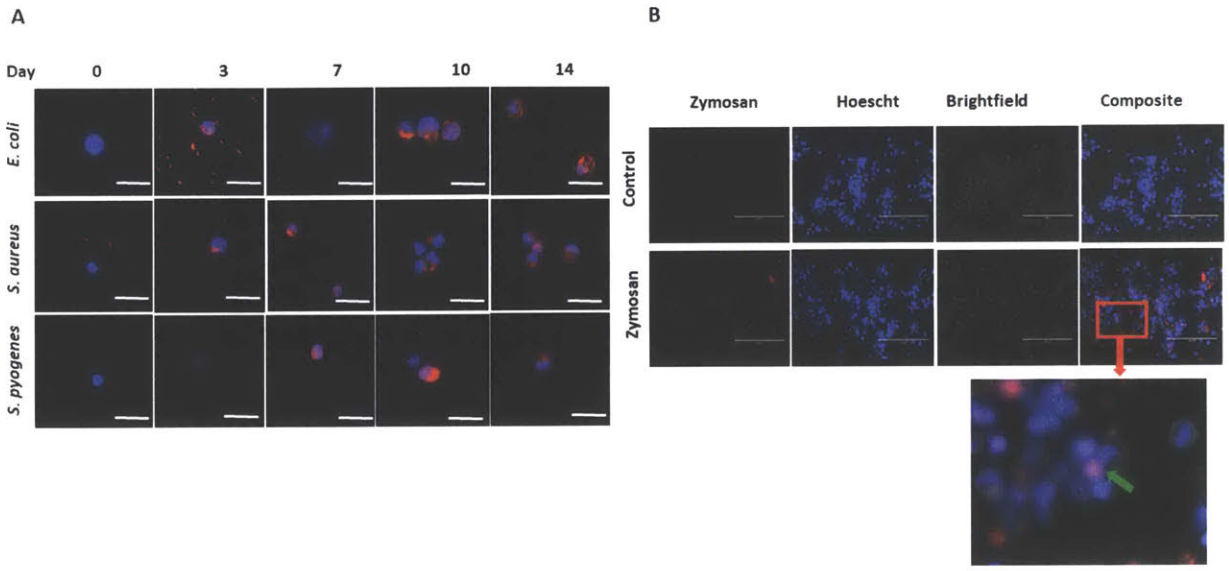

Figure 2-4: Megakaryocytes are capable of phagocytosis throughout differentiation.

CB MKs are functional phagocytes starting at day 3 of differentiation. (A) CB MKs were co-incubated with live pHrodo-conjugated bacteria on days 0, 3, 7, 10, and 14 of differentiation and were noted to be capable of phagocytosis starting on day 3 of differentiation. Scale bars are 20 μm. (B) Meg-01 cells were co-incubated with zymosan particles overnight and then imaged. The red zymosan particles appear fluorescent red within the cytoplasm of the Meg-01 cell when phagocytosed. Zymosan particles, green arrow.

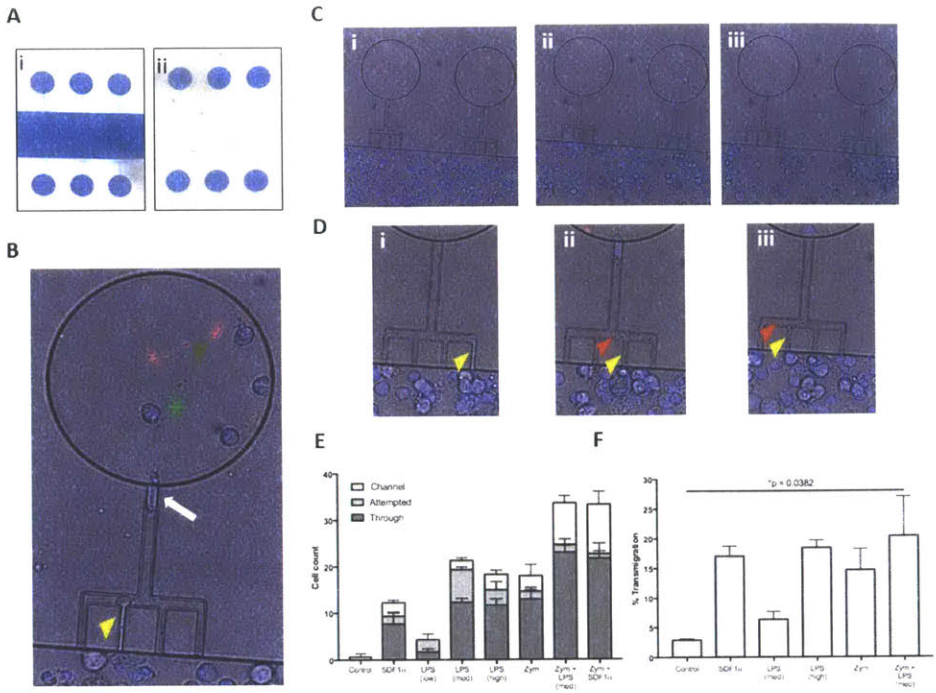

Figure 2-5: Meg-01 cells are capable of chemotaxis to pathogenic stimulus.

Meg-01 cells were tested for their ability to chemotax towards LPS and zymosan particles. (A) A microfluidic device was used for part of the chemotaxis experiments. In this device, the main channel is connected to a circular reservoir by four 6um channels and a larger 8 um connecting channel in a comb-like arrangement. The device is first primed with the condition (panel i) and the main channel is then flushed with media in order to create a concentration gradient from the 'lollipops' into the main channel (panel ii). (B) The MKs are stained with Hoechst for positive identification and then manually tracked. The behavior of the MK was divided into 3 categories: cells attempting to enter the channel (yellow arrowhead), cells inside the channel (white arrow), and cells through the channel and inside the reservoir (green arrowhead). Zymosan particles are marked with a green asterisk. (C) Time lapse image of MKs migrating into the lollipops which are primed with LPS (360 pg/mL) and zymosan particles. (D) Close-up of time-lapse image were MKs are observed to attempt to enter the channel, extend an 'arm' into the side channel (yellow arrowhead), and then bud off small platelet-like particles (red arrowhead). (E) Bar graph representing MK chemotaxis within the microfluidic device. (F) Bar graph representing MK chemotaxis within a transwell device, confirming the same observation as within the microfluidic device. LPS low, 22 pg/mL; LPS med, 220 pg/mL; LPS high, 2.2 ng/mL; Zym, zymosan particles; Zym+LPS, zymosan particles with 220 pg/mL LPS. Bar graphs are the mean with standard error bars.

Inside Circular Wells

	negative	positive	LPS lo	LPS m	LPS hi	Z	Z + L
positive	0.1408						
LPS lo	0.9978	0.3703					
LPS med	0.0051	0.6543	0.0173				
LPS hi	0.0083	0.794	0.0282	>0.9999			
Z	0.0031	0.5062	0.0106	>0.9999	0.9995		
Z + L	<0.0001	0.0006	<0.0001	0.0173	0.0106	0.0282	
Z + S	<0.0001	0.0015	<0.0001	0.0454	0.0282	0.0723	0.9995

Side Channels

	negative	positive	LPS lo	LPS m	LPS hi	Z	Z + L
positive	0.9435						
LPS lo	>0.9999	0.8279					
LPS med	0.9976	0.9996	0.9744				
LPS hi	0.8947	>0.9999	0.7462	0.9976			
Z	0.8947	>0.9999	0.7462	0.9976	>0.9999		
Z + L	0.0182	0.144	0.0098	0.0614	0.1877	0.1877	
Z + S	0.0039	0.0337	0.0021	0.0134	0.0456	0.0456	0.9908

Attempts

	negative	positive	LPS lo	LPS m	LPS hi	Z	Z + L
positive	0.9166						
LPS lo	0.5456	0.9947					
LPS med	0.0021	0.0225	0.0882				
LPS hi	0.2931	0.9166	0.9996	0.202			
Z	0.9166	>0.9999	0.9947	0.0225	0.9166		
Z + L	0.9166	>0.9999	0.9947	0.0225	0.9166	>0.9999	
Z + S	0.9947	0.9996	0.9166	0.0088	0.6888	0.9996	0.9996

Figure 2-6: Statistical summary of Meg-01 chemotaxis within a microfluidic device

One-way ANOVA was performed for each condition shown in Figure 2-5 E. Alpha = 0.05. LPS lo, 22 pg/mL; LPS med, 220 pg/mL; LPS hi, 2.2 ng/mL; Z, zymosan particles; positive, 220 ng/mL SDF1α; negative, media only; Z, zymosan particles; Z+L, zymosan with 220 pg/mL LPS.

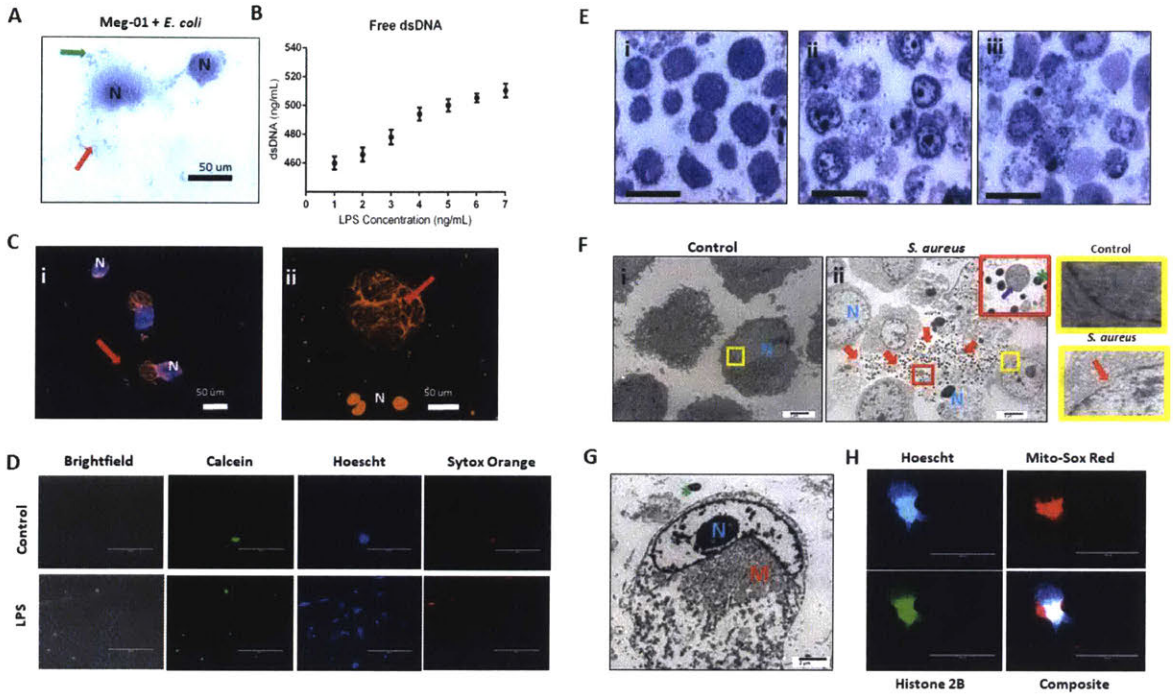

Figure 2-7: Megakaryocyte form extracellular traps (METs).

MKs were observed to form METs in response to pathogenic stimulus. (A) Meg-01 cells co-incubated with live *E. coli* and developed an ET-like morphology on light microscopy with diff-quick stain. This morphology consists of an open cell membrane with cytoplasm outside of the cell and a swollen nucleus. Green arrow, bacteria; red arrow, extracellular cytoplasm. (B) Meg-01 cells were co-incubated with various concentrations of LPS and free ds DNA was quantified using a PicoGreen assay. The amount of free dsDNA positively correlates with the increasing concentration of LPS. (C) CB MKs were co-incubated with live pHrodo-conjugated *E. coli* and were observed to have extracellular DNA. Live cells are stained blue with Hoechst, while extracellular DNA and dead cells are stained orange with SYTOX. (D) Meg-01 cells were incubated with just media or with LPS. Cells in the negative control were noted to have calcein staining (which indicates cell membrane) in the extracellular space, consistent with proplatelet budding; whereas cells incubated with LPS were noted to have calcein scant calcein stain and an abundance of extracellular DNA staining (red arrow). (E) Meg-01 cells were incubated with a variety of live bacteria. Light microscopy of these cells demonstrated swollen nuclei, broken nuclear membranes, extracellular DNA and granules, as well as bacteria associated with intra- and extracellular contents. Panel i is the control, and panel ii and ii are co-incubated with *E. coli* and *S. aureus*, respectively. (E) Transmission electron microscopy (TEM) of Meg-01 cells co-incubated with live bacteria. Panel I depicts a control cell with an intact nuclear membrane (right top panel) and limited extracellular content. Panel ii depicts multiple cells with swollen nuclei (N), broken nuclear membranes (bottom right panel),

extracellular cytoplasmic contents (including granules and mitochondria, purple arrow), and an abundance of bacteria primarily associated with cellular content. (G) TEM image of a Meg-01 cell co-incubated with live *E. coli* exhibiting a swollen nucleus and a rearrangement of mitochondria surrounding the nucleus. (H) Meg-01 cells transfected with Bacmam H2b-GFP were seen to form METs that were both positive for DNA (Hoechst) and histone 2B. Mitochondrial staining with MitoSox red shows active mitochondria in a perinuclear arrangement, confirming the TEM findings from panel G.

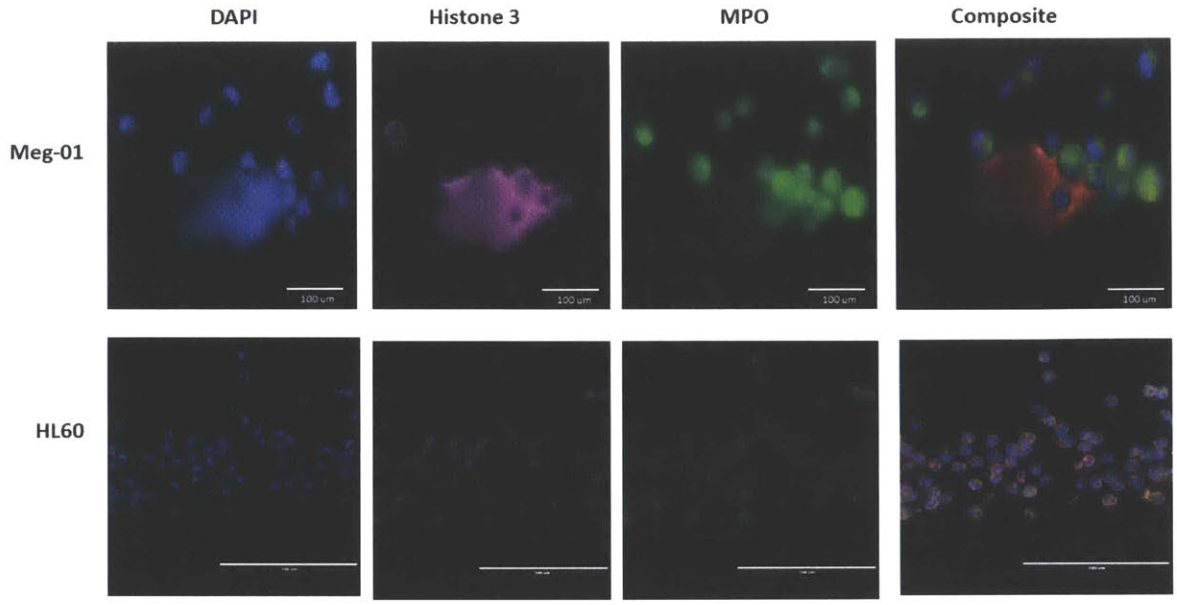

Figure 2-8: Megakaryocyte extracellular traps (METs) immunofluorescent staining.

Immunofluorescence was used to evaluate the extracellular traps made by Meg-01 cells. HL60 cells were used as a positive control for the immuno-stains. In these cells, DAPI (DNA stain) and Histone 3 (phospho Ser28) staining were both localized to the nucleus of the cells, while myeloperoxidase (MPO) was localized to the cytoplasm. In the Meg-01 cells, the METs stained positive for DAPI, Histone 3, and MPO.

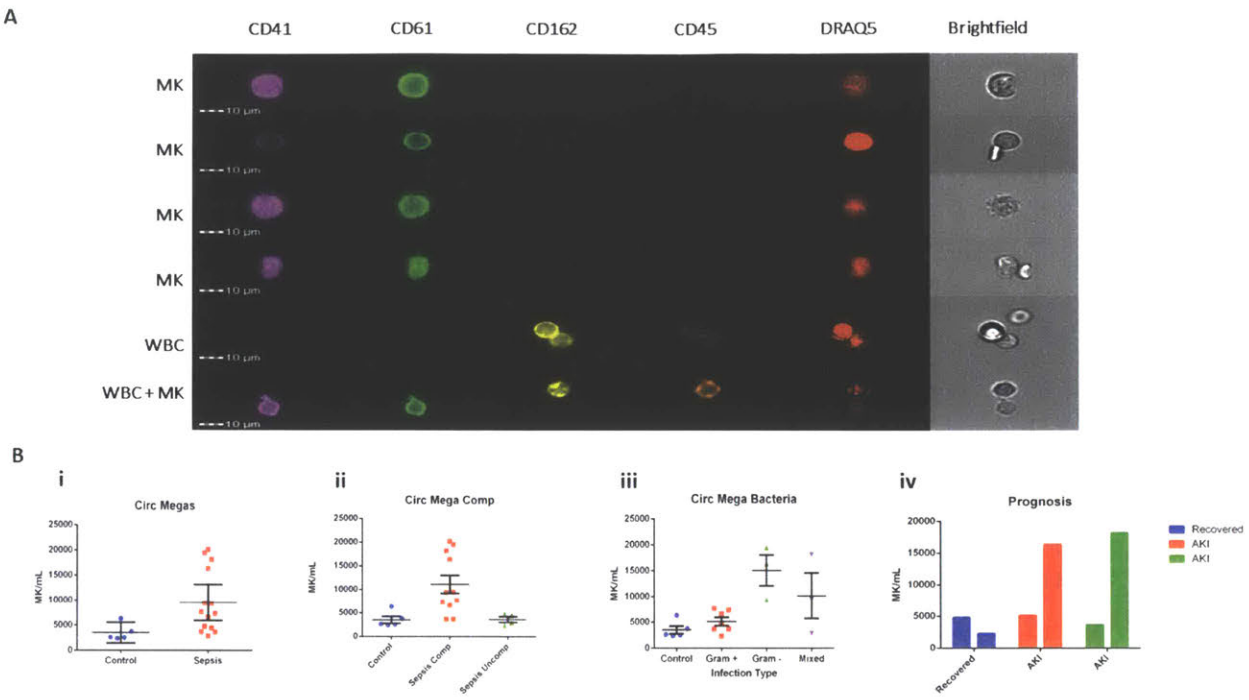

Figure 2-9: Megakaryocytes are present in increased amounts in the circulation during sepsis.

Samples from patients diagnosed with sepsis were evaluated for the presence of possible MKs. In order to positively identify MKs in the peripheral circulation, an MK was defined as CD41+CD61+ and DRAQ5+. (A) Imaging flow cytometry was used to identify and quantify circulating CD41+CD61+Draq5+ cells in the peripheral circulation. CD45 and CD162 were used as white blood cell markers. The top 4 panels show examples of MKs, while the bottom two panels have a white blood cell (bottom panel has an MK-WBC complex). (B) Circulating MKs were significantly higher in the peripheral circulation in patients with sepsis (i). The amount of MKs was correlated with sepsis-related complications, including ARDS and AKI, with 'complicated' sepsis having significantly higher MKs than 'uncomplicated' sepsis (ii). MKs were also noted to be higher in gram negative and mixed infections, as compared to gram positive only infections (iii). Sequential blood samples on day 1 and 3 of sepsis hospitalization suggested that there also may be a correlation with recovery and the development of sepsis complications, such as AKI (iv). Significance is calculated via student t-test with significance being defined as $p < 0.05$ (*).

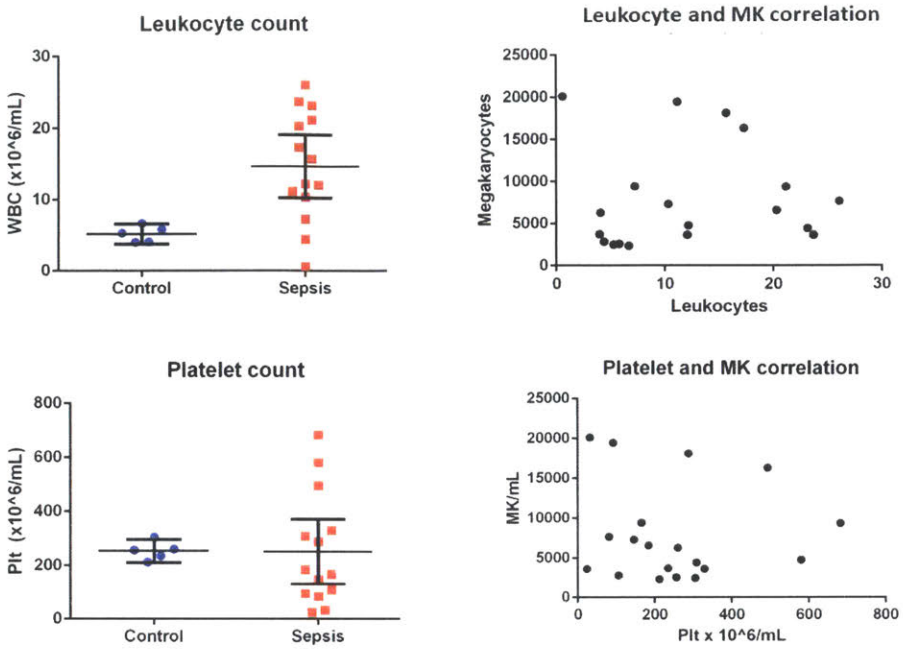

Figure 2-10: Correlation between CBC and Circulating megakaryocytes

Platelet and white blood cell (WBC; leukocyte) counts were compared to circulating MKs in patients. (A-B) Patients with sepsis had significantly increased WBC counts as compared to controls but there was no significant difference in platelet count. (C-D) There was no correlation between WBC or platelet count and circulating MK count (r2 =0.015 and 0.004, respectively).

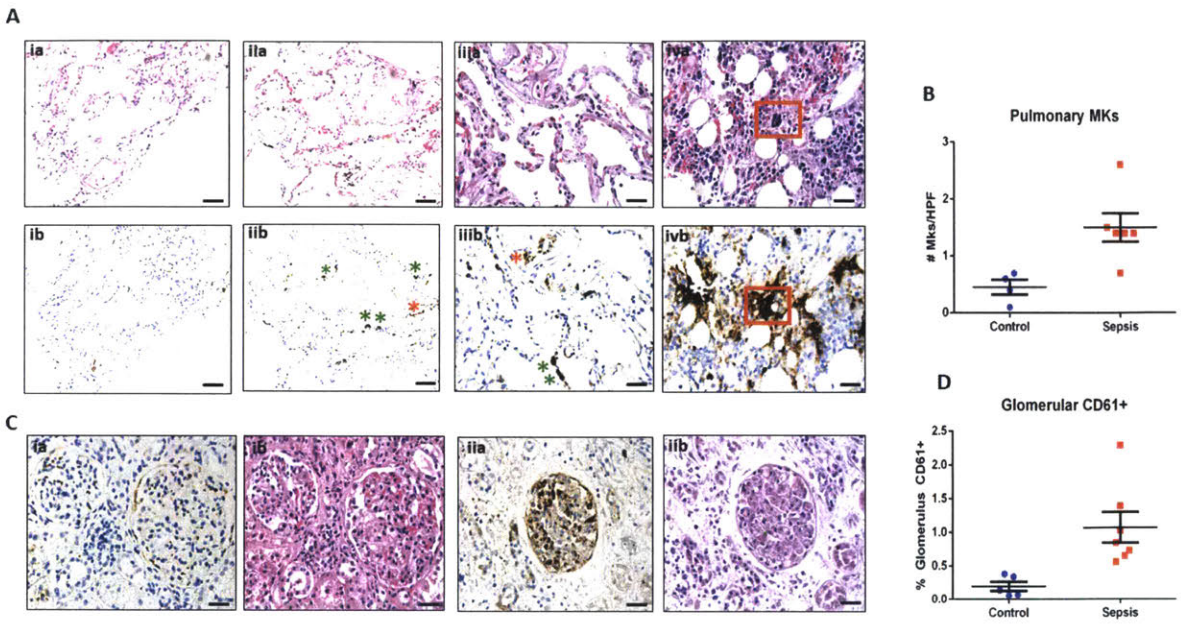

Figure 2-11: Megakaryocytes are present in the peripheral organs during sepsis.

Autopsy pathology samples from patients that died from sepsis were evaluated for MKs. (A) MKs in the lungs were defined as being large cells with dark, homogenous CD61+ staining (brown). An example of a lung image from a patient that died from heart disease as a negative control is shown in panel ia (hematoxylin and eosin, H&E) and ib (CD61). In these images there are no MKs observed. A representative image of two lung images from a patient that died from sepsis are shown in panel iia/iiia (H&E) and iib/iiib (CD61), showing multiple MKs (green asterisks). Platelet staining is also noted (red asterisks). While in some cases, a large dark staining basophilic nucleus can be seen in the H&E in the area of the CD61 staining, this is not always the case and may be due to sectioning through the sample and imaging different planes. This also suggests that CD61 may be more accurate when counting MKs than H&E. A sample of bone marrow from a sepsis patient is shown in panel iva (H&E) and ivb (CD61) as an example of a megakaryocyte with CD61 staining as a positive control (red box). (B) Glomeruli were also evaluated for the presence of increased CD61 staining. Individual MKs could not be reliable counted within the MKs, therefore percent of CD61 stain/glomeruli was evaluated. A glomerulus from a control patient is shown in panel ia (CD61) and ib (H&E), with minimal CD61 staining. This is in contrast to a glomerulus from a patient with sepsis and disseminated intravascular coagulation (DIC), which has much higher amounts of CD61 staining along with microvascular thrombi within the glomerular capillaries (green asterisk). Upon evaluation, there was significantly higher circulating MKs (C) and glomerular CD61 staining (D) in the sepsis patients as compared to control. Significance is calculated via student t-test with significance being defined as $p < 0.05$ (*). Scale bars are: Ai-ii, 100 µm, Aiii-iv and C, 50 µm.

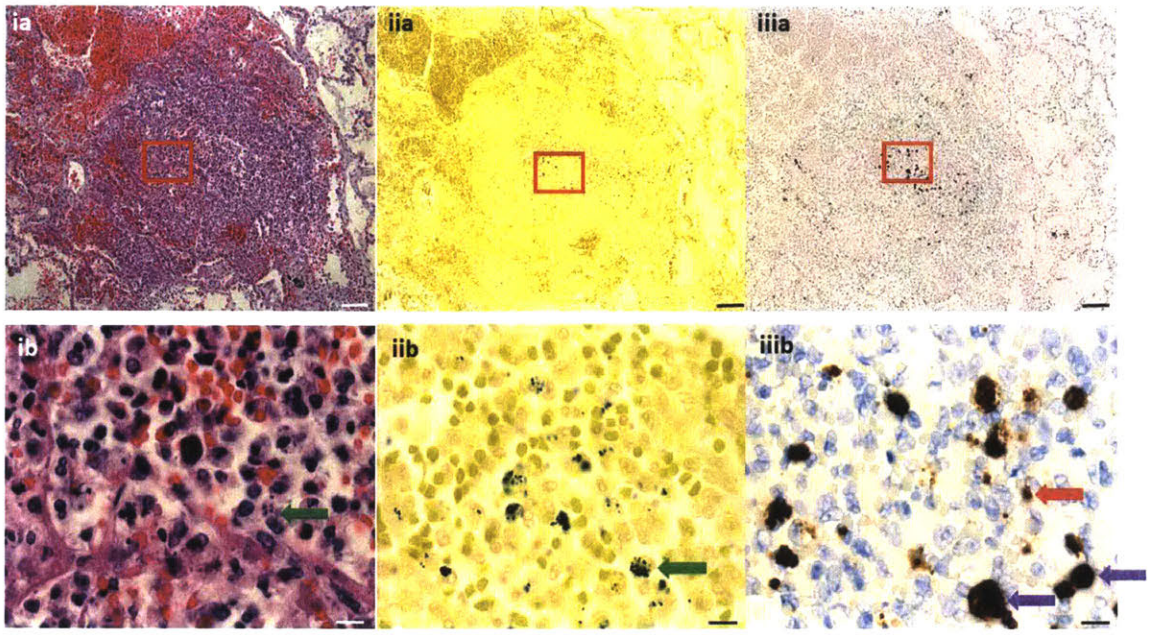

Figure 2-12: Pulmonary micro abscess in a septic patient

Histopathological evaluation of a pulmonary abscess in a patient that died from sepsis. Hematoxylin and Eosin (H&E) images of the abscess at 10x (ia) and 100X (iia) shows red blood cells, neutrophils, macrophages, and intracellular cocci (green arrow). Gram stain at 10x (iia) and 100x (iib) showing extra- and intracellular gram positive cocci (green arrow). CD61 staining at 10x (iiia) and 100x (iiib) showing multiple small CD61+ platelets (red arrow) and larger, dark-staining CD61+ cells suspected to be MKs (purple arrow). Scale bar top row, 100 μm (10X). Scale bar bottom row, 10 μm (100X).

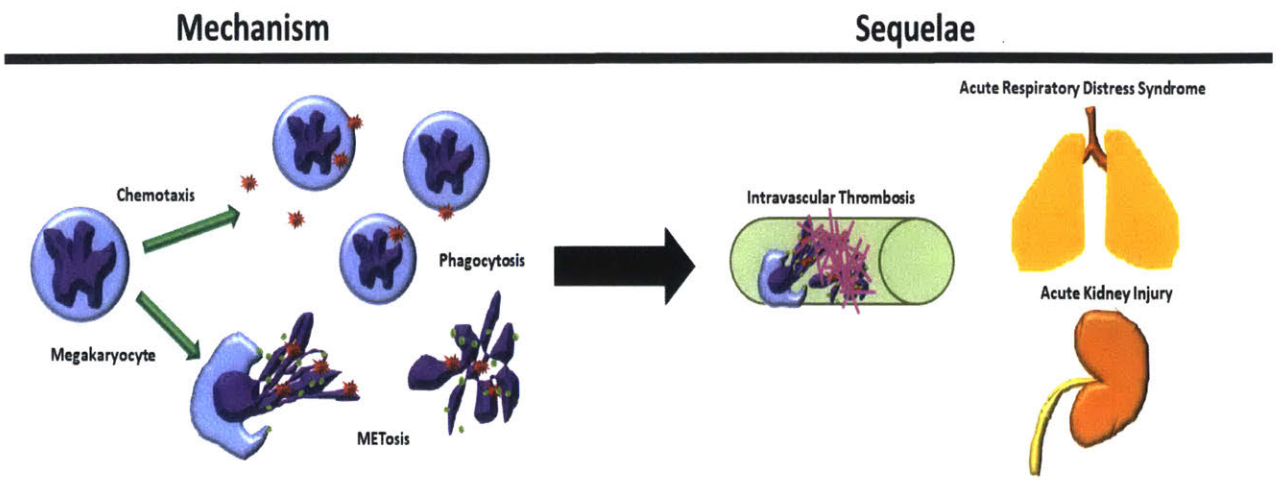

Figure 2-13: Proposed mechanism of megakaryocytes as immune cells

The megakaryocyte cell (left) is capable of chemotaxis towards pathogens (red stars). Upon contact with pathogenic stimulus, the megakaryocyte can perform phagocytosis (top left) or form an extracellular trap (bottom left) (DNA, purple; green, histones). These activated megakaryocytes and METs can then propagate intravascular thrombosis. This intravascular thrombosis can result in end organ damage if lodged within the lungs, resulting in acute respiratory distress syndrome, or the kidneys, resulting in acute kidney injury.

Tables:

Table 2-1: Patient descriptive statistics for circulating megakaryocytes

Patient ID	Sex/Age(yrs)	Infection/Source	MRSA/VRE	Notes	Circ MK (/mL)	Plt (x10^6/mL)	WBC(x10^6/mL)/Neut(%)
1	F/42	- Enterococcus/Urine - Candida albicans/Blood - Alpha hemolytic streptococcus/Blood	+/+	- Recurrent bacteremia	4791	206	5.9/22
2	M/34	- Not identified	-/-	- Septic shock - AKI - Aspiration pneumonia	4440	116	6.2/58.58
3	M/39	- Enterococcus faecalis/respiratory - Staph and yeast/urine		- Septic shock - ARF (chronic)	6593	296	18.1/64.3
4	M/51	- E. coli/blood - Enterobacter cloacae, Klebsiella pneumoniae/wound	-/-	- presumed anastomosis leak - AKI	9392	374	29.9/90
5	M/75	- Klabsiella oxytoca, Morganella morganii, staph aureus/wound	-/-		9454	259	7.3/78/7
6	M/67	- Serratia marcescens/urine - MRSA/blood	+/-	- AKI	3659	144	7.7/77.1
7	F/37	- Candida albicans/urine - Staph aureus, yeast/respiratory - Klebsiella (raultella)/respiratory		- Endocatditis	2840	130	9.5/92.8
8	M/51	- Pseudomonas and yeast/respiratory		- Septic shock - AKI - ARDS - MODS	19466	61	18.6/87.6
9	F/42	REPEAT (1)	+/+	- Recurrent bacteremia - Currently stable	2276	204	5.7/30.4
10	F/41	- Corynebacterium/respiratory - Yeast/urine		- ARDS	7679	256	6.8/71.8
11	M/51	REPEAT (4)	-/-		16352	436	24.8/83.8
12	M/67	REPEAT (6)	+/-		18144	159	6.9/75
13	M/51			- AKI	20126	209	10.3/
14	M/58	- Candida albicans and E. faecalis/respiratory - Candida albicans/urine		- ARDS	3659	114	
15	M/53	- Strep pneumoniae and staph aureus/respiratory		- ARDS - Pancreatitis	7319	93	18.8/

Table 2-2: Patient descriptive statistics for histopathology analysis

ID	Signalment Sex/Age (yr)	Path	Kidney	Lungs
2	M/68	- Coronary artery disease with infarcts and scarring	- Granular casts - Acute renal failure	- Mucopurulent bronchiolitis and pulmonary edema - Serosanguinous pleural fluid - E. coli and Stenotrophomas maltophilia (both G-)
3	M/69	- Pseudomembranous colitis with secondary C. diff infection - C. diff toxin + - Blood pos for Enterobacter cloacae and faecium	- Acute tubular necrosis	- No comments
4	F/82	- C. diff pseudomembranous colitis - acute hemorrhagic bronchopneumonia	- No comments	- Acute hemorrhagic bronchopneumia - Purulent pleural effusion, bilateral
6	F/44	- Diffuse alveolar damage complicating sepsis from staphylococcal bacteremia	- Acute tubular necrosis - Benign nephrosclerosis - Punctate parenchymal hemorrhage	- Diffuse alveolar damage - Exudate phase - Focal bronchopneumonia, patchy
7	F/63	- Autolytic changes - Pseudomembranous colitis - Ischemic change and sepsis suspect - History of recent bacteremia (IV line)	- Nephroclerosis - Acute tubular necrosis suspected	- Edematous
8	F/87	- Sepsis with heart disease - Necrotizing cellulitis - Blood+ for B-hem strep	- Moderate nephreloscleros is	- Serosanguinous pleural effusion - Centriacinar emphysema
9	F/58	- History of MM and influenza - Autolysis present - Sepsis and diffuse alveolar damage associated with disseminated candidiasis	- Candida abscesses - Nephlerosclerosis - Kapp staining - Chronic tubular injury	- Active diffuse alveolar damage - Focal bronchopneumonia with gram + cocci and candida species
10	F/84	- Dementia complicated by severe right lower lobe pneumonia - Resp MRSA+	- Severe nephrosclerosis	- Severe hemorrhagic bronchopneumonia - Pulmonary hypertension - emphysema
11	F/81	- Ischemic bowel arising in the context of MODS - Small bowel transmural necrosis with thrombus - autolysis - Suspect cardiac source of death	- glomerulosclerosis and autolysis	- diffuse alveolar damage - congestion - regional necrosis
5	F/90	- Terminal heart failure	- Nephlerosclerosis	- Pulmonary edema and congestion
1	F/68	- Sarcoidosis - Alzheimers - Ischemic event – cardiac	- Nephlerosclerosis - Diabetic glomerlosclerosis	- Patchy acute bronchopneumonia, acute, right lung - AFB and GMS negative
12	M/77	- Pulmonary hypertension - Coronary artery disease	- Mild nephrelosclerosis	- Pulmonary hypertension - Interstitial pneumonitis - Edema and congestion
13	M/60	- Diffuse cardiac ischemia	- Nephlerosclerosis - Diabetic nephlerosclerosis	- Bilateral congestion - Hemorrhage LUL - Mild emphysema
14	M/71	- Liver and heart disease	- Moderate glomerulosclerosis - Acute tubular injury	- Emphysema - Patchy interstitial airway inflammation and edema

Path, Cause of death determined by pathologist;

Kidney and Lung, histopathology findings as determined by pathologist.

Videos:

Video 2-1: Zymosan particles co-incubated with Meg-01 cells.

Meg-01 cells were co-incubated with zymosan particles overnight. In this video z-stack image, the particles appear to possible be associated with the cell membrane, but no internalization is observed. Zymosan, red; Nuclear stain (Hoechst), blue; Membrane stain, calcein, green.

Video 2-2: Zymosan particles are internalized by Meg-01 cells.

Meg-01 cells were co-incubated with zymosan particles overnight. In this z-stack image video, one of the cells is observed to have internalized the red zymosan particles. Zymosan, red; Nuclear stain (Hoechst), blue; Membrane stain, calcein, green.

Video 2-3: Chemotaxis of Meg-01 cells.

Meg-01 cells chemotaxing from the main channel into the side comb and side channel into the circular well containing LPS and zymosan particles. Zymosan, red; Nuclear stain (Hoechst), blue.

Video 2-4: Platelet-like particle budding within a well after chemotaxis.

Meg-01 cell that has entered a circular well primed with SDF1α is observed undergoing apoptosis and budding platelet-like particles within the well. Interestingly, some of the platelet-like particles remain Hoechst-positive, indicating that there is DNA within some of the particles. NOTE: This video was created on a different chemotaxis chamber design, where there is no comb and only one side-channel leading into the well.

Video 2-5: Cytoskeletal rearrangement during chemotaxis.

Continuation of Video 2. Large Meg-01 cell undergoes active cytoskeletal rearrangement with Hoechst-positive granules proximal to the nucleus. The cell is chemotaxing into a circular well that has SDF1α and platelet-like particles from a Meg-01 cell that had undergone apoptosis and budded particles. This large cell fills up the entire length of the side channel and then appears to get stuck and stops moving. NOTE: This video was created on a different chemotaxis chamber design, where there is no comb and only one side-channel leading into the well.

Video 2-6: Meg-01 cell carrying zymosan particle during chemotaxis.

Meg-01 cells are observed to chemotax towards wells primed with zymosan particles. One zymosan particle is noted to be within the comb and is carried into the circular well by a cell as it moves into the well. Zymosan, red; Nuclear stain (Hoechst), blue.

Video 2-7: Meg-01 cell budding platelet-like particles in the presence of zymosan and LPS.

Meg-01 cell is observed to migrate into a well primed with zymosan and LPS and then proceeds to form connecting platelet-like particles. Zymosan, red; Nuclear stain (Hoechst), blue.

Video 2-8: Meg-01 cell budding platelets in the presence of SDF1α.

A meg-01 cells is observed to migrate within the side channel, towards a well primed with SDF1α. Right before it enters the circular well, the cell stops migration and starts to undergo cytoskeletal rearrangement and buds what appears to be platelet-like particles. The cell does not migrate further once the cytoskeletal changes occurs and appears 'stuck' within the channel. Nuclear stain (Hoechst), blue.

Video 2-9: Meg-01 cell chemotaxis negative control.

Meg-01 cells are not observed to migrate to the negative control (RPMI + 10% FBS) within the microfluidic device.

Chapter 3

Megakaryocytes and Platelets Contain Extranuclear Histones

3.1 Abstract

Histones can be very dangerous when they are located in the extracellular compartment, promoting inflammation and coagulation in various disease states. Patients with sepsis are known to have increased extracellular histones, and these histones have been shown to correlate with prognosis and the development of sepsis-related sequelae, such as end organ damage. Until now, the primary source of extracellular histones during sepsis has been neutrophils. In this paper, we perform a set of *in vitro* experiments demonstrating that megakaryocytes commonly contain extranuclear histones; additionally, they appear to transmit these histones to their platelet progeny. We also performed imaging flow cytometry on isolated platelets from patients with sepsis and demonstrated that these patients do have increased platelet-associated histones as well as an activated platelet phenotype. Taken together, these results suggest that the megakaryocyte and platelet may be a source of extracellular histones during sepsis and should be further explored.

3.2 Introduction

Traditionally, histones have been recognized as a functional 'glue' for genetic material, wherein core histones (H2A, H2B, H3, and H4) form octamers and linker histones (H1 and H5) hold DNA together in specific conformations. Specific histone post-translational modifications (PTSMs) also directs site-specific activation or silencing of transcription. (Venkatesh S, 2015) While histones are typically located within the nucleus of the cell, they can also be located within the cytoplasm, the cell membrane, or can even be extracellular. (Chen R, 2014) When histones are located outside of the cell they can change roles and serve as damage-associated molecular patterns (DAMPs) and be dangerously proinflammatory and cytotoxic. (Chen R, 2014; Parseghian MH, 2006) Extracellular histones have been shown to be associated with life-threatening inflammatory conditions, such as sepsis and its' secondary complications, including

acute respiratory distress syndrome (ARDS) and acute kidney injury (AKI). (Xu Z, 2015; Miki T, 2015; Li Y, 2009; Jansen MPB, 2017; Kalbitz M, 2015)

One of the primary sources of extracellular histones during sepsis is thought to be neutrophils, via the formation of neutrophil extracellular traps (NETs). (Xu Z, 2015; Chaput C, 2009) NETs are essentially a type of cell death where a neutrophil releases intracellular material – namely DNA and associated histones. Extracellular DNA and histones have been shown to be both proinflammatory and thrombogenic. (Fuchs TA, 2007) Circulating histones can result in activation of nearby platelets and leukocytes, can activate thrombin to exacerbate intravascular clot formation, and can initiate endothelial and epithelial cell death via Toll-like receptor-2 and -4 (TLR2 and TLR4) signaling. (Xu Z, 2015; Chaput C, 2009; Gould TJ, 2015; Varju I, 2015)

In Chapter 2, 'Megakaryocytes as Functional Immune Cells', we showed that megakaryocytes, the precursors to platelets, are capable of forming megakaryocyte extracellular traps (METs) in response to pathogenic stimuli. We have also shown that megakaryocytes appear to be increased both in the peripheral circulation as well as in the peripheral organs (kidney and lungs) during sepsis. In this set of experiments, we explore whether megakaryocytes can be a source of extracellular histones, not only through MET formation, but also through the development of histone-rich platelets. We also show that platelets from patients with sepsis have significantly higher levels of platelet-associated histones and may themselves be a source of extracellular histones during severe infection and inflammation.

3.3 Methods and Materials

3.3.1 Cell culture

Cord blood $CD34^+$ stem cells were purchased and cultured in StemSpanII media with the megakaryocyte supplemental cytokines, according to the culture and differentiation protocols from Stemcell Technologies (Stemcell Technologies Inc. Cambridge, MA). A megakaryoblastic cell line (Meg-01) was purchased and cultured in RPMI with 10% FBS, according to the standard cultures protocols from ATCC (American Type Culture Collection, Manassas, VA).

3.3.2 Platelet and white blood cell isolation

Platelets and platelet-rich plasma was collected for most of these experiments. Neutrophils were isolated as a positive control for histone staining. Platelets were prepared from blood collected into 2.9 ml trisodium citrate Vacutainer tubes (Sarstedt, N¨umbrecht, Germany). Platelet-rich plasma (PRP) was first prepared by centrifugation of the whole blood at 210 g, 22°C, for 20 min. The PRP supernatant was gently pipetted into a new tube with 20% volume ACD solution (Boston Bioproducts, Ashland, MA, USA) and then centrifuged at 1900 g, 22°C, for 10 min. The platelet-poor plasma (PPP) was removed, leaving a platelet pellet. Neutrophils were isolated from whole blood collected in ACD BD Vacutainer tubes (Becton Dickinson, Franklin Lakes, NJ, USA) using a negative-selection protocol. In brief, neutrophils were isolated using a density gradient with HetaSep (Stemcell Technologies, Vancouver, BC, Canada) and then purified with EasySep Human Neutrophil Kit (Stemcell Technologies), following the manufacturer's protocol.

3.3.3 Immunofluorescence Imaging

Both Meg-01 and cord-blood derived MKs (CB MKs) were fixed and stained for the evaluation of cellular histone localization using immunofluorescence staining. Meg-01 cells were co-incubated with various concentrations of *E. coli* lipopolysaccharide (LPS) (O111:B4; Sigma Aldrich, St Louis, MO), for 60 minutes at 37°C on poly-lysine coated slides (Sigma Aldrich, St Louis, MO, USA) and then fixed with 4% paraformaldehyde (Santa Cruz Biotechnology, Dallas, TX, USA). Platelet pellets were prepared as described in the 'Blood cell sample preparation' section above. CB MKs, at day 14 of differentiation, and platelet pellets were fixed with 4% paraformaldehyde for 30 minutes and then concentrated onto a poly-lysine coated slide using the Cytospin 4 cytocentrifuge (Thermo Fisher Scientific), for 5 minutes at 1250 rpm, rinsed once with di-water and stored at -80°C until staining and evaluation. For staining, the slides were thawed at room temperature and blocked with 5% donkey serum (Jackson Immunoresearch) for 2 hours. The slides were rinsed three times with PBS and then treated with various combinations of the following primary antibodies for two hours: rat anti-Histone H3 (phospho S28) antibody (HTA28; Abcam, Cambridge, MA, USA) at 1:500, rabbit anti-Histone H4 (39270; Active Motif, Carlsbad, Ca, USA), rabbit anti-Histone H2A.X (Active Motif), rabbit anti-Histone 3 (ab1791; Abcam, Cambridge, MA, USA), and mouse anti-Histone 3 (96C10; Cell Signaling Technology,

Danvers, MA, USA). The slides were then rinsed three times with PBS and incubated with various combinations of the following secondary antibodies: mouse anti-human CD41 (GPIIb) 488 or 647 (Biolegend, San Diego, Ca, USA) at 1:250, donkey anti-rabbit 488, donkey anti-rat 647, and donkey anti-mouse 568 (Life Technologies) at 1:500 for 30 minutes. Slides were then rinsed three times with PBS and then covered with Vectashield antifade mounting medium with DAPI (Vector Labs, Burlingame, Ca, USA). The cells were then imaged with one of two fluorescent microscopes: Life Technologies EVOS FL (Thermo Fisher Scientific) or Nikon Eclipse 90i microscope (Nikon Instruments Inc., Melville, NY).

3.3.4 Histone-2B BacMam transfection of Meg-01 cells

Meg-01 cells were transfected with GFP-Histone 2B (H2B) for localization of cellular histone. Meg-01 cells were transfected with CellLight Histone 2B-GFP (BacMam 2.0, ThermoFisher Scientific) at 30 uL/mL for 48-72 hours. Cell were then labeled with MitoSox Red mitochondrial superoxide indicator (ThermoFisher Scientific) at 1:1000 Hoechst at 1:2000 for 30 minutes. Cells were then pelleted at 1,900 x g for 10 minutes and rinsed twice with PBS. Cells were then concentrated onto a poly-lysine coated slide using the Cytospin 4 cytocentrifuge (Thermo Fisher Scientific), for 5 minutes at 1250 rpm. Slides were then rinsed with DI water, cover slipped, and imaged on an EVOS fluorescent microscope.

3.3.5 Histone purification

Histones were extracted from both platelet pellets and Meg-01 cells for histone quantification. For sample preparation, venous whole blood collected in acid citrate dextrose tubes (Research Blood Components LLC, Boston, MA, USA). Platelet pellets were isolated as described in the section above, 'Blood cell sample preparation'. Meg-01 cells were pelleted down at 1900 x g for 10 minutes. For histone purification the Active Motif Histone Purification Mini Kit (Active Motif) was utilized per the manufacturer's instructions. Briefly, platelet and cell pellets were washed twice with hepes-tyrode buffer and 20% acid citrate dextrose buffer (Boston BioProducts, Boston, MA, USA). Pellets were then re-suspended in ice-cold Extraction Buffer. Samples were homogenized in the Extraction Buffer using for 30 minutes and then left overnight at 4°C. The samples were then spun at maximum speed (18,000 x g) in a microfuge for 5 minutes at 4°C. The supernatant, containing the crude histones, was then transferred to a new tube and

neutralized with 5X Neutralization Buffer to a pH of 8. One aliquot of crude histones was saved for downstream analysis. Spin columns provided by the kit were then equilibrated and the crude histones along with the Elution Buffer were run through the columns at 500 x g for 3 minutes. One aliquot of the eluted histones was saved for downstream analysis. Histones were then precipitated with perchloric acid. Briefly, histones were precipitated overnight at 4°C with 4% perchloric acid. The histones were then spun down at maximum speed for 1 hour at 4°C. The pellet was washed with 1 mL cold 4% perchloric acid, then twice in ice cold acetone with 0.2% HCl, and then twice in ice cold acetone. The resulting pellet was air dried for 10 minutes and then re-suspended in sterile water. All histones and aliquots were stored at -80°C until the samples were analyzed.

3.3.6 Histone quantification

Histone quantification was performed using two methods: absorbance measurements and ELISAs. For the absorbance measurements, both total protein and histone-specific absorbances were performed as follows using the DS-11 Spectrophotometer (DeNovix Inc., Wilmington, DE, USA): 230 nm for total protein, 280 nm for histone quantification with the following molecular weight extinction coefficients, as recommended by Active Motif (Table 3-1). Histones purified from calf thymus (Sigma-Aldrich, St. Louis, MO, USA) were used as a positive control at 2 mg/mL. For histone quantification using ELISAs the Luminex Histone H3 PTM Multiplex Assay (Active Motif) was used according to the manufacturer's protocol. For sample preparation, serial dilutions of Meg-01 and platelet pellet purified histones were prepared. For the positive control, the purified histone 3 protein that was provided with the kit was used in this assay. Both total Histone 3 (H3) and H3 post-translational modifications (PTSMs) were evaluated for each sample (Table 3-2). Briefly, the samples were co-incubated with multiple magnetic beads, were conjugated to antibodies targeted to specific H3 PTSM, on a shaker plate for 2 hours. The beads were then washed 3 times and incubated with biotinylated anti-H3 antibodies on a shaker plate for 30 minutes. The beads were then washed 3 times and then incubated with streptavidin-phycoerythrin for 30 minutes, followed by the final washes. Samples were read by using a Flexmap 3D (Luminex). The standard curve was generated by using 5-parametric-curve fitting with platform-specific software (xPONENT

Software Solutions, Luminex, Austin, TX). Samples were run in duplicate on each plate for quality control.

3.3.7 Flow cytometry

Flow cytometry was performed in order to evaluate cells and platelets for histone expression. Meg-01 cells, platelet, and whole blood were fixed with 4% paraformaldehyde with or without 0.1% Triton™ X-100 detergent (Sigma-Aldrich) for permeabilization for a total of 10 minutes. Samples were then pelleted down at 1,900 x g for 10 minutes and re-suspended in PBS. Cells were first incubated with primary, unconjugated antibodies, rabbit anti-Histone 3 (ab1791; Abcam) or rat anti-Histone H3 (phosphoS28) antibody (HTA28; Abcam) at 1:400 for 20 minutes and were then washed twice with PBS. Cells were then stained with a combination of conjugated primary antibodies and secondary antibodies for 15 minutes, including: mouse anti-human CD41 PacBlue, mouse anti-human CD45 594, mouse anti-human CD162P PE, mouse anti-human CD62P PE, mouse anti-human CD61 FITC (Biolegend, San Diego, Ca), and goat anti-rabbit 488 or donkey anti-rat 647 (Thermo Fisher Scientific, Waltham, MA) at 1:200 for 15 minutes, with the exception of CD41 which was at 1:100. Cells were then stained with Draq5 (Thermo Fisher Scientific, Waltham, MA) at a concentration of 1:10000 for 5 minutes. Data was obtained through the Amnis ImageStreamX Mark II imaging flow cytometer and INSPIRE Software (EMD Millipore, Billerica, MA). The accompanying IDEAS Software was used to perform data analysis. Data is reported as the percent of the total cell population that stained positive for the specific marker.

3.3.8 Transmission electron microscopy and immune-gold labeling

For transmission electron microscopy, cells were fixed in 2.5% gluteraldehyde, 3% paraformaldehyde with 5% sucrose in 0.1M sodium cacodylate buffer (pH 7.4), scraped, pelleted in a small eppendorf tube. Wash with 0.1M sodium cacodylate buffer 3x, post fixed in 1% OsO_4 in veronal-acetate buffer 1 hour. The pellet was stained overnight with 0.5% uranyl acetate in veronal-acetate buffer, dehydrated and embedded in Embed 812 resin. Sections were cut on a Leica Ultracut UCT microtome with a Diatome diamond knife at a thickness setting of 50 nm, stained with uranyl acetate, and lead citrate. The sections were examined using a FEI Tecnai spirit at 80KV.

For the immunogold labeling protocol, the protocol was as follows. (Tokuyasu KT, 1980) The cells were fix mildly Using PLP (paraformaldehyde / lysine / sodium periodate) fixative for 4 hours. Cells were pelleted and trimmed into small (<1mmsq) blocks. Infused with a cryo-protectant for at least one hour (PVP/ sucrose). Blocks were mounted onto cryo-pins, and snap frozen in liquid nitrogen. Ultrathin sections were cut at -110 degrees C with a Leica UC7 equipped with a FC7 cryo-stage using a glass knife, and immunolabeled, stained and embedded using the Tokuyasu technique. For the immmunolabeling, rabbit anti-histone 4 antibody (39270; Active Motif) was used. The material was examined using a FEI techni Spirit biotwin.

3.3.9 Patient sample collection

Venous blood from patients diagnosed with sepsis was collected and evaluated for histone-associated platelets (IRB protocol numbers, MGH No: 2014P002087; MIT No:150100681R001). A patient was categorized as sepsis when one of the diagnoses for the patient was 'sepsis' and when there was a confirmed infection. Twenty-one samples were evaluated with 16 sepsis samples (age 36-85 yrs., 4 females, 12 males) collected from MGH and 5 healthy control samples purchased from Research Blood Components (Research Blood Components, LLC, Boston, MA) (Table 3-3). Platelet pellets were isolated as described in the 'Histone purification' section from venous blood collected in vacutainer EDTA tubes and then frozen at -80°C until analyzed. Flow cytometry was performed as described above, in the 'Flow cytometry' section. In order to assess for the effect of platelet activation in the expression of histone as well as to account for the effects of freeze-thawing of the patient platelet pellets, one set of control samples and one sepsis sample was pre-treated with the following conditions: paraformaldehyde fixation, fixation with 0.1% Triton™ X-100 permeabilization, activation with 1 μg/mL α-thrombin (coagulation Factor IIa; Haematologic Technologies, Essex Junction, VT, USA), 0.2 mM $CaCl_2$, and vortexing for 10 seconds, freeze at -80°C followed by thaw in 4% paraformaldehyde (how the sepsis samples were treated), and free at -80°C followed by thaw in 4% paraformaldehyde with 0.1% Triton™ X-100. Samples were evaluated as described in the section above, 'Flow cytometry'.

3.3.10 Statistical analysis

Platelet were evaluated both as 'singles' and as 'clusters' in order to parse between the more

activated platelets that are more likely to be present as clusters and individual platelets in circulation. Statistics were performed using both Excel (Microsoft, Redmond, WA, USA) and GraphPad Prism Software (GraphPad Software, Inc.). Either one-way ANOVA or student t-tests were performed to compare between conditions. Pearson's correlation was used to determine whether there was a correlation present between platelet phenotype and platelet count or white blood cell count. A p-value of <0.05 was considered significant.

3.4 Results

3.4.1 Megakaryocytes contains extranuclear histones

Immunofluorescent imaging used to localize histones within megakaryocytes showed that extranuclear histones are common in both Meg-01 cells and in cord blood-derived (CB) MKs (Figure 3-1). Histone 3 phosphorylated at position serine 28 (PhosphoH3; Ser28; H3s28ph) was used as a histone marker. Ser28 increases in response to activation of the MAPK pathway and is increased during mitosis. (Dunn KL, 2005. Light granular staining was seen diffusely throughout the Meg-01 cell membrane and cytoplasm, with an increase in staining at the nucleus of cells with mitotic figures (Figure 3-1 A). CB MKs were also positive for Ser28, with small, round quiescent cells having mainly cell membrane and cytoplasmic staining, while more activated cells appeared to have positive staining within cellular extensions at, what appears to be, the uropod of the cell (Figure 3-1 B). Upon stimulation with *E. coli* LPS, CB MKs were observed to form MET-like structures, as previously described in Chapter 2, with extracellular histones and DNA; Meg-01 cells displayed histone staining within what appeared to be proplatelet buds (Figure 3-1 C).

BacMam technology was used to transfect Meg-01 cells with GFP-Histone 2B (H2B) in order to allow for a non-antibody-dependent method of confirming the presence of extracellular histones within megakaryocytes. In the majority of the cells, H2B appeared to be primarily located to the nucleus. Rarely, extranuclear histone was visualized within the cytoplasm of the cell or within platelet-like particles within the cell culture (Figure 3-2). The visualization of GFP-H2B is less likely to be artifact or background, as compared to antibody-dependent methods, such as

immunofluorescent staining, because the GFP-H2B must be synthesized by the cell itself. It was observed that the cells that appeared to have cytoplasmic GFP-H2B also had very strong GFP signal within the nucleus, which may either indicate that the cell is overexpressing the histone or the cell is polyploidy and approaching its apoptotic stage, where histones are likely to end up within the cytoplasm of the cell. (Chen R, 2014; Gabler C, 2004; Zhao B, 2016) These results strongly suggest that both Meg-01 cells and CB MKs appear to have extranuclear histones, although perhaps H2B is not the most prominent extranuclear histone in these cells.

3.4.2 Platelet contain histones

Immunofluorescent imaging was used to probe whether peripheral blood platelets are positive for histones. Isolated neutrophils were used as a positive control for the Ser28 staining and confirmed the nuclear localization of this stain (Figure 3-3 A). Buffy coats were then stained with Ser28 and showed that platelets did appear to stain positive for histones; where Ser28 appeared to be primarily around the platelet membrane, while CD41 positively identified the platelet and had diffuse staining (Figure 3-3 B). White blood cells noted on the slide were used as an internal positive control. Platelets were then probed with a generic Histone 3 (H3) and Histone (4) antibody to further confirm the presence of platelet histones (Figure 3-3 C & D). Imaging flow cytometry was then used to further test for the presence of platelet-associated histones in both permeabilized and non-permeabilized cells. Interestingly, staining with the generic H3 antibody was positive in the non-permeabilized cells, and appeared to be localized to the platelet membrane; whereas the permeabilized cells stained the entire platelet (Figure 3-4 A). Ser28, on the other hand, did not stain the non-permeabilized platelets, but did appear to stain the permeabilized platelets (Figure 3-4 B). These results suggest that there are Ser28, H3, and H4 platelets-associated histones.

Transmission electron microscopy (TEM) immuno-gold imaging was then used to attempt to determine the cellular localization of histones within platelets. Platelets stained positive for H4 (Figure 3-5). Interestingly, the labeling appeared to be fairly diffuse throughout the cytoplasm of the cell. There were pockets of more concentrated labeling, which tended to be either on the platelet membrane or on electron-dense areas of the TEM image. There was little-to-no immuno-

gold labeling within the platelets granules or mitochondria. These findings suggest histones are present diffusely within the platelets and are not packaged within platelet granules.

3.4.3 Histone quantification

Platelet histone quantification was attempted utilizing a combination of methods, including: absorbance and bead-based ELISA assays. The absorbance method for total protein and histone quantification results are shown in Table 3-1. The total protein was calculated with the following equation (Eq. 1):

Eq. 1: *(OD 0.42) / (1 mg/mL) = (measured OD at 230 nm)/ (X mg/mL)*
X = total protein concentration

Calf thymus histones were used as a positive control for this methodology and showed a relatively good agreement between the expected total protein concentration (10 mg/mL) and the measured total protein concentration (10.35 mg/mL). The Meg-01 histones were calculated to be at a concentration or 7.07 mg/mL and the two platelet extracts that were tested were calculated to be 0.18 mg/mL and 0.15 mg/mL. The samples were then evaluated for individual histone concentrations using their expected molecular weights and extinction coefficients. The total histone concentration (H2A, H2B, H3, and H4) of the calf thymus, Meg-01 cells, and both platelet extracts were 9.75 mg/mL, 6.28 mg/mL, 1.51 mg/mL, and 1.17 mg/mL, respectively. Although the histone concentrations are close to the total protein concentrations for the calf thymus and the Meg-01 cells, they were about ten times higher than the protein concentrations for the platelet extracts. The lower detection limit of the absorbance reader was 0.04 mg/mL; therefore, we do believe that the concentration should be within the detectable range for the reader.

Next we used a bead-based ELISA assay for the quantitation of histone 3 and a few specific histone 3 post-translational modifications. (Table 3-2). Sequential dilutions of the Meg-01 purified histones were performed in order to verify the assay protocol as well as derive the histone concentration in the platelet extract sample (Figure 3-6 A & Table 3-4). The dilution curve for the Meg-01 cells fit a logarithmic line (Eq. 2) with an R-squared value of 0.99.

Eq. 2: $Y = 614.9\ ln(X) + 462.9$

Y = MFI, mean fluorescent intensity; X = histone concentration (ng/uL)

Using eq. 2, the MFI for the platelet histones was used to back-calculate the total histone concentration in the sample. This concentration was then used to calculate the total amount of H3 per platelet (Eq. 3), using an estimated input platelet count of 300 x 10^6 platelets.

Eq. 3: $Y = X / A$

Y = ng / platelet; X = total His3 concentration (ng); A = platelet count (x 10^6)

According to Eq. 3, the estimated His3 concentration in platelets was 0.42-0.46 ng / 10^6 platelets. This protein concentration is within the range of other protein concentrations, as calculated by Peterson JE, et al (2010). (Peterson JE, 2010) Total estimated concentration for each of the His3 modifications measured with the bead-based assay are listed in Table 3-5. Although we were able to calculate the best-fit line for total H3, this was not able to be done for the H3 PTSMs tested because we did not know the initial input of each of these PTSMs; therefore, these specific histones are expressed in terms of percent of total H3 expressed. As seen in Table 3-6, H3kme4 and H3k27me3 were the PTSMs expressed in the highest abundance in the Meg-01 cells, as compared to H3k56ac and H3s10ph. In the platelet extracts, the histone PTSM expression appeared to follow a similar trend as the Meg-01 cells, with both H3k56ac and H3s10ph appearing to be below the limit of detection (Figure 3-6 B). Here we have demonstrated that, in addition to total H3, we can also detect specific PTSMs within platelets. At this point in time, we cannot draw any conclusions as to what these specific PTSM patterns signify, as the histones tested were 'total' histone extracts and were not specific for any gene sequence.

3.4.4 Sepsis results in increased platelet-associated histones

In order to evaluate whether platelet-associated histones were increased in patients with sepsis, we performed imaging flow cytometry on isolated platelet pellets. The markers that were evaluated included: CD34, which can either be increased if budding off of immature megakaryoblasts or can be decreased if platelets are activated, Draq5$^+$ which may be present in some platelets if platelet-formation results in DNA-containing platelets, as seen in Chapter 2

(Video 2-4), His3, which we hypothesize to be increase in patients with sepsis, and $Draq5^{+}His3^{+}$ cells, which may indicate that His3 and DNA are bound together within the platelet. Platelets were positively identified by gating for small $CD41^{+}$ (GPIIb) cells. Platelet analysis was also further subdivided into 'single' platelets and 'clustered or aggregated' platelets. The reasoning for this classification is because it is much more likely for platelets that are in aggregates to express higher levels of activation markers, and possible different amounts of DNA or His3.

To account for the sample storage and preparation conditions of the patient platelets, which included platelet isolation followed by storage at -80°C, we first evaluated the effect of these conditions on control platelets from healthy patients (Figure 3-7). When comparing the fresh platelets to the freeze-thawed platelets, there were changes in cell surface marker expression, for both single and clustered platelets, including: an increase in $His3^{+}$ platelets (plts) (1.8 ± 0.6 and 28.9 ± 1.7 % $His3^{+}$ plts vs. and 7.0 ± 1.6 and 52.9 ± 5.5 % $His3^{+}$ plts, respectively), an increase in $CD34^{+}$ plts (2.0 ± 1.8 and 28.9 ± 1.7 % $CD34^{+}$ plts vs. and 9.4 ± 1.9 and 52.9 ± 5.5 % $CD34^{+}$ plts, respectively), a decrease in $Draq5^{+}$ plts (4.9 ± 6.0 and 47.4 ± 17.7 % $Draq5^{+}$ plts vs. and 0.05 ± 0.02 and 14.3 ± 1.4 % $Draq5^{+}$ plts, respectively) and $Draq5^{+}His3^{+}$ plts (0.5 ± 0.9 and 25.3 ± 4.6 % $Draq5^{+}His3^{+}$ plts vs. and 0.02 ± 0.01 and 13.9 ± 1.3 % $Draq5^{+}His3^{+}$ plts, respectively. There was also decrease in the percent of platelets that are within clusters or aggregates (51.1 ± 17.8 vs. 24.1 ± 3.7 % Clusters, respectively). The same changes were seen in the single and clustered groups, although to a greater extent in the clustered, likely due to increased activation. At this point in time, we are not sure why $CD34^{+}$ increased with freeze thawing, as it has previously been shown to decrease with platelet activation; this may be due to rupture of the platelet membrane upon thawing and increased exposure of internal CD34 resulting in increased $CD34^{+}$ cells. Due to the differences in platelet phenotype with freeze-thawing, we treated all controls to freeze-thawing and used those values as the negative control to the sepsis patients; this would allow us to compare relative changes between groups.

As expected, patients with sepsis did have a different platelet phenotype than the control patients (Figure 3-8). There were significantly more $His3^{+}$ plts in the sepsis group as compared to the control group for both the single plts (27.1 ± 20.6 and 7.0 ± 1.6 % $His3^{+}$ plts, respectively), whereas there were significantly less $His3^{+}$ plts the clustered platelets (27.3 ± 13.4 and 52.9 ± 5.5

% $His3^+$ plts, respectively). There was no significant difference in $Draq5^+$ platelets in the sepsis group as compared to the control group, for both single and clustered platelets (4.2 ± 4.7 and 0.05 ± 0.02 % $Draq5^+$ plts vs. 33.5 ± 21.7 and 14.3 ± 1.4 % $Draq5^+$ plts, respectively). $CD34^+$ platelets were significantly decreased in patients with sepsis as compared to controls, for both single and clustered platelets (2.6 ± 3.6 and 9.4 ± 1.8 % $CD34^+$ plts vs. 24.4 ± 12.3 and 80.1 ± 2.4 % $His3^+$ plts, respectively). $Draq5^+His3^+$ platelets were significantly increased in the single platelets (0.8 ± 0.8 and 0.02 ± 0.01 % $Draq5^+His3^+$ plts, respectively), but not in the clustered platelets (14.2 ± 8.2 and 13.9 ± 1.3 % $Draq5^+His3^+$ plts). Notably, there was no significant difference in the number of platelet clusters between control and sepsis patients (21.1 ± 11.5 and 24.1 ± 3.7 % Clustered plts, respectively), further supporting that the changes in the platelet phenotype are not simply due to increase platelet activation and aggregation. There was no correlation between platelet phenotype and platelet count or total white blood cell count. Interestingly, $His3^+$ platelets in sepsis patients also appeared to have two different populations, a $His3^{lo}$ and a $His3^{hi}$ population; these two populations were not seen in the control groups (Figure 3-8 E). $His3^+$ cells also appeared to be at higher levels in patients diagnosed with Gram positive bacterial infections, as compared to gram – infections (Figure 3-8 F).

Changes in platelet phenotype were also explored over time in patients with sepsis (Figure 3-9). Nine patients were followed on sequential days during hospitalization and it was noted that $His3^+$ platelets were significantly higher during early sepsis than on subsequent days in six of the patients (Fig 9A). There were two patients that did not follow this trend: patient 2, which was diagnosed with sepsis but by the time the blood sample was collected, the urine culture was negative (who was subsequently not included in analysis), and patients 11 and 12, which were both diagnosed with chronic sepsis, were under 'palliative care', had been in and out of the hospital for weeks-months prior to sample collection, and did not recover from this event. The platelet phenotype was also different for both Gram positive and mixed infections, with a mixed infection being defined as at least 2 or more of the following: Gram negative bacteria, Gram positive bacteria, fungal organism, viral organism (Fig 9B-F). Cumulatively, these results suggest that, in addition to increased platelet activation, as noted by decreases in $CD34^+$ platelets, there was an increased number of platelets that had associated DNA (Draq5) and His3.

3.5 Discussion

Histones are an essential building block for nuclear material, helping form chromatin and acting as control switches for the transcription of DNA. In addition to their essential role in transcriptional regulation, histones also have important roles outside of the nucleus, including serving as damage-associated molecular patterns (DAMPs). (Xu Z, 2015; Miki T, 2015) When histones are outside of the cell, they bind to a number of different receptors on white blood cells and platelets, such as toll-like receptor 2 and 4 (TLR2 and TLR4). (Chaput C, 2009; Silk E, 2017; Russell RT, 2017; Semeraro F, 2011) Extracellular histones are typically degraded by a variety of enzymes, such as histone deacetylases (HDACs); but when they are significantly increased they can bind and activate the surrounding cells and may result in white blood cell activation, platelet activation, and endothelial cell damage. (Eckaney ML, 2014) Extracellular histones can be significantly increased during sepsis and are thought to play an integral role in the pathophysiology of severe systemic inflammation and immunothrombosis. (Li Y, 2009; Eckaney ML, 2014; Garcia-Gimenez JL, 2017; Kim JE, 2015; Kimball AS, 2016) Experimental treatment with TLR4 receptor inhibitors and HDACs in animal models of sepsis have helped support this mechanistic hypothesis. (Savva A, 2013; Fenhammer J, 2014; Ciarlo E, 2013; Takebe M, 2014; Li Y, 2015; Li Y, 2014) Up until now, platelets have been shown to bind extracellular histones through TLR2 and TLR4 receptors and also liberate histones from bound DNA through the release of highly positively charged platelet factor 4 (PF4), but platelets have not been explored as a potential source of extracellular histones themselves. (Semeraro F, 2011; Gollomp K, 2015) In this paper, we demonstrated that megakaryocytes (MKs) commonly contain extranuclear histones, and that that the 'parent' MKs may transmit these histones to their 'daughter' platelets, resulting in an additional source of extracellular histones during severe inflammation and platelet activation, such as in sepsis. We also demonstrated that patients with sepsis appear to have increased platelet-associated histones.

Although histones are most commonly located within the nucleus of a cell, extranuclear histones have been demonstrated in a variety of cells and in a number of conditions. The role histones outside of the nucleus is not completely clear, but they have been shown to be extremely

proinflammatory and even prothrombotic. (Chen R, 2014; Parseghian MH, 2015; Xu Z, 2015; Miki T, 2015) There are a number of mechanisms by which histones can be found outside of the nucleus, including extracellular trap formation, apoptosis, via escape or leakage through nuclear membrane pores, and as a functional protein within the mitochondrial membrane. (Chen R, 2014; Fuchs TA, 2007; Gabler C, 2004; Zhao B, 2016) As hematopoietic stem cells (HSCs) differentiate into MKs and mature into platelet-producing cells, they typically undergo controlled apoptosis (Discussed in more detail in Section 1.2, 'Platelet production'). (Kile BT, 2014; Joseffson EC, 2011; Li J, 2001; Kozuma Y, 2009; Clarke MCH, 2003; De Bottom S, 2002) During this, typically, caspase-mediated apoptosis, it is not surprising that MKs likely develop nuclear membrane pores, where intranuclear material, such as histones, can leak out into the cytoplasm. (Gabler C, 2004; Zhao B, 2016; Gabler C, 2003) In this paper, we have demonstrated that MKs do in fact commonly contain histones in both their cytoplasm and along their cell membrane. The exact role of the histones in these compartments of cells is not currently understood.

Platelets are organized buds composed of MK cell membrane and cytoplasmic material; therefore, it is not out of the question for extranuclear histones within the cell membrane and cytoplasm of the MK to be a part of the resultant platelet (Figure 3-10). Platelets have been shown to bind to extracellular histones via TLR receptors, potentially playing a role in the proinflammatory and prothrombotic nature of extracellular histones during sepsis and its' related complications. (Xu Z, 2015; Semeraro F, 2011; Semple JW, 2011) Up until now, platelets have not been explored as potential sources of histones themselves. One paper by Stewart D.I.H., et al. (1983), did show that protein isolation of platelet pellets contained small concentrations of histone proteins, but at the time this was attributed to likely contamination of the platelet pellet with nucleated white blood cells and was disregarded. (Stewart DIH, 1983) Although we were able to confirm these findings through histone purification and quantitation, there is always the possibility that there were contaminating nucleated cells within our platelet pellets as well. More suggestive proof of platelet-associated histones was demonstrated by showing that platelets stain positive for H4 in both the cytoplasm as well as the cell membrane on electron microscopy.

We next explored whether there was an association between the presence of platelet-associated histones and sepsis. Our results demonstrated that there was an increase in $His3^+$ platelets, as well as an increase in $Draq5^+$ platelets and $Draq5^+/His3^+$ platelets. Although this is suggestive that there may be an increase in platelet-associated histone and DNA content during sepsis, we cannot rule out that the histones and platelets were not just bound to the platelet membrane from the circulation, as plasma histones and DNA are known to be increased during sepsis. (Xu Z, 2015; Gould TJ, 2015) There was also a significant decrease in $CD34^+$ platelets, which is suggestive of platelet activation, although platelet clusters, another sign of platelet activation, was not increased in sepsis patients. (Lewandoaska K, 2003) Interestingly, this unique phenotype lacking platelet aggregation but having an increase in platelet activation is consistent with previous research demonstrating that platelets from patients with sepsis are more likely to spontaneously activate but are less likely to aggregate in response to various platelet agonists. (Hurley SM, 2016; Layois N, 2017; Woth G, 2011; Davies GR, 2014) This unique platelet phenotype was also observed to revert to 'normal' over time as a patient was treated for sepsis, suggesting that this may also be an early indicator of sepsis. The increase in platelet-associated histones may also be another mechanism by which platelets form platelet-leukocyte aggregates (PLAs) and are increasingly cleared or sequestered, leading to peripheral thrombocytopenia; both of which are known consequences of sepsis. (Gabler C, 2003; Grozovsky R, 2010; Ma R, 2017; Rondina MT, 2015; Tejera P, 2017)

In conclusion, this set of experiments has demonstrated that platelets may contain extranuclear histones, and that platelet-associated histones are increased in patients with sepsis. Due to the small concentration of platelet histones that we identified, we do not think that platelets are a primary source of plasma histones during sepsis; although, when platelets are activated, whether the histones are released or whether they are brought to the plasma membrane, these may be stimulatory enough to propagate intravascular inflammation and thrombosis (Figure 3-11). Future studies to further explore this potential source of extracellular histones during sepsis includes testing platelets for histone release upon activation and testing the platelet-associated histones for their proinflammatory and prothrombotic properties. Additionally, because platelets appear to have various H3 PTSMs, testing whether these are bound to DNA or whether the

different histone PTSMs have specific interactions with the immune and coagulation system, as seen with CitH3, would also potentially be very valuable.

3.6 Acknowledgements

Dr. Charles Vanderburg helped with the protein isolation and quantification. Dr. Keith Wong provided guidance in the immunofluorescent staining. Nicki Watson performed the immuno-gold labeling for the electron microscopy images. This work was supported by the T32-0D019078-28 (JGF), the P30-ES002109 (JGF), the P50-GM021700 (RGT), the GM092804 and AI113937 (to D.I.), and the Harvard NeuroDiscovery Center. All microfabrication procedures were performed at the BioMEMS Resource Center (EB002503).

3.7 References

1. Venkatesh S, Workman JL. Histone exchange, chromatin structure and the regulation of transcription. Nature Reviews Molecular Cell Biology, 2015;16:178-179.
2. Chen R, Kang R, Fan X-G, et al. Release and activity of histone in diseases. Cell Death and
3. Parseghian MH, Luhrs KA. Beyond the walls of the nucleus: the role of histones in cellular signaling and innate immunity. Biochem Cell Biol, 2006;84:589-604.
4. Xu Z, Huang Y, Mao P, et al. Sepsis and ARDS: the dark side of histones. Mediators of Inflammation, 2015; 2015:205054.
5. Miki T, Iba T. Kinetics of circulating damage-associated molecular patterns in sepsis. J Immunol Research, 2015;2015:424575.
6. Li Y, Liu B, Eugene Y, et al. Identification of Cit H3 as a potential serum protein biomarker in a lethal model of LPS-induced shock. Surgery, 2011;150(3):442-451.
7. Chaput C, Zychlinsky A. Sepsis: the dark side of histones. Nature Medicine, 2009;15:1245-1246.
8. Jansen MPB, Emal D, Gwendoline TJD, et al. Release of extracellular DNA influences renal ischemia reperfusion injury by platelet activation and formation of neutrophil extracellular traps. Kidney International, 2017;91(2):352-364.
9. Kalbitz M, Grailer JJ, Fattahi F, et al. Role of extracellular histones in the cardiomyopathy of sepsis. FASEB J, 2015;29(5):2185-2193.
10. Fuchs TA, Abed U, Goosman C, et al. Novel cell death program leads to neutrophil extracellular traps. JCB, 2007;176(2):231-241.
11. Gould TJ, Lysov Z, Liaw PC. Extracellular DNA and histones: double-edged swords in immunothrombosis. J Thromb Harmost, 2015;13(Supp 1):S82-91.
12. Varju I, Longstaff X, Szabo L, et al. DNA, histones and neutrophil extracellular traps exert anti-fibrinolytic effects in a plasma environment. Thromb Haemost, 2015;113(6):1289-98.
13. Tokuyasu K.T. (1980). Immunochemistry on ultrathin frozen sections. Histochem. J. 12: 381-403.
14. Dunn KL, Davie JR. Stimulation of the Ras-MAPK pathway leads to independent phosphorylation of histone H3 on serine 10 and 28. Oncogene, 2005;24:3492-3502.
15. Gabler C, Blank N, Hieronymus T, et al. Extranuclear detection of histones and nucleosomes in activated human lymphoblasts as an early event in apoptosis. Ann Rheum Dis, 2004;63:1135-1144.
16. Zhao B, Mei Y, Schipma MJ, et al. Nuclear condensation during mouse erythropoiesis requires caspase-3-mediated nuclear opening. Dev Cell, 2016;36(5):498-510.
17. Peterson JE, Zurakowski D, Italiano JE Jr, et al. Normal ranges of angiogenesis regulatory proteins in human platelets. Am J Hematol, 2010;85(7):487-493.
18. Silk E, Zhao H, Weng H, et al. The role of extracellular histone in organ injury. Cell Death and Disease, 2017;8(5):e2812.
19. Russell RT, Christiaans SC, Nice T, et al. Histone-complexed DNA fragment levels are associated with coagulopathy, endothelial cell damage, and increased mortality after severe pediatric trauma. Shock, 2017;doi.10.1097/SHK.0000000000000902.
20. Semeraro F, Ammollo CT, Morrissey JH, et al. Extracellular histones promote thrombin generation through platelet-dependent mechanisms: involvement of platelet TLR2 and TLR4. Blood, 2011;118(7):1952-1961.
21. Ekaney ML, Otto GP, Sossdorf M, et al. Impact of plasma histones in human sepsis and their contribution to cellular injury and inflammation. Crit Care, 2014;18(5):543.

22. Garcia-Gimenez JL, Roma-Mateo C, Carbonell N, et al. A new mass spectrometry-based method for the quantification of histones in plasma from septic shock patients. Scientific Reports; 2017;7:10643.
23. Kim JE, Lee N, Gu JY, et al. Circulating levels of DNA-histone complex and dsDNA are independent prognostic factors of disseminated intravascular coagulation. Thrombosis Research, 2015;135(6):1064-1069.
24. Kimball AS, Obi AT, Diaz JA, et al. The emerging role of NETs in venous thrombosis and immunothrombosis. Front Immunol, 2016;7:236.
25. Savva A, Roger T. Targeting toll-like receptors: promising therapeutic strategies for the management of sepsis-associated pathology and infectious diseases. Front Immunol, 2013;4:387.
26. Fenhammer J, Rundgren M, Hultenby K, et al. Renal effects of treatment with a TLR4 inhibitor in conscious septic sheep. Critical Care, 2014;18:488.
27. Ciarlo E, Savva A, Roger T. Epigenetics in sepsis: targeting histone deacetylases. Int J Antimicrob Agents, 2013;42Supp:S8-12.
28. Takebe M, Oishi H, Taguchi K, et al. Inhibition of histone deacetylases protects septic mice from lung and splenic apoptosis. J Surg Res, 2014;187(2):559-570.
29. Li Y, Zhao T, Liu B, et al. Inhibition of deacetylase 6 improves long-term survival in a lethal septic model. J Trauma Acute Care Surg, 2015;78(2):378-385.
30. Li Y, Liu Z, Liu B, et al. Citrullinated histone 3 – a novel target for treatment of sepsis. Surgery, 2014;156(2):229-234.
31. Gollomp K, Ian J, Fatoumata D, et al. The NET effect: platelet factor 4 and DNA-histone interactions in sepsis. Blood, 2015;126:2197.
32. Kile BT. The role of apoptosis in megakaryocytes and platelets. BJH, 2014;165(2):217-226.
33. Joseffson EC, James C, Henley KJ, et al. Megakaryocytes possess a functional intrinsic apoptosis pathway that must be restrained to survive and produce platelets. JEM, 2011;208(10):2017.
34. Josefsson EC, Burnett DL, Lebois M, et al. Platelet production proceeds independently of the intrinsic and extrinsic apoptosis pathways. Nature Comm, 2014;3455.
35. Li J, Kuter DJ. The end is just the beginning: megakaryocyte apoptosis and platelet release. Int J Hematol, 2001;74(4):365-374.
36. Kozuma Y, Yuki S, Ninomiya H, et al. Caspase activation is involved in early megakaryocyte differentiation but not in platelet production from megakaryocytes. Leukemia, 2009;23:1080-1086.
37. Clarke MCH, Savill J, Jones DB, et al. Compartmentalized megakaryocyte death generates functional platelets committed to caspase-independent cell death. JCB, 2003;160(4):577-587.
38. De Bottom S, Sabri S, Dougas E, et al. Platelet formation is the consequence of caspase activation within megakaryocytes. Blood, 2002;100(4):1310-1317.
39. Gabler C, Blank N, Winkler S, et al. Accumulation of histones in cell lysates precedes expression of apoptosis-related phagocytosis signals in human lymphoblasts. ANNALS, 2003;1010:221-224.
40. Semple JW, Italiano JE, Freedman J. Platelets and the immune continuum. Nature Reviews, 2011:264-274.
41. Stewart DIH, Golosinska K, Smillie LB. Identification of a troponin-I like protein in platelet preparations as histone H2B. FEBS, 1983;157(1):129-132.

42. Lewandowska K, Kaplan D, Husel W. CD34 expression on platelets. Platelets, 2003;14(2):83-87.
43. Hurley SM, Lutay N, Holmqvist B, et al. The dynamics of platelet activation during the progression of streptotoccal sepsis. PLOS One, 2016;11(9):e0163531.
44. Layios N, Delierneux C, Hego A, et al. Sepsis prediction in critically ill patients by platelet activation markers on ICU admission: a prospective pilot study. Intensive Care Med Exp, 2017;5(1):32.
45. Woth G, Varga A, Ghosh S, et al. Platelet aggregation in severe sepsis. J Thromb Thrombolysis, 2011;31(1):6-12.
46. Davies GR, Mills GM, Lawrence M, et al. The role of whole blood impedance aggregommetry and its utilization in the diagnosis and prognosis of patients with systemic inflammatory response syndrome and sepsis in acute critical illness. PLoS One, 2014;9(9):e108589.
47. Grozovsky R, Hoffmeister KM, Falet H. Novel clearance mechanisms of platelets. Curr Opin Hematol, 2010;17(6):585-589.
48. Ma R, Xie R, Yu C, et al. Phosphatidylserine-mediated platelet clearance by endothelium decreases platelet aggregates and procoagulant activity in sepsis. Sci Rep, 2017;7:4978.
49. Rondina MT, Carlisle M, Fraughton T, et al. Platelet-monocyte aggregate formation and mortality risk in older patients with severe sepsis and septic shock. J Gerontology, 2015;70(2):225-231.
50. Tejera P, Zhang R, Su L, et al. Immature platelet fraction and in vivo markers of platelet function in sepsis. Am Journ Resp and Crit Care Med, 2017;195:A7451.

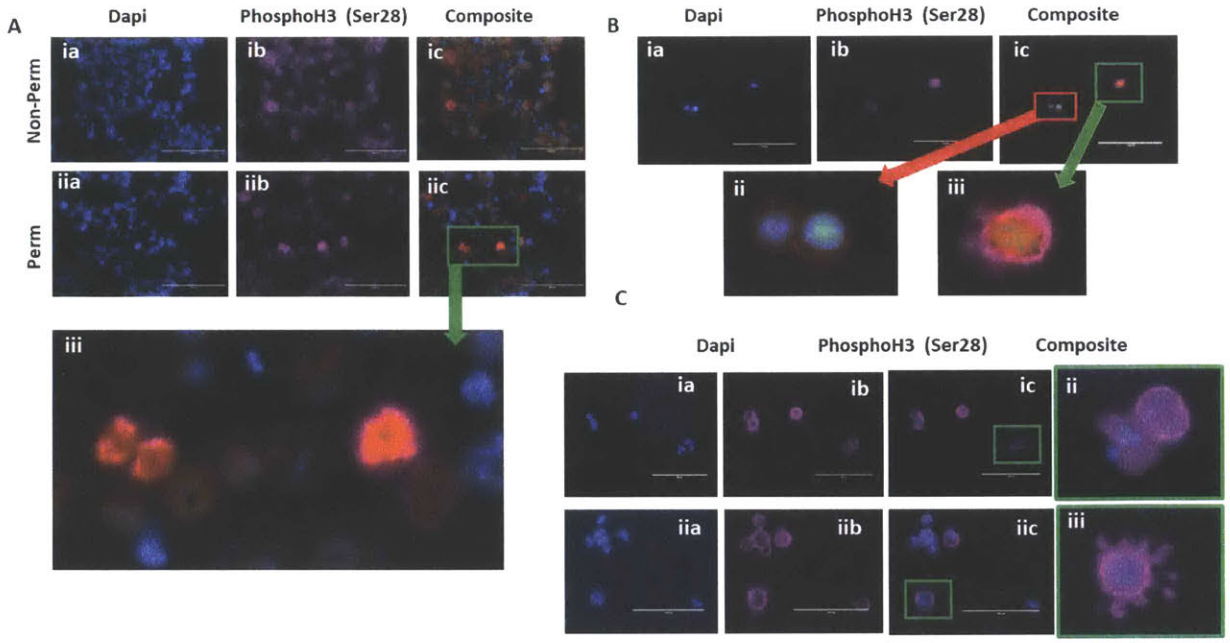

Figure 3-1: Megakaryocytes have extranuclear histones.

Immunofluorescent images of megakaryocytes demonstrating extranuclear localization of PhosphoH3 (Ser28) histones. (A) Meg-01 cells are observed to have histone staining throughout the cell, including the cell membrane and cytoplasm. Permeabilized Meg-01 cells (iia-c) demonstrate strong nuclear staining, specifically in cells with mitotic figures, such as those shown in the bottom left panel (iii). (B) CB MKs at day 10 of differentiation were fixed, permeabilized prior to staining and imaging. Cells on the bottom left panel (ii) appear to be quiescent and round, while the cell on the bottom right panel (iii) has much stronger histone staining and what appears to be pseudopods or proplatelet buds that stain positive for histones. (C) CB MKs (i) and Meg-01 cells (ii) were co-incubated for 1 hour with 3 µg/mL and 30 pg/mL *E. coli* LPS, respectively. The cells were then fixed, permeabilized, stained and imaged. The top right panel (ii) is representative of cells that were observed to have a break in the cell membrane and release extracellular DNA and histones, likely forming extracellular traps. The bottom right panel appears to be a cell extending histone-positive proplatelet buds (iii).

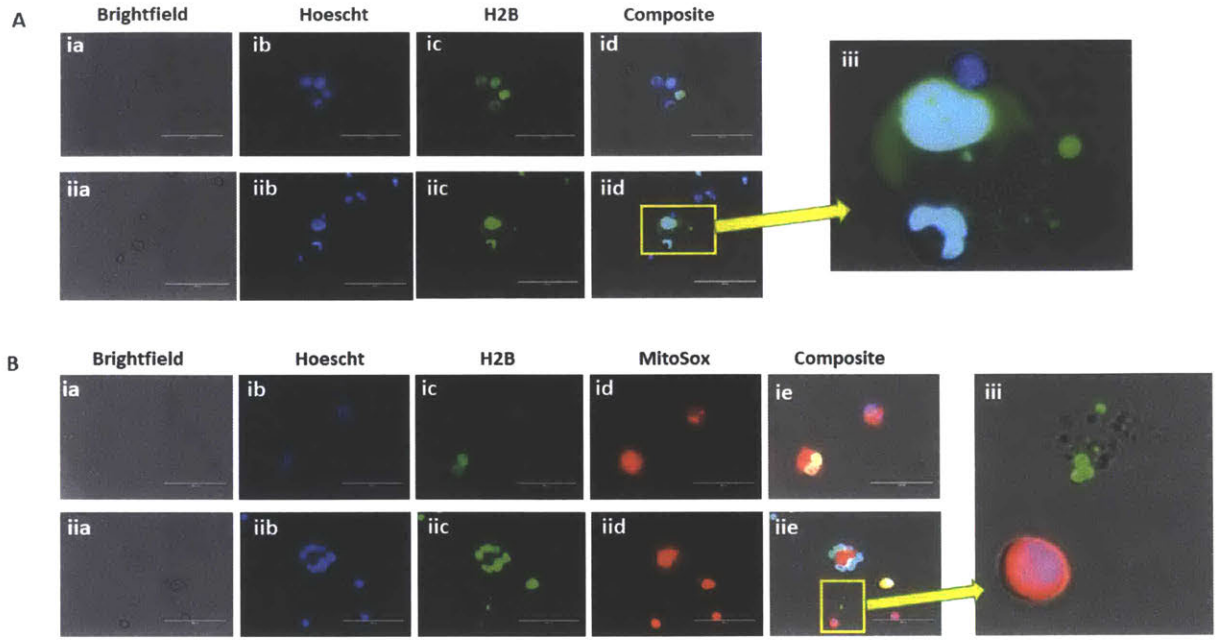

Figure 3-2: GFP-H2B expressing Meg-01 cells have extranuclear histones.

Meg-01 cells were transfected with GFP-Histone 2B (H2B) BacMam to explore the cellular localization of H2B in megakaryocytes. (A) H2B was mostly observed to be restricted to the nucleus within Meg-01 cells (i); although, occasionally cells were noted to have some extranuclear histones, such as the cells in the panel on the right (ii). (B) Cells were co-incubated with MitoSox red in order to show the cytoplasmic location of metabolically active mitochondria. While H2B was normally within the nucleus and within the boundaries of the cell membrane, isolated platelet-like particles with H2B expression were noted as well (ii).

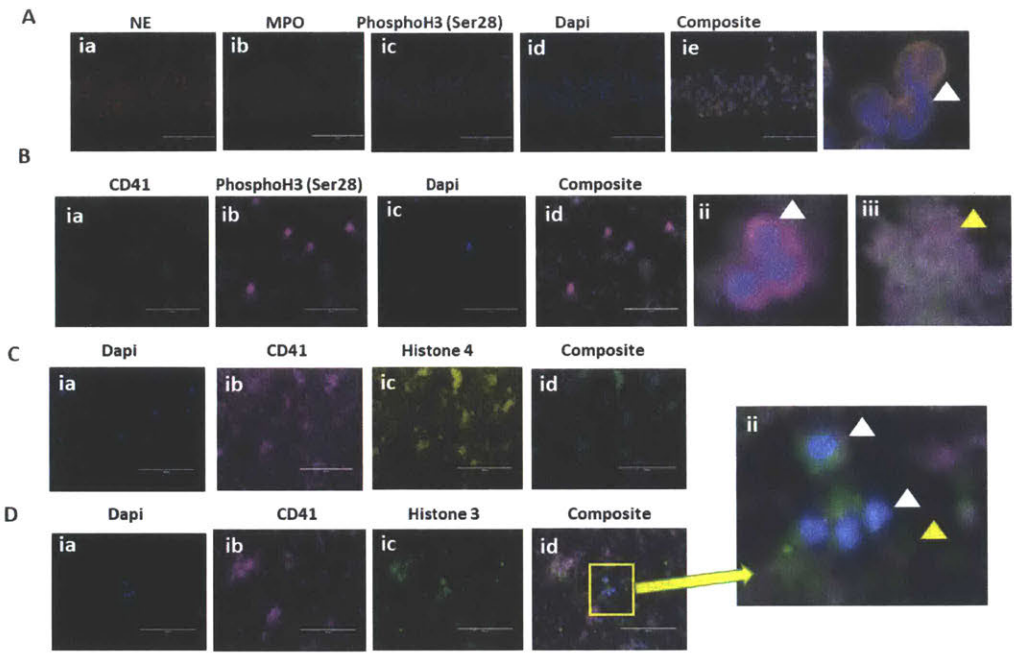

Figure 3-3: Immunofluorescent images of platelet-associated histones.

Immunofluorescent images of white blood cells and platelets confirm the presence of platelet-associated histones. (A) Isolated human neutrophils were used as a positive control to demonstrate the specificity of the PhosphoH3 (Ser28) antibody to the nucleus of the cell. A close-up of this image is seen on the right (ii). (B) Platelet-rich plasma was fixed, permeabilized, and probed for the presence of Ser28 and showed positive staining both within white blood cells (ii) and platelets (iii). Notably, it appeared that the CD41 platelet staining was towards the center of the platelets, while the Ser28 staining was concentrated around the periphery. (C) Platelet pellets were further probed with anti-Histone 3 (i) and anti-Histone 4 (ii) antibodies, which both stained positive for white blood cells and platelets, as seen in the close up of the anti-Histone 4 composite image on the lower right panel (iii). White blood cell, white arrowhead; Platelets, yellow arrowhead.

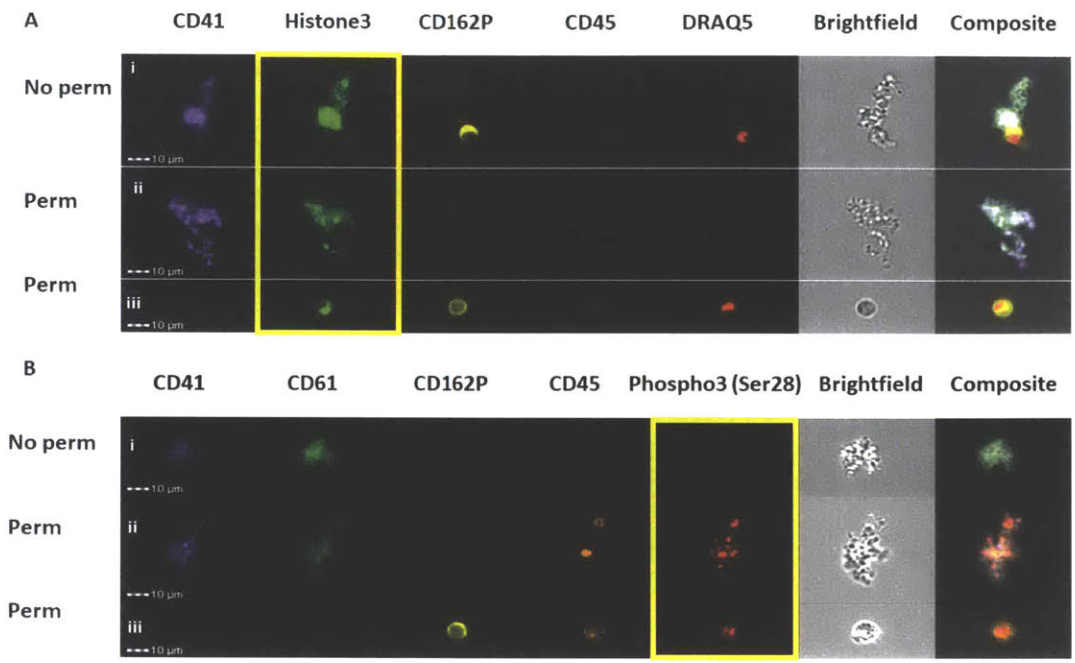

Figure 3-4: Imaging flow cytometry shows platelet-associated histones.

Flow cytometry was used to probe for histones in platelets. (A) Histone 3 appeared to be present around the platelet membrane in the non-permeabilized cells (i) and throughout the cell in the permeabilized cells (ii). A white blood cell used as an internal control has histone 3 nuclear staining (iii). (B) Phospho3 (Ser28) did not stain the non-permeabilized cells (i), but did stain the permeabilized cells (ii). A white blood cell did stain positive for nuclear Phospho3 (Ser28) (iii). Yellow box is around the histone-stain channel.

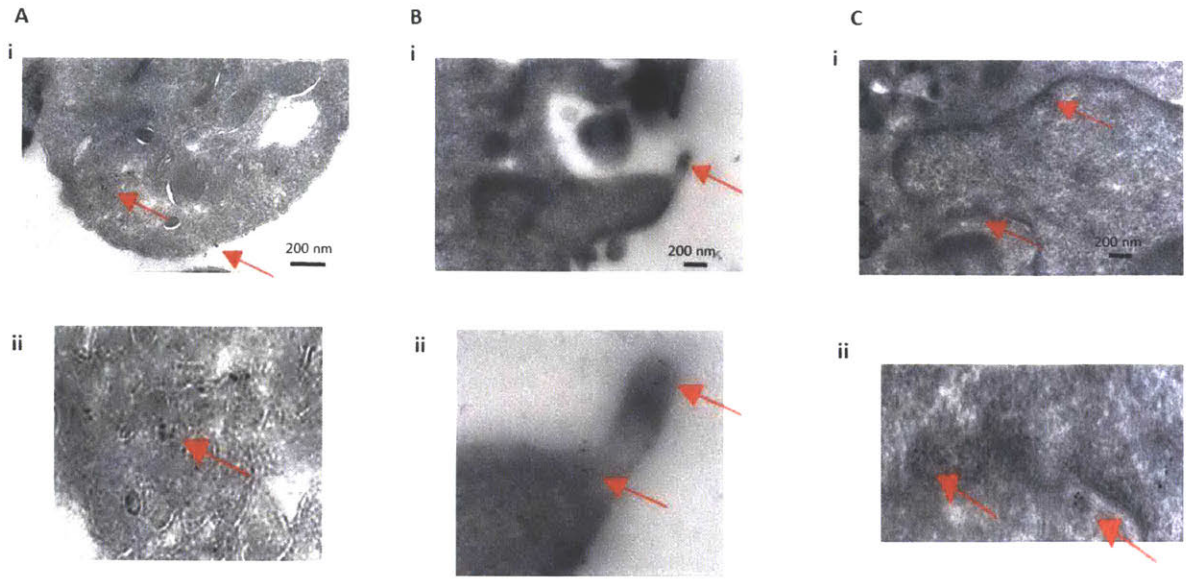

Figure 3-5: Transmission electron microscopy and immuno-gold labeling of platelet histones.

Cells were immuno-gold labeled with anti-histone 4 antibodies and then imaged with transmission electron microscopy. (A-B) Platelets are shown to label positive for histone 4 in their cytoplasm as well as on their cell membrane. Magnified images are shown in the bottom panels (Aii and Bii). (C) HT-29 cells were also immuno-labeled and imaged as a positive control and showed nuclear labeling of histone 4. Magnification of the nuclear envelope with labeling is shown on the bottom panel (Cii). Red arrows point towards immuno-gold particles (6nm).

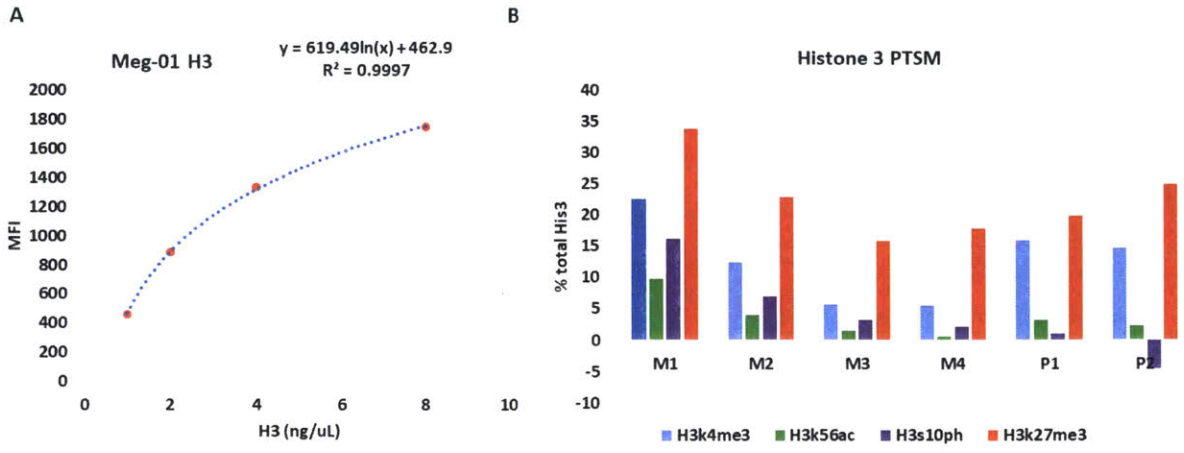

Figure 3-6: Histone quantification using bead-based ELISA assays.

Histones extracted and purified from Meg-01 cells and platelet pellets were quantified. (A) Meg-01 cell histone-extract serial dilutions were run on the ELISA assay. His3 concentration based on absorbance measurements were used to extrapolate the histone concentration input (ng/uL) in each dilution. These concentrations were then plotted against the mean fluorescence intensity (MFI) reading from the ELISA assay. The points were then fit with a logarithmic best-fit line, which has an R^2 value of >0.99. (B) The Meg-01 and platelet histone extracts were also assessed for various H3 PTSMs. These are expressed in terms of % of total H3 based on MFI readings. M1, Meg-01 at a 1:250 dilution; M2, Meg-01 at a 1:500 dilution; M3, Meg-01 at a 1:1000 dilution; M4, Meg-01 at a 1:2000 dilution; P1, Platelet at a 1:25 dilution; P2, Platelet at a 1:50 dilution.

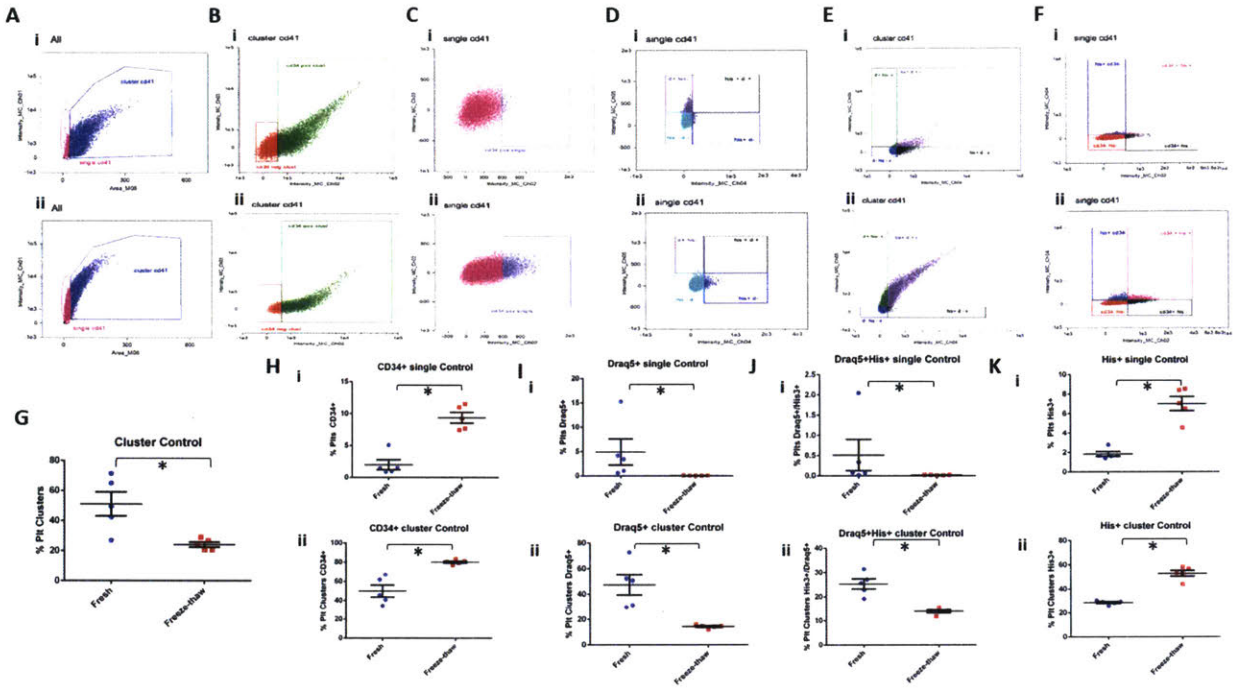

Figure 3-7: Flow cytometry comparison of fresh versus freeze-thawed platelets.

Flow cytometry was performed on both fresh and freeze-thawed platelets, in order to control for the effects of storage conditions on the patient platelet analysis. (A-F) Representative scatter plots of flow cytometry results comparing fresh platelets (i) and freeze-thawed platelets (ii). (G-K) Scatter plots with mean and standard error bars comparing fresh compared to freeze-thawed platelets for both single platelets (i) and clustered platelets (ii). Student unpaired t-test was performed, with significance defined as $p \leq 0.05$ according to a paired student t-test for all samples. d, Draq5; h, His3.

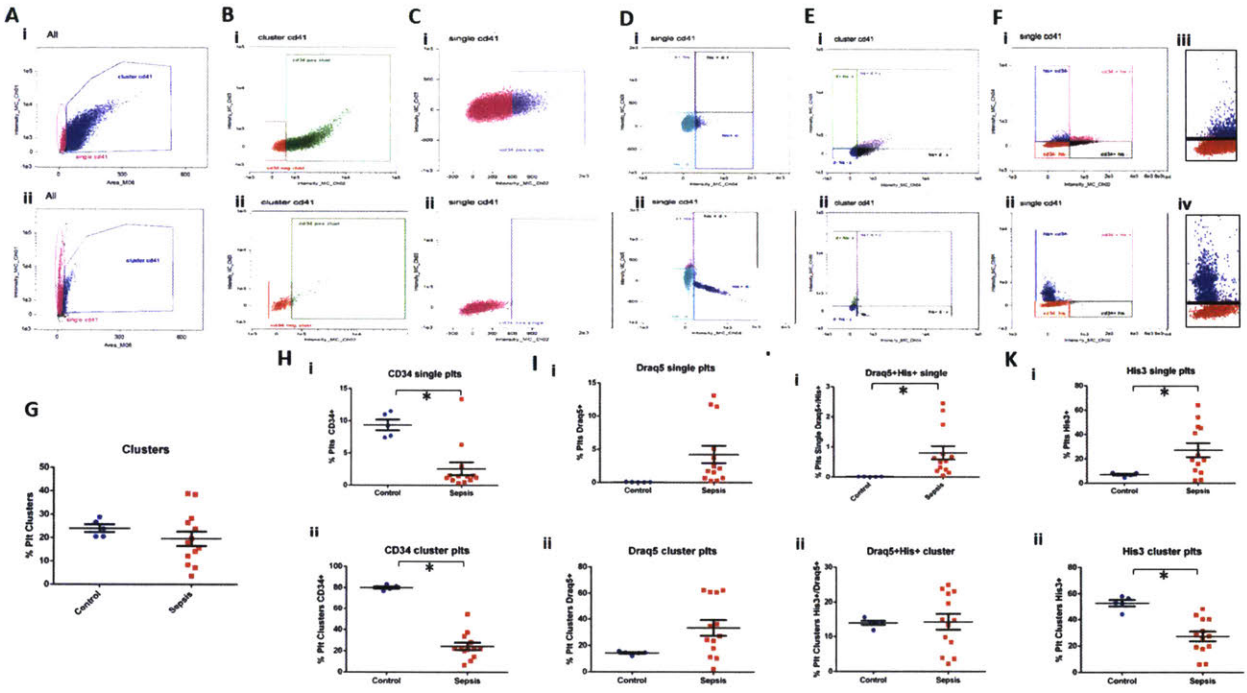

Figure 3-8: Flow cytometry analysis of platelets from patients diagnosed with sepsis.

Flow cytometry was performed in order to explore the platelet phenotype of (A-F) Representative scatter plots of flow cytometry results comparing control patients (i) and sepsis patients (ii). A magnified example of single platelet-associated His3 signal is represented for both the control patient (Eiii) and the sepsis patient (Eiv) (G-K) Scatter plots with mean and standard error bars comparing fresh compared to freeze-thawed platelets for both single platelets (i) and clustered platelets (ii). Student unpaired t-test was performed, with significance defined as $p \leq 0.05$ according to a paired student t-test for all samples. d, Draq5; h, His3.

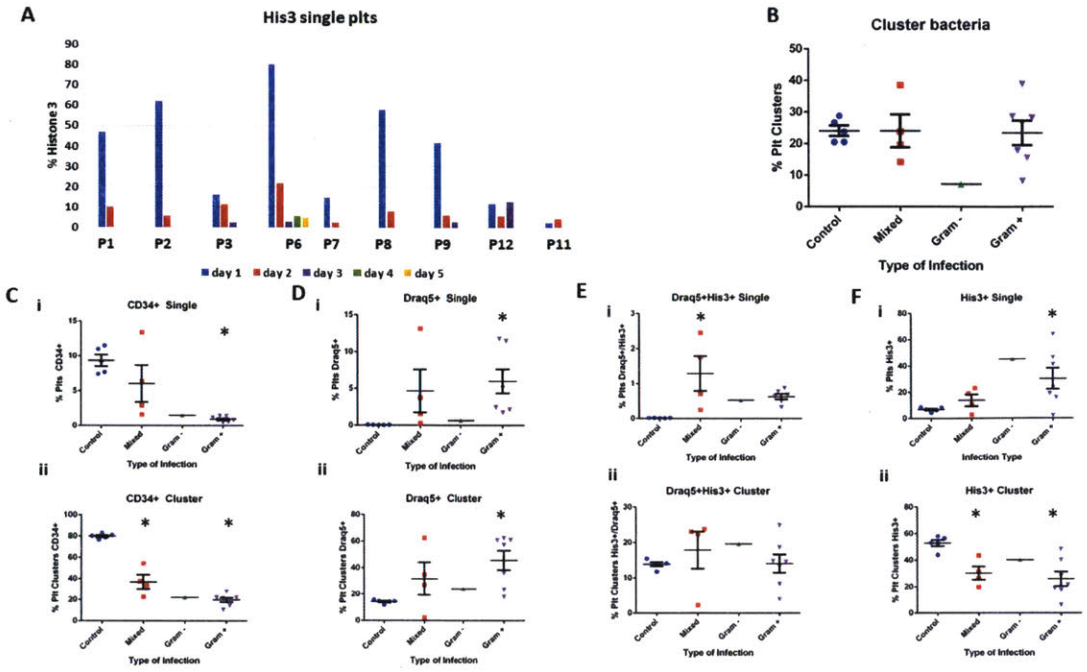

Figure 3- 9: Platelet phenotype is associated with type of infection.

Flow cytometry was performed to evaluate platelet phenotype from patients diagnosed with sepsis. (A) Platelet were evaluated on multiple days of hospitalization. $His3^{+}$ platelets appeared to be highest in patients with acute sepsis and on day 1 of evaluation and decreased as the patient was treated (P1,2,3,6,7,8,9). Patients with chronic sepsis that had been in the hospital for a prolonged period did not have the same changes in $His3^{+}$ platelets and these patients did not recover. (B-F) Platelet phenotype was also compared for patients with different types of infection: Gram positive, Gram negative, or Mixed. Single platelets (i) and clustered platelets (ii) were evaluated. One-way ANOVA testing was performed comparing the type of infection to the control group, with significance being defined as $p < 0.05$ (*). Statistics were not performed on the Gram – group as there was only one patient in this group.

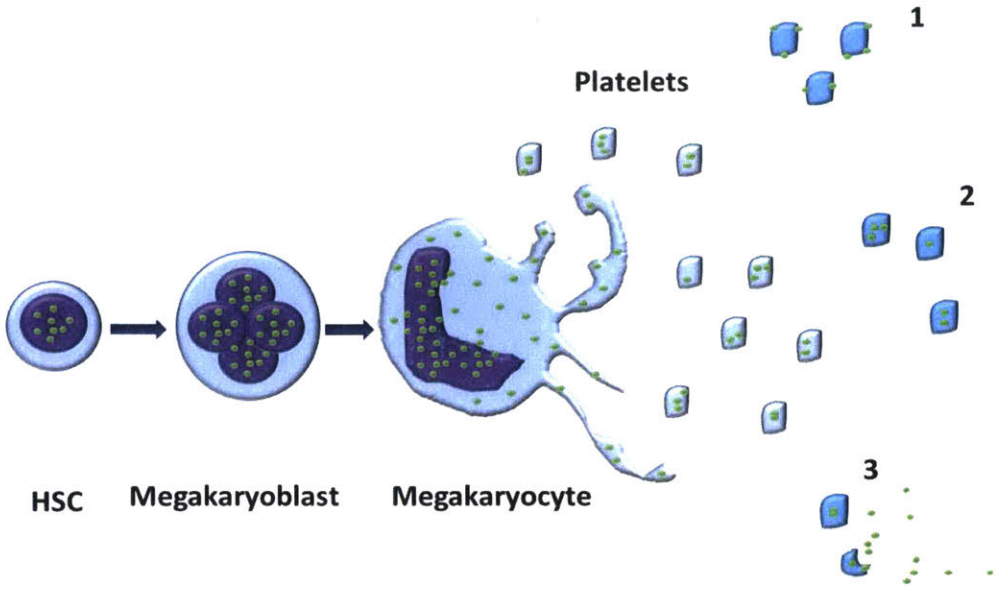

Figure 3-10: Megakaryocytes contain extranuclear histones, which are passed on to platelets.

The proposed mechanism for the development of platelet-associated histones. A mononuclear hematopoietic stem cell (HSC) differentiates into a megakaryoblast and undergoes endomitoses to form multiple nuclei. The nuclei (purple) contain various intranuclear histones (green circles). Once differentiation is complete and a mature megakaryocyte is made, the cell begins undergoing a controlled apoptosis, where the nuclear membrane develops pores and histones begin to leak into the cytoplasmic compartment. Upon the formation of proplatelet buds, the cytoplasmic and cell membrane-associated histones are also packed into the resultant platelets. The histones can be present in histones either primarily bound to the cell membrane (1), primarily within the cytoplasm (2), or a combination of the 1 and 2, where platelet activation results in the increased expression of histones on the cell membrane and possible release into the environment accompanied by degranulation.

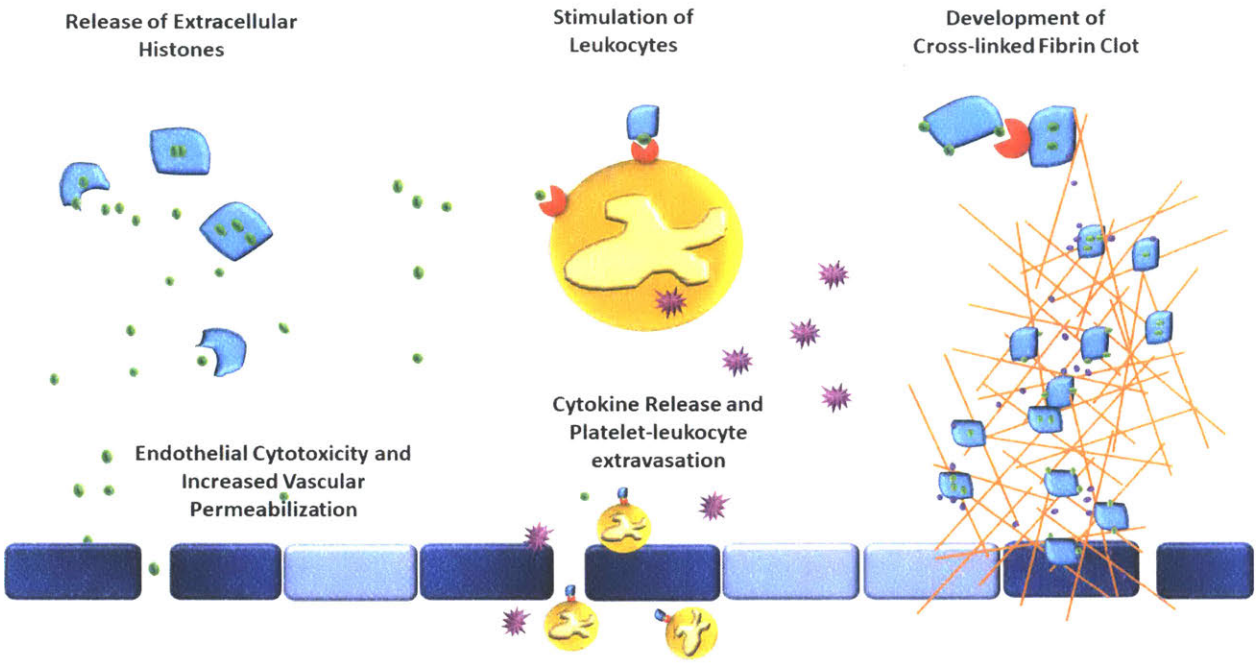

Figure 3-11: Potential sequela of platelet-associated histones

Platelet-associated histones can affect the inflammation and coagulation system via various mechanisms. Platelets (light blue polygons) can either release extracellular histones (green circles) upon stimulation or express them on their cell membranes. The release of extracellular histones (top left) can result in direct cytotoxicity of endothelial and epithelial cells (dark blue rectangles), resulting in both, increased vascular permeability, and a prothrombotic surface. The binding of both platelet-associated histones and extracellular histones to leukocytes (orange circle) (top middle) can result in the development of platelet-leukocyte aggregates (PLAs), as well as stimulate the cell to increase production and release proinflammatory cytokines (purple stars). These PLAs can then either diapedese across the endothelium or escape through the increase endothelial permeability into extravascular tissue (bottom middle) and further propagate inflammation. Thrombosis can be initiated and propagated through various mechanisms (right), where platelet-associated histones can bind to each other through TLR receptors (top right) which results in subsequent activation and an increase in thrombin generation and release (purple circles). Extracellular histones are also themselves, prothrombotic and anti-fibrinolytic, promoting thrombosis.

Tables:

Table 3-1: Histone protein measurement.

Histone	MW (kDa)	E/1000
Histone 2A	13.960	4.05
Histone 2B	13.774	6.07
Histone 3	15.273	4.04
Histone 4	11.236	5.40

Table 3-2: Histone post-translational modifications

Histone Modification	Residue	Modification	Functions
H3k4me3	Lys4	Tri-methylation	Euchromatin, transcriptional activation
H3k56ac	Lys56	Acetylation	DNA damage repair, chromatin assembly
H3s10ph	Ser10	Phosphorlyation	Mitosis, immediate early gene activation
H3k27me3	Lys27	Tri-methylation	Transcriptional silencing
H3s28ph	Ser28	Phosphorylation	Mitosis
Cit H3	N/A	Citrullination	Catalyzed by PAD4
H2A.X	N/A	N/A	DNA damage repair, response to double strand DNA breaks

Table 3-3: Patient descriptive statistics

Patient ID	Signalment (sex/age)	Infectious Agent	Source of Infection	Bacterial Classification
1	F/82	- *Klebsiella pneumoniae* - Influenza	- Urine	Mixed
2	M/36	- *Pseudomonas aeruginosa*	- Urine	Gram negative
3	M/67	- *Enterococcus faecalis* - *Staphylococcus aureus* - *Streptococcus pneumoniae* - Yeast	- Lungs - Lungs - Lungs - Lungs	Mixed
4	M/73	- *Pseudomonas aeruginosa* - *Enterococcus faecium* - Yeast	- Lungs and Urine - Lungs - Lungs	Mixed
5	M/85	- *Enterococcus faecium* - Coagulase-negative *Staphylococcus* - *Candida albicans* - Yeast	- Wound - Lungs - Wound - Lungs	Mixed
6	M/49	- β-*hemolytic Streptococcus A* - *Staphylococcus aureus* - *Enterococcus faecium* - *Aspergillus fumigatus* - Yeast	- Lungs - Lungs - Lungs - Lungs	Mixed
7	M/61	- *Streptococcus pneumoniae* - Multi-drug resistant *Staphylococcus aureus* - Influenza	- Lungs - Lungs	Mixed
8	M/71	- *Enterococcus faecalis* - *Enterobacter aerogenes* - *Corynebacterium*	- Blood - Lungs - Lungs	Mixed
9	M/62	- Multi-drug resistant *Staphylococcus aureus* - *Enterobacter aerogenes*	- Blood - Blood	Mixed
10	M/61	- *Staphylococcus aureus*	- Lungs	Gram positive
11	M/77	- *Streptococcus intermedius*	- Pleural fluid	Gram negative
12	M/59	- *Klebsiella pneumoniae* - *Proteus mirabilis* - *Enterococcus*	- Blood and Lungs - Blood - Blood	Mixed
13	F/76	- Metapneumovirus - No positive bacterial cultures	- N/A	Mixed
14	F/73	- *Escherichia coli* - *Staphylococcus epidermidis*	- Blood and Urine - Blood	Mixed
15	F/67	- *Escherichia coli* - *Staphylococcus epidermidis*	- Blood and Urine - Blood	Mixed
16	M/81	- *Enterococcus faecalis*	- Blood	Gram positive

Table 3-4: Histone protein quantification

Sample	Total Protein (OD)[1]	Total Protein[1] (mg/mL)	H2A[2] (mg/mL)	H2B[3] (mg/mL)	H3[4] (mg/mL)	H4[5] (mg/mL)
Calf thymus	0.57[7]	10.35[6]	2.81	1.8	3.3	1.84
Meg-01 cells	2.97[7]	7.07	1.76	1.4	2	1.12
Platelet 1	0.074	0.18	0.27	0.62	0.44	0.18
Platelet 2	0.064	0.15	0.36	0.18	0.34	0.29

1. 230 nm
2. 280 nm; MW (kDa), 13.960; E/1000, 4.05
3. 280 nm; MW (kDa), 13.774; E/1000, 6.07
4. 280 nm; MW (kDa), 15.273; E/1000, 4.04
5. 280 nm; MW (kDa), 11.236; E/1000, 5.40
6. Expected concentration is 10 mg/mL total histones
7. Sample diluted 1:10

Table 3-5: Histone post-translational modification quantification

Sample	Total H3[1]	H3k4me3[1]	H3k56ac[1]	H3s10ph[1]	H3k27me3[1]
Positive Control[2] (1:25)	3278.5	3360	2006	2170	2196
Blank	18	9	13	14	10
Meg-01 (1:250)	1760	401	185	296.5	598
Meg-01 (1:500)	1354	175.5	66	108	315
Meg-01 (1:1000)	909	60.5	27	43	151.5
Meg-01 (1:2000)	477	35	16	24	92
Platelet (1:25)	108	23.5	16	15	28
Platelet (1:50)	62	15.5	14	12	21

1. All measurements are provided as MFI (mean fluorescent intensity), with the exception of the LOD row.
2. Positive control of HeLa cell extract, estimated to be 0.5 mg/mL total protein; information provided by Active Motif.

Table 3-6: Histone post-translational modification percentages

Sample	Total H3[1]	H3k4me3[2]	H3k56ac[2]	H3s10ph[2]	H3k27me3[2]
Meg-01 (1:250)	200.0 / 1970.9	22.5	9.9	16.2	33.8
Meg-01 (1:500)	100.0 / 2046.7	12.5	4.0	7.0	22.8
Meg-01 (1:1000)	50.0 / 1995.8	5.8	1.6	3.3	15.9
Meg-01 (1:2000)	25.0 / 1987.4	5.7	0.7	2.2	17.9
Platelet (1:25)	13.75 / 0.46[3]	16.1	3.3	1.1	20.0
Platelet (1:50)	12.75 / 0.42[3]	14.8	2.3	-4.5	25.0
LOD[4]	2	30	7.8	8	3

1. Total input per well in ng / Concentration in units of ng/uL of stock protein
2. % of total H3 based on MFI
3. LOD, Limit of detection. Based on purified histones input. Total ng input.

Chapter 4

Development of Microfluidic Device for the *In Vitro* Exploration of the Platelet-Neutrophil Interaction at a Single-Cell Level

As published in:

Frydman GH, Anna Le, Ellet F, Jorgensen J, Fox JG, Tompkins RG, Irimia D. **Technical Advance: Changes in neutrophil migration patterns upon contact with platelets in a microfluidic device.** J Leukoc Biol, 2017; 101(3):797-806.

4.1 Abstract

Neutrophils are traditionally regarded as the "first responders" of the immune system. However, recent observations revealed that platelets often respond earlier to recruit and activate neutrophils within sites of injury and inflammation. Currently, platelet–neutrophil interactions are studied by intravital microscopy. Although such studies provide exceptional, physiologic in vivo data, they are also laborious and have low throughput. To accelerate platelet–neutrophil interaction studies, we have developed and optimized an ex vivo microfluidic platform with which the interactions between platelets and moving neutrophils are measured at single-cell level in precise conditions and with high throughput. With the use of this new assay, we have evaluated changes in neutrophil motility upon direct contact with platelets. Motility changes include longer distances traveled, frequent changes in direction, and faster neutrophil velocities compared with a standard motility response to chemoattractant fMLP. We also found that the neutrophil– platelet direct interactions are transient and mediated by CD62P–CD162 interactions, localized predominantly at the uropod of moving neutrophils. This "crawling," oscillatory neutrophil behavior upon platelet contact is consistent with previous in vivo studies and validates the use of this new test for the exploration of this interactive relationship.

4.2 Introduction

Activation of the acute innate immune response is complex, consisting of both cellular and soluble components. In tissue injury and infection, neutrophils were long thought to be the first and most robust responders, being recruited by both the pathogenic stimulus and the tissue resident cells. (Kim ND, 2015; Kumar V, 2010) Platelets are increasingly recognized as key players in the innate immune responses, being activated by tissue injury and several infections before neutrophils and subsequently, recruiting and activating them. (Engelman B, 2013; Semple JW, 2010; Sreeramkumar V, 2014) Platelets can be activated in hundreds of milliseconds, faster than neutrophils activate. (Frojmovic MM, 1999) Platelet adhesion to pathogens or injured vessel walls results in platelet activation and has been described to facilitate binding to neutrophils, the release of neutrophil chemotactic substances, and the formation of neutrophil extracellular traps. (Engelman B, 2013; Ghasemzadeh M, 2013; Hurley SM, 2015; Kim KH, 2013)

In this study, we optimized and validated a microfluidic platform that enabled us to examine platelet–neutrophil interactions *ex vivo* with single-cell resolution. We found that upon contact with PRPt, neutrophils migrate spontaneously in the absence of chemoattractant gradients. Neutrophils appear to associate and dissociate frequently from platelets during migration, and the interactions are mediated by CD62P. In straight channels, neutrophils move in an oscillatory pattern between platelets, similar to the crawling behavior described *in vivo*. (Sreerkumar V, 2014)

4.3 Materials and Methods

4.3.1 Platelet preparation

Blood was collected from healthy volunteers in accordance with Institutional Review Board protocols (2009-P-000295). Platelets were prepared from blood collected into 2.9 ml trisodium citrate Vacutainer tubes (Sarstedt, N¨umbrecht, Germany). PRPt was prepared by centrifugation of the whole blood at 210 g, 22°C, for 20 min. The PRPt supernatant was gently pipetted into 2 tubes. In 1 tube, 20% vol ACD solution (Boston Bioproducts, Ashland, MA, USA) was added, and

the PRPt was incubated at 37°C until the start of the experiment. The second tube was centrifuged at 1900 g, 22°C, for 10 min. The PPP was removed, leaving a platelet pellet. IMDM buffer with 20% FBS was used to resuspend the platelet pellet, and ACD was added to the PPP and the platelet suspension. Platelet cell membrane was stained with 1:1000 calcein green (Thermo Fisher Scientific, Waltham, MA, USA). Total platelet count was performed on all samples, with acceptable purity defined as ,2% WBC or RBC contaminant. PPP acellularity (,2%) was also verified using a hemocytometer. The PRP platelet count ranged from 25 to 45 3 109 platelets/ml, whereas the WP count ranged from 15 to 25 3 109 platelets/ml; decreased platelet count in WP was most likely a result of platelet loss during the washing step. All plasma preparations were kept at 37°C until the start of the experiment.

4.3.2 Neutrophil isolation

Blood was collected in ACD BD Vacutainer tubes (Becton Dickinson, Franklin Lakes, NJ, USA). Neutrophils were isolated from whole blood using a negative-selection protocol, as previously described [10]. In brief, neutrophils were isolated using a density gradient with HetaSep (Stemcell Technologies, Vancouver, BC, Canada) and then purified with EasySep Human Neutrophil Kit (Stemcell Technologies), following the manufacturer's protocol. Neutrophil purity was assessed to be .98%, and cell count was performed using a hemocytometer. Neutrophils were subsequently resuspended in IMDM with 20% FBS (Thermo Fisher Scientific) for a total neutrophil concentration of 5–6 3 106 cells/ml. The cellular nucleic acid was stained with 1:2000 Hoechst Dye 33342 (Thermo Fisher Scientific) for 20 min, followed by 1 wash step. For experiments that evaluated the effect of blocking CD162, neutrophils were also stained with 1:200 mouse antihuman CD162 (clone KPL1; BioLegend, San Diego, CA, USA) for 20 min, followed by 1 wash step. Samples were processed within 1 h of blood draw and were maintained at 37°C.

4.3.3 Design and fabrication of the microfluidic devices

The microfluidic devices were manufactured using standard microfabrication techniques. In brief, a 2-layer photoresist design (SU-8; MicroChem, Newton, MA, USA), with a first and second layer (3 and 50 mm thick, respectively), was patterned on 1 silicon wafer via sequentially aligned photolithography masks and processing cycles, according to the manufacturer's protocols. The resulting patterned wafer was then used as a mold to produce PDMS (Thermo Fisher Scientific)

devices, which were subsequently, irreversibly bonded to glass slides (1 3 3 in.; Thermo Fisher Scientific). Gradients were generated between an array of orthogonal side channels (6 mm width, 800 mm height), primed with the chemoattractant and serving as the source (of chemoattractant), and a central channel (500 mm width, 50 mm height), serving as the sink (Figure 4-1 A).

4.3.4 Priming and loading the microfluidic devices

The microfluidic devices were loaded with various solutions uniformly or used to generate chemical gradients, as previously described. (Jones CN, 2014; Butler KL, 2010) To generate gradients, a 2-step process was involved. The microfluidic devices were primed with various solutions: media (negative control), fMLP (100 nM, positive control), PRPt, PPP, or WP. Because the side channels are closed at the distal end, when the main channel is washed with media, a linear gradient is formed along the length of the side channel (Figure 4-1 B). To load a device, a 1 ml syringe filled with solution was connected to 1 port of the device and the solution pushed through the main channel, and then the outlet port was clamped off. With the application of steady pressure to the syringe, the solution was infused into the device, displacing the air into the PDMS. Once the solution was infused, the neutrophils were loaded into the main channel of the device and allowed to settle by clamping off both ports of the device.

4.3.5 Neutrophil motility analysis

Neutrophil migration was recorded, starting within 15 min of neutrophil loading, using time-lapse imaging on a fully automated Nikon Ti-E microscope with the biochamber at 37°C and 80% humidity and in the presence of 5% carbon dioxide gas. Images of the neutrophils were acquired automatically, every 2.5–3.5 min for up to 2 h, from at least 5 distinct locations on each of 4 microfluidic devices run in parallel in the same experiment. ImageJ manual tracking software (U.S. National Institutes of Health, Bethesda, MD, USA) was used for the analysis of neutrophil migration and behavior. Previous reports showed that when neutrophils are mechanically confined to the smaller side channels during migration, the cell trajectories and velocities can be measured more easily and with higher precision than any of the current assays. (Jones CN, 2014)

4.3.6 Platelet–neutrophil interactions

Platelet–neutrophil interactions were analyzed using multiple parameters. For each side channel in which there was neutrophil migration, the total number of platelets within the channel was counted; this included platelets that were attached to neutrophils as they entered from the main channel. Neutrophils traveling in channels containing no platelets were not included in statistical analyses for platelet interactions. Neutrophil–platelet interactions were categorized as "arrested" or "carrying." Arrested contact involved a migrating neutrophil stopping at the position of the platelet, in contact with the platelet, for one time-frame (i.e., at least 2.5 min; Figure 4-2A). Platelet carrying occurred when neutrophils and platelets moved together through the channel for at least one time-frame (Figure 4-2 B). The platelet–neutrophil interaction was further categorized by the number of times that a neutrophil carried a platelet, the total distance it carried the platelet, and the duration of time a platelet was carried. The mean and SD of each of these conditions were calculated for all groups that had contact with platelets, and Student's 2-tailed t-tests were carried out to compare the behavior of the PRPc with the PRPn.

4.3.7 Flow cytometry

Phlebotomy was performed with a 24-gauge butterfly needle, and blood was collected into an 8.5 ml ACD BD Vacutainer tube (Becton Dickinson). Isolated neutrophils were stained with 1:200 mouse anti-human CD162 antibodies (clone KPL1; BioLegend) and incubated with PRP. For the negative control, neutrophils were neither stained with anti-CD162 nor incubated with PRP. For the positive control, neutrophils were not stained with anti-CD162 and were incubated with PRP. All samples were stained with 1:200 mouse anti-human CD66b (clone G10F5; BD Biosciences, San Jose, CA, USA) and 1:200 mouse anti-human CD41 (clone HIP8; BioLegend) markers. Data were obtained through the Amnis ImageStreamX Mark II imaging flow cytometer and INSPIRE software (EMD Millipore, Billerica, MA, USA). The accompanying IDEAS software (EMD Millipore) was used to perform data analysis.

4.3.8 Statistical analysis

For determination of the neutrophil phenotype upon interaction with platelets, all cells in each condition (fMLP, PRPt, PPP, and WP) were manually tracked, and the total distance traveled, time spent in a side channel, and average velocity were calculated for each individual neutrophil.

Histograms were prepared for all conditions and the skewness, intermediate quartile range, and 95% CI were reported. The number of directional changes a neutrophil made within a channel described neutrophil oscillatory behavior. A change in directionality was defined as when a neutrophil traveled for a minimum of 50 mm in one direction after a turn. Changes in direction were calculated for each neutrophil in all conditions. Arrested contact with a platelet was defined as a neutrophil stopping and interacting with a platelet for one time frame (2–3.5 min) and traveling a distance of ,50 mm in any direction. The mean and SD for each condition was calculated and compared across conditions (fMLP, PRPt, PRPc, PRPn, PPP, and WP) using Student's 2tailed t tests, with $P < 0.05$ considered significant. The experiment was performed for a total of 5 biologic replicates for interdonor comparison. Four intradonor samples were compared and were not found to be significantly different. The same analysis was performed on the samples that were blocked with anti-CD162 antibody, and this was performed on 3 biologic replicates. Statistical analysis was performed using Excel (Microsoft, Redmond, WA, USA).

The flow cytometry experiments to determine the effectiveness of the antiCD162 antibody were conducted on 3 biologic replicates. Each neutrophil that had a platelet attached was defined as a PLA. The percentage of PLAs in each was calculated, and the number of neutrophils that were determined to be PLAs was compared between experimental conditions. The percent of "PLA inhibition" was determined by calculating the difference in the percent of PLAs formed with and without anti-CD162 antibody. Statistical analysis was performed using Excel (Microsoft)

4.4 Results

4.4.1 Spontaneous migration of neutrophils in the absence of chemoattractant

Spontaneous neutrophil migration into the side channels occurred in the absence of a chemoattractant. Surprisingly, neutrophils migrated into the side channels for both the PRPt and PPP (231 and 182 total neutrophils, respectively), equivalent to the migration of neutrophils when exposed to fMLP (201 total neutrophils). Neutrophil migration in the WP was rare (18 total neutrophils). Interestingly, the average velocity of the migrating neutrophils in the PRPt and PPP was, 28.4 ± 5.8 μm/min and 29.5 ± 5.8 μm/min respectively, as compared to the fMLP, $19.5 \pm$

9.1 μm/min (Table 4-1). Evaluating the representative histogram curves of average velocity for all conditions, the neutrophils in fMLP were clustered on the left, while the neutrophils in PRPt and PPP were clustered towards the right (Figure 4-3 and Table 4-2). This implies that PRPt and PPP stimulation of neutrophils results in neutrophils moving at higher velocities than those stimulated by fMLP. This phenomenon is not seen with platelets without the plasma component (WP). This is notable, as fMLP is one of the most potent neutrophil chemoattractants currently known (12).

This data suggests that there are factors within the plasma that result in spontaneous neutrophil migration. These soluble factors may include: exosomes; microparticles; members of the coagulation and fibrinolysis cascade; complement, or the leukotriene family. (Boneschansker L, 2014; Nakagawa H, 1993; Patrick RA, 1980; Paegelow I, 2002; Schuliga M, 2015) The discovery and analysis of plasma factors that may stimulate neutrophils is beyond the scope of this paper, but is important and should be pursued in future studies. Additionally, although there are minimal platelets in PPP, and spontaneous chemotaxis is seen in the PRPt without direct contact with platelets, there may be platelet activation during both processing of the plasma, as well as the plasma loading into the microfluidic device. This may result in a number of factors being released by the platelets, including microparticles and exosomes; many of which have been shown to result in neutrophil activation. (Yanez-Mo M, 2015) The lack of spontaneous migration observed in the WP group provides a useful negative control for presence of ACD, and suggests that if platelet activation is responsible for neutrophil migration, additional plasma-derived components must also be required to stimulate this activity.

4.4.2 Frequent directional changes by neutrophils after interaction with platelets

Neutrophils in PRPt changed directions in the side channels more frequently than those in PPP or in fMLP (Figure 4-4). Plotting of representative neutrophil velocities versus time showed a clear phenotypic difference between PRPt, PPP, and fMLP (Figure 4-4 B-D). Additionally, neutrophils that came into contact with a platelet often displayed an oscillatory behavior, switching directions within the side channel at a higher rate than those without platelet contact (Figure 4-5 A, Table 4-1). The majority neutrophils in fMLP and WP changed directions only once (68.7% and 76.5%, respectively) and usually at the end of the channels, as reported

previously (14) (Figure 4-5 A, Table 4-1, and Video 4-1). By comparison, a large proportion of neutrophils in PRPt and PPP changed in direction 3 or more times (34.6% and 25.3%, respectively) (Figure 4-5 A, Table 1, and Video 4-2). The difference in proportions of neutrophils changing directions 3 or more times was statistically significant between fMLP and PRPt (p-value <0.01) (Table 4-3). This data shows that there is a unique oscillatory phenotype present in neutrophils when exposed to PRP and PPP, as opposed to WP and fMLP. The PRPc neutrophils made significantly more directional changes in the side channel than the PRPn neutrophils (50.6% and 25.7% respectively, p-value <0.01), and this was in the absence of any exogenous chemoattractant (Table 4-1 and 4-2). This oscillatory behavior seen in neutrophils exposed to plasma, and exacerbated by direct contact with platelets, is similar to the 'crawling' behavior observed *in vivo* (5).

4.4.3 Time and distance traveled by neutrophils after interactions with platelets

The time spent in the channel by neutrophils also revealed differences between neutrophil migration patterns in each condition. Neutrophils exposed to PRPt, PPP, and fMLP spent an average of 61.4 $\pm$ 29.8 min, 53.0 $\pm$ 30.4 min, and 64.0 $\pm$ 36.2 min in the side channels, respectively (Figure 4-5 Bi and Table 4-1). The distributions for fMLP and washed platelets demonstrated bimodality, indicating that the behavior of these neutrophils is bimodal (Figure 4-3 and Supp. Table 4-1). Conversely, the distributions for PRPt and PPP followed a normal distribution curve. The distance traveled in the side channels is also influenced by both PRP and the interaction with platelets. The average total distance traveled in the PRPt and PPP was, 1695.7 $\pm$ 811.0 μm and 1470.3 $\pm$ 736.8 μm respectively, as compared to the fMLP, 1047.7 $\pm$ 460.3 μm. (Figure 4-5 Bii and Table 4-1). Statistical comparisons between all conditions is summarized in Table 4-3. Overall, the neutrophil phenotype of fMLP was similar to that of WP, while the phenotype of PRPn was similar to that of PPP, with the exception of the velocity of the neutrophil. When comparing PRPc to PRPn, it is apparent that, with the exception of the velocity of the neutrophil, contact with platelets does significantly change the migration behavior of the neutrophil.

4.4.4 Neutrophils migrate faster after direct, physical interaction with platelets

Direct platelet-neutrophil interactions resulted in either the arrest of neutrophil motility after contact with a platelet (20.1 % of interactions), or in the neutrophil carrying the platelet (67.3% of interactions) (Table 4-1). The duration of time that a neutrophil carried a platelet along the side channel was indicative of the transient nature of the platelet-neutrophil interactions, with most neutrophils carrying platelets for less than 4 minutes over a distance of approximately 120 μm. Surprisingly, some neutrophils carried platelets for up to one hour and for more than 2100 μm (Figure 4-2 C). Occasionally, neutrophils were noted to carry a platelet from the main channel into a side channel; these neutrophils exhibited a similar phenotype to the neutrophils that came into contact with a platelet within the side channel. Initial contact with the platelet mostly involved the leading edge of the neutrophil due to the spatial constraints within the side channels of the device. Interestingly however, the neutrophils that did attach to and carry platelets along the channels appeared to bind at the uropod (the trailing edge). This is consistent with previously published literature establishing that two of the main receptors involved in the platelet-neutrophil interaction are CD62P on the surface of the activated platelets and CD162 on the uropod of the activated neutrophil (5, 15, 16). Further experiments to validate the binding of the platelet to the neutrophil uropod are described later, in the section concerning neutrophil phenotypes following blockage of CD162.

Direct contact with platelets had an effect on the time spent in the side channel, the total distance traveled, and the velocity, with neutrophils in the PRPc group having faster velocities and spending longer time in the channels than the PRPn group, 71.5 ± 28.0 and 55.7 ± 29.4 min, 2029.7 ± 812.9 and 1508.4 ± 749.8 μm, and 29.1 ± 5.7 and 28.0 ± 5.9 μm/min, respectively (Figure 4-5 4Bi-iii and Table 4-1). Histograms of these behaviors were also plotted (Figure 4-3 and Table 4-2). The difference between PRPc and PRPn was statistically significant for both the total time spent in the channel (p-value <0.01) and the total distance traveled (p-value <0.01) (Table 4-3). These observations indicate that interactions between neutrophils and platelets result in an altered neutrophil phenotype, making them significantly more mobile than neutrophils that simply migrate into the channels.

4.4.4 The platelet-neutrophil interaction is mediated by CD62P-CD162 interactions

To further verify the utility of this assay and validate the importance of the CD62P-CD162 interaction in the platelet-neutrophil interaction, CD162 was blocked. Blocking of CD162 on neutrophils resulted in a decrease in the amount of PLA formation *ex vivo* (Figure 4-6). Flow cytometry experiments showed that co-incubation of isolated neutrophils with PRP resulted in an increase in PLA formation (1.3 $\pm$ 0.9% compared to 39.4 $\pm$ 17.4%); however, when neutrophils were treated with anti-CD162 antibody prior to co-incubation with PRP, formation of PLAs decreased (39.4 $\pm$ 17.4% compared to 14.1 $\pm$ 1.8%) (Figure 4-6 B and C). We also compared the amount of PLA formation before and after neutrophil isolation (4.0 $\pm$ 0.8% as compared to 1.3 $\pm$ 0.9%) to show that there was minimal PLA formation with the blood collection technique, and that neutrophils resulting from the negative isolation technique used were primarily not bound to platelets (Figure 4-6 B and C).

The microfluidic assay was then run using CD162-blocked neutrophils, to determine whether a change in platelet-neutrophil interaction would be observed. Activation and polarization of CD162 at the uropod of the neutrophil was clearly visualized in both the main channel and the side channel of the microfluidic device (Figure 4-7 A). There was no significant difference in migration behaviors for the neutrophils with and without CD162 blocked upon exposure to fMLP (Figure 4-7 and Tables 4-4 and 4-5). There was a significant difference in migration behavior between neutrophils in PRP with and without blocking of CD162, for both the total distance traveled ($p < 0.01$) and the average velocity ($p < 0.01$) (Table 4-5). As expected, there was also a significant decrease in the amount of neutrophils that bound to and carried platelets when CD162 was blocked in PRP (Table 4-6). There was no significant different in neutrophil migration behavior for neutrophils that did not come into contact with a platelet (PRPn and PRPn+anti-CD162), although there were significant differences in behavior with the neutrophils that came into contact with platelets (PRPc and PRPc+anti-CD162) (Figure 4-7 B-E and Tables 4-4 and 4-5). These findings demonstrate that blocking CD162 on neutrophils does significantly inhibit initial platelet-neutrophil binding, although if a platelet was bound, neutrophils displayed a phenotype consistent with platelet interaction.

4.5 Discussion

Neutrophil-platelet interactions and their role in the initiation of innate immune responses are under intense scrutiny. (Sreeramkumar V, 2014) However, previous studies were limited by the techniques available. While intravital microscopy has contributed a great deal of knowledge regarding this relationship, it has its limitations as well; including the use of live animals, highly technical equipment, and microsurgical training. (Xu N, 2011) Additionally, although the utilization of *in vivo* experiments has an essential role in exploring physiology, complex mechanistic studies can sometimes be better teased apart under highly controlled conditions, restricting the number of variables. The *ex vivo* assay we have developed for the study of the platelet-neutrophil interaction utilizing microfluidic devices fills this void, enabling precise control of soluble and cellular inputs and analysis at the single-cell level. Using this assay, we studied the effect of various platelet containing solutions on neutrophil motility, and the changes of neutrophil motility after direct, physical interactions with platelets.

Using this new microfluidic technique, we observed spontaneous migration of neutrophils to both PRPt and PPP, although the average velocity of neutrophils in PRPt was almost double of that in fMLP. This suggests that either soluble components or microparticles within the plasma result in spontaneous neutrophil migration. Additionally, there were significant differences in the number of neutrophil directional changes, velocity, and total time spent in the side channels, dependent on whether the neutrophils made direct contact with platelets. This spontaneous migration and oscillatory phenotype has been reported before in the context of sepsis after burn injuries. (Jones CN, 2014) This is the first time that this behavior has been recapitulated in an *ex vivo* system. Platelets can play both pro- and anti-inflammatory roles. For instance, CD62P-CD162 interactions can instigate the activation and 'crawling' of neutrophils, and neutrophils can utilize platelet arachidonic acid for the biosynthesis of leukotrienes; these events can take place in both the circulatory system as well as in peripheral organs. (Sureerkumar V, 2014; Antoine C, 1992) A better understanding of neutrophil-platelet interactions could help advance our understanding of neutrophil dysfunction and mechanisms leading to sepsis. (Gawaz M, 1997; Opal SM, 2003; Russwurm S, 2002)

Our observations of the interactions between platelets and moving neutrophils, in conditions of mechanical confinement, are suggestive of a mechanism by which neutrophils may transport platelets inside tissues. This biological property is likely relevant to certain disease states, when platelets do not always remain within the circulatory system. On many occasions, platelets have been noted to be present in extravascular spaces, suggesting a mechanism for platelet diapedesis. Platelets and neutrophils have been observed in the skin of rats after intradermal injection of platelet activating factor and in the sinusoidal and perisinusoidal Disse spaces in the liver of mice and rats after injection of lipopolysaccharide. (Endo Y, 1993; Endo Y, 1992; Nakamura M, 1998; Pons F, 1993; Pirotzky E, 1984) The recent study by Zuchtriegel G., et al. (Zuchtriegel G, 2016), investigating the binding of CD162 by CD62P showed that this interaction leads to ERK1/2 MAPK-dependent conformational changes of leukocyte integrins, promoting the successive extravasation of neutrophils and monocytes. Importantly, this study also revealed that platelet-directed, spatiotemporally organized crosstalk between platelets and leukocytes are essential in the trafficking of neutrophils towards sites of inflammation. One hypothesis emerging from this literature suggests that neutrophils mediate transport of platelets, and that the role of this behavior in disease should be studied in more detail. These interactions may also serve a protective function during inflammation and injury, as suggested by the biosynthesis of inflammation resolution mediators such as Maresin 1. (Abdulnour RE, 2014) In our study, some neutrophils in the PRPt were noted to migrate from the main channel into the side channel with a platelet already adhered, demonstrating that this *ex vivo* technique could potentially provide a platform for the study of platelet extravasation secondary to neutrophil diapedesis.

The development of microfluidic techniques for the study of platelet-neutrophil interactions at a single-cell level can provide new insights into innate immune cell behavior. In this study, phenotypic changes of the neutrophil upon platelet binding are identified and described in detail. Future applications of the assay presented here can be broadened to explore the effect of drugs, molecules and various disease states on the neutrophil-platelet interaction.

4.6 Acknowledgements

Dr. Caroline Jones helped design the microfluidic device for neutrophil migration. Dr. Felix Ellet and Anna Le helped perform experiments and with image analysis. Alyssa Pappa helped with the manuscript preparation. Financial support was provided by The U.S. National Institutes of Health through grants T32-0D019078-27 and P30-ES002109 (to J.G.F.) and GM092804 and AI113937 (to D.I.). All microfabrication procedures were performed at the BioMEMS Resource Center (EB002503).

4.7 References

1. Kim, N. D., and Luster, A. D. The role of tissue resident cells in neutrophil recruitment. Trends in immunology, 2015;36:547-555.
2. Kumar, V., and Sharma, A. Neutrophils: Cinderella of innate immune system. International immunopharmacology, 2010;10:1325-1334.
3. Engelmann, B., and Massberg, S. Thrombosis as an intravascular effector of innate immunity. Nature reviews. Immunology, 2013;13:34-45.
4. Semple, J. W., and Freedman, J. Platelets and innate immunity. Cellular and molecular life sciences : CMLS, 2010;67:499-511.
5. Sreeramkumar, V., Adrover, J. M., Ballesteros, I., et al. Neutrophils scan for activated platelets to initiate inflammation. Science, 2014;346:1234-1238.
6. Frojmovic, M. M. Platelet Biorheology: Adhesive interactions in Flow. In Handbook of Platelet Physiology and Pharmacology (Rao, G. H., ed), 1999, Springer Science and Business Media, New York, NY
7. Ghasemzadeh, M., and Hosseini, E. Platelet-leukocyte crosstalk: Linking proinflammatory responses to procoagulant state. Thrombosis research, 2013;131:191-197.
8. Hurley, S. M., Kahn, F., Nordenfelt, P., et al. Platelet-Dependent Neutrophil Function Is Dysregulated by M Protein from Streptococcus pyogenes. Infection and immunity, 2015;83:3515-3525.
9. Kim, K. H., Barazia, A., and Cho, J. Real-time imaging of heterotypic platelet-neutrophil interactions on the activated endothelium during vascular inflammation and thrombus Formation in live mice. Journal of visualized experiments : JoVE, 2013;e50329.
10. Jones, C. N., Moore, M., Dimisko, L., et al. Spontaneous neutrophil migration patterns during sepsis after major burns. PloS One, 2014;9:e114509.
11. Butler, K. L., Ambravaneswaran, V., Agrawal, N., et al. Burn injury reduces neutrophil directional migration speed in microfluidic devices. PloS One, 2010;5:e11921.
12. Boneschansker, L., Yan, J., Wong, E., et al. Microfluidic platform for the quantitative analysis of leukocyte migration signatures. Nature communications, 2014;5:4787.
13. Xu, N., Lei, X., and Liu, L. Tracking neutrophil intraluminal crawling, transendothelial migration and chemotaxis in tissue by intravital video microscopy. Journal of visualized experiments : JoVE, 2011;e3296.
14. Hamza, B., Wong, E., Patel, S., et al. Retrotaxis of human neutrophils during mechanical confinement inside microfluidic channels. Integr Biol (Camb), 2014;6:175-183
15. Xu, T., Zhang, L., Geng, Z. H., et al. P-selectin cross-links PSGL-1 and enhances neutrophil adhesion to fibrinogen and ICAM-1 in a Src kinase-dependent, but GPCR-independent mechanism. Cell adhesion & migration, 2007;1:115-123.
16. Moore, K. L., Patel, K. D., Bruehl, R. E., et al. P-selectin glycoprotein ligand-1 mediates rolling of human neutrophils on P-selectin. The Journal of cell biology, 1995;128,:661-671.
17. Nakagawa, H., and Komorita, N. Complement component C3-derived neutrophil chemotactic factors purified from exudate of rat carrageenin-induced inflammation. Biochemical and biophysical research communications, 1993;194:1181-1187.
18. Patrick, R. A., Hollers, J. C., Liu, D. Y., et al. Effects of human complement component 1 inactivator on neutrophil chemotaxis and chemotactic deactivation. Infection and immunity, 1980;28:700-707

19. Paegelow, I., Trzeczak, S., Bockmann, S., et al. Migratory responses of polymorphonuclear leukocytes to kinin peptides. Pharmacology, 2002;66:153-161.
20. Schuliga, M. The inflammatory actions of coagulant and fibrinolytic proteases in disease. Mediators of inflammation, 2015;437695.
21. Yanez-Mo, M., Siljander, P. R., Andreu, Z., et al. Biological properties of extracellular vesicles and their physiological functions. Journal of extracellular vesicles, 2015;4:27066.
22. Antoine, C., Murphy, R. C., Henson, P. M., et al. Time-dependent utilization of platelet arachidonic acid by the neutrophil in formation of 5-lipoxygenase products in platelet-neutrophil co-incubations. Biochimica et biophysica acta, 1992;1128:139-146.
23. Gawaz, M., Dickfeld, T., Bogner, C., et al. Platelet function in septic multiple organ dysfunction syndrome. Intensive care medicine, 1997;23:379-385.
24. Opal, S. M., and Esmon, C. T. Bench-to-bedside review: functional relationships between coagulation and the innate immune response and their respective roles in the pathogenesis of sepsis. Crit Care, 2003;7:23-38.
25. Russwurm, S., Vickers, J., Meier-Hellmann, A., et al. Platelet and leukocyte activation correlate with the severity of septic organ dysfunction. Shock, 2002;17:263-268.
26. Endo, Y., and Nakamura, M. Active translocation of platelets into sinusoidal and Disse spaces in the liver in response to lipopolysaccharides, interleukin-1 and tumor necrosis factor. General pharmacology, 1993;24:1039-1053.
27. Endo, Y., and Nakamura, M. The effect of lipopolysaccharide, interleukin-1 and tumour necrosis factor on the hepatic accumulation of 5-hydroxytryptamine and platelets in the mouse. British journal of pharmacology, 1992;105:613-619.
28. Nakamura, M., Shibazaki, M., Nitta, Y., et al. of platelets into Disse spaces and their entry into hepatocytes in response to lipopolysaccharides, interleukin-1 and tumour necrosis factor: the role of Kupffer cells. Journal of hepatology, 1998;28:991-999.
29. Pons, F., Rossi, A. G., Norman, K. E., et al. Role of platelet-activating factor (PAF) in platelet accumulation in rabbit skin: effect of the novel long-acting PAF antagonist, UK-74,505. British journal of pharmacology, 1993;109:234-242.
30. Pirotzky, E., Page, C. P., Roubin, R., et al. PAF-acether-induced plasma exudation in rat skin is independent of platelets and neutrophils. Microcirculation, endothelium, and lymphatics, 1984;1:107-122.
31. Zuchtriegel, G., Uhl, B., Puhr-Westerheide, D., et al. Platelets Guide Leukocytes to Their Sites of Extravasation. PLoS biology, 2016;14:e1002459
32. Abdulnour, R. E., Dalli, J., Colby, J. K., et al. Maresin 1 biosynthesis during platelet-neutrophil interactions is organ-protective. Proc Natl Acad Sci USA, 2014;111(46):16526-16531.

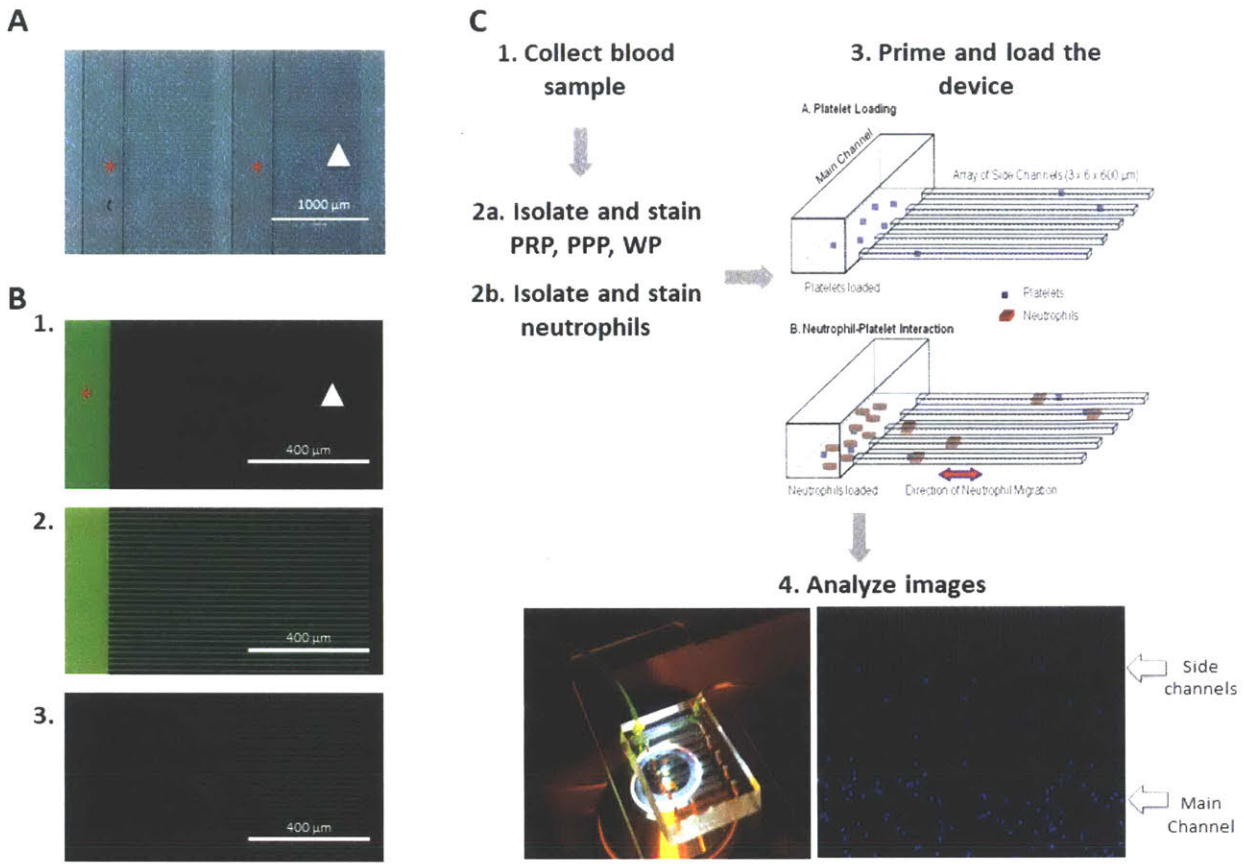

Figure 4-1: Microfluidic device work-flow.

Ai) Photomicrograph of the microfluidic device prior to priming and loading. The main channel (red star) of the device is loaded with fluorescein (ii). One end of the main channel is clamped off and fluorescein is pushed into the side channels (white arrowhead), displacing the air and filling them with dye (iii). The main channel is opened and is flushed with buffer, creating a fluorescein concentration gradient within the device (iv). B) Schematic of neutrophil migration protocol. Blood is collected (1) and aliquoted into two samples, one for neutrophil isolation and one for platelet isolation. Experimental conditions, PRP, PPP, and WP are prepared via differential centrifugation and stained with Calcein (2a) and neutrophils are collected via negative isolation and stained with Hoechst dye (2b). The microfluidic device is primed using the plasma preparation (3a) and then the neutrophils are loaded into the main channel (3b). Image analysis is then performed on time-lapse fluorescence microscopy of the neutrophils in the different experimental conditions (4). fMLP is used as a positive control that triggers persistent neutrophil migration.

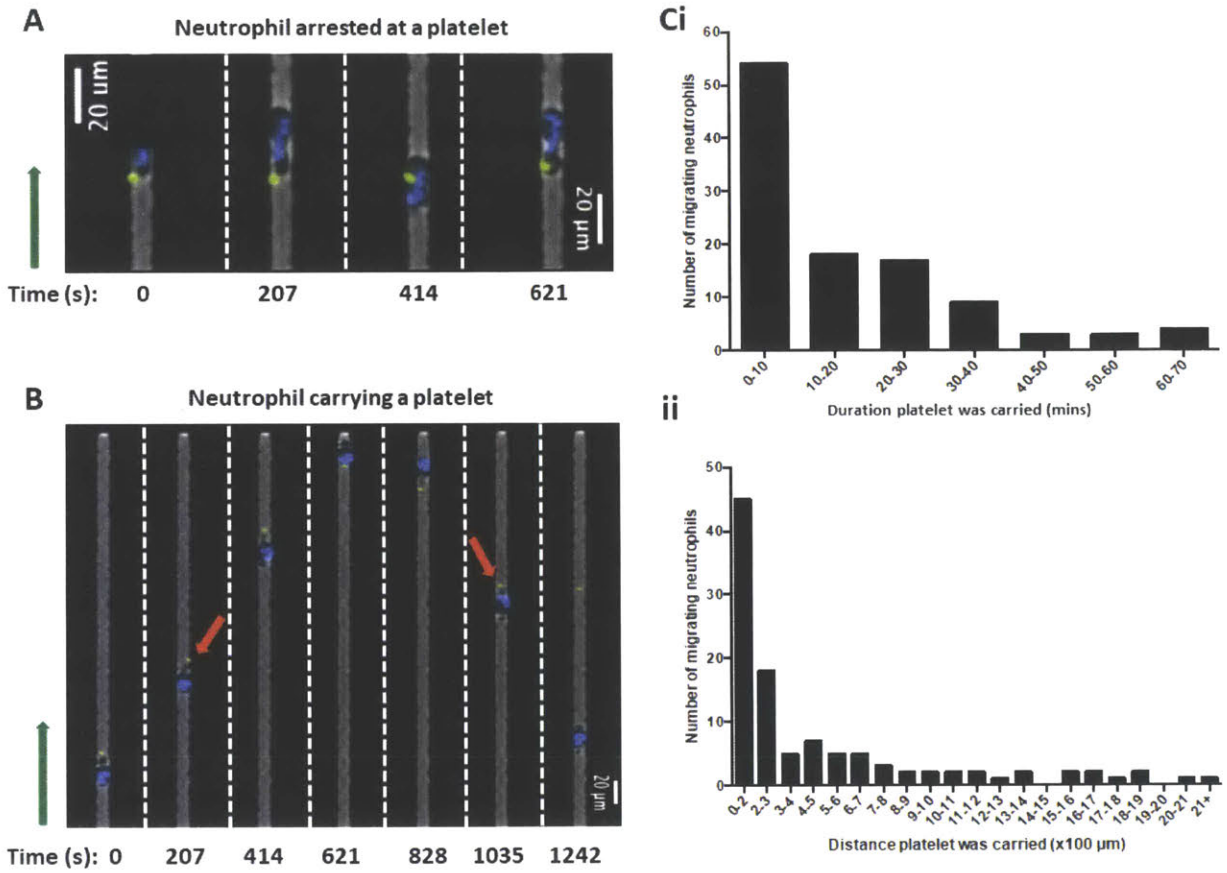

Figure 4-2: Definition of platelet-neutrophil interactions.

A) Montage of time-lapse fluorescent imaging of the platelet-neutrophil interaction. A neutrophil (Hoechst, blue) in PRP is shown to stop in place and interacting with a platelet (Calcein, green) for 10.35 minutes. B) A neutrophil is shown migrating down a side-channel towards a platelet, then attaching and carrying the platelet on its uropod (red arrow) as it changes directions. Direction towards the blind end of the side channel is indicated by the green arrow. C) Graphs of the total amount of neutrophils migrating as a function of duration of time that a platelet was carried by a neutrophil (i) and the total distance that a platelet was carried by a neutrophil (ii).

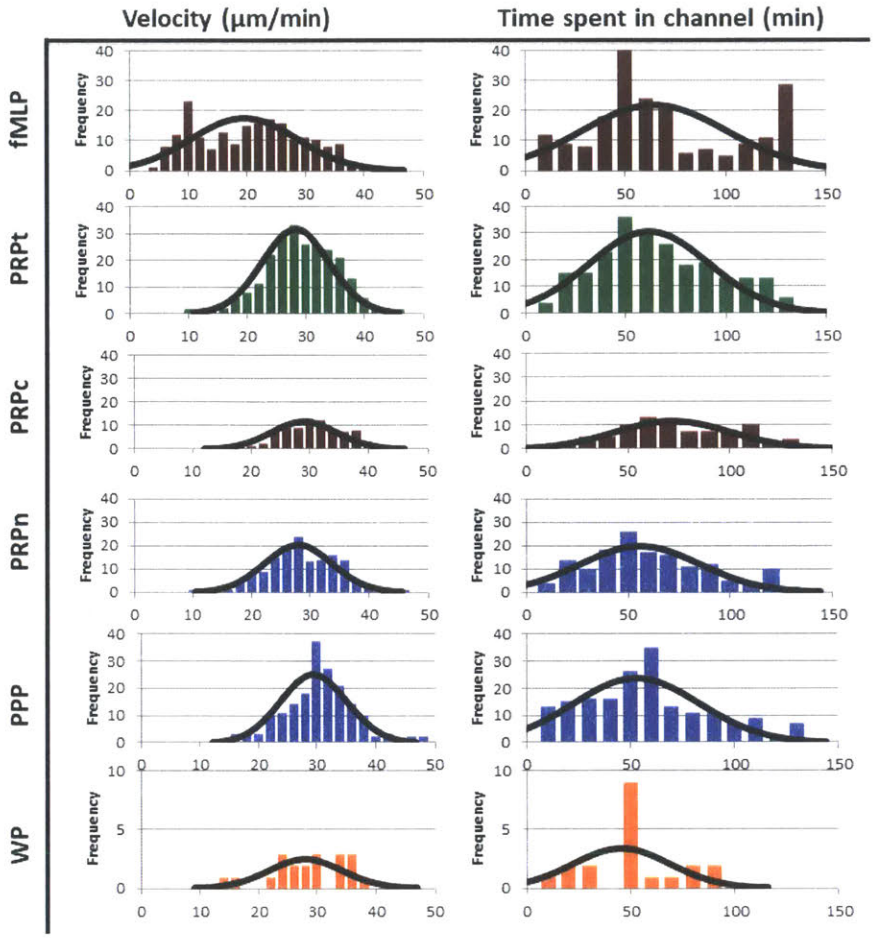

Figure 4-3: Distribution curves.

Distribution curves for average speed (um/min), total time spent in the side channel (min), and total distance traveled (um) for all four conditions (fMLP, PRPt, PPP, WP).

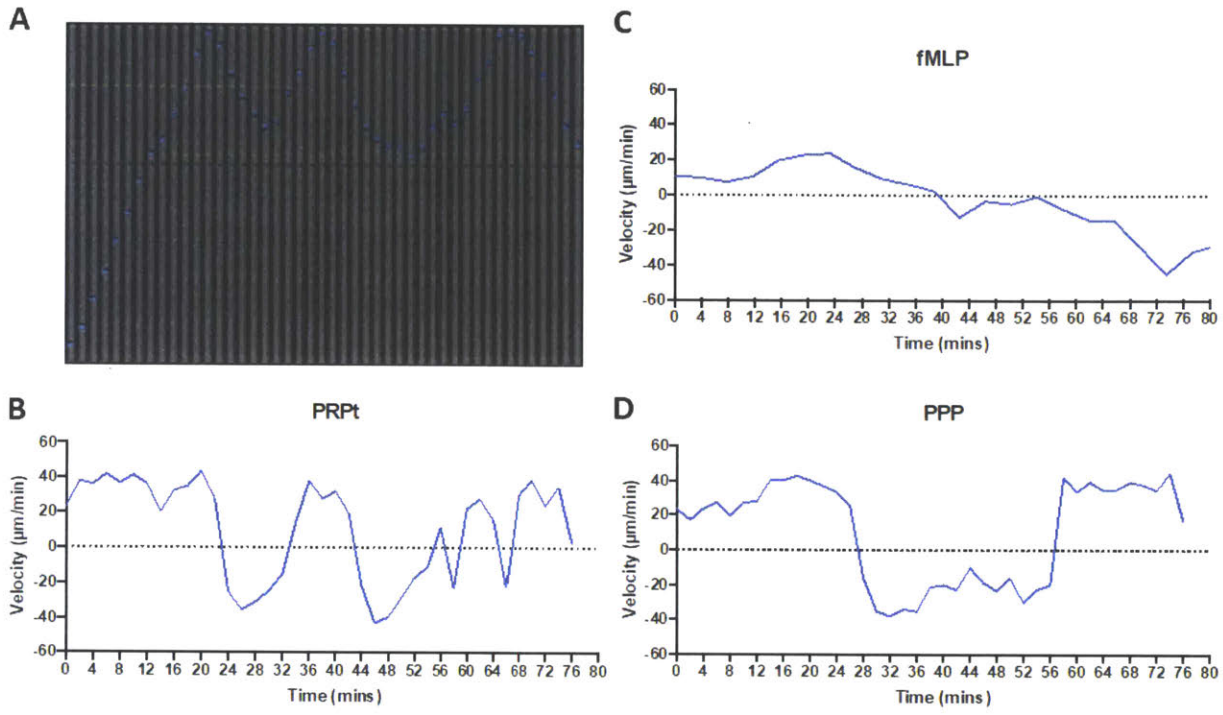

Figure 4-4: Neutrophil directionality.

Neutrophil behavior was evaluated in microfluidic devices, with individual velocities recorded and analyzed. A) A montage of time-lapse (207 seconds) fluorescent imaging shows a representative neutrophil (Hoechst, blue) in PRPt (Calcein, green), migrating and interacting in a side channel. B) The velocity of this individual neutrophil towards the end of the channel was tracked and displayed on a graph over time. The migratory behavior of a representative neutrophil is also displayed for fMLP (C) and PPP (D).

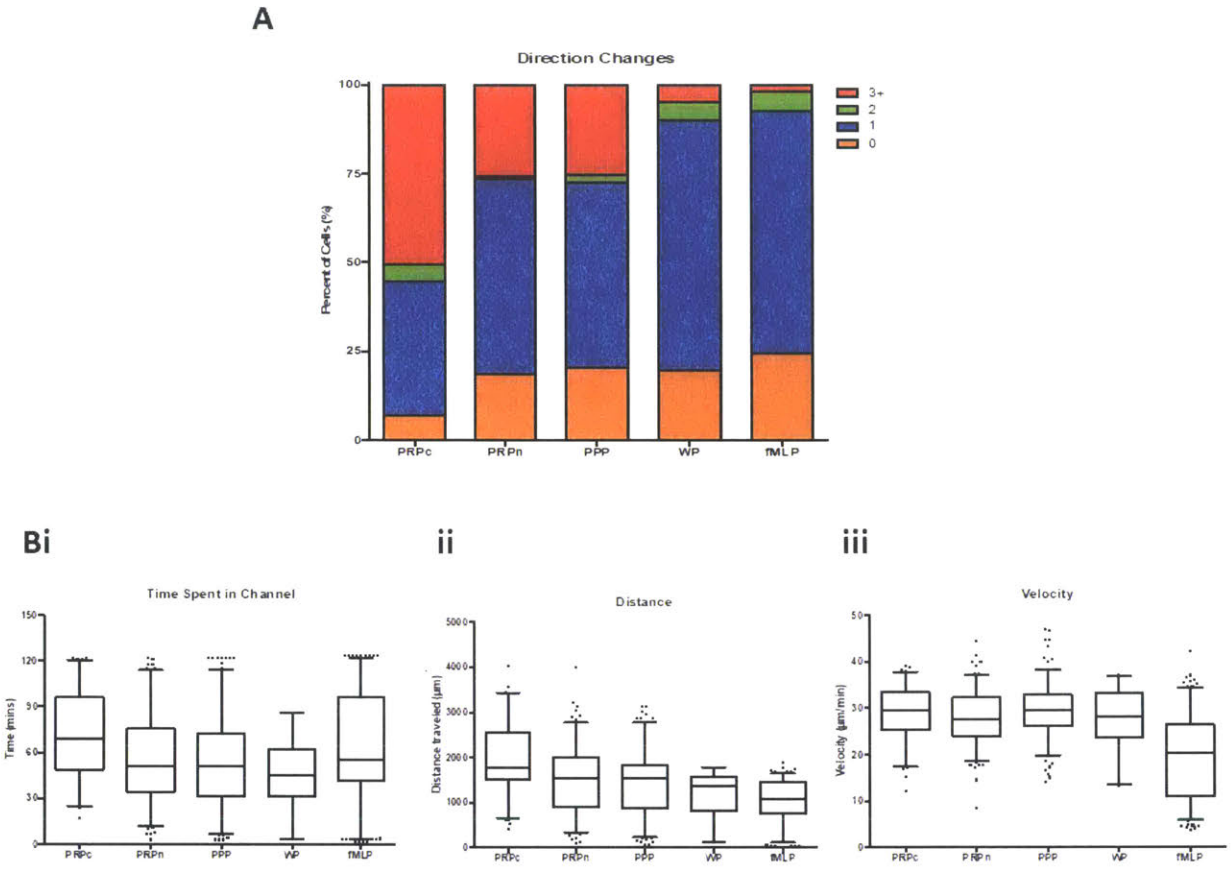

Figure 4-5: Neutrophil phenotype in various conditions.

Neutrophil phenotype was evaluated in all four conditions (PRPc, PRPn, PPP, WP, and fMLP). A) Bar graph represents the percent of neutrophils that displayed a certain number of directional changes (orange, 0; blue, 1; green, 2; red, 3+). B) Box scatter plots showing the 95% confidence intervals are shown for time spent in the side channel (i), the distance traveled within the side channel (ii), and the velocity (iii).

A

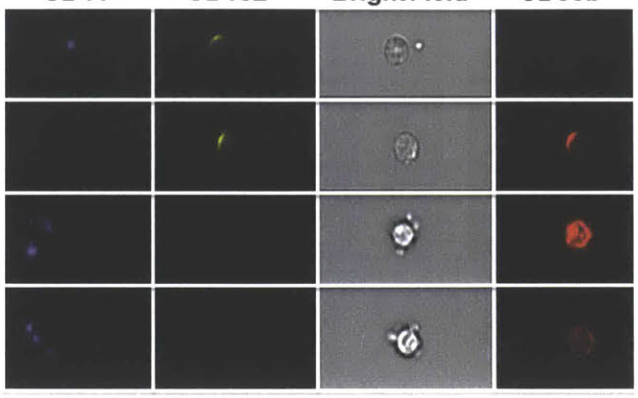

B

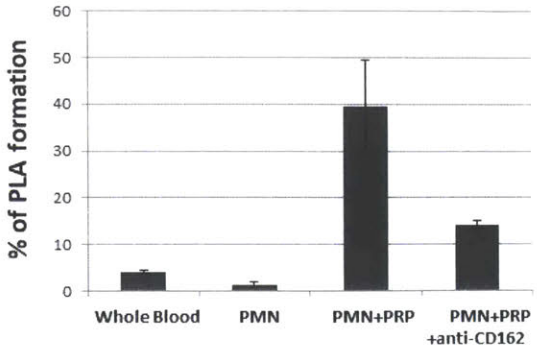

C

	Average PLA (%)	SD	SEM
Whole blood	4.0	0.8	0.5
PMN	1.3	0.9	0.5
PMN + PRP	39.4	17.4	10.0
PMN + CD162 + PRP	14.1	1.8	1.0

Figure 4-6: Inhibition of platelet-neutrophil complexes with anti-CD162 antibody.

Various of preparations of blood were treated with anti-CD162 antibodies. (A) Imaging flow cytometry was used to confirm dissociation of PLA. (B&C) % of PLA formation was observed to be significantly decreased in the PMN+PRP condition treated with anti-CD162 antibodies.

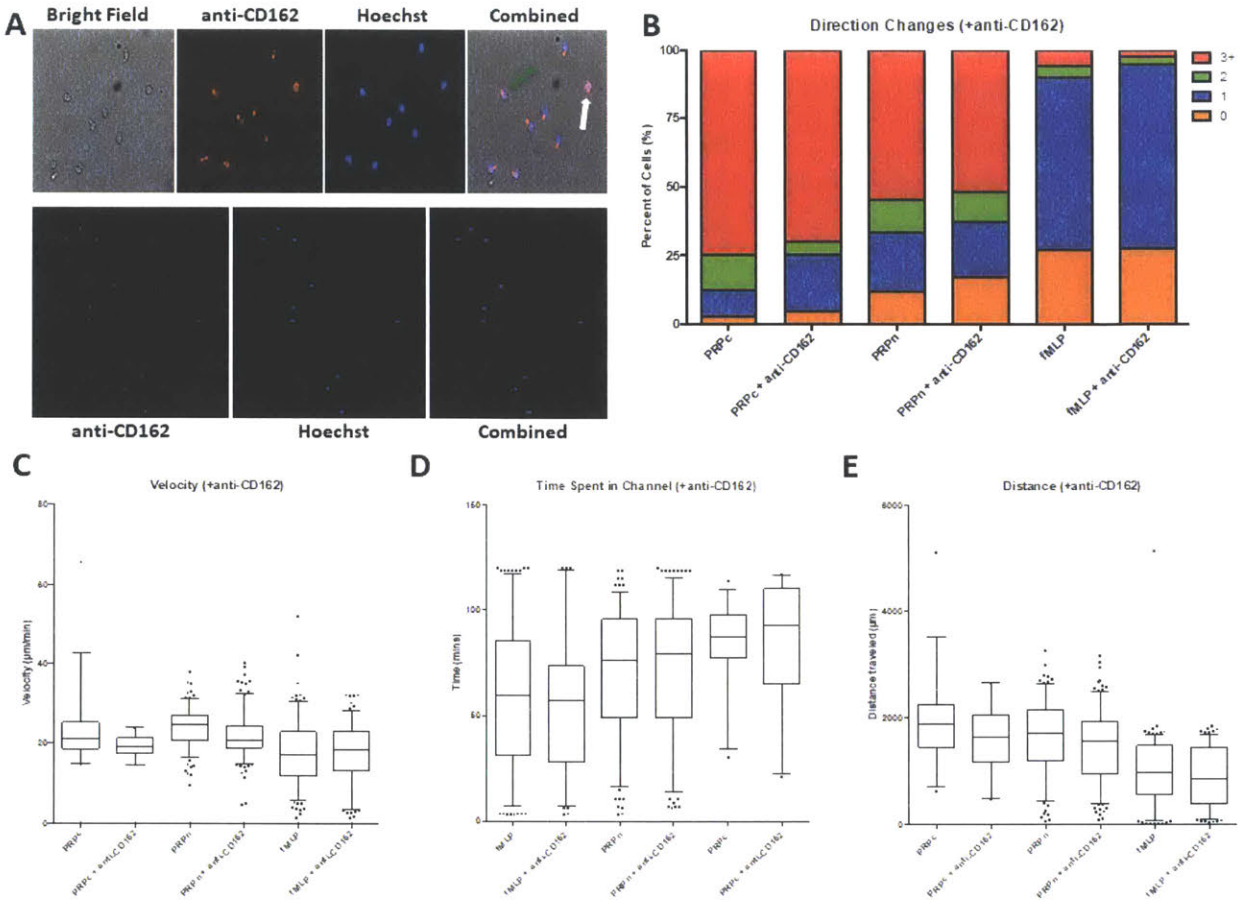

Figure 4-7: Neutrophil phenotype after treatment with anti-CD162 antibody.

A) Neutrophils in the microfluidic device, stained with both Hoechst (blue) and anti-CD162 antibody (red). The top 4 photos show the neutrophil within the main channel. Activation of the neutrophil is characterized by the polarization of the uropod and the localization of the anti-CD162 staining (green arrow). Neutrophils that are not activated are not polarized and display CD162 staining diffusely throughout their cell membrane (white arrow). B) Bar graph represents the percent of neutrophils that displayed a certain number of directional changes (orange, 0; blue, 1; green, 2; red, 3+). Neutrophil phenotype was evaluated in all four conditions (fMLP, fMLP + anti-CD162, PRPc, PRPc + anti-CD162, PRPn, PRPn + anti-CD162). Box scatter plots showing the 95% confidence interval are shown for velocity (C), time spent in the side channel (D), and the distance traveled within the side channel (E).

Tables:

Table 4-1: Comparison of neutrophil migration and interaction with platelets

Condition	Number of neutrophils migrating	Number of directional changes[1]				Total distance traveled (μm)[2]	Velocity μm/min	Time spent in channel (min)	Neutrophil arrest near platelet[3]	Neutrophil carrying platelet[4]	Total distance platelet carried (μm)[2]	Time platelet carried (min)[2]
		0	1	2	3+							
fMLP	201	24.9%	68.7%	4.5%	2.0%	1047.7 ±460.3	19.5 ±9.1	64.0 ±36.2	NA	NA	NA	NA
PRPt	231	14.7%	48.5%	2.2%	34.6%	1695.7 ±811.0	28.4 ±5.8	61.4 ±29.8	20.1%	67.3%	468.3 ±507.1	16.1 ±16.4
PRPc	83	7.2%	37.4%	4.8%	50.6%	2029.7 ±812.9	29.1 ±5.7	71.5 ±28.0	20.1%	67.3%	468.3 ±507.1	16.1 ±16.4
PRPn	148	18.9%	54.7%	0.7%	25.7%	1508.4 ±749.8	28.0 ±5.9	55.7 ±29.4	NA	NA	NA	NA
PPP	182	20.9%	51.7%	2.2%	25.3%	1470.3 ±736.8	29.5 ±5.8	53.0 ±30.4	0.0%	1.1%	475.3 ±517.3	17.4 ±19.7
WP	17	23.5%	76.5%	0.0%	5.9%	1155.5 ±510.1	27.0 ±7.6	44.6 ±22.9	0.0%	0.0%	NA	NA

[1]Percent of neutrophils moving in a given number of directions within two hours.
[2]Mean (± SD)
[3]cent of neutrophils in channels which arrested at the position of a platelet for more than one time frame.
[4]Percent of neutrophils in channels which grabbed and carried a platelet once or more for at least one time frame.

Table 4-2: Data from histogram curves

		fMLP	PRPt	PRPc	PRPn	PPP	WP
Average velocity (µm/min)	*Count*	199	231	83	148	181	20
	Mean	19.5	28.4	29.1	28.0	29.5	28.0
	Median	20.2	28.1	29.5	27.6	29.5	28.3
	Variance	81.8	33.7	32.4	34.2	33.0	39.5
	SD	9.0	5.8	5.7	5.9	5.7	6.3
	SEM	0.6	0.4	0.6	0.5	0.4	1.4
	Skewness	0.1	-0.2	-0.5	-0.0	0.1	-0.5
	IQR	15.4	8.2	8.1	8.3	6.8	9.6
	95% CI lb	18.3	27.6	27.9	27.0	28.7	25.1
	95% CI ub	20.8	29.1	30.3	28.9	30.4	31.0
Time spent in the side channel (min)	*Mean*	64.0	61.4	71.5	55.7	53.0	45.6
	Median	55.7	55.7	69.0	51.0	51.0	45.3
	Variance	1312.5	888.3	785.0	861.6	923.5	552.4
	SD	36.2	29.8	28.0	29.4	30.4	23.5
	SEM	2.6	2.0	3.1	2.4	2.3	5.3
	Skewness	0.3	0.3	0.1	0.4	0.4	0.0
	IQR	55.2	41.8	44.7	39.9	40.7	17.4
	95% CI lb	59.0	57.5	65.5	51.0	48.6	34.6
	95% CI ub	69.1	65.2	77.5	60.4	57.4	56.6

Table 4-3: Comparison of neutrophil behavior in different conditions

Condition	# of directional changes	Distance traveled	Velocity	Time spent in channel
fMLP v. PRPt	<0.01	<0.01	<0.01	0.40
fMLP v. PRPn	<0.01	<0.01	<0.01	0.02
fMLP v. PRPc	<0.01	<0.01	<0.01	0.09
fMLP v. PPP	<0.01	<0.01	<0.01	<0.01
fMLP v. WP	0.80	0.21	<0.01	0.03
PRPt v. PPP	0.02	<0.01	0.05	0.01
PRPn v. PPP	0.97	0.64	0.02	0.42
PRPc v. PPP	<0.01	<0.01	0.59	<0.01
PRPt v. WP	0.01	0.01	0.79	0.02
PRPn v. WP	0.12	0.06	0.98	0.14
PRPc v. WP	<0.01	<0.01	0.46	<0.01
PPP v. WP	0.11	0.09	0.28	0.29
PRPc v. PRPn	<0.01	<0.01	0.16	<0.01

Table 4-4: Comparison of neutrophil migration and interaction with platelets in the presence of anti-CD162 antibody

Condition	Number of neutrophils migrating	Number of directional changes[1]				Total distance traveled (μm)[2]	Velocity (μm/min)	Time spent in channel (min)	Neutrophil arrest near platelet[3]	Neutrophil carrying platelet[4]	Total distance platelet carried (μm)[2]	Time platelet carried (min)[2]
		0	1	2	3+							
fMLP	189	27.0%	63.0%	8.0%	11.0%	991.9 ±600.2	17.8 ±1.4	60.6 ±33.4	NA	NA	NA	NA
fMLP + anti-CD162	153	27.5%	67.3%	4.0%	4.0%	909.2 ±553.0	17.7 ±7.2	56.3 ±33.5	NA	NA	NA	NA
PRPt	207	10.6%	19.3%	12.1%	58.0%	1700.1 ±693.1	23.8 ±5.6	73.5 ±28.0	8.3%	17.4%	449.1 ±531.0	16.0 ±16.5
PRPc	32	3.1%	9.4%	12.5%	75%	1902.8 ±781.7	23.0 ±1.8	83.5 ±20.7	8.3%	17.4%	449.1 ±531.0	16.0 ±16.5
PRPn	173	12.1%	21.4%	11.6%	54.9%	1664.8 ±586.4	19.3 ±2.7	86.4 ±25.9	NA	NA	NA	NA
PRPt + anti-CD162	228	16.2%	19.7%	10.5%	53.5%	1516.7 ±645.4	21.8 ±5.3	73.5 ±31.4	6.25%	7.6%	214.04 ±202.9	10.4 ±9.3
PRPc + anti-CD162	20	5.0%	20.0%	5.0%	70%	1647.3 ±658.3	23.9 ±4.8	71.2 ±28.7	6.25%	7.6%	214.04 ±202.9	10.4 ±9.3
PRPn + anti-CD162	208	17.3%	19.7%	11.1%	51.9%	1502.5 ±650.3	22.0 ±5.4	72.3 ±31.7	NA	NA	NA	NA

[1]Percent of neutrophils moving in a given number of directions within two hours.
[2]Mean (± SD)
[3]cent of neutrophils in channels which arrested at the position of a platelet for more than one time frame.
[4]Percent of neutrophils in channels which grabbed and carried a platelet once or more for at least one time frame.

Table 4-5: Comparison of neutrophil behavior in different conditions in the presence of anti-CD162 antibodies

Condition	# of directional changes	Distance traveled	Velocity	Time spent in channel
fMLP v. fMLP+anti-CD162	0.21	0.19	0.89	0.24
fMLP v. PRPt	<0.01	<0.01	<0.01	<0.01
fMLP v. PRPt+anti-CD162	<0.01	<0.01	<0.01	<0.01
fMLP+anti-CD162 v. PRPt	<0.01	<0.01	<0.01	<0.01
fMLP+anti-CD162 v. PRPt+anti-CD162	<0.01	<0.01	<0.01	<0.01
PRPt v. PRPt+anti-CD162	0.74	<0.01	<0.01	0.99
PRPc v. PRPc+anti-CD162	0.89	0.25	0.07	0.66
PRPc v. PRPn+anti-CD162	0.09	<0.01	0.36	0.05
PRPn v. PRPn+anti-CD162	0.54	0.03	<0.01	0.73
PRPn v. PRPc+anti-CD162	0.04	0.91	<0.01	0.02
PRPn v. PRPc	0.02	0.05	<0.01	<0.01
PRPn+anti-CD162 v. PRPc+anti-CD162	0.13	0.28	0.03	0.06

Table 4-6: Comparison of neutrophil migration and platelet interaction in the presence of anti-CD162 antibodies

	PRPc[1]	PRPc + anti-CD162[1]	P-value[2]
Distance platelet was carried (μm)	449.1 ± 113.2	214.0 ± 64.2	0.19
Time duration platelet was carried (min)	16.0 ± 3.5	10.4 ± 2.9	0.32
% Neutrophils carrying platelets	17.4	7.6	0.01
% Neutrophils in arrested near platelets	8.3	6.3	0.47
Time duration of arrested platelet contact (min)	4.9 ± 2.3	5 ± 2.8	0.94

[1]Mean (± SD)
[2]Two-tailed student t-test between the PRP and PRP+PSGL1 group

Videos:

Video 4-1: Neutrophil motility in the presence of PRP.

Neutrophils (Hoechst, blue) migrate into the side channel and interact with platelets (green) in PRP.

Video 4-2: Neutrophil chemotaxis towards fMLP.

Positive control. Neutrophils (Hoechst, blue) undergo 1 or 2 direction changes.

Chapter 5
Conclusions and Future Work

Megakaryocytes (MKs) have traditionally played a primary role in hemostasis as precursors to platelets. Recently, platelets have been shown to play a key role in the immune system, often playing the role of 'first responder.' Once activated by an inflammatory or pathogenic stimulus, platelets can both directly stimulate neighboring white blood cells as well as release signals into the surrounding area, which can propagate inflammation and thrombosis formation. (Semple JW 2011) While platelets are studied for their various roles in inflammation, the role of MKs within the innate immune system has, until now, gone unexplored. Taking into consideration that 'daughter' platelets derive their form, function, and intracellular content from their 'parent' MK, we hypothesized that the MK also harbors innate immune cell functions. The overall objectives of this project were thus to explore the role of the MK as a functional innate immune cell, to delineate the role that platelets have in inflammation at the origin of the 'parent' MK, and to demonstrate how this may tie into the pathophysiology of sepsis.

In a series of comprehensive *in vitro* experiments, we have demonstrated that both cord blood-derived MKs (CB MKs) and MKs from a megakaryoblastic lineage (Meg-01) have innate immune cell functions, including phagocytosis, formation of extracellular traps, and chemotaxis towards pathogenic stimuli (Chapter 2). Samples from patients diagnosed with sepsis were evaluated and demonstrated both an increase in $CD61^{+}CD41^{+}$ cells in the venous blood as well as an increase in total $CD61^{+}$ staining within renal glomeruli and the lungs. The amount of MKs also appeared to correlate with both type of infection, with Gram negative bacteria proving the most significant, as well as the development of complications, such as acute respiratory distress syndrome (ARDS) and acute kidney injury (AKI). In addition to a primary role as immune cells, MKs were also shown to contain extranuclear histones, which the MKs appear to release within budding platelets into the peripheral circulation (Chapter 3). We then evaluated platelets from patients with sepsis and demonstrated that platelet-associated histones are significantly increased in patients with sepsis; this is also correlated with the type of infection and prognosis. Platelets from patients with sepsis also appeared to have a specific phenotype, including increased

activation and increased DNA and histone staining.

We also developed new tools in order to evaluate the interaction between platelet and leukocytes in an *in vitro* system (Frydman GH 2017). By creating a microfluidic chip for the single-cell evaluation of platelet-neutrophil interactions, we were able to characterize the change in neutrophil migration behavior upon contact and bonding with platelets (Chapter 4). We then performed preliminary *in vitro* experiments (Appendix) exploring the effect of endotoxin on megakaryocyte differentiation in order to help elucidate the origin of platelet phenotype changes during sepsis. These preliminary results demonstrate that if MKs are exposed to endotoxin during differentiation, they can develop an alternate phenotype that may have downstream effects on the resultant platelets.

In summary, the studies comprising this thesis explore a newly recognized role of the MK as a functional innate immune cell and demonstrate that MKs, both directly and indirectly, through their platelets, may have a significant role in the pathophysiology of sepsis and its related complications. These findings have many implications for the pathophysiological mechanisms underlying sepsis and end organ dysfunction, as well as for the potential future discoveries for the early diagnosis and treatment of this complex and deadly syndrome. While the inflammation and coagulation system are intimately intertwined, it is only recently that scientists have elucidated that inflammatory cells play a major role in coagulation and that cells originally thought to only be important in coagulation, play an essential role in inflammation. By understanding that the different conversation that cells have with each other may have downstream effects on cellular phenotype and behavior, we will allow ourselves to be open-minded enough to discover the complexity of systemic inflammation and infections.

One example of the effect of this cross-talk and cell phenotype change occurs during a post-sepsis complication termed compensatory anti-inflammatory response syndrome (CARS). Patients fortunate enough to survive sepsis are at an increased risk for having CARS, which results in chronic immune-suppression and a number of other complications which sometimes permanently effects quality of life. (Adib-Conquy M 2009) Studies have shown that sepsis and bacterial infections can cause permanent changes to leukocytes starting at the bone marrow level

through mechanisms such as modification of histone post-translational modifications (PTSMs), which, in turn, results in endotoxin tolerance (Hamon MA 2008; Weiterer S 2015). As demonstrated in this thesis, megakaryocytes may play an important role in the immune and coagulation systems during sepsis; therefore, it is also plausible that during sepsis they may undergo similary phenotypic changes that have both immediate and long-term effects on patient prognosis and health. Because MKs are the source of platelets in the body, any change in the molecular signaling and phenotype of the MK may also change the downstream platelets. This thesis presents just one example of how one cell that has been traditionally overlooked, the megakaryocyte, can potentially be a key to the pathophysiology of some of the most dangerous inflammatory conditions, such as hemorrhagic fevers, autoimmune diseases, and sepsis.

References

1. Semple JW, Italiano JE, Freedman J. Platelets and the immune continuum. Nature Reviews Immunol, 2011;11:264-274.
2. Frydman GH, Le E, Ellett F, et al. Technical advance: changes in neutrophil migration patterns upon contact with platelets in a microfluidic assay. J Leukoc Biol, 2017;101(3):797-806.
3. Adib-Conquy M, Cavaillon JM. Compensatory anti-inflammatory response syndrome. Thromb Haemost, 2009;101(1):36-47.
4. Hamon MA, Cossart P. Histone modifications and chromatin remodeling during bacterial infections. Cell Host & Microbe, 2008;4:100-109.
5. Weiterer S, Uhle F, Lichtenstern C, et al. Sepsis induces specific changes in histone modification patterns in human monocytes. PLoS One, 2015;10(3):e0121748.

Figures:

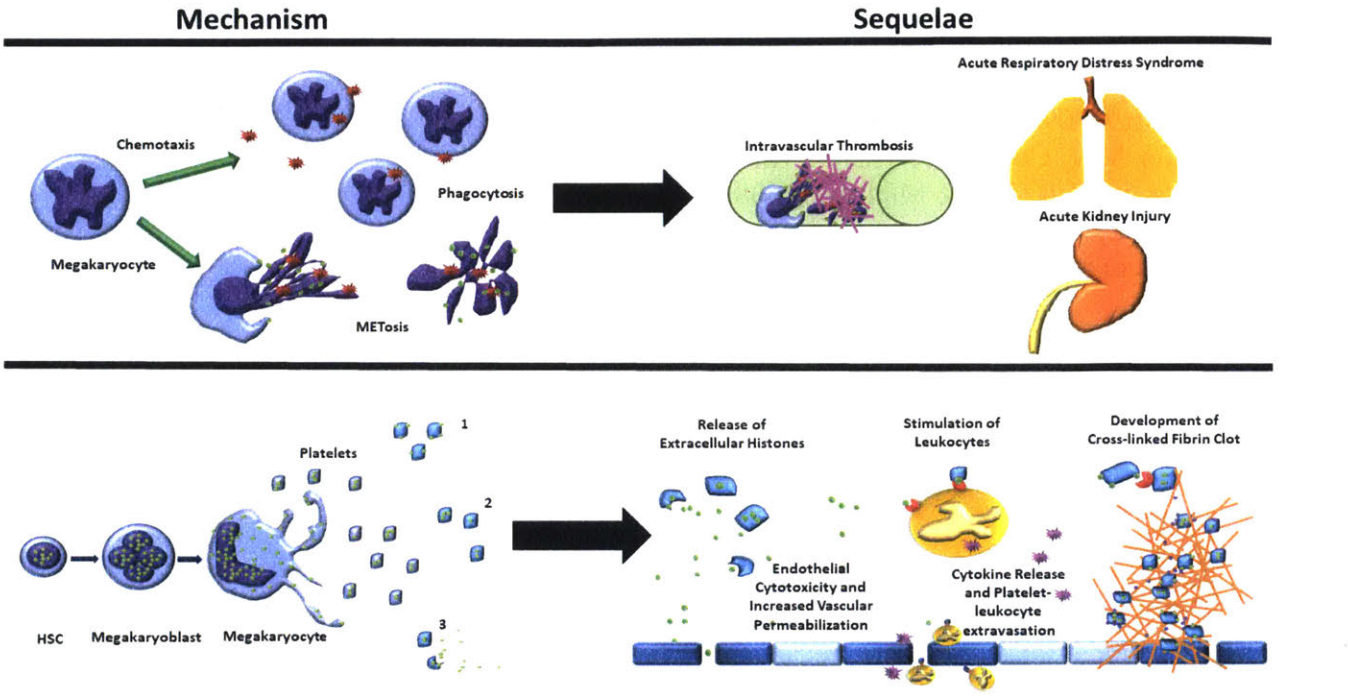

Figure 5-1: Proposed mechanisms and sequelae of megakaryocytes as immune cells

Presented above is a summary of the proposed mechanisms of the MK and the platelet within the immune and coagulation system. On the top panel is a summary of Figure 2-13 and the bottom panel is a summary of Figure 3-10 and 3-11.

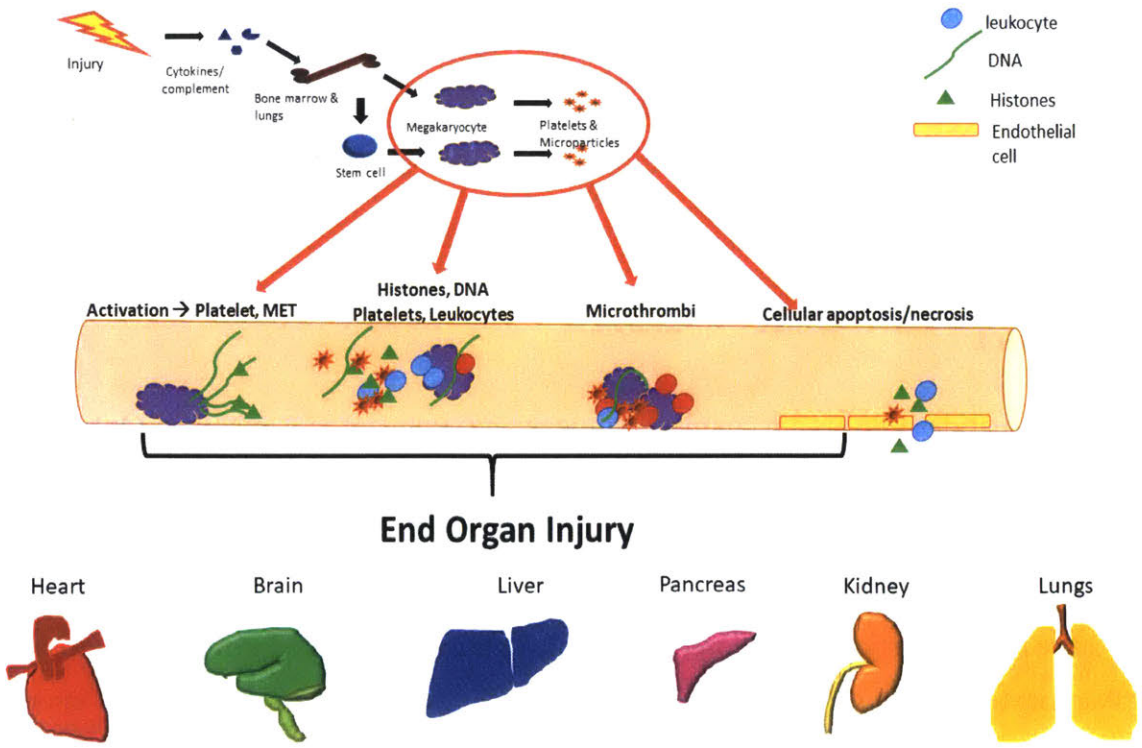

Figure 5-2: Proposed role of the megakaryocyte and platelet in sepsis

Here we propose one example of how megakaryocytes and platelets play a role in the pathophysiology of sepsis and end organ damage. An injury incites cytokine and complement/coagulation activation; these soluble signals and DAMPs travel through the circulation, where they reach sites of HSCs and MKs, such as the bone marrow and the lungs; here the MKs can be activate and function as primary innate immune cells, and their progeny platelets and microparticles can also play a role in inflammation and coagulation, such as being a source of extracellular histones. The MK and platelet activation can result in increased MET formation, circulating clusters of histones, DNA, and various cell types, white blood cell activation, microthrombi formation, and endothelial cell apoptosis or necrosis. Depending on the physiological localization of these events, end organ damage can occur and result in severe injury and increased morbidity and mortality.

Appendix

The Effect of Lipopolysaccharide on Megakaryocyte Differentiation

1. Abstract

Lipopolysaccharide (LPS) is a recognized mitogen and stimulant of leukocytes. One situation in which a person's bone marrow may be exposed to LPS is during Gram negative sepsis. Patients with sepsis often have abnormal platelet indices, including changes in mean platelet volume, reticulated platelets, and cell surface markers. Although alterations in platelet phenotype during sepsis have been superficially explored, very little research has looked at their 'parent' megakaryocytes. In this paper, we perform a preliminary set of *in vitro* experiments in order to determine if hematopoietic stem cell exposure to *Escherichia coli (E. coli)* LPS during megakaryocyte differentiation would result in an altered megakaryocyte phenotype. The results of these studies are suggestive of an altered phenotype, including changes in cell number, cell size, nuclear content, cell surface markers, and ultrastructure. Although this study merely grazing the surface, it is highly suggestive that LPS exposure may result in aberrant megakaryo- and thrombopoiesis, potentially producing abnormal platelet phenotypes, such as those identified in patients with sepsis.

2. Introduction

Megakaryocytes have been shown to pass on their form and function to platelets during thrombopoiesis. Perturbations during megakaryo- or thrombopoiesis can result in changes in the circulating platelet phenotype. Sepsis is a syndrome where changes in platelet indices have been shown to be important indicators of condition and prognosis. (Gao Y, 2014; Ramesh Bhat Y, 2017; Enz Hubert RM, 2015) Changes in megakaryocytes during sepsis have also started to be explored. (Brown RE, 2008; Freishtat RJ, 2009) In depth studies into the morphological, transcriptional, and translational effects of sepsis on the development of the MK cell and its' progeny platelets have yet to be explored.

Previous literature demonstrates that different types of stimulus can result in both transcriptional and translational changes in megakaryocytes, resulting in changes in the platelet cargo and function. The platelet transcriptome during certain disease states, such as lupus and sickle cell, has revealed variations from normal platelets. (Lood C, 2011; Raghavachari N, 2007; Healy AM, 2006) Sepsis-associated changes in MK and platelet mRNA have been identified. In mice, septic megakaryocytes and platelets were found to have increased expression of granzyme-B mRNA, and these platelets exhibited increased *in vitro* lymphotoxicity. (Freishtat RJ 2009) Both platelets from septic patients and normal platelets stimulating with endotoxin contained splicing of *tissue factor* pre-mRNA and accelerated plasma clotting, suggesting that this may be a marker to an altered platelet phenotype and function in sepsis. (Rondina MT, 2011) A thorough evaluation of the megakaryocyte and platelet axis has not yet been evaluated in sepsis.

In this study, we perform a set of preliminary *in vitro* experiments investigating the effect of lipopolysaccharide (LPS) on the differentiation and maturation of the MK. Here we show that there are changes in cell count, cellular ultrastructural morphology, and even cell surface marker expression.

3. Materials and Methods

3.1 Cell culture

Cord blood $CD34^+$ hematopoietic stem cells and Meg-01 cells were cultured and differentiated into megakaryocytes (CB MKs). Cord blood $CD34^+$ hematopoietic stem cells were purchased and cultured in StemSpanII media with the megakaryocyte supplemental cytokines, according to the culture and differentiation protocols from Stemcell Technologies (Stemcell Technologies Inc. Cambridge, MA). Cell cultures were co-incubated with *E. coli* lipopolysaccharide at 360 pg/mL starting at day 7 of differentiation (0111: B4, γ-irradiated for cell culture; Sigma Aldrich, St. Louis, MO, USA) (Figure A1-1).

3.2 Cell morphology analysis

Cell cultures were analyzed for total cell numbers as well as cell size. Manual cell counts were performed using hemacytometers (INCYTO C-Chip Disposable Hemacytometers; Fisher Scientific, Pittsburgh, PA, USA) on each culture at day 1 and day 14 of differentiation. Brightfield pictures of the cells were taken on day 14 of differentiation with one of two fluorescent microscopes: Life Technologies EVOS FL (Thermo Fisher Scientific) or Nikon Eclipse 90i microscope (Nikon Instruments Inc., Melville, NY). Cell size was measured using Fiji software (NIH). (Shindelin J, 2012)

3.3 Flow cytometry

Flow cytometry was performed in order to verify appropriate cellular differentiation and for the evaluation of cell surface markers. Briefly, cells were stained with antibodies at a concentration of 1:200 for 15 minutes, with the exception of CD41, which was at a concentration of 1:100. Cells were then stained with Draq5 (Thermo Fisher Scientific, Waltham, MA) at a concentration of 1:10000 for 5 minutes. Antibodies included: anti-human HLA-ABC (MHC class I), HLA-DR (MHC class II), CD162 (p-glycoprotein-1; SELPG), CD41 (GPIIb), CD34 (Biolegend, San Diego, Ca), and CD62P (P-selectin) (BD Biosciences, San Jose, CA). Data was obtained through the Amnis ImageStreamX Mark II imaging flow cytometer and INSPIRE Software (EMD Millipore, Billerica, MA). The accompanying IDEAS Software was used to perform data analysis. Data is reported as the percent of the total cell population that stained positive for the specific marker.

3.4 Transmission electron microscopy (TEM)

Cord blood-derived MKs were cultured until day 14 of differentiation, with or without *E. coli* LPS. The cells were then pelleted down at 1900 g for 10 minutes. Immediately after removal of the culture medium, KII fixative (2.5% glutaraldehyde, 2.0% paraformaldehyde, 0.025 % Calcium Chloride in a 0.1M Sodium Cacodylate buffer, pH 7.4) was added to the cell pellet, mixed, and allowed to fix for 20 minutes. A rubber tipped cell scraper was then used to gently remove the fixed monolayer from the plastic substrate. The samples were centrifuged, the fixative removed, replaced with buffer, and stored at 4°C until further processing. To make a cell block, the material was centrifuged again and resuspended in warm 2% agar in a warm water

bath to keep the agar fluid. The material was then centrifuged again and the agar allowed to gel in an ice water bath. The tissue containing tip of the centrifuge tube was cut off resulting in an agar block with the material embedded within it. This agar block was then processed routinely for electron microscopy in a Leica Lynx™ automatic tissue processor. Subsequent processing was done using a Lieca Lynx™ automatic tissue processor. Briefly, they were post-fixed in osmium tetroxide, stained En Bloc with uranyl acetate, dehydrated in graded ethanol solutions, infiltrated with propylene oxide/Epon mixtures, embedded in pure Epon, and polymerized overnight at 60°C. One micron sections were cut, stained with toluidine blue, and examined by light microscopy. Representative areas were chosen for electron microscopic study and the Epon blocks were trimmed accordingly. Thin sections were cut with an LKB 8801 ultramicrotome and diamond knife, stained with lead citrate, and examined in a FEI Morgagni transmission electron microscope. Images were captured with an AMT (Advanced Microscopy Techniques) 2K digital camera.

3.5 Ultrastructural Image Analysis

TEM images were analyzed using Fiji software. Image thresholding and quantification was performed in order to calculate the percent of white space, which would represent either vacuoles or open canalicular spaces, as a percent of the total cell area imaged. (Eckly A, 2009)

3.6 Statistical Analysis

Statistics were performed using both Microsoft Excel and GraphPad Prism Software (GraphPad Software, Inc.). Paired student t-tests were performed to compare between conditions for each experiment, with the exception of an un-paired student t-test for the EM thresholding analysis. Each parameter evaluated in this study had at least 3 experimental groups evaluated. A p-value of <0.05 was considered significant.

4. Results

4.1 LPS treatment results in decreased cell count and cell size

Cord blood-derived (CB) MKs appeared to have a change in gross cell morphology upon treatment with *E. coli* LPS during differentiation (Figure A1-2). Upon microscopic evaluation, the cells appeared to be subjectively smaller in size and were frequently found in clusters (Figure A1-2 A). Cells counts were evaluated by calculating the average number of MKs in culture per each input hematopoietic stem cell (HSC) (Eq 1&2).

Eq. 1: *(# CB MKs on day 14) / (# input HSC on day 1) = # CB MKs/HSC*
Eq. 2: *((LPS # CB MKs/HSC) / (Control # CB MKs/HSC) * 100) – 100 = % change LPS CB MKs/HSC*

The number of CB MKs/HSC was significantly higher in the LPS-treated group as compared to the control group, as shown by the total percent change between groups (14-59%) (Figure A1-2 B). When cell size was evaluated, the cells were significantly decreased in the LPS-treated group as compared to the control group (11.3 ± 0.5 μm vs. 12.7 ± 0.8 μm, respectively). Cells in the LPS-treated group were also frequently found in clusters and with, subjectively less platelet buds, than the control group (Figure A1-2 C).

4.2 LPS treatment results in changes in nuclear content and cell surface markers

Imaging flow cytometry was performed on the CB MKs in order to evaluate any changes in their cell surface marker or nuclear content phenotype. Cells were divided into 'nucleated' or 'pyknotic' cells, based on their nuclear content, as estimated by Draq5 staining intensity, and by their accompanying image (Figure A1-3 A). The mean Draq5 DNA staining intensity for nucleated cells were then compared between LPS-treated and control cells, and showed that there was a statistically significant decrease in Draq5 staining in the LPS-treated group (7.8-71.7% decrease in Draq5 staining intensity) (Figure A1-3 B). This decrease in staining intensity can be due to a number of causes, including being associated with decreased cell size, or having a decrease in endomitosis, resulting in a decrease in nuclear content.

Cell surface markers were also evaluated for each LPS and control groups, for both nuclear and pyknotic cells. There was a significant increase in the percent of $CD62P^{+}CD34^{+}$ and a significant decrease in the percent of $CD62P^{-}CD34^{-}$ cells, nucleated and pyknotic ($p = 0.020$ and $p = 0.004$ vs. $p = 0.006$ and 0.014). There was no significant difference in the percent of $CD162^{+}$ cells. Statistics were not performed on HLA-ABC, HLA-DR, and von Willebrand factor (vWF) because they were only evaluated in two experimental groups; while there did not appear to be a difference between the two groups for both MHC-receptors, there did appear to be a decrease in the average vWF staining intensity in the LPS-treated group. There was a significant increase in the amount of $CD34^{+}$ pyknotic cells in the LPS group as compared to the control group ($p = 0.011$), but no significant difference in nucleated $CD34^{+}$ cells between groups ($p = 0.073$). This phenotype change indicates an increase in immature apoptotic cells within the LPS-treated group.

4.3 LPS treatment results in ultrastructural changes

Transmission electron microscopy (TEM) images of the CB MKs demonstrated some subtle differences in the ultrastructural morphology of the LPS and control groups. One of the more significant difference noted was the change in the amount of 'empty' spaces within the cell (Figure A1-4 A); these spaces were either vacuoles or were part of the open canalicular network system. To quantify the 'empty' space within the cells, we used imaging software to threshold the white space and then quantify the % of the cell that was taken up by this white space (Figure A1-4 B). This approach demonstrated that there was a significantly increased amount of 'empty' space within each cell in the LPS-treated groups, as compared to the control group (33.3 ± 7.9 % white space vs. 21.8 ± 13.5% white space, respectively; $p < 0.001$). This increase in 'empty' space is consistent with a number of hereditary MK disorders, which are associated with a subsequent abnormality in platelet formation and platelet granule content. Another unique finding was the presence of small intracytoplasmic inclusion bodies (Figure A1-4 C). At this point in time, we are not sure of the significance of this finding, as it was not seen in all samples, but the inclusions appear to resemble 'Döhle bodies', which are abnormal cytoskeletal inclusions due to defect in Nonmuscle Myosin Heavy Chain IIA. The potential significance of these ultrastructural changes will be explored further in the 'Discussion' (section 1.5).

5. Discussion

Exposure to *E. coli* lipopolysaccharide (LPS) is known to have mitogenic effects on multiple cell types. (Skidmore BJ 1975; Goodman GW 1979) In order to explore the effects of *E. coli* LPS on the differentiation and maturation of the MK cell, we performed some a set of preliminary experiments and exposed cord blood-derived MKs to LPS starting at day 7 of differentiation and compared their phenotype at day 14 to the control cells. Early results demonstrate that their does appear to be a phenotypic change in MK cells upon exposure to LPS during differentiation, including changes in cell count, cell size, ultrastructural morphology, as well as cell surface markers.

MKs are one of the only cell types in the body to undergo endomitosis; the replication of chromosomes in the absence of cell or nuclear division, which, in MKs, results in polyploid cells. Exposure to LPS starting at day 7 of differentiation resulted in an increase in cell count and a decrease in cell size and nuclear content. LPS is a known mitogen, resulting in an increase in cell division; therefore, it is no surprise that exposure to LPS resulted in an increase in MK cell count. The decrease in nuclear content could be a result of either an increase in complete mitosis, or it may simply be related to the decrease in cell size. Previous literature has confirmed these findings in mice, demonstrating that exposure to LPS resulted in an increase in CFU-MK (colony-forming unit MKs) and an increase $CD41^+$ expression, however, LPS was also found to increase MK polyploidization in this study. (Wu D 2015) These differences in the effects of LPS can be a result of species difference in the origin of the cells or can be a result of the difference between adult and neonatal megakaryocytes, which are known to have differences in both cell morphology, nuclear ploidy, and cell surface marker expression. (Mattia G, 2002)

Cell surface markers were also observed to change with LPS-treatment, resulting in an increase in $CD34^+$ pyknotic cells. MKs undergo a controlled apoptosis when fully differentiated and when undergoing thrombopoiesis (see section 1.2.2, 'Thrombopoiesis'). One of the explanations for this increase in $CD34^+$ pyknotic cells could be that the MKs are prematurely undergoing thrombopoiesis. This finding could potentially explain one of the mechanisms by which patients that are exposed to LPS, such as in the case of sepsis, have increased circulating reticulated

platelets, which represent an immature platelet fraction. (Enz Hubert RM, 2015) The likelihood of the LPS being cytotoxic after 7 days of culture is not likely, but if some cells bound more LPS than others, then this is still a possibility.

The ultrastructural changes identified in the MKs exposed to LPS may explain the changes in platelet morphology and function seen in patients with sepsis. Platelet indices have been shown to be correlated with sepsis and prognosis, with reticulated platelets and mean platelet volume (MPV) being increase in septic patients. (Gao Y, 2014; Ramesh Bat, 2017; Enz Hubert RM 2015) Stimulation of toll-like receptor 4 (TLR4) has been suggested to play a role in MK thrombopoiesis. (Beaulieu LM, 2010) Platelet function has also been noted to be altered, with septic patients having platelets that spontaneously activate but have a defect in agonist-dependent aggregation. (Hurley SM, 2016; Yaguchi A, 2004; Woth G, 2011; Alt E, 2004) The increase in MK 'empty' space identified in the LPS-treated cells could result in large, hypogranular, abnormally functioning platelets; such as those seen in other MK abnormalities, including Grays Platelet Syndrome and May Hegglin Anomaly. (Eckly A, 2009; Kahr WHA, 2013) The occasional cytoskeletal inclusion bodies noted in the MKs appear to be morphologically similar to döhle bodies. Döhle bodies are inclusion bodies, most commonly described to be due to abnormalities in *MYH9*, resulting in myosin aggregates within the cytoplasm of the cell. Interestingly, döhle bodies are present during both hereditary abnormalities, such as May Hegglin anomaly, as well as during sepsis. (Oski FA, 1962; Easton JA, 1966; Botero JP, 2016; Lazarchick J, 2010; Labert JL, 2016) During sepsis, one of the classic changes seen in leukocytes, specifically neutrophils, is toxic change consisting of: foamy basophilic cytoplasm, hyper segmented nuclei, and döhle body inclusions; interestingly, the ultrastructural evaluation of neutrophil döhle bodies in toxic neutrophils are described as being rough endoplasmic reticulum (RER) aggregates and not cytoskeletal inclusions. (McCall CE, 1969) It is also important to note that patients with May Hegglin anomaly also usually also have a macrothrombocytopenia, which is also seen during sepsis. (Oski FA, 1962; Ruhoy SM, 2016) The mechanism by which döhle bodies appear in neutrophils during sepsis is not currently known; perhaps the finding of döhle bodies in MKs as a result of LPS exposure is an indication towards a mechanism.

Together, these preliminary results demonstrate that LPS exposure during MK differentiation may result in abnormal MK differentiation and maturation. Although these are not conclusive, this approach may help to understand the etiology of the abnormal circulating platelet during sepsis, and may help elucidate novel mechanisms of cellular dysfunction in the face of endotoxemia.

6. Acknowledgements

Skyler Kauffman helped perform cytotoxicity assays (data not shown). Martin Selig and Nicki Watson performed the transmission electron microscopy. This work was supported by the T32-0D019078-28 (JGF), the P30-ES002109 (JGF), the P50-GM021700 (RGT), and the Harvard NeuroDiscovery Center.

7. References

1. Gao Y, Li Y, Xuehong Y, et al. The impact of various platelet indices as prognostic markers of septic shock. PLoS One, 2014;9(8):e103761.
2. Ramesh Bhat Y. Platelet indices in neonatal sepsis: A review. World J Clin Infect Dis, 2017;7(1):6-10.
3. Enz Hubert RM, Rodrigues MV, Andreguetto BD, et al. Association of the immature platelet fraction with sepsis diagnosis and severity. Sci Rep, 2015;5:8019.
4. Brown RE, Rimsza LM, Pastos K, et al. Effects of sepsis on neonatal thrombopoiesis. Pediatr Res, 2008;64(4):399-404.
5. Freishtat RJ, Natale J, Benton As, et al. Sepsis alters the megakaryocyte-platelet transcriptional axis resulting in granzyme B-mediated lymphotoxicity. Am J Respir Crit Care Med, 2009;179(6):467-73.
6. Lood C, Amisten S, Gullstrand B, et al. Platelet transcriptional profile and protein expression in patients with systemic lupus erythematosus: up-regulation of the type I interferon system is strongly associated with vascular dis- ease. Blood, 2010;116(11):1951-1957.
7. Raghavachari N, Xu X, Harris A, et al. Amplified expression profiling of platelet transcriptome reveals changes in arginine metabolic pathways in patients with sickle cell disease. Circulation, 2007;115(12):1551-1562.
8. Healy AM, Pickard MD, Pradhan AD, et al. Platelet expression profiling and clinical validation of myeloid- related protein-14 as a novel determinant of cardiovascular events. Circulation, 2006;113(19):2278-2284.
9. Rondina MT, Schwertz H, Harris ES, et al. The septic milieu triggers expression of spliced tissue factor mRNA in human platelets. J Thromb Haemost, 2011; 9(4): 748-58.
10. Skidmore BJ, Chiller JM, Morrison DC, et al. Immunologic properties of bacterial lipopolysaccharide (LPS): correlation between mitogenic, adjuvant, and immunogenic activities. J Immunol, 1975;114(2pt2):770-775.
11. Goodman GW, Sultzer BM. Endotoxin protein is a mitogen and polyclonal activator of human B lymphocytes. J Exp Med, 1979;149:713-723.
12. Wu D, Xie J, Wang X, et al. Micro-concentration lipopolysaccharides as a novel stimulator of megakaryopoiesis that synergizes with IL-6 for platelet production. Sci Rep, 2015;doi:10.1038/srep13748.
13. Mattia G, Vulcano F, Milazzo L, et al. Different ploidy levels of megakaryocytes generated from peripheral cord blood CD34_ cells are correlated with different levels of platelet release. Blood, 2002;99(3):888-897.
14. Beaulieu LM, Freedman JE. The role of inflammation in regulating platelet production and function: Toll-like receptors in platelets and megakaryocytes. Thromb Res, 2010; 125(3): 205-209.
15. Hurley SM, Lutay N, Holmqvist B, et al. The dynamics of platelet activation during the progression of streptococcal sepsis. PLoS One, 2016;11(9):e0163531.
16. Yaguchi A, Lobo FL, Vincent JL, et al. Platelet function in sepsis. J Thromb Haemost, 2004;2(12):2096-2102.
17. Woth G, Varga A, Ghosh S, et al. Platleet aggregation in severe sepsis. J Thromb Thrombolysis, 2011;31(1):6-12.
18. Alt E, Amann-Vesti BR, Madl C, et al. Platelet aggregation and blood rheology in severe

sepsis/septic shock: relation to the Sepsis-related Organ Failure Assessment (SOFA) score. Clin Hemorrheol Microcirc, 2004;30(2):107-115.
19. Eckly A, Strassel C, Freund M, et al. Abnormal megakaryocyte morphology and proplatelet formation in mice with megakaryocyte-restricted MYH9 inactivation. Blood, 2009;113:3182-3189.
20. Kahr WHA, Lo RW, Li L, et al. Abnormal megakaryocyte development and platelet function in Nbeal2$^{-/-}$ mice. Blood, 2013;122:3349-3358.
21. Oski FA, Naiman JL, Allen DM, et al. Leukocyte inclusions—Dohle bodies—associated with platelet abnormality (the May-Hegglin anomaly). Report of a family and review of the literature. Blood, 1962;20:657-667.
22. Easton JA, Fessas CH. The incidence of Döhle bodies in various diseases and their association with thrombocytopenia. British J Hematol, 1966;12(1):54-60.
23. Botero JP, Patnaik M. Delayed diagnosis of MYH-9 related disorder and the role of light microscopy in congenital macrothrombocytopenia. Blood, 2016;127:1940-1940.
24. Lazarchick J. Döhle bodies – 1. Blood, 2010; image #00001069, ASH Image Bank.
25. Lambert JL, Fernandez NJ, Roy MF. Association of presence of band cells and toxic neutrophils with systemic inflammatory response syndrome and outcome in horses with acute disease. J Vet Intern Med, 2016;30(4):1284-1292.
26. McCall CE, Katayama I, Cotran RS, et al. Lysosomal and ultrastructural changes in human "toxic" neutrophils during bacterial infection. JEM, 1969;129(2):267.
27. Ruhoy SM, Yates A. Macrothrombocytopenia with Döhle body-like granulocyte inclusions: A case report of May-Hegglin anomaly in a 33-year-old white woman with an update on the molecular findings of *MYH9*-related disease. Lab Med, 2016;47(3):246-250.

Figures:

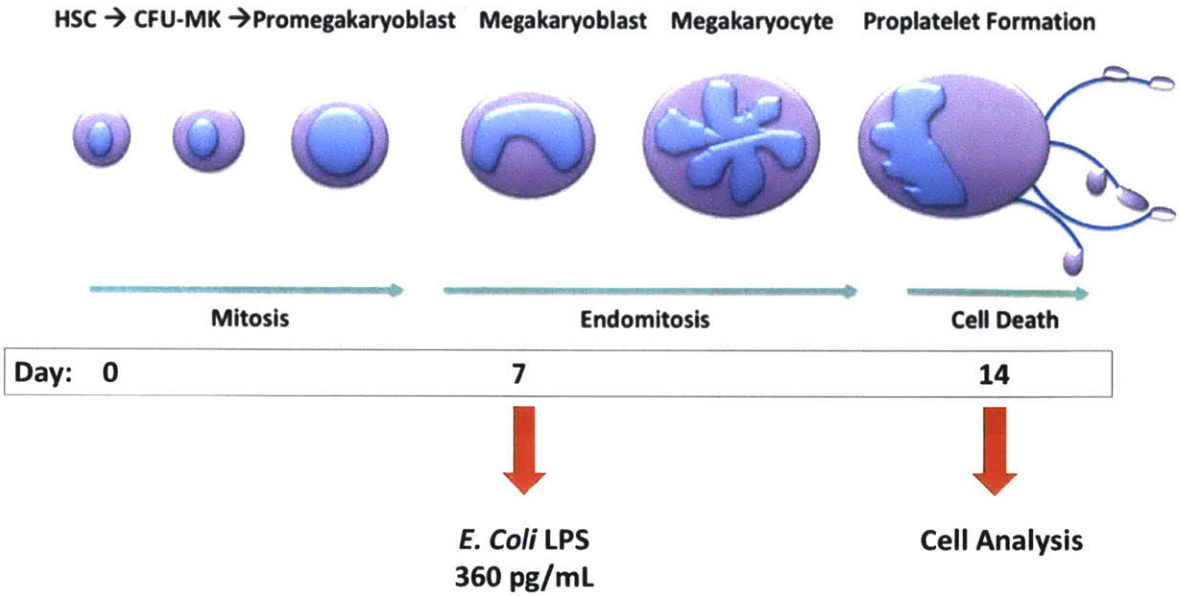

Figure A1-1: Experimental Design.

Cord blood-derived $CD34^+$ cells were cultured and differentiated into mature megakaryocytes over 14 days. *E. coli* LPS was added at a concentration of 360 pg/mL at day 7 of differentiation. Cells were then harvested at day 14 for subsequent analysis. MK, megakaryocyte; HSC, hematopoietic stem cell, $CD34^+$ cell; CFU-MK, colony-forming unit MK.

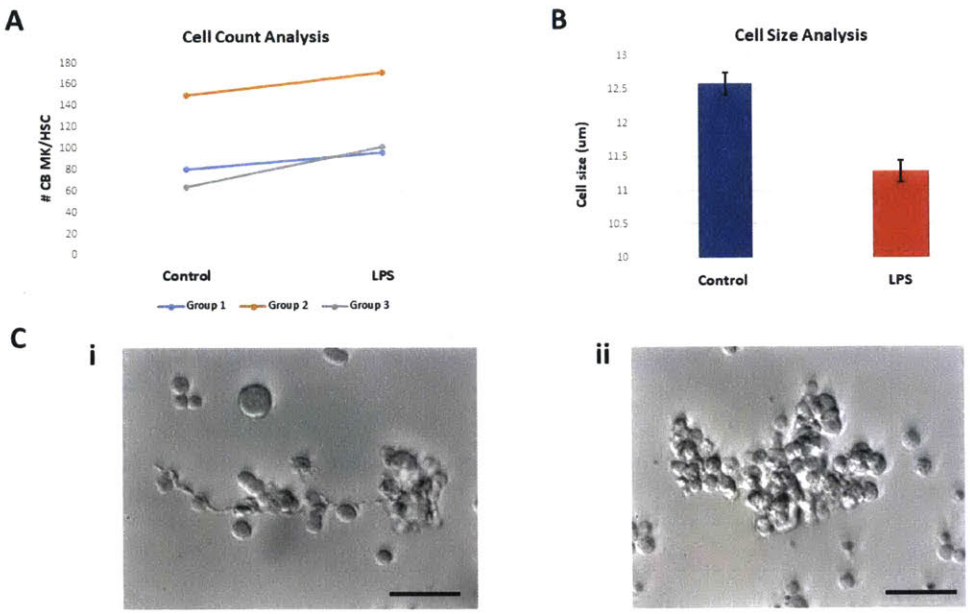

Figure A1-2: Megakaryocyte morphology after exposure to LPS.

MK cell count and cell size was evaluated and compared between LPS-treated and control groups. (A) Cell counts were significantly increase in the three LPS-treated groups evaluated ($p = 0.03$). (B) Cells size was significantly decreased in the LPS-treated cells as compared to the control cells ($p < 0.00$). (C) Images of the control (i) and LPS (ii) group showed morphology changes, including smaller cell size, increase cell clustering, and decreased proplatelet buds. Cell clustering and proplatelet bloods were not quantified. Scale bar is approximately 50 µm.

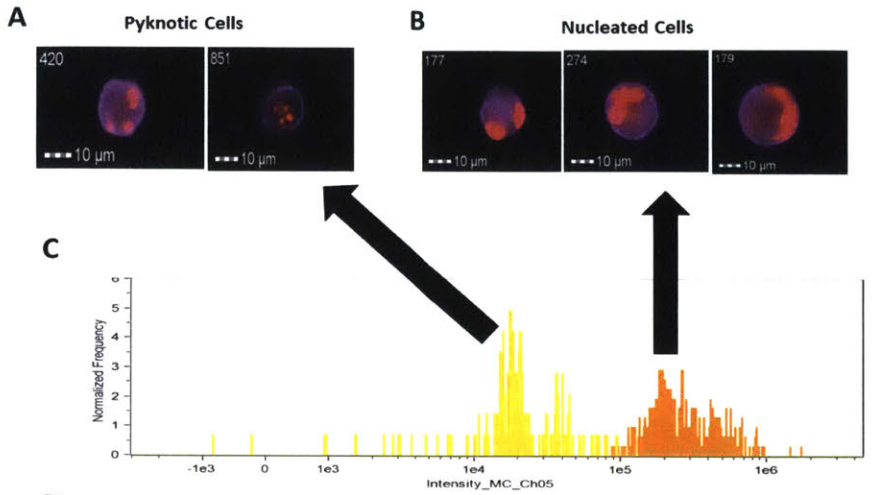

Population	Count	%Gated	Mean	Std. Dev.	Minimum	Maximum
pyknotic & singlets & CD41+	142	100	24182.09	16296.9	-824.7	94378.08
nucleated & singlets & CD41+	308	100	318178.21	203866.65	89080.09	1723761.94

Figure A1- 3: Evaluation of nuclear content.

Imaging flow cytometry was performed in order to evaluate the total DNA content (nuclear content) of the cells in culture. Cells were first identified as MKs ($CD41^+$ cells). These cells were then further subdivided into cells that were nucleated (meaning cells with identifiable nuclei) and cells that were pyknotic (small, segmented nuclear staining). This is shown in the images on the top two panels (A & B). The nuclei were stained with Draq5, which stains DNA. The histogram visualization of the mean intensity of the Draq5 staining enabled the segregation of the nucleated and pyknotic cells (C). The Ideas Software also allowed for the analysis of the Draq5 staining intensity for both groups, including, but not limited to: cell count, mean, standard deviation, minimum and maximum Draq5 staining intensity (D).

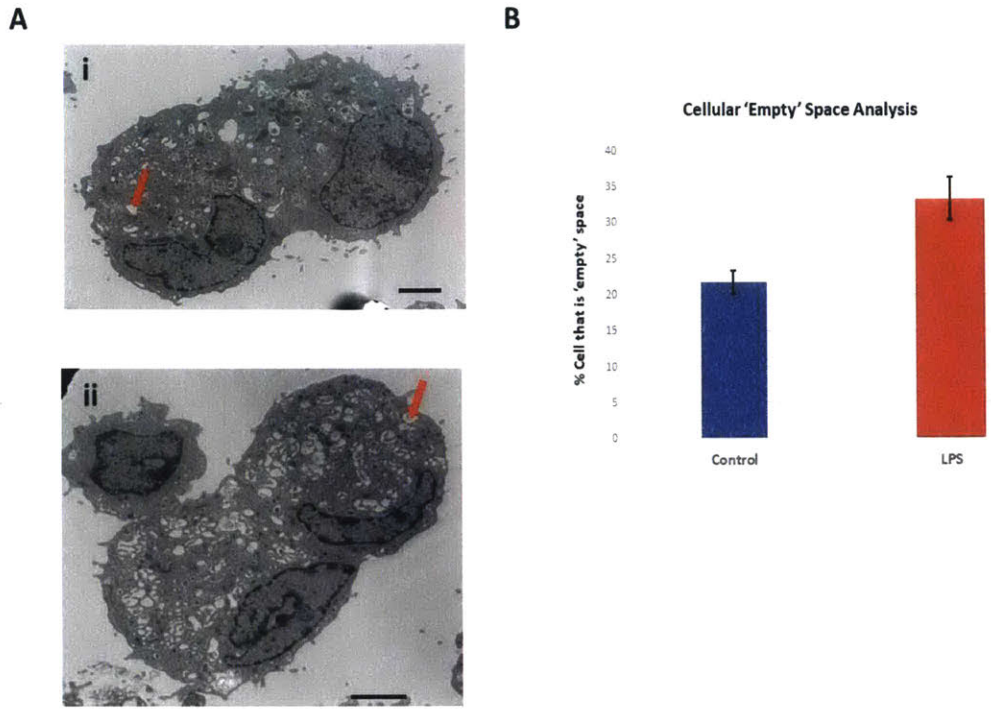

Figure A1-4: Evaluation of cellular 'empty' space.

Transmission electron microscopy (TEM) was performed on the LPS-treated and control MKs. (A) TEM images demonstrated that the control cells (i) subjectively had decreased 'empty' space (red arrow) within the cytoplasm as compared to the LPS-treated group (ii). (B) Image analysis software was used to quantify the percent of the cell that was occupied by this 'empty' space and confirmed that the LPS-treated cells had significantly more 'empty' space than the control cells ($p < 0.01$). Data is shown as a bar graph with standard error bars. Scale bar is approximately 2 μm.

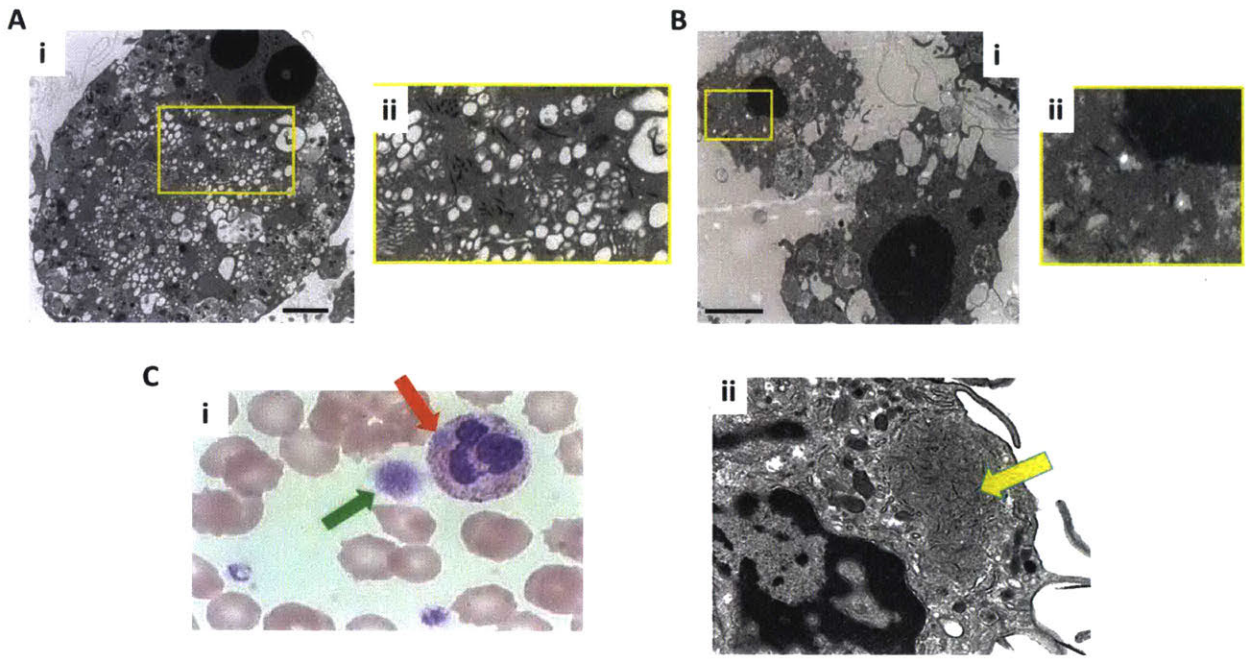

Figure A1-5: Megakaryocyte inclusion bodies

TEM imaging of MKs showed that there were occasional inclusion bodies within the cytoplasm of the cell. (A & B) These inclusion bodies appeared to have a sharp, linear, electron-dense morphology. Magnification of these inclusions are shown in panel Aii and Bii. Patients with May-Hegglin anomaly have a somewhat similar sharp, electron-dense inclusion body within neutrophils, termed döhle bodies. (C) A light micrograph of a neutrophil with a döhle body (red arrow) next to a giant platelet (green arrow) is shown (i) alongside the companion TEM of a neutrophil (ii) with a döhle body (yellow arrow). Scale bar is approximately 2 μm. Images for panel C are from: Botero JP, Patnaik MM. Delayed diagnosis of MYH9-related disorder and the role of light microscopy in congenital macrothrombocytopenias. Blood, 2016;127:1940.